# Intra-genomic variation in symbiotic dinoflagellates: recent divergence or natural hybridization?

**Shaun Peter Wilkinson**

A thesis submitted to the Victoria University of Wellington in fulfilment of the requirements for the degree of Doctor of Philosophy

Victoria University of Wellington

2015

# Abstract

The perpetuity of coral reefs will ultimately depend on the ability of corals to adapt to changing conditions. Inter-specific hybridization can provide the raw genetic material necessary for adaptation, and stimulate macro-evolutionary leaps during periods of environmental upheaval. Though well-documented in corals, hybridization has yet to be identified in their dinoflagellate symbionts (genus *Symbiodinium*), despite growing evidence of sexual reproduction in this genus. The integral roles that these symbiotic algae play in coral productivity, reef accretion and 'coral bleaching' emphasize the need to better understand their short-term evolutionary potential. In this thesis, I develop new molecular and statistical methodology, and combine lab- and field-based analysis to explore the potential for hybridization between divergent *Symbiodinium* taxa.

To screen for putative *Symbiodinium* hybrids, intra-genomic variation was examined within individual symbionts isolated from the reef-building coral *Pocillopora damicornis* at Lord Howe Island (Australia). A nested quantitative PCR (qPCR) assay was developed to quantify polymorphic internal transcribed spacer 2 (*ITS2*) sequences within the genome of each symbiont cell. Three genetically distinct *Symbiodinium* populations were detected co-existing within the symbiont consortium of *P. damicornis*. Mixed populations of 'pure' *Symbiodinium* types C100 and C109 coexisted with a population of cells hosting co-dominant C100 and C109 *ITS2* repeats. Genetically heterogeneous *Symbiodinium* cells were more common than homogeneous symbionts in four of the six colonies analysed, with a maximum proportional abundance of 89%.

Morphological, functional and ecological attributes of heterogeneous *Symbiodinium* cells were characterized to assess their candidacy as putative hybrids. The proportional abundance of genetically heterogeneous symbionts was spatially and temporally conserved within colonies, indicating a lack of competition between *Symbiodinium* populations. However, this abundance ratio varied considerably between colonies separated by metres to tens of metres, and to a greater extent between sites isolated by hundreds to thousands of metres. The local thermal maximum emerged as a significant predictor of the proportional abundance of genetically heterogeneous *Symbiodinium* cells, suggesting that the distribution of these 'putative hybrids' is influenced by a reduced affinity for thermal stress.

Genetically heterogeneous *Symbiodinium* cells were around 50% larger (by volume) than homogeneous cells, occupied tissue of the coral host at reduced densities, and showed relatively poor light-harvesting efficiency. Colonies hosting a higher proportion of these symbionts suffered a reduction in overall photosynthetic performance (maximum gross photosynthesis normalised to respiration; *P:R*) at the ambient temperature of 25 °C. This disparity was maintained when the temperature was elevated to simulate the maximum experienced within the LHI lagoon (29 °C). Under these stressful conditions, colonies dominated by putative *Symbiodinium* hybrids were only marginally capable of net oxygen production.

The influence of putative *Symbiodinium* hybrids on the growth and survival of *P. damicornis* was tested by reciprocally transplanting coral colonies between reef sites featuring distinct temperature regimes. Neither calcification nor mortality was influenced by the proportional abundance of genetically heterogeneous cells in the symbiont consortium. This uncoupling of symbiont performance and host fitness may be explained by stochastic events such as predation and disease, which substantially increase variation in growth and mortality in field experiments. Alternatively, it may represent some unknown benefit associated with hosting hybrid symbionts, belying their relatively poor photosynthetic performance, and explaining the widespread abundance of these heterogeneous *Symbiodinium* cells on the Lord Howe Island reef.

Our inability to maintain many clade C *Symbiodinium* types in culture prevents direct observations of hybridization between C100 and C109. Unequivocal evidence of this phenomenon will therefore likely remain elusive until high-resolution, single-copy nuclear markers can be developed, since the incomplete displacement of ancestral polymorphisms can leave a similar genomic signature to that of hybridization. However, this study serves to provide an initial proof-of-principle for hybridization between divergent *Symbiodinium* taxa. In doing so, it highlights the need to better understand the evolutionary processes underpinning coral- and symbiont-adaptation in a changing climate.

# Contributions and publications

This thesis is compiled as a series of manuscripts that have been submitted for publication or are in the preparation process. The thesis is the intellectual and analytical work of the author, with contributions as described below. Assoc. Prof. Simon Davy and Dr. Paul Fisher provided supervisory, intellectual and editorial assistance throughout, and Dr. Stefanie Pontasch assisted with field-work at Lord Howe Island.

**Chapter 2:** This chapter is formatted as an independent manuscript: Wilkinson SP, Fisher PL, Davy SK. Intra-genomic variation in symbiotic dinoflagellates: recent divergence or natural hybridization? This manuscript has been submitted for publication.

**Chapter 3:** This chapter is formatted as an independent manuscript: Wilkinson SP, Pontasch S, Fisher PL, Davy SK. The spatiotemporal distribution of putative *Symbiodinium* hybrids at Lord Howe Island, Australia.

**Chapter 4:** This chapter is formatted as an independent manuscript: Wilkinson SP, Pontasch S, Fisher PL, Davy SK. Poor functional performance of putative *Symbiodinium* hybrids and their coral hosts at a high-latitude, marginal coral reef.

**Chapter 5:** This chapter is formatted as an independent manuscript: Wilkinson SP, Pontasch S, Fisher PL, Davy SK. Reduced functional performance in putative *Symbiodinium* hybrids does not impair coral growth and survival in their natural habitat.

Financial support was provided by a VUW Vice Chancellor's Strategic PhD Scholarship, a J. L. Stewart Scholarship, a VUW PhD Submission Scholarship and a Faculty Strategic Research Grant, awarded to the author. Additional assistance for field-work costs was provided by a Royal Society Marsden Fund Grant awarded to Assoc. Prof. Simon Davy and Dr. Paul Fisher (contract number VUW0902). Corals were collected under New South Wales Department of Primary Industries permit number P10/0042-1.1. The work was made possible with the help of the Lord Howe Island Marine Parks Authority.

# Acknowledgements

I am very grateful for the sources of funding that made this project possible. In particular, I wish to extend my gratitude to Victoria University of Wellington for deeming me a worthy recipient of the VUW Vice Chancellor's PhD Scholarship.

This thesis represents a large amount of work, much of which came from the efforts of other people. I would initially like to thank Simon Davy for being the consummate supervisor. Simon seemed to have an unwavering belief in me, and remained interested and helpful even when the project drifted far from his academic comfort zone, battling through my stats jargon and always providing valuable feedback. This work would also not have been possible without the help of my co-supervisor Paul Fisher, who willingly passed on his skills and knowledge, and whose original idea it was to attempt genetic quantification on a single symbiont cell.

Carrying out field-work in the pristine Lord Howe Island Marine Park was an extraordinary experience, and I thank all the people who made it possible. I would especially like to thank my research buddy Stefanie Pontasch; our mission was never going to be an easy one, and with resourcefulness, determination, and copious amounts of coffee, we got there! I also wish to thank the people at the Lord Howe Island Marine Parks Authority, particularly Ian Kerr, Sallyann Gudge, Jimmy Maher and Tas Douglass. You guys were so welcoming, helpful, generous, understanding, and actively engaged in our research. Thanks also to Tim Solomon and Rebecca Moran for hosting me on the island, and to the many other locals who helped turn our ambitious plans into a reality. I'd especially like to thank Ian Fitzgerald for volunteering a huge amount of time and effort, and Brian Busteed at Howea Divers for making our diving experience unforgettable. Thanks also to the many academics we met on the island and provided much needed guidance to a couple of early-career researchers. In particular, thanks to Professor Peter Harrison, whose advice I found invaluable.

It seems that all academics have an unmanageable amount of work, and I am very appreciative of those who sacrificed their time to improve the scientific quality of this thesis. I am deeply grateful for the help and advice I received from Shirley Pledger, Nicole Phillips, Xavier Pochon, Michael Stat, Scott Santos, and Joe Zuccarello. Thanks also to Madeleine van Oppen for sharing her unpublished work, and to Ruth Gates for showing an interest in my research and keeping me in high spirits during the write-up. I'd also like to take this

opportunity to thank the anonymous reviewers who provided detailed and constructive feedback on my earlier manuscript drafts, ultimately making this thesis a much better product. A big thanks to Luke Thomas for inviting me along on his research expedition to the Houtman Abrolhos, and teaching me his own unique brand of resourcefulness. Thanks to Emma Gibbin and Katie Hillyer for compensating for my not-so-good admin skills, and to the rest of the Davy Lab group for providing a stimulating research environment. Cheers to my office mates Luke, Karl and Gagan for making my time at Vic an enjoyable one. Thanks also to everyone that brought my pies and helped me get to the symbiosis conference in Poland!

There are many people who gave me a great deal of personal support along the way. Thanks to my family, Mum, Dad, Naomi and family, Kath, Claire, Jules and my Nana Dawn. I'd especially like to thank my parents Pete and Jen for fostering my interest in science from an early age. Over the past few years I have received an enormous amount of support from the Bourke family, John, Trish, Anna, Mike, Lou, Carel, Frank and Anna. A special thank you to Trish for all the wonderful meals, and to John for convincing me that I should go to university. Without that piece of advice I would be much less stimulated mentally, though probably a lot better off financially. Thanks to Franky for being a good mate, and understanding why I've had to neglect the extreme catamaraning and spearfishing over the past few months. Finally, thanks to my patient and understanding soon-to-be wife Alice, for providing a little extra encouragement to get this thesis into the hand-in box, and for making life great.

# List of abbreviations

| | |
|---|---|
| **$\alpha$** | Light-harvesting efficiency |
| **ABH** | Adaptive bleaching hypothesis |
| **AFLP** | Amplified fragment length polymorphism |
| **AGF** | Assisted gene-flow |
| **AIC** | Akaike information criterion |
| **AICc** | Corrected Akaike information criterion |
| **AIMS** | Australian Institute of Marine Science |
| **ANCOVA** | Analysis of covariance |
| **ANOVA** | Analysis of variance |
| **BLAST** | Basic local alignment search tool |
| **BSA** | Bovine serum albumin |
| **bp** | Base pair |
| **$C_{C100}$** | The total number of *Symbiodinium* clade C *ITS2* sequence copies of type C100 |
| **$CO_2$** | Carbon dioxide |
| **$C_t$** | Cycling threshold value |
| **$C_{TOTAL}$** | The total number of *Symbiodinium* clade C *ITS2* sequence copies |
| **CDS** | Coding sequence |
| **Chl** | Chlorophyll |
| **df** | Degrees of freedom |
| **DGGE** | Denaturing gradient gel electrophoresis |
| **DMSO** | Dimethyl sulfoxide |
| **DNA** | Deoxyribonucleic acid |
| **DNAB** | DNA buffer |
| **EDTA** | Ethylenediaminetetraacetic acid |
| **ENSO** | El Niño Southern Oscillation |

| | |
|---|---|
| **FISH** | Fluorescence *in situ* hybridization |
| **FSW** | Filtered seawater |
| **GBR** | Great Barrier Reef |
| **GPS** | Global positioning system |
| **$H_2O$** | Water |
| **HCl** | Hydrochloric acid |
| **HKY** | Hasegawa Kishino Yano model |
| **HRF** | Host release factor |
| **ICEAP** | Incomplete concerted evolution of ancestral polymorphisms |
| **$I_C$** | Compensation irradiance |
| **$I_K$** | 50% saturating irradiance |
| **IPTG** | Isopropyl β-D-1-thiogalactopyranoside |
| ***ITS2*** | Internal transcribed spacer 2 |
| **L-BFGS-B** | Limited memory Broyden-Fletcher-Goldfarb-Shanno algorithm with bound constraints |
| **LHI** | Lord Howe Island |
| **LHIMPA** | Lord Howe Island Marine Park Authority |
| **LSU** | Large subunit of ribosome-coding DNA |
| **MANCOVA** | Multivariate analysis of covariance |
| **MANOVA** | Multivariate analysis of variance |
| **MINQUE** | Minimum norm quadratic unbiased estimation |
| **MLG** | Multi-locus genotype |
| **MS** | Mean squared error |
| **NaCl** | Sodium chloride |
| **NDP** | Non-diagnostic polymorphism |
| **NGS** | Next generation sequencing |
| **$O_2$** | Molecular oxygen |

| | |
|---|---|
| ***P:R*** | Ratio of maximum gross photosynthesis to respiration |
| **PAGE** | Poly-acrylamide gel electrophoresis |
| **PAM** | Pulse amplitude modulation |
| **PAR** | Photosynthetically active radiation |
| **PCR** | Polymerase chain reaction |
| $P_{GROSS}$ | Maximum gross photosynthetic rate |
| **PI** | Photosynthesis-irradiance |
| $P_{NET}$ | Maximum net photosynthetic rate |
| $psbA^{ncr}$ | Non-coding region of the plastid psbA minicircle |
| **qPCR** | Quantitative PCR, also known as real-time PCR or quantitative real-time PCR |
| ***R*** | Respiration rate |
| **RAPD** | Random amplified polymorphic DNA |
| **rDNA** | Ribosome-coding DNA |
| **rmANOVA** | Repeated measures analysis of variance |
| **RNA** | Ribonucleic acid |
| $\mathbf{R_n}$ | Fluorescence normalized to specific passive dye signal (qPCR) |
| **ROS** | Reactive oxygen species |
| **Rubisco** | Ribulose-1,5-bisphosphate carboxylase/oxygenase |
| **scPCR** | Single-cell PCR |
| **SCUBA** | Self-contained underwater breathing apparatus |
| **SE** | Standard error |
| $\boldsymbol{S_H:S_T}$ | Abbreviated form of $Symbiodinium_{\mathrm{HETEROGENEOUS}}$: $Symbiodinium_{\mathrm{TOTAL}}$, the proportional abundance of genetically heterogeneous *Symbiodinium* cells in the symbiont consortium. |
| **SS** | Sum of squared errors |
| **SSU** | Small subunit of ribosome-coding DNA |
| **TAE** | Tris-acetate-EDTA |

| | |
|---|---|
| **TE** | Tris-EDTA |
| **$T_m$** | Melting temperature (qPCR product) |
| **UK** | United Kingdom |
| **UV** | Ultraviolet |
| **VUW** | Victoria University of Wellington |
| **WGA** | Whole genome amplification |
| **$w_i$** | Akaike weight |
| **XGAL** | 5-bromo-4-chloro-3-indolyl-β-D-galactopyranoside |

# Glossary

| | |
|---|---|
| **Acclimation** | Changes that occur within an organism in response to experimentally-induced changes in its environment |
| **Acclimatization** | Changes that occur within an organism in response to changes in its natural environment |
| **Adaptation** | A heritable modification that makes an organism more fit for existence under the conditions of its environment |
| **Admixture** | A population consisting of two or more divergent lineages that undergo interbreeding/hybridization |
| **Allopolyploid** | An individual carrying two or more sets of chromosomes originating from different lineages |
| **Backcrossing** | The crossing of fertile hybrids with individuals from one or both progenitor populations |
| **Cross-hybridization** | An artifactual fluorescence signal arising from a lack of sequence specificity in a fluorogenic probe (qPCR) |
| **Diagnostic locus**: | A locus that is fixed for alternate alleles in different species |
| **Diploid** | An organism/cell carrying twice the haploid number of chromosomes |
| **Epistasis** | The interaction between genes at two or more loci resulting in a different phenotype to that expected under independent expression |
| **Excystment** | Emergence from a resting cyst stage |
| **Fitness** | The genetic contribution of an individual to the subsequent generation |
| **Haploid** | An organism/cell carrying a single set of unpaired chromosomes |
| **Haplontic** | A type of sexual life-cycle where haploid gametes fuse to form a diploid zygote, which then undergoes meiosis to restore the haploid condition |
| **Heterosis** | Superior fitness in early-generation hybrids (relative to their parents) arising from increased heterozygosity. Also known as ‘hybrid vigour’ |
| **Hermatypic** | Reef-building (coral) |
| **Heterogeneous** | Characterized by a co-dominant or near co-dominant mixture of genetic sequences |
| **Heterotrophy** | A feeding mode involving the assimilation of organic carbon |

**Holobiont** The community of organisms constituting the entire coral entity

**Homogeneous** Characterized by a pure or near-pure array of genetic sequences

**Hybridization** The crossing of individuals from genetically-divergent lineages

**Hypnozygote** A resting cyst produced from the union of two haploid gametes

**Introgression** The flow of genes between lineages, arising from the progressive backcrossing of $F_1$ and later-generation hybrids with progenitors

**Nested PCR** PCR amplification in two or more stages, using a series of primers that bind to progressively inner regions of the target sequence

**Ortholog** A sequence variant arising from the divergence of separate lineages

**Paralog** A sequence variant arising within a lineage as a result of gene or genome duplication

**Polyploid** An organism/cell carrying more than twice the haploid number of chromosomes

**Progenitor** One of the original ancestors of a hybrid lineage

**Ribotype** A particular rDNA nucleotide sequence

**Scleractinia** The order of corals that includes reef-building species (Class: Anthozoa, Subclass: Hexacorallia)

**Transgressive segregation** The production of $F_2$, backcross, or later-generation hybrids with more extreme phenotypes than the phenotypic range of the parental populations

# Table of contents

# List of figures

# List of tables

# Chapter 1: General introduction

## 1.1. The value of coral reefs

"Anybody who has had the privilege of diving on a coral reef will have seen the natural world at its most glorious, diverse and beautiful". The description given by veteran naturalist and broadcaster Sir David Attenborough accurately depicts the spectacular biodiversity of the reef environment. Coral reefs and their inhabitants generate a valuable global eco-tourism industry, and the economies of many developing countries strongly rely on this source of income (Burke *et al.* 2011). Yet the economic contribution of the world's coral reefs extends well beyond the tourist dollar. More than 10% of the world's population lives within 100 km of a coral reef, and many people directly depend on the reef system for nutrition and coastal stability (Bryant *et al.* 1998; Burke *et al.* 2011). Around 10% of the global fishery catch takes place in reef areas (Smith 1978), and this figure can exceed 25% in some developing Indo-Pacific nations (Cesar 1996). Coral reefs also play an important role in climate regulation, and while they comprise only 0.17% of Earth's ocean surface area (Smith 1978), reefs sequester more atmospheric carbon dioxide per square meter than any other marine ecosystem (Nybakken & Bertness 2005). Moreover, corals and other reef-associated fauna have been recognized as an important source of bioactive compounds, with the potential to greatly benefit the field of human medicine (Carté 1996).

Placing a monetary value on the goods and services provided by coral reefs is necessary for the purposes of conservation prioritisation (Costanza *et al.* 1997). Yet this is made difficult by the inter-connectivity of coral reefs with the broader ecological 'seascape' (Ogden 1988). The productivity and complex three-dimensional architecture afforded by coral reefs support an astonishing diversity of flora and fauna in otherwise desolate tropical waters (Odum & Odum 1955), with estimates of up to 9 million species worldwide (Small *et al.* 1998). Reefs also promote coastal stability through dissipation of wave energy at reef margins, thus enabling the development of other important tropical ecosystems such as mangrove forests and seagrass beds (Hoegh-Guldberg 1999). Therefore, while current evaluation estimates their ecosystem services at US $375 billion annually (Costanza *et al.* 1997), the true value of coral reefs to the human population is certainly much higher.

### 1.2. The distribution of coral reefs

For net reef accretion to occur, corals require warm temperatures, high levels of photosynthetically active radiation (PAR), and saturation or near-saturation of aragonite, the inorganic substrate necessary for calcification (Barnes & Chalker 1990). As such, contiguous coral reef structures are predominantly confined within the equatorial band from 30 °N to 30 °S (Sheppard *et al.* 2009; Figure 1.1). Maximum diversity occurs within the Indo-Australian archipelago (the 'Coral Triangle'), an area inhabited by some 500 coral species (Briggs 1999; Green & Mous 2008). Coral diversity generally diminishes with distance from this biodiversity hotspot, with only around 50 species found at the Galapagos Islands (Briggs 1999; Knowlton 2001). At higher latitudes, communities of corals can be found interspersed among macroalgal assemblages; however they do not form contiguous reef structures due to suboptimal abiotic conditions and competition with macroalgae (Veron 1995; Paulay 1997). The world's northernmost coral reefs occur at Bermuda and Okinawa (Japan; 33 °N), and the southernmost reef is that of Lord Howe Island (Australia; 31.5 °S). Despite being situated at the transition zone between coral- and macroalgal-dominated benthic systems, these 'marginal reefs' can feature high levels of biodiversity. In particular, the isolated reef of Lord Howe Island includes more than 83 scleractinian coral species, many of which are endemic (Veron & Done 1979; Harriott *et al.* 1995).

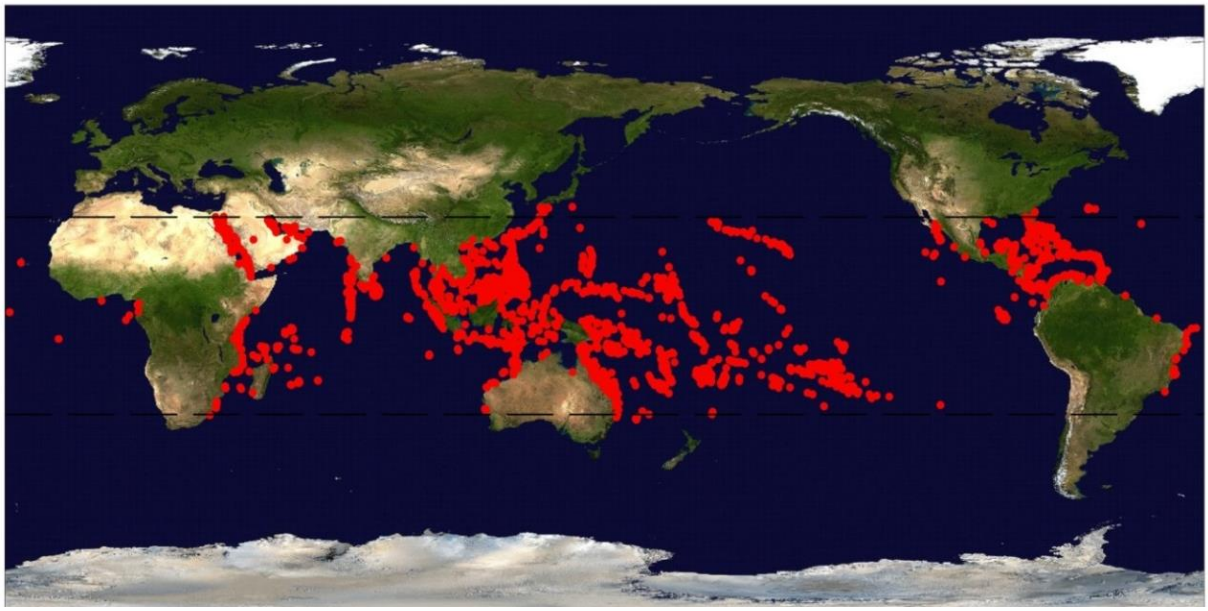

**Figure 1.1 (previous page) The worldwide distribution of coral reefs**
Dashed lines show the latitudinal band of 30 °N and 30 °S, within which the majority of coral reefs are concentrated. GPS data and satellite pictures were obtained from ReefBase, with coral reef locations provided by the United Nations Environment Programme World Conservation Monitoring Centre (UNEP-WCMC; downloaded from http://reefgis.reefbase.org/ on 07/07/2014).

## 1.3. The coral symbiosis: form and function

Coral growth and reef formation are fundamentally supported by symbiosis, the persistent intimate coexistence of different species. The entire coral entity (referred to as the 'holobiont') is composed of a diverse community of organisms, including a cnidarian host (Anthozoa: Scleractinia), single-celled dinoflagellate algae of the genus *Symbiodinium* (also known as 'zooxanthellae'; Freudenthal 1962), and various other micro-eukaryotes, prokaryotes and viruses (Rohwer *et al.* 2001, 2002). A complex array of inter-specific interactions underlie the function of the coral holobiont, spanning the continuum from mutualism (both partners benefit) to parasitism (one partner benefits to the other's detriment). Yet the ecological prosperity of scleractinian corals primarily stems from the mutualistic symbiosis between the cnidarian host and the dinoflagellate symbiont. The symbiont inhabits the cells of the host's gastrodermis (Trench 1987; Figure 1.2) at densities that can exceed $10^6$ cells per $cm^2$ (Drew 1972), releasing photosynthetically-derived organic compounds such as glycerol and/or glucose, fatty acids, organic acids and amino acids (Trench 1971; Whitehead & Douglas 2003; Davy *et al.* 2012). The coral host may receive up to 90% of the total carbon fixed by its symbionts (Steen & Muscatine 1984), a nutritional contribution that can fulfil its energetic requirements under well-lit conditions (Muscatine 1990). The symbiont also plays an integral role in the nitrogen status of the symbiosis, assimilating inorganic nitrogen from environmental sources (e.g. dissolved nitrate) and waste products of host metabolism (predominantly ammonium), into host-accessible compounds (Wang & Douglas 1998; Tanaka *et al.* 2006; Burriesci *et al.* 2012; Kopp *et al.* 2013). Moreover, other essential micronutrients such as phosphorus and sulphur are also assimilated into organic compounds by the symbiont and potentially translocated to the host (Cook 1971; Muller-Parker & D'Elia 1997; Davy *et al.* 2012). This highly efficient closed-system of nutrient retention and recycling underpins the characteristically high productivity and diversity of coral reefs in nutrient-poor tropical oceans (Goreau & Goreau 1959; Muscatine & Porter 1977; Muscatine 1990; Yellowlees *et al.* 2008). Finally, the photosynthetic activity of the symbiont ultimately

supports the calcium carbonate deposition of the host, without which reef accretion would not occur (Pearse & Muscatine 1971; Vandermeulen *et al.* 1972; Colombo-Pallotta *et al.* 2010).

The evolution of the cnidarian-dinoflagellate symbiosis has given rise to a wide variety of behavioural and physiological adaptations. Symbionts can be inherited from parent to offspring, *via* infection of the gamete and/or asexual larvae (vertical transmission), or they can be acquired anew each generation from environmental source populations (horizontal transmission; see Baird *et al.* 2009 for a review). In some cases, both horizontal and vertical transmission strategies may be employed (Byler *et al.* 2013). In the case of horizontal symbiont transmission, the establishment and maintenance of a stable endosymbiosis involves a complex system of symbiont recognition, assortment and phagocytosis ('winnowing'; Nyholm & McFall-Ngai 2004; Dunn & Weis 2009). The winnowing process involves an array of surface receptor proteins (including glycan-binding lectins), and potentially the exchange of metabolites (reviewed in Davy *et al.* 2012). Lectin binding is also believed to play a role in the permanent transition of the symbiont from the motile, flagellated free-living phase to the sedentary coccoid form that the symbiont exhibits when in symbiosis (Koike *et al.* 2004). Once endosymbiosis is established, the symbiont is housed within a membrane complex consisting of a host vacuole (the 'symbiosome membrane') and a series of inner membranes of symbiont origin (Wakefield *et al.* 2000; Wakefiel & Kempf 2001). Nutritional exchange across the symbiosome membrane is regulated by a suite of membrane-bound and cytoplasmic macro-molecules, which may include an enigmatic 'host release factor' (HRF; Gates *et al.* 1995; Wang & Douglas 1997; Ritchie *et al.* 1997). While our understanding of these cellular interactions is in its infancy, emerging 'big-data' fields such as metabolite profiling (metabolomics), high-throughput RNA-transcript and protein sequencing (transcriptomics and proteomics) and whole genome sequencing (genomics) promise to revolutionize our understanding of the functional adaptations underlying the establishment and maintenance of the symbiotic condition (Davy *et al.* 2012).

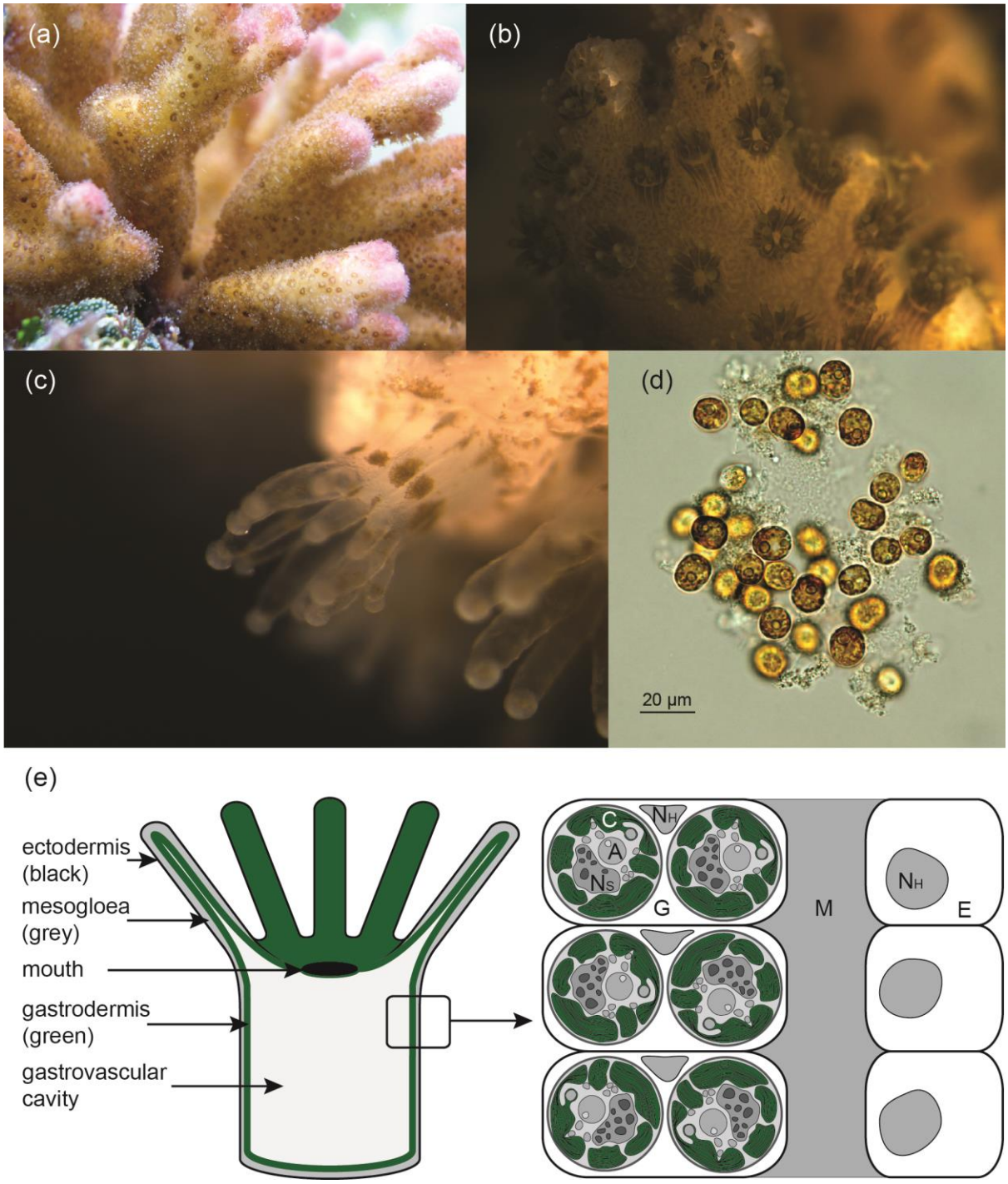


**Figure 1.2 Anatomy of the cnidarian-dinoflagellate symbiosis**
Scleractinian corals consist of a colony of interconnected clonal polyps with an underlying calcium carbonate skeleton. Images show: (a-c) *Pocillopora damicornis* with polyps extended, at increasing levels of magnification; (d) coccoid *Symbiodinium* cells under a light microscope; and (e) schematic cross-section of an individual polyp with a close-up view of the three body layers, the gastrodermis G, the mesogloea M, and the ectodermis E (host nucleus $N_H$). In *P. damicornis*, a bilayer of coccoid *Symbiodinium* cells are enclosed in the gastrodermal cells of the host (chloroplast C, accumulation body A, and nucleus $N_S$; modified from Gates *et al.* 1992; Allemand *et al.* 2011). Photo credits: Emma Gibbin (b and c) and Tom Hawkins (d).

## 1.4. Threats to coral reefs

Corals have evolved in concert with symbiotic dinoflagellates for over 230 million years, forging an obligate association (Coates & Jackson 1987; Stanley & Swart 1995; Veron 1995; Glynn 1996). Yet the symbiotic condition renders both partners extremely vulnerable to environmental disturbance. Even marginal abiotic stress can push the 'holobiont' beyond narrowly defined physiological thresholds, leading to symbiotic dysfunction (Hoegh-Guldberg 1999). Corals are especially vulnerable to elevated temperature (Jokiel & Coles 1977; Iglesias-Prieto *et al.* 1992), excess irradiance (Lesser & Shick 1989; Gleason & Wellington 1993), and in particular, a synergistic temperature-light interaction (Coles & Jokiel 1978; Lesser *et al.* 1990; Fitt & Warner 1995; Lesser & Farrell 2004). These factors stimulate the production of reactive oxygen species (ROS) such as hydrogen peroxide, singlet oxygen, and hydroxyl, perhydroxyl, and superoxide anion radicals. ROS are continually produced at low levels in both symbiotic partners, where they are scavenged and neutralized by a suite of antioxidant molecules (reviewed in Lesser 2006). However, ROS can overwhelm the natural antioxidant defences under stressful conditions (Cadenas 1989), disrupting the cellular constituents of both symbiotic partners through protein denaturation, mutagenic DNA damage, and the peroxidation of plasma membranes (particularly those of the mitochondria and chloroplast; Lesser 2006).

A major source of ROS is the thylakoid membrane of the symbiont chloroplast. Here, temperature-induced uncoupling of the photosynthetic electron transport chain can lead to the transfer of electrons to oxygen, forming the highly toxic superoxide anion (the Mehler reaction; Jones *et al.* 1998). Chronic photoinhibition arises from oxidative damage to the D1-protein and plastiquinone binding proteins of photosystem II, and the primary carboxylating enzyme RUBISCO (Renger *et al.* 1989; Lesser 1996, 1997; Lupínková & Komenda 2004). The loss of photosynthetic function and increased flux of ROS can induce the coral host to eliminate its symbionts, either by exocytosis (Steen & Muscatine 1987; Lesser 1996, 1997), detachment of whole gastrodermal cells (Gates *et al.* 1992), or intracellular degradation (Titlyanov *et al.* 1996). The loss of symbionts renders the coral tissue transparent, exposing the underlying white coral skeleton in a conspicuous phenomenon known as 'coral bleaching' (Figure 1.3).

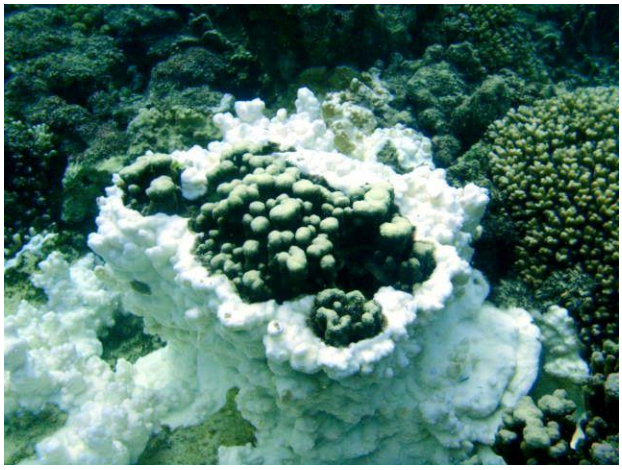

**Figure 1.3 Coral bleaching**
A partially bleached *Porites* colony at Lord Howe Island (Australia). The loss of *Symbiodinium* exposes the underlying coral skeleton, manifesting in a conspicuous white appearance. Bleaching often leads to colony mortality *via* starvation, unless the coral can quickly regenerate its symbiont population (pending subsistence of environmental stress) or compensate by switching to a heterotrophic feeding mode (e.g. Grottoli *et al.* 2006).

Depending on the severity, coral bleaching can result in whole-colony mortality, a process that can occur *en masse* (Hoegh-Guldberg 1999). The frequency and severity of coral bleaching events has increased in recent decades, primarily due to rises in ocean temperatures associated with anthropogenic carbon dioxide emissions. In a particularly severe case, the 1997-1998 El Niño Southern Oscillation (ENSO) caused a devastating bleaching episode that resulted in significant reef declines in all major geographical areas on Earth (Wilkinson *et al.* 1999). As such, coral bleaching has been identified as a key threat to the perpetuity of coral reefs in the 21$^{st}$ century (Hughes *et al.* 2003; Hoegh-Guldberg *et al.* 2007; Pandolfi *et al.* 2011).

While bleaching poses a significant threat to the world's corals, a suite of other impacts also endanger these vulnerable organisms. Episodes of coral disease have increased sharply in recent decades as a consequence of elevated temperature and declining habitat quality (Rosenberg & Ben-Haim 2002; Bruno *et al.* 2007). Ocean acidification arising from the dissolution of anthropogenic $CO_2$ also poses a significant threat to corals, by inhibiting calcification (Orr et al. 2005), and impeding physiological function (Anthony *et al.* 2008). As such, a continued reduction below pH 7.7 will likely initiate major ecosystem transitions at the expense of coral reefs (Fabricius *et al.* 2011; Bell *et al.* 2013). Moreover, ecosystem disruption arising from overfishing and pollution can lead to outbreaks of corallivores such as the crown-of-thorns starfish (*Acanthaster planci*; Brodie *et al.* 2005), and nutrient enrichment from terrestrial runoff and sewage can lower coral performance and fecundity (Tomascik & Sander 1985, 1987a; b). Through the combined assaults of bleaching, disease, ocean acidification, storm damage, overfishing, destructive fishing, predator outbreaks, pollution,

coastal development, and other human impacts, the majority of coral species have recently suffered a sharp increase in extinction risk (Carpenter *et al.* 2008). Concurrently, a prolific research effort has sought to predict the ability of corals to acclimatize and adapt to an environment modified by anthropogenic activity (Hoegh-Guldberg *et al.* 2007).

## 1.5. *Symbiodinium* diversity

### *1.5.1. Genetic diversity*

Members of the genus *Symbiodinium* form symbiosis with a diverse array of marine organisms. These include corals, other cnidarians such as zoanthids, octocorals, jellyfish and sea anemones, and several other phyla, including platyhelminths, molluscs, foraminiferans, ciliates and poriferans (Trench 1993; Rowan 1998; Carlos *et al.* 1999; Pawlowski *et al.* 2001; Lobban *et al.* 2002). These symbiotic dinoflagellates were all formerly considered to represent a single pandemic species (*Symbiodinium microadriaticum*; Freudenthal 1962), a paradigm that was supported by early morphological assessments (Kevin *et al.* 1969; Taylor 1969, 1974). However, different growth rates of homologous and heterologous algae *in situ* (Schoenberg & Trench 1976), and corresponding differences in host performance (Kinzie & Chee 1979) gave credence to the emerging hypothesis that the genus *Symbiodinium* harboured a trove of hidden diversity. This was affirmed by early assessments of genetic distance based on isoenzyme polymorphism (Schoenberg & Trench 1980a), that correlated with subtle differences in size and ultrastructure (Schoenberg & Trench 1980b). A further correlation was shown between symbiont growth rates within the anemone *Aiptasia tagetes* (= *pallida*) and the similarity of isoenzymes to those of the homologous *A. tagetes* symbiont (Schoenberg & Trench 1980c). Following these pioneering studies, assessments of host specificity, morphology, physiology and biochemistry were used to describe three new *Symbiodinium* species (*S. goreauii*, *S. kawagutii* and *S. pilosum*; Trench & Blank 1987). Yet the apparent absence of sexual reproduction hindered formal genetic analysis (Trench 1987). The increased availability of PCR during the early 1990s facilitated the detection of sequence variation in the highly conserved *nr18S* gene (nuclear ribosomal DNA small-subunit or SSU rDNA Rowan & Powers 1991a; b, 1992; McNally *et al.* 1994). The *nr18S* phylogeny was supported by similar topologies obtained from the more rapidly-evolving *nr28S* rDNA region (Wilcox 1998; Pochon *et al.* 2001), and a hyper-variable region within domain V of the plastid-encoded *cp23S* gene (Santos *et al.* 2002). These congruent phylogenetic patterns

enabled the organization of the *Symbiodinium* complex into well-supported clades. The recent discovery of a novel *Symbiodinium* lineage in symbiosis with benthic Foraminifera in Hawaii extends the current phylogeny to nine major taxonomic clades, designated A-I (Pochon & Gates 2010; Figure 1.4). This delineation is supported by genetic distances that approximate order- or even class-level divergence in free-living dinoflagellates and other algae (Blank & Huss 1989; Rowan & Powers 1992), thus effectively invalidating the single-genus classification (Pochon & Gates 2010). However, a general consensus on *Symbiodinium* systematics has yet to be reached, primarily due to the existence of substantial genetic diversity within many of the major taxonomic clades.

Strong purifying selection operates on rDNA coding sequences (CDS) and hence identical or similar sequences may occur among different species (Nei & Rooney 2005). Indeed, the *nr18S* clade-system proposed by Rowan & Powers (1991) appears to grossly underestimate the actual taxonomic diversity within the *Symbiodinium* complex (Sampayo *et al.* 2009; LaJeunesse *et al.* 2010a; LaJeunesse & Thornhill 2011). This limitation has been partially overcome by the development of high-resolution, rapidly evolving genetic markers, including two internal transcribed spacers of the rDNA cistron (*ITS1* and *ITS2*; LaJeunesse 2001, 2002; Rodriguez-Lanetty 2003; Coffroth & Santos 2005). In particular, sequence variation within the *ITS2* region has revealed hundreds of sub-cladal phylotypes, particularly within the highly divergent clade C (Baker 2003; LaJeunesse 2005; Thornhill *et al.* 2013a). Recently, several studies have explored the fine-scale genetic diversity within these *ITS2* phylotypes by analysing polymorphic microsatellite loci and other rapidly evolving genetic regions (Santos *et al.* 2003b; Magalon *et al.* 2006; Thornhill *et al.* 2013a; b, 2009, 2010; Kirk *et al.* 2009; Howells *et al.* 2009, 2013; Andras *et al.* 2011; Pettay *et al.* 2011; Baums *et al.* 2014). These studies show that geographically-defined population structure and host specificity often occur within widely distributed *ITS2* populations, intimating the existence of yet another level of diversity beneath the subclade level.

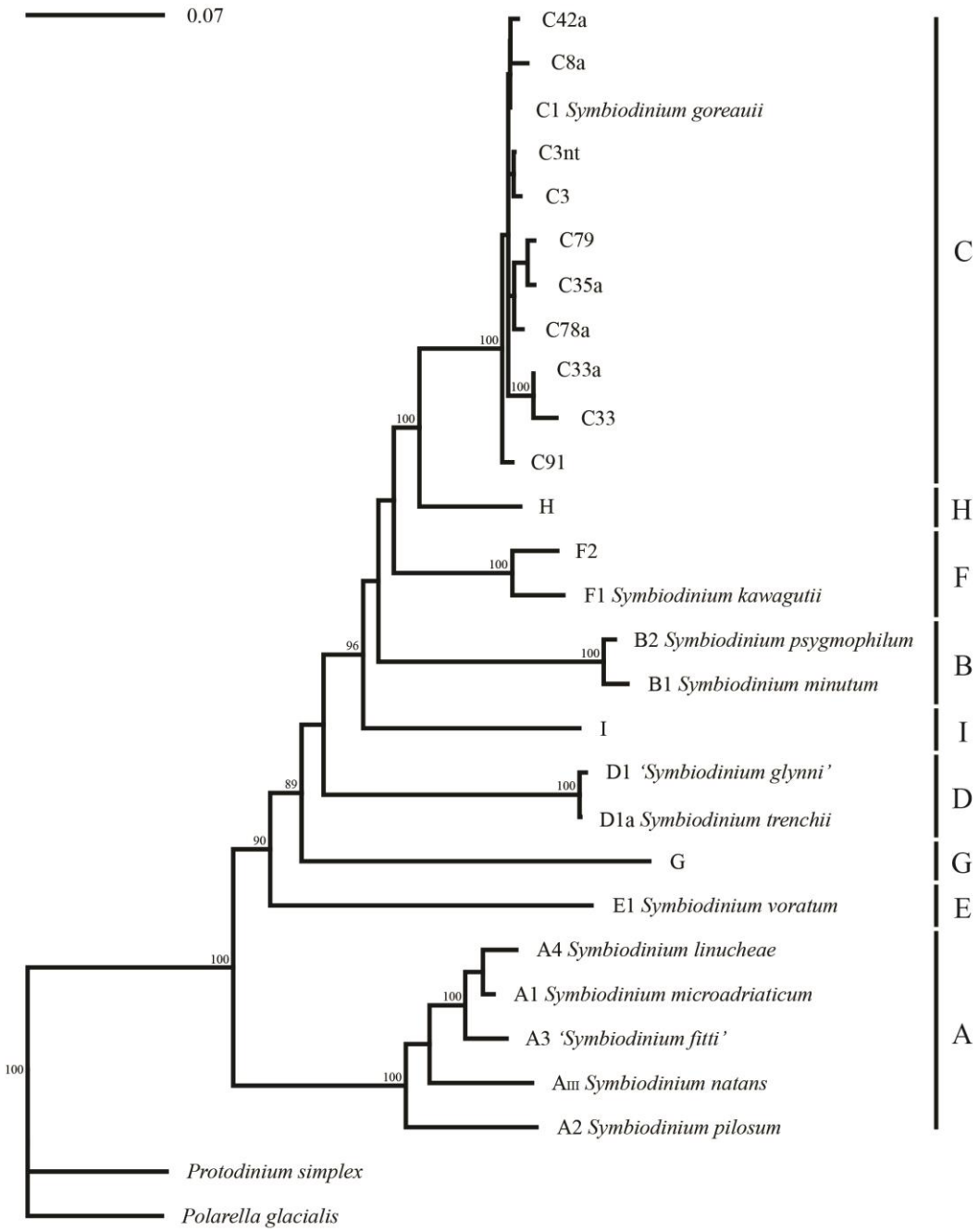


**Figure 1.4 *Symbiodinium* rDNA phylogeny**

Neighbour-joining tree of manually assembled rDNA concatenations of the partial *18S*, complete *ITS1*, *5.8S* and *ITS2*, and the D1-D2 domain of the *28S* large ribosomal subunit gene (maximum 1534 bp), as would be amplified using the primers ITS1CLAMP (LaJeunesse *et al.* 2008) and 28S-reverse (Zardoya *et al.* 1995). The nucleotide alignment and tree were constructed in Geneious v7.0 (Biomatters) using the HKY five-parameter evolutionary model (Hasegawa *et al.* 1985), with *Polarella glacialis* and *Protodinium simplex* as outgroups. The scale bar indicates the number of nucleotide substitutions per sequence position. Numbers at branch nodes are consensus support values (%) with those above 80% included in the figure. Each lineage is labelled using standard alphanumeric nomenclature (LaJeunesse 2001), and species names where applicable. Species in inverted commas lack formal description (*nomen nudum*; see Table 1.2). Large block letters indicate cladal membership (*sensu* Rowan & Powers 1991). See *Appendix A* for Genbank accession numbers of sequences used in rDNA concatenations.

### *1.5.2. Functional diversity*

Divergent evolutionary trajectories have fostered extensive functional variation among many *Symbiodinium* taxa. This is evident in clade- and subclade-specific differences in photochemical efficiency (Savage *et al.* 2002; Rowan 2004; Goulet *et al.* 2005), growth rates (Kinzie *et al.* 2001), host infectivity (Schoenberg & Trench 1980c; Davy *et al.* 1997; Xiang *et al.* 2013; Starzak *et al.* 2014), and in the quantity and quality of photosynthates translocated to the host (Markell & Trench 1993; Loram *et al.* 2007b; Stat *et al.* 2008b; Cantin *et al.* 2009). Physiological and biochemical mechanisms underpinning these functional disparities include differences in chlorophyll distribution among chlorophyll-protein complexes (Iglesias-Prieto & Trench 1997), variation in the regulation of photo-protective compounds (Banaszak *et al.* 2000), and differential lipid saturation in thylakoid membranes (Tchernov *et al.* 2004). The potential for dynamic photo-acclimation also varies between *Symbiodinium* taxa (Chang *et al.* 1983). Disparity in photo-physiological plasticity arises from differences in the regulation of chlorophyll-protein complexes (Iglesias-Prieto & Trench 1994), the cycling of xanthophylls in non-photochemical quenching (Iglesias-Prieto & Trench 1997), and in the ability to repair and/or replace the integral D1 protein of the photosystem II reaction centre (Warner *et al.* 1999; Ragni *et al.* 2010).

While the physiology of the host is important in determining its bleaching susceptibility (e.g. Fitt *et al.* 2009; Wicks *et al.* 2012; Paxton *et al.* 2013; Hawkins *et al.* 2014), the thermal adaptation of the symbiont can mean the difference between coral survival and mortality under stressful conditions (Baker *et al.* 2004; Rowan 2004; Berkelmans & van Oppen 2006; Jones *et al.* 2008; Sampayo *et al.* 2008). Differences in temperature and light optima are evident both between and within clades, and there is a strong correlation between the thermal optimum of the symbiont and that of the host (Iglesias-Prieto & Trench 1997; Warner *et al.* 1999; Savage *et al.* 2002; Rowan 2004; Tchernov *et al.* 2004; Goulet *et al.* 2005; Loram *et al.* 2007b; Sampayo *et al.* 2008; Fisher *et al.* 2011; Howells *et al.* 2011). The most striking example of symbiont thermal adaptation occurs in the *Symbiodinium* clade D species complex (*S. trenchii, S. boreum, S. eurythalpos* and *S. glynni nomen nudum*; LaJeunesse *et al.* 2014). While *S. trenchii* associates with many coral genera (LaJeunesse *et al.* 2009, 2010a), *S. boreum* and *S. eurythalpos* occur exclusively with *Oulastrea crispata* (LaJeunesse *et al.* 2014), and *S. glynni* is found only with *Pocillopora* spp. in the Indo-Pacific region (LaJeunesse *et al.* 2010b; Putnam *et al.* 2012). Despite their ecological differences, these symbionts can all confer a critical measure of thermal tolerance to their hosts under stressful

conditions (LaJeunesse *et al.* 2014). In Guam, *Pocillopora verrucosa* colonies hosting *S. glynni* showed considerably higher photosynthetic efficiency than those hosting clade C at 32 °C, while efficiencies were similar at 28. 5 °C (Rowan 2004). Likewise, colonies of the brain coral *Platygyra verwyei* in close proximity to a hot water discharge from a nuclear power station in Taiwan exclusively harboured *S. trenchii*, with the prevalence of the heat-sensitive C3 gradually increasing with distance from the outlet (Keshavmurthy *et al.* 2012).

While *Symbiodinium* clade D represents a known thermo-tolerant lineage, there is otherwise a general lack of correlation between physiological performance and cladal membership (Savage *et al.* 2002). This is primarily due to the large amount of functional variability within clades, with sub-cladal congeners often showing pronounced differences in stress tolerance. For example, *Stylophora pistillata* colonies on the Great Barrier Reef (GBR) hosting symbiont types C78 or C8a were significantly less prone to thermal bleaching and mortality than those hosting C79 or C35a (Sampayo *et al.* 2008). Differences in thermal optima have even been reported between members of the same subclade. Temperature stress caused photo-damage and host-bleaching in a population of the subclade C1 (= *S. goreauii*) from a relatively cool region of the GBR, while a conspecific population from a warmer habitat remained relatively unaffected (Howells *et al.* 2011). Significant differences in thermal tolerance between minimally divergent populations suggest that functional adaptation may occur on small evolutionary time-scales, providing some optimism for the outlook of coral reefs in a rapidly changing climate (van Oppen *et al.* 2011; Howells *et al.* 2011).

### *1.5.3. Ecological diversity*

The primary axis for niche diversification and speciation in *Symbiodinium* is the host taxon (LaJeunesse 2005). Host-symbiont combinations are conspicuously non-random, reflecting a complex co-evolution driven by cellular recognition and functional adaptation to the distinct, host-specific intracellular habitat (Trench 1997; Thornhill *et al.* 2013a). In a fine-scale genetic study of *Symbiodinium* phylotypes in the Caribbean, 32 out of 35 lineages within the subclade C3 were found to exclusively associate with a single host taxon (Thornhill *et al.* 2013a). Though host-symbiont fidelity appears to be the prevailing condition given current data, the degree of host-specificity can vary widely among symbiont taxa. For example, in a large-scale survey of symbiont diversity within the Indian Ocean, *S. trenchii* associated with

26 out of 58 host genera in Thailand and 11 of 70 genera in Zanzibar (LaJeunesse *et al.* 2010a).

Functional differences between *Symbiodinium* types are also reflected in their spatial distribution patterns (Iglesias-Prieto & Trench 1994, 1997; Toller *et al.* 2001a). Environmental niche partitioning represents a secondary axis of diversification, and has been reported over latitudinal gradients (Loh *et al.* 2001; Rodriguez-Lanetty *et al.* 2001; Macdonald *et al.* 2008), between temperature microhabitats on a reef (Oliver & Palumbi 2011; Keshavmurthy *et al.* 2012), over different depth ranges (Rowan *et al.* 1997; Iglesias-Prieto *et al.* 2004; Sampayo *et al.* 2007; Frade *et al.* 2008), and between sites featuring distinct turbulence regimes (Ulstrup & van Oppen 2003). The irradiance microhabitat even explains the vertical zonation of symbiont taxa within some individual coral colonies (Rowan & Knowlton 1995; Rowan *et al.* 1997; van Oppen *et al.* 2001). However, *S. trenchii* again provides an exception to this general rule, showing a wide distribution across all major geographic regions (LaJeunesse *et al.* 2010a).

The lack of conformity by *S. trenchii* and other types to a single host taxon or habitat type can be explained by invoking the equilibrium-opportunist continuum as a third axis of diversification. Niche partitioning over both host-taxon and geographic/environmental axes is commonly observed in specialized types that show traits consistent with an 'equilibrium' life history. In particular, many phylotypes within *Symbiodinium* clade C exclusively associate with a single, vertically transmitting host species (LaJeunesse *et al.* 2003; Sampayo *et al.* 2007; Thornhill *et al.* 2013a). The resulting coevolution fosters a productive mutualism, characterized by highly beneficial nutritional reciprocity between symbiotic partners (Stat *et al.* 2008b; Cantin *et al.* 2009). Equilibrium taxa typically show a low affinity for physiological stress (Jones *et al.* 2008), and thus distribute within a narrowly defined habitat. On the other hand, 'opportunistic' types such as *S. trenchii* and *S. minutum* associate with multiple host taxa, exhibit a high tolerance of physiological stress, and show a widespread but patchy distribution (Toller *et al.* 2001b; LaJeunesse 2005; Stat *et al.* 2008b; LaJeunesse *et al.* 2009, 2010a). A trait commonly associated with an opportunistic life history involves a reduction in nutritional value to the host (Cantin *et al.* 2009), sometimes to the point of marginal mutualism (Stat *et al.* 2008b). The disturbance created by bleaching and disease can facilitate 'outbreaks' by opportunistic symbionts, leading to conspicuous shifts in dominance across the reef (Baker *et al.* 2004; LaJeunesse *et al.* 2009, 2010b; Correa & Baker 2011). This is generally a transient state, with return of conditions to pre-stress levels facilitating the

succession of equilibrium taxa (Thornhill *et al.* 2006b; Jones *et al.* 2008; LaJeunesse *et al.* 2009, 2010b).

## 1.6. *Symbiodinium* systematics

### *1.6.1. Assigning species nomenclature*

The *Symbiodinium* genus clearly represents a genetically, functionally and ecologically diverse complex. Assigning binomial species nomenclature to the many different 'types' is an important endeavour for comparing, aligning and integrating global research efforts, and evaluating conservation status (Green 2005). Yet efforts to formally describe *Symbiodinium* species are hampered by morphological similarities between divergent phylotypes, and their primarily asexual mode of reproduction (Sampayo *et al.* 2009; Stat *et al.* 2012; LaJeunesse *et al.* 2012). Alternatives to the classic biological species concept (also known as the isolation species concept; Mayr 1942, 1963) such as the ecological species concept (ESC; van Valen 1976; Andersson 1990) and the cohesion species concept (CSC; Templeton 1989) provide suitable criteria by which to delineate *Symbiodinium* species (Correa & Baker 2009; Thornhill *et al.* 2013a). Both provide faculty for clonal or predominantly clonal lineages, whose species candidacy cannot be assessed on the basis of reproductive isolation (Mayr 1999). However, the delineation of species boundaries using both sets of criteria hinge on building well-supported phylogenetic trees based on molecular sequence data.

### *1.6.2. The internal transcribed spacer 2 (*ITS2*)*

The *ITS2* has emerged as the most extensively utilised marker for resolving fine-scale *Symbiodinium* systematics (Franklin *et al.* 2012; Tonk *et al.* 2013), and can provide taxonomic resolution roughly corresponding to the species level (LaJeunesse 2001). This marker can be used in conjunction with denaturing gradient gel electrophoresis (DGGE) to provide a relatively fast, cost-effective and reproducible means of establishing the dominant *Symbiodinium* phylotype(s) within a coral colony (LaJeunesse & Trench 2000; LaJeunesse 2001, 2002). However, *ITS2* sequence diversity may not always provide an accurate reflection of species diversity. Sequence variation in the *ITS2* region may provide a level of resolution that is too coarse to distinguish species within the more derived *Symbiodinium*

lineages such as C1 and C3, necessitating the use of more rapidly evolving markers (Thornhill *et al.* 2013a). In other lineages, phylogenetic inference based on *ITS2* variation can result in inflated diversity estimates. For example, Litaker *et al.* (2007) showed that inter-genomic *ITS* sequence variation occurs within several well-defined species of free-living dinoflagellates. A cluster-based approach has been proposed to control for diversity inflation in *Symbiodinium* (Correa & Baker 2009); yet this method merely highlights groups of *ITS2* phylotypes that require further genetic, physiological and ecological analysis (Stat *et al.* 2012).

The multiple-copy nature of rDNA imposes a further limitation on the phylogenetic utility of the *ITS2*. rDNA genes in dinoflagellates (and most other eukaryotes) are arranged in extensive tandem arrays (Hackett *et al.* 2004; Zhang *et al.* 2006; Figure 1.5a), with some free-living species hosting chromosomes almost entirely composed of rRNA repeats (Figueroa *et al.* 2014). A mutation occurring within an rDNA repeat may be eliminated, or promoted to fixation throughout the genome *via* stochastic DNA repair/replication processes that stimulate gene conversion or duplication/deletion. These processes include unequal crossover during meiosis (Figure 1.5b), transposition, retrotransposition, slipped-strand mispairing and intra-strand exchange within and between chromatids (reviewed in Nei & Rooney 2005). The effect of these processes is to homogenize intra-genomic sequence variation and cause repetitive genetic elements to evolve in concert ('concerted evolution'; Brown *et al.* 1972; Arnheim *et al.* 1980; Figure 1.5c) While concerted evolution acts to eliminate intra-genomic sequence variation, mutations continuously arise during DNA replication and repair (paralogs; Hou & Lin 2009). It may take many generations for a mutated rDNA copy to be eliminated from the genome or to reach fixation, particularly if ribosome-coding genes occupy chromosomal positions near the centromere (Cronn *et al.* 1996). Hence a non-diagnostic polymorphism (NDP) may remain within a lineage for extended periods of evolutionary time (Álvarez & Wendel 2003). The intra-genomic persistence of NDPs can yield false diversity signals and lead to incorrect phylogenetic inference, particularly when detected in plasmid cloning assays of bulk-cell *Symbiodinium* samples (van Oppen & Gates 2006; LaJeunesse & Pinzón 2007; Thornhill *et al.* 2007; Miranda *et al.* 2012). Single-cell PCR (scPCR) offers a solution, controlling for inflated diversity estimates and providing increased accuracy in phylogenetic reconstruction (Miranda *et al.* 2012). However, the difficult and time-consuming nature of this technique has prevented its widespread utility in *Symbiodinium* systematics.

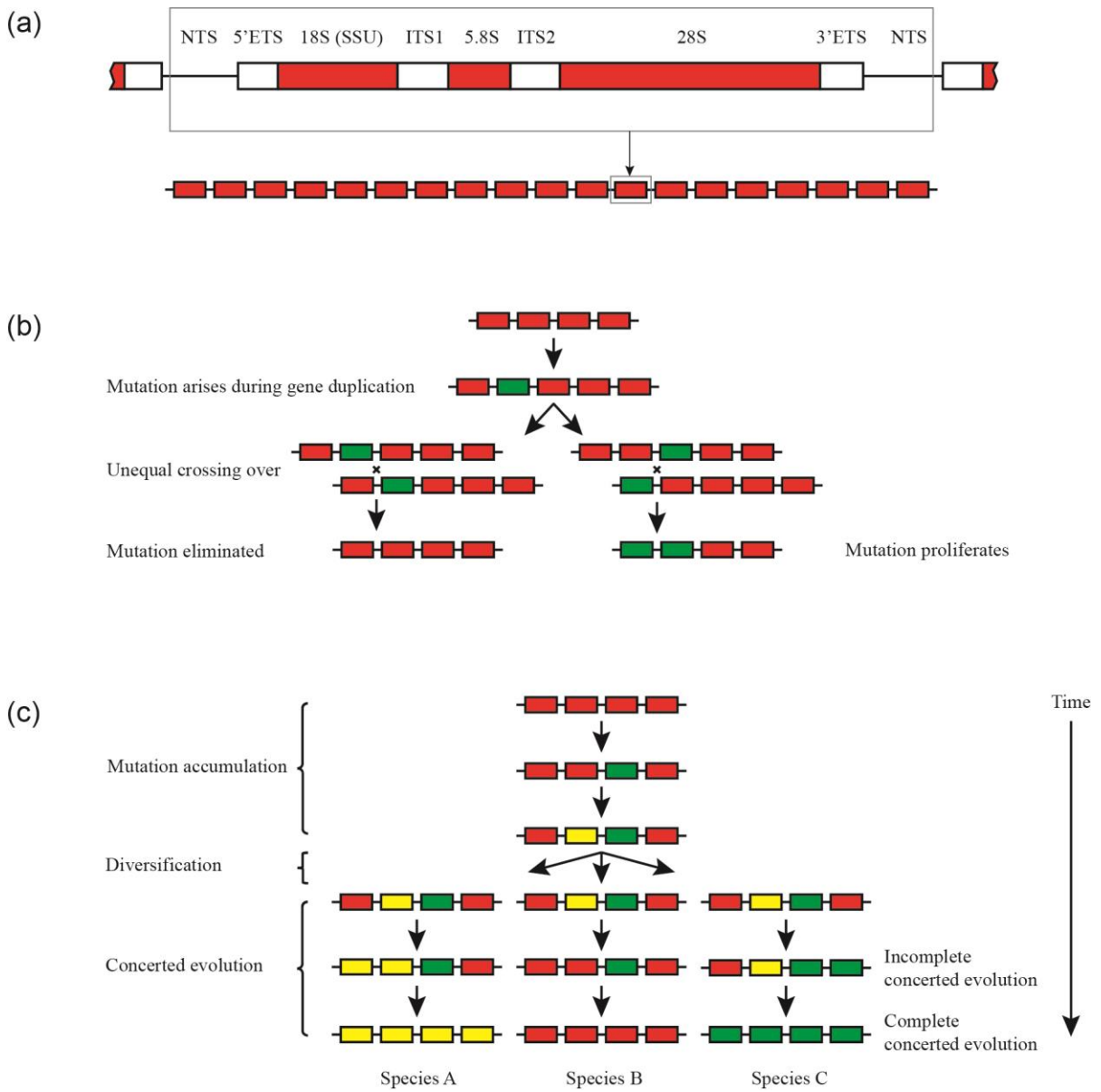


**Figure 1.5 Concerted evolution of rDNA in the nuclear genome**

The eukaryote nuclear genome contains rDNA genes in tandem arrays (a), with copy numbers ranging from less than 100 to several hundred thousand. Each rDNA repeat comprises two external transcribed spacers (5'*ETS* and 3'*ETS*), a small subunit gene (SSU; *18S*), two internal transcribed spacers (*ITS1* and *ITS2*), and the *5.8S* and *28S* genes that collectively code for the large ribosomal subunit (LSU). Each tandem repeat is separated from its neighbour by a non-transcribed spacer (*NTS*). A mutation may occur in an rDNA repeat during gene duplication or repair (b; mutated copy shown in green), and the resulting polymorphism may either dissipate from the genome or ascend to fixation through concerted evolutionary processes such as unequal crossing-over during meiosis. Concerted evolution can take many generations to homogenize all copies within the genome (c; polymorphic copies shown in different colours). When concerted evolution is complete, rDNA arrays are useful for inferring phylogenetic relationships; however when arrays are in a state of incomplete homogenization (e.g. following divergence or hybridization), rDNA markers can yield ambiguous sequence reads, inflated diversity estimates and incorrect phylogenies (Buckler *et al.* 1997; Álvarez & Wendel 2003).

### *1.6.3. Alternative genetic markers*

The limitations accompanying the use of the *ITS2* for phylogenetic inference have prompted assessments of several alternative candidate markers. Yet each has their drawbacks and a general consensus on a benchmark 'species' level marker for *Symbiodinium* has yet to be reached. The nuclear-encoded *actin* gene provides an acceptable level of resolution (Pochon *et al.* 2012) and has seen limited utility (Mieog *et al.* 2009; Cunning *et al.* 2013; Cunning & Baker 2013); however it occurs in multiple copies and appears to follow the 'birth and death' model of evolution, thus facilitating the accumulation of intra-genomic variation arising from the degeneration of pseudo-genes (Kim *et al.* 2011). Indeed, 10 of the 46 *actin* genes in the genome of the free-living dinoflagellate *Amphidinium carterae* were identified as pseudo-genes (Bachvaroff & Place 2008). Despite this, the *actin* copy number is suitably low in *Symbiodinium*, estimated at 7 in clade C and just a single copy in clade D (Mieog *et al.* 2009). This is considerably lower than the *ITS2*, which numbers in the hundreds to tens of thousands of copies per *Symbiodinium* genome (Mieog *et al.* 2009). Length heteroplasmy in a hyper-variable area of domain V in the *cp23S* plastid rDNA can be assessed using poly-acrylamide gel electrophoresis (PAGE) to rapidly identify dominant and coexisting symbiont types at the sub-cladal level (Santos *et al.* 2003a). However, while useful in screening taxa within clades A and B, this technique is not sufficiently sensitive to resolve the more recently-diverged members of clade C (Sampayo *et al.* 2009). Alternatively, the non-coding region of the plastid-encoded photosystem II D1 protein gene (*psbA*$^{ncr}$) can show substantially higher rates of divergence than either the *ITS2* or the *cp23S* (Thornhill *et al.* 2013a), while generally maintaining low copy numbers (but see Koumandou & Howe 2007) and similarly low intra-genomic variation (Moore 2003; LaJeunesse & Thornhill 2011). However, universal *Symbiodinium* primers are not available for *psbA*$^{ncr}$, and hence specific primers must be tailored for individual clades. Microsatellite flanking regions such as *Sym15* and *Si4.86* also show high sensitivity and have the added advantage of occurring in a single-copy per genome (Santos *et al.* 2004; Pettay & LaJeunesse 2007). By targeting these markers, Finney *et al.* (2010) showed that the *ITS2* lineage B1 (or *cp23S* lineage B184) consists of a diverse assemblage of putative species. Yet similar to the *psbA*$^{ncr}$, all microsatellite flanking regions characterized to date require primers that are clade- or even subclade-specific. The mitochondrial-encoded (mtDNA) cytochrome oxidase genes *cob* (Zhang *et al.* 2005) and *coI* (or *cox1*; Takabayashi *et al.* 2004) have also been used in *Symbiodinium* systematics. A large and expanding dataset of *coI* sequences is available through the 'barcode of life' project

(www.barcoding.si.edu), making this marker particularly appealing (Stern *et al.* 2010). However, mtDNA genes tend to be highly conserved in dinoflagellates, obscuring fine-scale diversity (Takabayashi *et al.* 2004; Zhang *et al.* 2005; Sampayo *et al.* 2009; Pochon *et al.* 2014).

### *1.6.4. A consensus on* Symbiodinium *systematics?*

Despite promising progress in the development of alternative markers, the rDNA cistron remains the benchmark for *Symbiodinium* systematics. In a recent evaluation of candidate markers, the *Symbiodinium* rDNA phylogeny resolved that of the combined multi-gene concatenation better than any of the plastid or mitochondrial genes assessed (*cp23S*, *psbA*$^{ncr}$, *coI* and *cob*; Pochon *et al.* 2014). This may reflect well-documented errors in organelle phylogenies that arise from lineage sorting, organelle capture and hybridization (Rieseberg & Soltis 1991; Rieseberg *et al.* 1996; Tsitrone *et al.* 2003). For these and other reasons, the 'barcode of life' consortium recommends that rDNA markers are more appropriate than mtDNA or chloroplast DNA (cpDNA) for systematic barcoding in protists (Pawlowski *et al.* 2012).

In practice, the most suitable gene(s) to target depends on the taxonomic question being addressed (Pochon *et al.* 2012, 2014). To formally describe *Symbiodinium* species, an agreeing phylogenetic topology from a combination of coding and non-coding nuclear, mitochondrial, and chloroplast sequences, as well as corroborative morphological, physiological and ecological data are necessary (Sampayo *et al.* 2009; LaJeunesse *et al.* 2012).To date, twelve *Symbiodinium* species have been described (Table 1.1) and a further five have been assigned tentative species names (*nomena nuda*; Table 1.2). Yet the vast majority of diversity within this genus awaits taxonomic description (LaJeunesse *et al.* 2012). Several recent advances in molecular methodology facilitate progress in this area. These include the assembly and public availability of the *Symbiodinium* nuclear and plastid genomes (Shoguchi *et al.* 2013; Barbrook *et al.* 2014), the increased accessibility and utility of high-throughput sequencing platforms (Quigley *et al.* 2014; Thomas *et al.* 2014), and the centralization of multi-gene sequence data within comprehensive databases (Franklin *et al.* 2012; Tonk *et al.* 2013). Such developments will likely be of considerable benefit in the effort to characterize new molecular markers, assign species nomenclature, establish diversity estimates, and reconstruct the evolutionary history of the *Symbiodinium* complex.

**Table 1.1 List of formally described *Symbiodinium* species**

| Species name | Synonyms | *ITS2* type | Host (holotype) | Reference |
|---|---|---|---|---|
| ***Symbiodinium boreum*** | | D15 | *Oulastrea crispata* | (LaJeunesse *et al.* 2014) |
| ***Symbiodinium eurythalpos*** | | D8, D8-12, D12-13, D13 | *Oulastrea crispata* | (LaJeunesse *et al.* 2014) |
| ***Symbiodinium goreauii*** | *S. goreaui* | C1 | *Ragactis lucida* | (Trench & Blank 1987; Trench 2000) |
| ***Symbiodinium kawagutii*** | | F1 | *Montipora verrucosa* | (Trench & Blank 1987; Trench 2000) |
| ***Symbiodinium linucheae*** | *Gymnodinium linucheae* | A4 | *Linuche unguiculata* | (Trench & Thinh 1995) |
| ***Symbiodinium microadriaticum*** | | A1 | *Cassiopeia xamachana* | (Freudenthal 1962) |
| ***Symbiodinium minutum*** | | B1 | *Aiptasia* sp. | (LaJeunesse *et al.* 2012) |
| ***Symbiodinium natans*** | | A | Free-living (Tenerife) | (Hansen & Daugbjerg 2009) |
| ***Symbiodinium pilosum*** | *S. meandrinae, S. corculorum* | A2 | *Zoanthus sociatus** | (Trench & Blank 1987; Trench 2000) |
| ***Symbiodinium psygmophilum*** | | B2 | *Oculina diffusa* | (LaJeunesse *et al.* 2012) |
| ***Symbiodinium trenchii*** | *S. trenchi* | D1a | Unspecified | (LaJeunesse *et al.* 2014) |
| ***Symbiodinium voratum*** | *S. californium, S. varians* | E1 | Free-living (South Korea) | (Jeong *et al.* 2014) |

*This holotype may not represent the dominant symbiont of *Z. sociatus*, since *S. pilosum* is not known to form endosymbiosis with other cnidarians (LaJeunesse 2002) and free-living types are known to out-compete and over-grow symbiotic strains in culture (Santos *et al.* 2001).

**Table 1.2 List of *Symbiodinium* species lacking formal description (*nomen nudum*)**

| Species name | Synonyms | *ITS2* type | Host | Reference |
|---|---|---|---|---|
| ***Symbiodinium bermudense*** | *S. pulchrorum* | B1 | *Aiptasia pallida, A. pulchella* | (Banaszak *et al.* 1993) |
| ***Symbiodinium cariborum*** | *S. microadriaticum* subsp. *Condylactis* | A1.1 | *Condylactis gigantea* | (Blank & Huss 1989; Banaszak *et al.* 1993) |
| ***Symbiodinium fitti*** | | A3 | *Acropora* spp., *Tridacna* spp. | (Pinzón *et al.* 2011) |
| ***Symbiodinium glynni*** | | D1 | *Pocillopora* spp. | (LaJeunesse *et al.* 2010b) |
| ***Symbiodinium muscatineii*** | *S. muscatinei* | B4 | *Anthopleura elegantissima* | (LaJeunesse & Trench 2000) |

## 1.7. Coral-symbiont adaptation and acclimatization

### *1.7.1. 'Adaptive' bleaching*

The realization that genetic, functional and ecological diversity exists within the *Symbiodinium* complex prompted the formulation of the somewhat contentious 'adaptive bleaching hypothesis' (ABH; Buddemeier & Fautin 1993). The ABH postulated that, rather than representing an ominous threat to coral reefs, bleaching might serve as an adaptive mechanism by which corals could survive periods of climatic upheaval. According to the ABH, coral bleaching "provides an opportunity for the host to be repopulated by a different type of partner", and altered environmental conditions "favour establishment of combinations of symbionts that were less adaptive under previous conditions" (Buddemeier & Fautin 1993). A central assumption of the ABH in its original form was that established coral colonies can switch to a new symbiont phylotype obtained from an environmental source population (Kinzie *et al.* 2001). 'Symbiont switching' (Figure 1.6a) has been induced in the laboratory in anemones, octocorals and scleractinians (e.g. Schoenberg & Trench 1980; Davy *et al.* 1997; Kinzie *et al.* 2001; Lewis & Coffroth 2004; Coffroth *et al.* 2010). However, the experimentally manipulated host-symbiont associations in corals are generally transient, reverting to the original combination over time (Coffroth *et al.* 2010). Furthermore, there remains no evidence that a novel symbiont can colonize and ascend to dominance within a coral after a natural bleaching event. A post-bleaching change in dominant symbiont was reported as evidence of 'adaptive bleaching' in transplanted coral colonies (Baker 2001); however this interpretation drew criticism. In particular, Hoegh-Guldberg *et al.* (2002) pointed out that Baker had not shown evidence of adaptation, but rather an acclimatization mechanism, one of many that corals have at their disposal to cope with environmental stress (e.g. Falkowski & Dubinsky 1981; Palumbi *et al.* 2014). Fautin & Buddemeier (2004) provided semantic clarification stating that 'adaptation' was intended in the English sense, defined as "modification of an organism or its parts in a way that makes it more fit for existence under the conditions of its environment", thereby extending its definition to include acclimation and acclimatization (note that this definition differs fundamentally from that used in evolutionary biology, in which adaptive modification is heritable, and therefore genetically encoded; Dobzhansky 1968). The concept of adaptive bleaching was thus generalized to include an acclimatory change in the relative proportion of pre-existing types (i.e. 'symbiont shuffling'; Figure 1.6b and c), and extended to encompass the entire continuum from

catastrophic bleaching to visually undetectable symbiont turnover (Fautin & Buddemeier 2004).

### *1.7.2. Mixed symbiont populations and symbiont shuffling*

Until recently, mixed *Symbiodinium* infections were thought to occur in only a minority of coral species (Diekmann *et al.* 2002; Goulet 2006). However, modern ultra-sensitive molecular techniques such as qPCR, fluorescence *in situ* hybridization (FISH) and next generation sequencing (NGS) increasingly reveal cryptic symbiont populations (Baker & Romanski 2007; Loram *et al.* 2007a; Mieog *et al.* 2007; Correa *et al.* 2009; Silverstein *et al.* 2012; Quigley *et al.* 2014; Thomas *et al.* 2014). For example, Silverstein *et al.* (2012) surveyed the symbiont consortia of 39 coral species (including 26 'symbiont specialists') using a clade-specific qPCR assay, and found representatives from all species that hosted at least two *Symbiodinium* clades. Within-colony symbiont diversity remains particularly unexplored in Indo-Pacific corals, many of which simultaneously host multiple, closely related types within clade C (Baker 2003; LaJeunesse *et al.* 2004; LaJeunesse 2005; Baker & Romanski 2007; Stat *et al.* 2011).

Theoretical virulence models predict that mixed symbiont infections should be less mutualistic than monoclonal populations, due to the tendency of related symbionts to compete for host resources (van Baalen & Sabelis 1995; Frank 1996b). Yet there remains no evidence of direct antagonism between symbionts within a cnidarian host (Dunn & Weis 2009). Furthermore, if mixed infections promote symbiotic disruption, selection should favour vertical transmission (Douglas 1998), whereas only around 15-30% of coral species transmit symbionts from parent to offspring (Fadlallah 1983; Harrison & Wallace 1990; Richmond & Hunter 1990; Baird *et al.* 2009). Moreover, the limited empirical evidence specifically addressing symbiont competition in cnidarians suggests that mixed infection is not synonymous with symbiotic disruption. In a study tracking the fate of photosynthetically fixed carbon in the giant sea anemone *Condylactis gigantea*, Loram *et al.* (2007b) showed that the amount of translocated photosynthate was simply an additive function of the specific productivity and relative abundance of each of the types present (*Symbiodinium* clades A and B), indicating that their coexistence did not have negative implications for the host. Symbiont competition therefore appears to be predominantly or exclusively under the auspices of host-regulation. This control may be exerted through symbiont compartmentalisation (Correa &

Baker 2011), within-colony niche partitioning (Rowan & Knowlton 1995; Rowan *et al.* 1997), and/or the regulation of symbiont biomass *via* selective expulsion/degradation, nutrient limitation and chemical signalling (see Davy *et al.* 2012 for a review). The persistence of mixed infections despite host regulation suggests that, rather than promoting virulence, this condition may actually confer a selective advantage under certain conditions.

Mixed symbiont infections may benefit the host by providing an 'insurance policy' (*sensu* Yachi & Loreau 1999), conferring resilience against abiotic stress by increasing the capacity to maintain function in the face of environmental change (Nyström 2006). If the dominant symbiont is suddenly rendered ill-adapted to a modified environment, a cryptic, more suitably-adapted type may take its place, thus enabling the host to survive (Baker 2003). Dominance shifts have been well-documented within the symbiont consortia of corals and anemones following changes in their environment (Rowan *et al.* 1997; Baker 2001; Toller *et al.* 2001b; Chen *et al.* 2005; Berkelmans & van Oppen 2006; Thornhill *et al.* 2006b; Jones *et al.* 2008; Sampayo *et al.* 2008; Venn *et al.* 2008; Jones & Berkelmans 2010). In the majority of cases, a symbiont change was stimulated by bleaching, with the disturbance facilitating the proliferation of a previously cryptic population (Figure 1.6b). For example, Berkelmans & van Oppen (2006) transplanted colonies of *Acropora millepora* to an area featuring a higher average temperature, and observed a post-bleaching change in the dominant symbiont type from the naturally present clade C in favour of clade D. Repopulation by *Symbiodinium* D conferred a 1-1.5 °C increase in heat tolerance, and enabled affected colonies to survive the disturbance (Berkelmans & van Oppen 2006).

Though not as well-characterized as bleaching-induced symbiont shuffling, changes within the symbiont consortium can also occur in the absence of bleaching (dynamic symbiont shuffling; Figure 1.6c). In this case, succession occurs through gradual symbiont turnover, effected by differential elimination and regeneration (Yamashita *et al.* 2010). In many horizontal-transmitting species, symbiont succession is evident during the early stages of ontogeny, prior to the establishment of more stringent symbiont-specificity (Coffroth *et al.* 2001; Little *et al.* 2004). Dynamic symbiont shuffling also occurs in disease-affected adult corals, possibly arising from compromised immunity (Toller *et al.* 2001b), and in healthy adults in response to natural environmental variation (Chen *et al.* 2005; Venn *et al.* 2008).

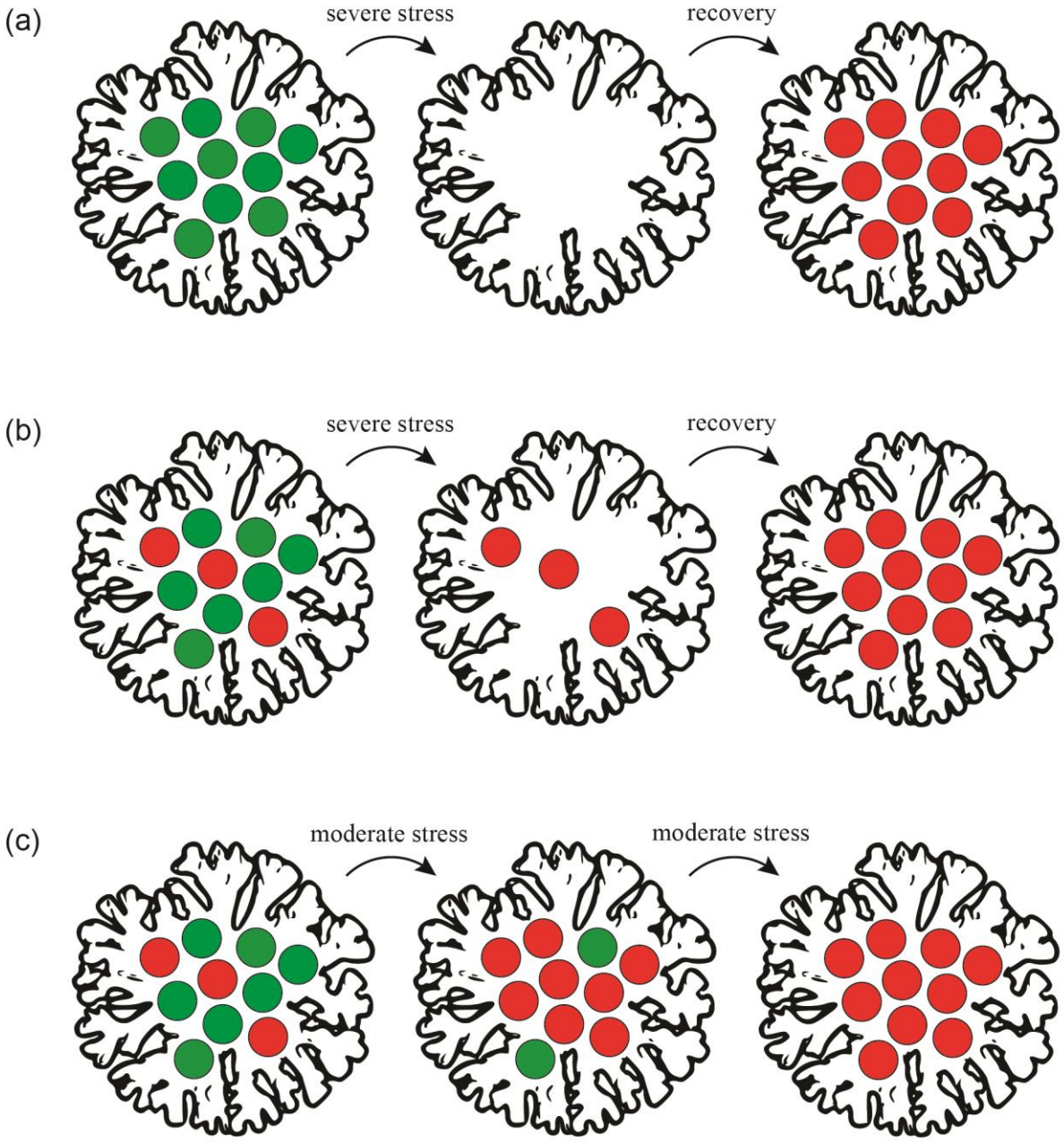


**Figure 1.6 Symbiont switching and shuffling**
A change in symbiont dominance within a coral colony from a heat-sensitive type (green) to a heat tolerant type (red) can occur *via* (a) a switch to a new symbiont from an environmental source population following bleaching-related disturbance; (b) the post-bleaching proliferation of a residual, thermally tolerant type (bleaching-induced symbiont shuffling); or (c) gradual symbiont turnover in response to environmental change (dynamic symbiont shuffling). Symbiont 'switching' has not been documented in the natural environment.

While symbiont shuffling appears to offer improved host benefit relative to symbiont switching, optimistic predictions for corals in the face of warming temperatures are accompanied by several major caveats. First, similar to symbiont switching, host-symbiont associations modified by symbiont shuffling appear to be transient, and long-term follow up studies generally reveal post-bleaching reversion (Thornhill *et al.* 2006b; Jones *et al.* 2008; LaJeunesse *et al.* 2009; but see Sampayo *et al.* 2008). Second, symbiont shuffling may involve severe physiological trade-offs for the host. Opportunistic symbionts that proliferate within the tissue of corals after bleaching may offer comparatively less nutritional value (Stat *et al.* 2008b; Cantin *et al.* 2009), resulting in slower coral growth rates (Little *et al.* 2004; Jones & Berkelmans 2010) and increased susceptibility to disease (Stat *et al.* 2008b). Surviving corals may therefore suffer drastic reductions in fecundity, and take many years to fully recover (Hoegh-Guldberg 1999). Third, it is not known how many coral species are able to 'shuffle' symbionts. While the symbiont consortium is dynamic in some species, host-symbiont co-evolution has fostered rigid fidelity in others (Stat *et al.* 2006; Putnam *et al.* 2012). This is evident in several fine-scale population studies that reveal the multi-year persistence of a single clonal genotype within individual colonies (Goulet & Coffroth 2003a; Kirk *et al.* 2005; Thornhill *et al.* 2006a, 2009; Andras *et al.* 2011; Pettay *et al.* 2011). In particular, vertical-transmitting species characteristically show a reduced affinity for symbiont shuffling (Thornhill *et al.* 2006a). This is highlighted by the disproportionate number of studies reporting symbiont shuffling in horizontal-transmitting species (Rowan *et al.* 1997; Coffroth *et al.* 2001; Baker 2001; Toller *et al.* 2001b; Little *et al.* 2004; Chen *et al.* 2005; Berkelmans & van Oppen 2006; Thornhill *et al.* 2006b, 2009; Jones *et al.* 2008; Venn *et al.* 2008; Jones & Berkelmans 2010; but see Sampayo *et al.* 2008). Symbionts are vertically-transmitted in around 15-30% of scleractinian coral species (Baird *et al.* 2009), suggesting that symbiont shuffling may not be a universally available acclimatory mechanism. Finally, symbiont shuffling appears to offer a maximum increase in thermal tolerance of around 1-1.5 °C (Berkelmans & van Oppen 2006). Given that recent model simulations predict a 1.5-3 °C increase by the year 2050 (Kirtman *et al.* 2013), symbiont shuffling will unlikely mitigate the environmental stress that corals are expected to face in the near future. Therefore, while 'adaptive bleaching' *sensu lato* has provided a source of optimism for the outlook of corals in the face of warming ocean temperatures (Baker 2001; Fautin & Buddemeier 2004; Berkelmans & van Oppen 2006), the persistence of corals in a changing climate will ultimately depend on the ability of both symbiotic partners to acquire functional adaptations to cope with abiotic stress. A shift in focus towards evolutionary

adaptation *sensu stricto* is clearly necessary if we are to gain a realistic insight into the future of coral reefs.

## 1.8. *Symbiodinium* evolution

### *1.8.1. Asexual reproduction in* Symbiodinium

The classic model of *Symbiodinium* evolution depicts an asexual, permanent haploid lineage that diversifies through host-specialization and geographic isolation (LaJeunesse 2005). Genetic variation accumulates through somatic mutation, and similar to asexual prokaryotic lineages, evolution is characterised by punctuated speciation events and 'selective sweeps'(LaJeunesse 2005; Correa & Baker 2009). This is consistent with theoretical models that predict a higher affinity for asexual reproduction in mutualistic symbionts than in pathogens, whose inclination towards sexual reproduction is driven by a continuous evolutionary 'arms race' with their hosts (Law & Lewis 1983; Maynard Smith 1998). The proposed loss of sexual reproduction in *Symbiodinium* has led some authors to conclude that the evolutionary responsiveness within this lineage is likely minor (Buddemeier & Fautin 1993). However, the short generation times observed in symbiosis (Wilkerson *et al.* 1988) and the high frequency at which somatic mutations occur (van Oppen *et al.* 2011) suggest that rapid adaptation could occur during periods of environmental change. This is exemplified by the free-living asexual dinoflagellate *Prorocentrum triestinum*, in which somatic mutations alone conferred a 5 °C increase in thermal tolerance within around 400 generations (Flores-Moya *et al.* 2008).

While somatic mutations could explain the broad genetic and functional diversity within the *Symbiodinium* complex, exclusive clonality presents a paradox when one considers the long evolutionary persistence of this lineage (over 50 million years; Tchernov *et al.* 2004). With very few exceptions (e.g. bdelloid rotifers, darwinuloid ostracods and arbuscular mycorrhizal fungi), the loss of sexual reproduction condemns lineages to early extinction (Judson & Normark 1996). Muller's ratchet dictates that the gradual, irreversible accumulation of deleterious somatic mutations (genetic load) in an asexual population inevitably leads to the erosion of mean fitness over time (Felsenstein 1974). Genetic information is eventually lost through stochastic genetic drift, and high-fitness genotypes are successively replaced by deleterious mutants (Crow 1994). It is thought that mutation accumulation can only truly be

overcome by meiotic recombination, explaining the persistence of sexual reproduction despite its high cost in comparison to clonality (Muller 1964). Haploidy can lessen the speed of the ratchet since the mutation rate within the genome is effectively halved and deleterious alleles are always expressed (and hence exposed to stronger selection). However, haploids are not immune to 'ratchet clicks', even when population sizes are large (Gordo & Charlesworth 2000). Highly efficient DNA repair mechanisms in some asexual lineages have been implicated in reducing genetic load (Schön & Martens 1998). In particular, ameiotic recombination *via* reciprocal crossover or non-reciprocal gene conversion can reduce the accumulation of deleterious alleles in asexual diploid crustaceans (*Daphnia* spp.; Omilian *et al.* 2006) and tetraploid rotifers (*Adienta vaga*; Flot *et al.* 2013). Yet in the absence of homologous chromosomes to use as templates for gene-conversion, how has genetic load not led to the extinction of the haploid, asexual *Symbiodinium* lineage?

### *1.8.2. Sexual reproduction in* Symbiodinium

In his initial species description of *Symbiodinium microadriaticum*, Freudenthal (1962) reported putative cysts with developing stages resembling isogametes. Small zoospores resembling gametes were also observed by Taylor (1973, 1974), and Schoenberg & Trench (1980a), but the critical processes of fusion and recombination remained elusive. These observations, in addition to their own, led Fitt & Trench (1983) to form the hypothesis that the *Symbiodinium* life cycle includes a sexual stage. Specifically, their hypothesis suggested that haploid zoospores fuse and undergo plasmogamy to form a transient diploid zygote, which then undergoes meiosis to restore the haploid condition (i.e. a haplontic life cycle; Figure 1.7). This is consistent with the majority of free-living dinoflagellates, nearly all of which are haplontic (Pfiester & Anderson 1987; Pfiester 1989; Elbrächter 2003).

The initial molecular evidence that *Symbiodinium* undergoes cryptic meiotic recombination came from isoenzyme analyses. Incongruence between isoenzyme phylogenies and those constructed from both RAPD (Baillie *et al.* 1998, 2000) and *ITS2* sequence variation (LaJeunesse 2001) implicated allelic recombination, consistent with criteria outlined to distinguish between clonal and sexual eukaryote populations (Tibayrenc *et al.* 1991). More recently, meiotic recombination has been inferred from linkage disequilibrium between microsatellite loci (Santos *et al.* 2003b; Pettay *et al.* 2011; Thornhill *et al.* 2013a; LaJeunesse *et al.* 2014; Baums *et al.* 2014), indicating that extensive shuffling of alleles has occurred

within several *Symbiodinium* lineages. Additionally, a recent meta-genomic analysis revealed the presence of six meiosis-specific and 25 meiosis-related functional genes in published *Symbiodinium* genomes (Chi *et al.* 2014), suggesting that the loss of sexual reproduction has not occurred in this genus.

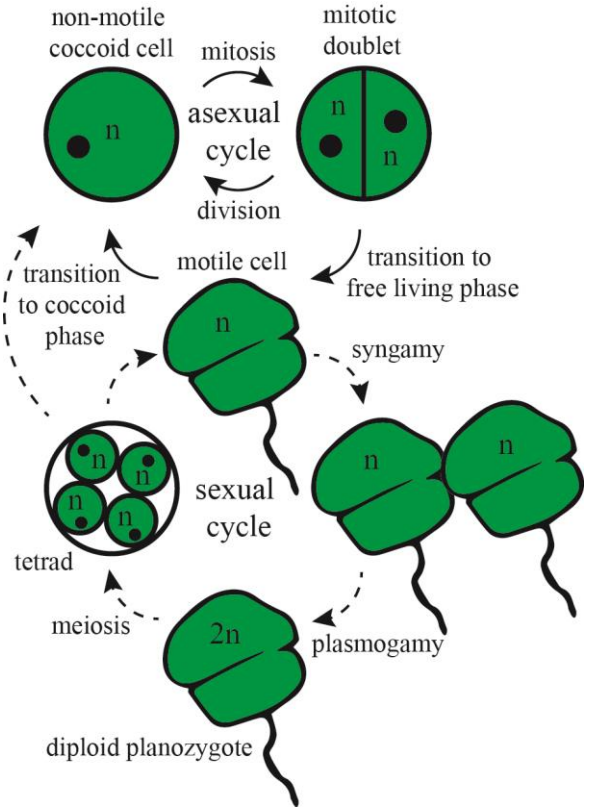


**Figure 1.7 The putative haplontic life-cycle of *Symbiodinium***
Closed arrows show observed processes and dashed arrows represent those that are inferred. While the sexual life cycle has not been directly observed, cryptic recombination is evident from several multi-locus genotyping studies (see below). *Symbiodinium* cells are coccoid and non-motile when in symbiosis (black circles represent accumulation bodies, visible under the light microscope) and transition to the flagellate motile form when in the free-living phase. Coccoid and flagellate cells are primarily haploid (n). The putative zygote is diploid (2n) before undergoing meiosis to restore the haploid condition (modified from Stambler 2011).

While symbiotic dinoflagellates do appear to undergo cryptic recombination, it remains unknown when and where sexual reproduction occurs. The *Symbiodinium* life cycle involves both a sedentary coccoid phase and a dispersive motile phase (Freudenthal 1962; Fitt & Trench 1983). When in symbiosis, the coccoid, non-motile symbionts are enclosed in membrane-bound vacuoles within the host's gastrodermal cells (Trench 1987), presumably isolating them from potential mates. Reproduction occurs exclusively through mitotic division of haploid, vegetative cells (Santos & Coffroth 2003), a process that is tightly regulated by the host (Davy *et al.* 2012). When in the free-living phase, longitudinal and transverse flagella develop and cells closely resemble *Gymnodinium* spp. (Kawaguti 1944; Fitt & Trench 1983; Trench & Thinh 1995). Free-living *Symbiodinium* cells are motile,

chemotactic (Fitt 1984; Pasternak *et al.* 2006) and phototactic (Hollingsworth *et al.* 2005), and viable cells are found in high abundance in the reef sediment and water column (Coffroth *et al.* 2006; Littman *et al.* 2008; Pochon *et al.* 2010; Takabayashi *et al.* 2011). Access to potential mates therefore appears to be unlimited *ex hospite*, presenting an ideal environment for sexual reproduction to occur (Trench 1997). Yet the conditions required to induce the sexual life-cycle in *Symbiodinium* continue to evade researchers, presenting a challenging obstacle to its thorough characterization.

Aside from providing the opportunity to eliminate deleterious mutations, recombination may lead to the acquisition of environmental adaptations, through the generation and proliferation of adaptive allele combinations under selection (Baillie *et al.* 1998; LaJeunesse 2001; Pettay *et al.* 2011). In the extreme case, recombination between divergent *Symbiodinium* lineages could facilitate the exchange of genetic material, vectored by a series of hybrid and backcross intermediates (introgression). Introgressive hybridization may provide the opportunity for a host-compatible symbiont lineage to rapidly acquire functional adaptations, supporting the evolution of the symbiosis. For these reasons, characterizing the sexual life-cycle and establishing the barriers of reproductive isolation in the *Symbiodinium* genus are important objectives in the effort to predict the ecological and evolutionary responses of corals in a changing climate.

### *1.8.3. Hybridization in* Symbiodinium*?*

The crossing of individuals from genetically divergent lineages (hybridization; Arnold 1997) is evident in around 25% of plant species and 10% of animal species (Mallet 2005). Hybridization is thought to be common in the marine environment (Gardner 1997), though few studies have examined its occurrence in marine micro-eukaryotes (Casteleyn *et al.* 2009). While *Symbiodinium* does appear to reproduce sexually, it is not known whether members of different species, clades or subclades are sexually compatible or able to produce viable progeny. Analyses of polymorphic microsatellite loci have shown evidence of allelic recombination within, but not between *Symbiodinium cp23S*, *ITS2* and *psbA*$^{ncr}$ lineages (Santos *et al.* 2003b, 2004; Pettay *et al.* 2011; Thornhill *et al.* 2013a; LaJeunesse *et al.* 2014). In a phylogenetic analysis of clade C phylotypes on the GBR, organelle phylogenies were highly congruent with those of the nuclear rDNA, again indicating an absence of hybridization (Sampayo *et al.* 2009). Yet these studies represent only a small fraction of the

worldwide *Symbiodinium* diversity, and hence more extensive sampling is needed to establish whether hybridization naturally occurs in this group. Furthermore, *ITS* sequence variants that produce additive patterns when visualized on electrophoretic gels (such as DGGE and SSCP) are often dismissed as co-dominant paralogs, without considering alternative explanations for their intra-genomic coexistence (or indeed determining whether the observed sequence variation is intra-genomic). For example, the *Symbiodinium* C1c *ITS2* sequence was initially reported as a paralogous intra-genomic variant of C1, since the former was only found in association with the DGGE profile of the latter (LaJeunesse *et al.* 2003); however C1c was later assigned the alphanumeric status C45 when further sampling revealed its presence in isolation of C1 (LaJeunesse 2005). It is therefore possible that the additive pattern observed by LaJeunesse *et al.* (2003) could have resulted from hybridization between *Symbiodinium* C1 and C45.

Though yet to be identified in *Symbiodinium*, hybridization has been reported between members of divergent free-living dinoflagellate taxa (Edvardsen *et al.* 2003; Hart *et al.* 2007; Brosnahan *et al.* 2010). For example, Brosnahan *et al.* (2010) recovered hypnozygote cysts from Belfast Lough in Northern Ireland, and used nested single-cell qPCR (targeting the hyper-variable D1 and D2 regions of LSU rDNA) to demonstrate their hybrid origin. The progenitor taxa were identified as members of two ribosomal clades within the *Alexandrium tamarense* species complex (groups I and III). However, experimental crosses between these strains failed to yield viable progeny, with recombinant offspring undergoing no more than three cell divisions (Brosnahan *et al.* 2010). While post-zygotic mating barriers can cause hybrid lethality or sterility in crosses involving widely divergent taxa, more closely-related lineages can show comparatively weak reproductive isolation. For example, crosses of recently diverged, geographically isolated dinoflagellates within the *Gymnodinium catenatum* complex produced hypnozygotes with high excystment success and viable offspring (Blackburn *et al.* 2001). Successful hybridization is also apparent between the free-living dinoflagellates *Dinophysis acuminata* and *D. norvegica*, a species pair distinguished by eight nucleotide substitutions in the *ITS1-5.8S-ITS2* region (Edvardsen *et al.* 2003). This level of divergence appears to be near the upper limit for reproductive compatibility in dinoflagellates, a threshold that roughly corresponds with other micro-eukaryote groups. In the freshwater diatom family Eunotiaceae, reproductive isolation and hybrid sterility generally evolve in mating pairs featuring *ITS* sequence divergence above 10% (Vanormelingen *et al.* 2008; Casteleyn *et al.* 2009). Barriers to reproductive isolation are also

evident beyond ~10% *ITS* divergence in the haplontic green algal family Volvocaceae (Coleman *et al.* 1994). Given that ecologically divergent *Symbiodinium* taxa can be differentiated by just a single base pair in the *ITS1-5.8S-ITS2* region (0.2% divergence; e.g. subclades C1 and C3), a thorough investigation of the occurrence and potential evolutionary effects of hybridization in the *Symbiodinium* genus is warranted.

### 1.9. Inferring hybridization in *Symbiodinium*

Establishing the incidence of hybridization and introgression has proven difficult in many natural populations. Identifying the genealogical origin of *Symbiodinium* individuals is further complicated by their unicellularity, haploidy, and the inability to establish many types in culture. Hybridization is often revealed using standard genotyping techniques such as multi-locus microsatellite analysis and amplified fragment length polymorphism (AFLP); however these PCR-based methods require a multi-genomic DNA template, limiting their utility to multicellular or cultivable single-cell organisms. The recent development of single-cell whole-genome amplification (WGA) methodology can provide the means to increase DNA template concentrations to sufficient levels for multi-locus genotyping, but these are currently expensive and technically demanding procedures (Handyside *et al.* 2004; Coskun & Alsmadi 2007). Alternatively, a single locus may provide conditional evidence of hybridization provided that a suitable genetic region is targeted. Mitochondrial and chloroplast genomes are typically uniparentally inherited, and hence are rarely useful in identifying hybrids (Small *et al.* 2004). However, the intra-genomic co-dominance (additivity) of diagnostic nuclear alleles can provide convincing evidence that an individual is of hybrid origin (Soltis *et al.* 1992; Wendel *et al.* 1995; Sang *et al.* 1995; Brasier *et al.* 1999; Newcombe *et al.* 2000). Single-copy nuclear markers are preferable for such analyses, since they lack the NDPs often found in multi-copy gene families (Small *et al.* 2004). However, *Symbiodinium* is predominantly haploid (Santos & Coffroth 2003; but see LaJeunesse *et al.* 2014); therefore recombination ultimately leads to the uniparental inheritance of single-copy alleles. The intra-genomic coexistence of polymorphic, biparentally inherited nuclear genes such as those of the rDNA cistron can provide conditional evidence of hybridization (Sang *et al.* 1995; Morrell & Rieseberg 1998). In particular, the *ITS2* has been extensively utilized in plant systematics, revealing numerous cases of hybridization, hybrid speciation and reticulate evolution (reviewed in Álvarez & Wendel 2003). The multi copy nature of rDNA arrays also

make their constituent sequences amenable to single-cell PCR amplification, circumventing the need to perform a WGA step or establish isoclonal cultures. However, a major limitation of using rDNA markers in hybridization analysis is that a similar additive genomic signature can also arise from the vestigial persistence of ancestral intra-genomic polymorphisms. If the most recent common ancestor of two putatively hybridizing taxa carried both diagnostic rDNA alleles within its genome, and insufficient time has passed since divergence for concerted evolution to fully homogenize the rDNA arrays in each lineage, an individual carrying both alleles may simply represent a member of one taxon that has retained copies of the allele diagnostic of the other (see Figure 1.5c). As such, distinguishing hybridization from incomplete concerted evolution requires the application of specialized statistical techniques (e.g. Bayesian methods that enable the inference of hybridization and introgression from multi-locus haplotypes; Mallet 2005), and should be reinforced with morphological, physiological and ecological data (Peterson *et al.* 2004; Vriesendorp & Bakker 2005).

## 1.10. Aims and objectives of this study

This study aimed to establish whether hybridization occurs, or has occurred, between divergent *Symbiodinium* taxa. To address this question, a combination of genetic, physiological and ecological investigations were carried out on the reef-building coral *Pocillopora damicornis*, a widely distributed, vertically-transmitting species that hosts a diverse array of *Symbiodinium* taxa. Surveys and experiments were carried out at the high-latitude coral reef site of Lord Howe Island (LHI; Australia). The specific objectives were to:

1. Develop a single-cell PCR-DGGE protocol and a quantitative PCR (qPCR) assay to quantify *ITS2* ratios within individual *Symbiodinium* cells, and hence screen for putative hybrids.
2. Develop a statistical framework to simultaneously test three competing hypotheses explaining the patterns of *ITS2* additivity within *P. damicornis* symbionts: ($H_0$) colonies host a single clonal population of symbionts hosting a non-diagnostic polymorphism; ($H_1$) colonies host two populations of genetically distinct symbionts; and ($H_2$) three symbiont populations coexist within coral colonies, including two divergent taxa and an intermediate population of genetically heterogeneous *Symbiodinium* cells (putative hybrids).

3. Develop a method to convert bulk-cell qPCR data (*ITS2* sequence proportions) into the proportional abundance of genetically homogeneous and heterogeneous cells, and employ this method to model the spatiotemporal distribution of putative hybrids. The hypothesis tested in this objective was that homogeneous and heterogeneous symbionts undergo niche diversification, consistent with many natural hybrid-progenitor systems.
4. Assess the physiological performance of heterogeneous symbionts relative to their homogeneous congeners. It was hypothesized that the different cell types are morphologically and physiologically distinct, and that each performs differently under various environmental conditions.
5. Establish whether physiological differences between genetically heterogeneous and homogeneous symbiont cells translate to differences in host fitness. The hypothesis tested was that corals hosting different proportions of homogeneous and heterogeneous symbionts show different growth and mortality rates in their natural environment.

The four subsequent data chapters address these objectives in the following format:

**Chapter 2** addresses the first and second objectives. Individual symbionts were sampled from six *P. damicornis* colonies and analysed for intra-genomic *ITS2* ratios. A finite mixture model was applied to test the three competing hypotheses outlined in objective 2.

**Chapter 3** addresses the third objective by reconciling *ITS2* sequence proportions obtained from bulk-cell qPCR analysis with actual proportions of genetically homogeneous and heterogeneous cells. This facilitated a comprehensive analysis of the spatiotemporal distribution of each cell type within and between *P. damicornis* colonies on the LHI reef. Observed distribution patterns were correlated with a suite of environmental variables obtained from long-term monitoring.

**Chapter 4** employs the methods developed in chapters 2 and 3 to test the hypothesis outlined in the fourth objective. The proportional abundance of genetically heterogeneous *Symbiodinium* cells was quantified in each of 15 *P. damicornis* colonies, and analyses of photosynthetic and respiratory oxygen flux were carried out at both ambient and elevated temperature. Analyses of symbiont morphology and physiology were also performed to further assess the candidacy of heterogeneous cells as putative hybrids.

**Chapter 5** involves the reciprocal transplantation of coral colonies between two distinct reef habitats. Corals were switched between a warm, well lit inner-lagoon site and a reef margin location characterised by low light levels, strong wave action and high macroalgal growth. The growth and survival of corals were assessed in relation to the proportional abundance of genetically heterogeneous *Symbiodinium* cells within their symbiont consortia.

**Chapter 6** provides a review of the combined evidence for hybridization between *Symbiodinium* phylotypes, and speculates on the possible evolutionary implications thereof. Future directions are suggested for the unambiguous confirmation of hybridization in symbiotic dinoflagellates, and the establishment of its location, frequency, and consequences for coral fitness. The possible application of controlled hybridization in the 'evolutionary rescue' of corals in a deteriorating environment is also discussed.

# Chapter 2: Measuring intra-genomic variation in *Symbiodinium*

## 2.1. Introduction

Until the mid-20th century, hybridization was thought to occur rarely and have little evolutionary significance (Mayr 1963). However, a major paradigm shift extolled the incidence and importance of hybridization, led principally by the pioneering work of American botanist Edgar S. Anderson (Anderson 1949; Anderson & Stebbins 1954). This was articulated by his colleague Warren H. Wagner who recalled "We used to make fun of Edgar Anderson by saying that he was finding hybrids under every bush – then we realized that even the bushes were hybrids" (Abbott *et al.* 2013). The so-called 'molecular revolution' has increased our awareness of natural hybridization further still, with current estimates of around 25% of plant species and 10% of animal species undergoing hybridization (Mallet 2005). Yet the phylogenetic and statistical criteria that constitute convincing evidence of natural hybridization and introgression remain the subject of contention, and may depend on the life-history characteristics of the taxa in question (Vriesendorp & Bakker 2005).

Morphological similarities among symbiotic dinoflagellates highlight the need to use appropriate genetic tools when establishing the incidence of hybridization in this group. The internal transcribed spacer 2 (*ITS2*) region of nuclear ribosomal DNA (rDNA) is the most well-characterised and commonly-used marker in *Symbiodinium* systematics, primarily due to its high taxonomic resolution (van Oppen & Gates 2006; Stern *et al.* 2012). Unlike alternative mitochondrial- and chloroplast-encoded sequences and single-copy nuclear genes, the *ITS2* is bi-parentally inherited in most sexually-reproducing organisms, and hence the intra-genomic coexistence of divergent sequence variants can reveal the occurrence of ancient and recent hybridization events (Baldwin *et al.* 1995; Álvarez & Wendel 2003). However, the multiple-copy nature of the rDNA cistron renders it subject to intra-genomic variation from a variety of other processes, including the generation of paralogous somatic mutations and the degeneration of functional genes into pseudo-genes (Thornhill *et al.* 2007). Establishing whether a given ribotype is taxonomically meaningful requires the analysis of individuals rather than multi-genomic samples, necessitating a single-cell approach for unicellular organisms such as *Symbiodinium* (Correa & Baker 2009; Miranda *et al.* 2012). The generation of isoclonal cell-lines from individual *Symbiodinium* cells offers a partial solution

(Thornhill *et al.* 2007); however frequent somatic mutations may lead to cultures that are not representative of the original cell (van Oppen *et al.* 2011). Single-cell PCR (scPCR) provides an obvious advantage in distinguishing between intra and inter-genomic sequence variation (Tengs *et al.* 2000; Edvardsen *et al.* 2003); yet this method has not been widely used in *Symbiodinium* systematics. This is primarily due to its time-consuming nature, and the difficult task of disrupting the recalcitrant cell wall to extract the nucleic acids. A lack of suitable methodology for isolating, extracting and sequencing DNA from individual *Symbiodinium* cells has meant that intra-genomic variation in this genus has remained virtually unexplored (Stat *et al.* 2012).

While establishing the dominant ribotype within individual cells is necessary to establish diversity estimates (Correa & Baker 2009), it is also beneficial to quantify intra-genomic sequence variation when assessing the incidence of hybridization. This is because $F_1$ hybrids are expected to inherit relatively similar rDNA copy numbers from each parent (Baldwin *et al.* 1995; Brosnahan *et al.* 2010), and polymorphism ratios can indicate the direction of introgression and/or concerted evolution (Wendel *et al.* 1995; De Castro *et al.* 2013). Fluorogenic-probe based qPCR analysis now offers sufficient sensitivity to quantify *ITS2* variants at the subclade level, and when preceded by a PCR pre-amplification step (nested qPCR; e.g. Brosnahan *et al.* 2010), it can be used to quantify polymorphic ribotypes within the individual dinoflagellate genome. However, while the intra-genomic co-dominance (additivity) of diagnostic *ITS2* variants can allude to the occurrence of hybridization and even introgression, a similar genomic signature can also rise from the incomplete concerted evolution of ancestral polymorphisms (ICEAP). For this reason, a statistical framework is needed to distinguish between these conflicting origins of intra-genomic rDNA additivity.

In this chapter, I attempt to address these methodological limitations by developing: (1) a single-cell isolation and DNA extraction protocol for *Symbiodinium*; (2) a single-cell PCR-DGGE method to screen for *Symbiodinium* individuals with additive *ITS2* repeats; (3) a nested PCR-qPCR assay to quantify intra-genomic *ITS2* sequence polymorphisms within individual cells; and (4) a statistical framework to identify admixture in *Symbiodinium* populations based on proportions of *ITS2* sequence variants within the genome. The model selection criterion developed in (4) was then employed to test whether the *P. damicornis* symbiont consortium consists of ($H_0$) a single clonal population of symbionts featuring a non-diagnostic polymorphism (NDP); ($H_1$) two populations of divergent, homogeneous symbionts; or ($H_2$) a mixture of genetically homogeneous symbionts and heterogeneous cells,

representing putative hybrids (Figure 2.1a). The proportional abundance of *ITS2* polymorphisms within each *Symbiodinium* cell was also assessed to explore the potential for gene flow *via* introgressive hybridization (Figure 2.1b).

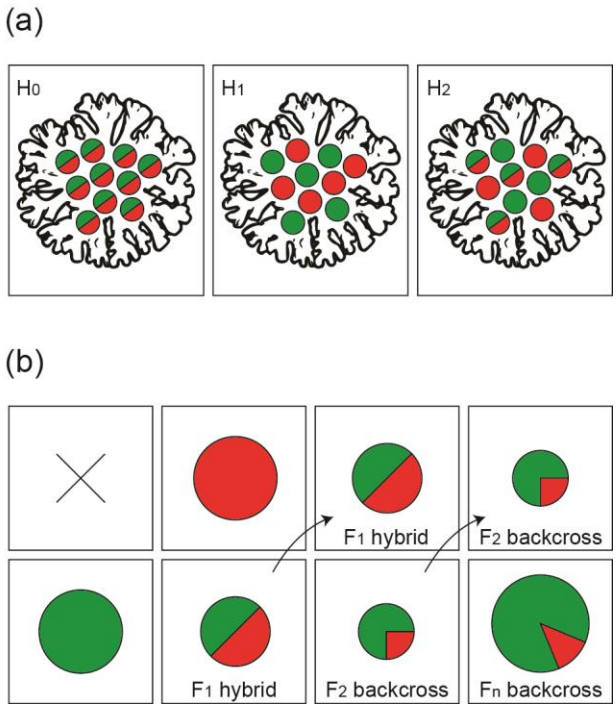


**Figure 2.1 Conflicting origins of intra-genomic variation in *Symbiodinium***
Red and green colorations represent divergent *ITS2* sequences, with monocoloured cells featuring homogeneous or near-homogeneous *ITS2* arrays and bicoloured cells hosting polymorphic ribotypes. Schematics show (a) competing hypotheses of sequence homology within *P. damicornis*-associated *Symbiodinium*, with a single clonal population hosting a non-diagnostic polymorphism (NDP) under $H_0$, exclusively homogeneous symbionts under $H_1$and hybridization between individuals from genetically distinct populations under $H_2$; and (b) introgressive hybridization, with differential fitness between hybrid classes (shown in a size gradient). Many backcross generations (*n*) may occur before an increase in fitness is realized. Genetic isolation occurs when one or more hybrid/backcross classes suffer from insurmountably low mean fitness.

## 2.2. Methods

### *2.2.1. Study species and location*

This study was carried out at the world's southernmost coral reef at Lord Howe Island (LHI; Australia). This isolated 14.5 $km^2$ volcanic remnant is located around 600 km east of the Australian mainland, and some 200km to the south of the Elizabeth and Middleton Reefs Marine National Park Reserve. The LHI reef hosts at least 83 species of scleractinian coral, (many of which are endemic; Harriott *et al.* 1995), and a correspondingly diverse and endemic *Symbiodinium* assemblage (Wicks *et al.* 2010). Reef fauna are regularly exposed to widely variable thermal conditions (Harriott & Banks 2002), and cold-stress is known to play a defining role in determining species boundaries at this site (Veron & Done 1979). In certain

reef-margin areas, a stark transition from coral- to macro-algal dominated benthic assemblages is apparent (Allen & Paxton 1974).

The host species investigated in this study was the widely-distributed coral *Pocillopora damicornis*, a thermally-sensitive but fast-growing species that forms a dominant component of many Indo-Pacific reefs (including that of LHI; Veron 2000). Colonies at LHI can grow to several metres in diameter in sheltered inner-lagoon habitats, and form a small compact clump-like morphology in exposed locations (Miller & Ayre 2004). *P. damicornis* is hermaphroditic and shows an unusual dual-reproductive mode, with the majority of offspring consisting of brooded asexual larvae, complimented by the cryptic simultaneous broadcast-spawning of sexual gametes in some areas (Combosch & Vollmer 2013). This species shows a predominantly sexual reproductive mode at LHI, where it occasionally undergoes intergeneric hybridization with *Stylophora pistillata* (Miller & Ayre 2004). This may arise from suboptimal abiotic conditions selecting for 'extreme' hybrid phenotypes, and/or a low availability of conspecific gametes (Willis *et al.* 2006). *P. damicornis* transmits symbionts vertically from parent to offspring, and can form a symbiotic relationship with a large array of genetically and physiologically distinct *Symbiodinium* taxa. In Australian waters alone, *P. damicornis* is found in association with *S. goreauii*, *S. glynni*, *S. trenchii*, and numerous other undescribed *ITS2* types including C1b, C1c, C1c-ff, C1h, C1j, C33, C33a, C42, C42a, C42b, C100, C103, C118, C125 and C126 (LaJeunesse *et al.* 2003, 2004; Sampayo *et al.* 2007; Ulstrup *et al.* 2008; Stat *et al.* 2008a; Wicks *et al.* 2010; Silverstein *et al.* 2011; Tonk *et al.* 2013). Of these, *P. damicornis* colonies have been reported hosting *Symbiodinium* C100, C103 and C118 at LHI (Wicks *et al.* 2010).

### *2.2.2. Sample collection and DNA isolation*

Coral sampling was carried out in March 2012 at North Bay and Ned's Beach, Lord Howe Island, Australia. Three *Pocillopora damicornis* colonies were sampled from each site by divers using snorkel (North Bay; depth 1-3 m) or SCUBA (Ned's Beach; depth 14-16m). In all cases, colonies were sampled at least 2 m from each other to reduce the risk of selecting ramets. Three small branch tips (~ 1 $cm^3$) were taken from each colony using diagonal pliers, and preserved in DMSO preservation buffer (20% DMSO, 250 mM EDTA, NaCl saturated, pH 8.0; Seutin *et al.* 1991). Coral samples were stored at -20 °C prior to DNA analysis. A 0.12 $cm^2$ area of tissue was removed from the skeleton in 1.5 ml of 0.22 µm filtered seawater

(FSW), delivered at high velocity through a circular stencil. A 10 µl sub-sample was taken and centrifuged at 16,100 x *g* for 5 min to pellet the *Symbiodinium* fraction. The supernatant was discarded and the pellet re-suspended in 100 µl DNA buffer (DNAB; 0.4M NaCl, 50mM EDTA, pH 8.0). Individual cells (*n* = 30 from each colony) were hand-picked under a light microscope using a heat-elongated glass micro-pipette. Each cell was washed three times in 2 µl DNAB, transferred to a 1.7 ml micro-centrifuge tube with 50 mg acid-washed glass beads (710-1180 µm; Sigma-Aldrich), and milled for 1 min at 50 Hz (Qiagen TissueLyser LT; Qiagen) to disrupt the cell-wall and release the nucleic acids. TE buffer (10 mM Tris-HCl; 1 mM EDTA; pH = 8.0) was then added to a final volume of 20 µl. For each colony, the extraction process was carried out with the symbiont cell omitted (but with coral tissue homogenate included), to ensure that only intracellular DNA contributed to the PCR amplification signal.

### *2.2.3. End-point PCR, DGGE and DNA sequencing*

Single-cell DNA template solutions generally contained insufficient DNA for direct PCR-DGGE and qPCR analysis. The partial *nr5.8S, ITS2* and partial *nr28S* regions were therefore pre-amplified using a shortened end-point PCR protocol, with the outer primers ITSintfor2 (LaJeunesse 2002) and ITS2Rev2 (Stat *et al.* 2009). Thermal cycling included an initial denaturation step of 3 min at 95 °C followed by 24 cycles of 15 seconds at 95 °C, 15 seconds at 56 °C and 10 seconds at 72 °C (carried out on an Applied Biosystems Veriti thermo-cycler). Each reaction contained 10 µl of DNA template solution, 1x MyTaq PCR reaction mix (Bioline), 15 pmol each primer, and deionised sterile water to a total volume of 25 µl. Multiple pre-amplification reactions on individual template solutions were prevented by the limited amount of target DNA available. A template-free control reaction was included with each run.

Pre-amplified PCR products were diluted $1{:}10^3$ (North Bay colonies) or $1{:}10^4$ (Ned's Beach colonies) in deionised sterile water prior to PCR-DGGE and qPCR analysis. These differences were due to shortages of DNA template solutions from the Ned's Beach colonies, which were used for the initial assay development and optimization process. PCR amplification for DGGE was carried out using the primers ITSintfor2 and ITS2CLAMP (LaJeunesse 2002). Cycling conditions were as described above, except an additional 16 thermal cycles were run (40 in total). PCR products (20 µl) were loaded on 200 x 200 x 0.75

mm, 8% denaturing polyacrylamide gels (25-50% denaturant gradient), and run in 1 x TAE at 150 V for 7 h at 60 °C (DCode system; BioRad) alongside known *ITS2* sequences of *Symbiodinium* C100 and C109. Following electrophoresis, gels were stained with ethidium bromide and viewed on a UV trans-illuminator (FirstLight UVP). Five representative (dominant) bands at each position were excised, milled for 1 minute at 50 Hz with 50 mg glass beads and 200 µl TE buffer, and re-amplified with both clamped and non-clamped primers (LaJeunesse 2002). DGGE was carried out on clamped PCR products to ensure a single band migrated to the identical position from where it was excised. Corresponding non-clamped products were cleaned with ExoSAP-IT (USB), and sequenced by the Macrogen Sequencing Service (Macrogen Inc., Seoul, South Korea). Sequences were manually checked and aligned in Geneious v 7.0 (Biomatters) and a BLAST search was carried out against *Symbiodinium ITS2* sequences available in Genbank. Novel sequences were assigned alphanumeric *ITS2* nomenclature (c.f. LaJeunesse 2001, 2002) and deposited into the Genbank database. The un-rooted statistical parsimony network of *Symbiodinium ITS2* phylotypes found within Pocilloporid corals at LHI (Wicks *et al.* 2010) was updated in TCS v 1.21 (95% connection limit; gaps assigned fifth character state; Clement *et al.* 2000).

### *2.2.4. qPCR analysis of* Symbiodinium ITS2 *ratios*

For qPCR analysis, the universal primers CInnerFor (5'-TGGCTTGTTAATTGCTTGGTTCT-3') and CInnerRev (5'-ACCTGCATCCCAGCGGTT-3') were developed, in addition to the custom TaqMan fluorogenic probes $C100^{+}$ and $C100^{-}$ (5'-TTTTACTTGAGTGACACCGC-3' and 5'-CTTTACTTGAGTGACGCTGC-3', respectively; Life Technologies). The probe $C100^{+}$ was designed to quantify the number of *ITS2* sequences of type C100 in a given sample (denoted $C_{C100}$), while the $C100^{-}$ probe was developed to quantify the copy-number of all clade C *ITS2* sequences other than type C100. All primers and probes were initially checked for specificity by conducting a BLAST search against sequences deposited in Genbank (Altschul *et al.* 1990). To obtain purified DNA sequences for qPCR calibration, PCR products (types C100, C103, C109 and C118 extracted from *P. damicornis*, and C3 obtained from the VUW *Symbiodinium* laboratory culture collection) were cloned using the TOPO TA kit (Invitrogen Life Technologies). Plasmid colonies were incubated overnight on selective LB agar plates containing ampicillin, IPTG and XGAL (Bioline). DNA was extracted from positive transformants, purified using a

plasmid Mini-Prep kit (Invitrogen Life Technologies), and sequenced as above with the M13 primer set. Plasmid DNA template concentrations were estimated using a Pearl Nanophotometer (Implen), diluted to approximately $10^{-3}$ ng $\mu l^{-1}$, and five $\log_{10}$ serial dilutions were constructed to generate standard curves and test the accuracy and precision of the assay. All qPCR reactions were carried out in triplicate (standard curves) or duplicate (template solutions) on an Applied Biosystems StepOne instrument (Life Technologies), alongside a template-free control reaction. Each TaqMan qPCR reaction contained 4 µl template, 1x TaqMan Universal Mastermix II (Life Technologies), 1x TaqMan fluorogenic probe (Life Technologies), 18 pmol each primer, and deionised sterile water to a total volume of 20 µl. Thermal cycling conditions involved an initial 10 min, 95 °C denaturation step followed by 40 cycles of 15 seconds at 95 °C and 1 min at 60 °C. Cycle threshold ($C_t$) values were determined as the cycle at which the change in fluorescence was significantly different to the background level ($\Delta R_n = 0.05$; obtained using the instrument's built-in algorithm). $C_t$ values below the standard curve intercept (see *Appendix B*) and featuring sufficiently low standard deviations (< 0.5) were included in the analysis.

To ensure that the TaqMan assays $C100^+$ and $C100^-$ detected all *Symbiodinium* clade C sequences present within each sample, the total *ITS2* copy number (denoted $C_{TOTAL}$) in each *Symbiodinium* cell from the North Bay colonies was also estimated using SYBR qPCR analysis. Reactions were carried out as above, except Power SYBR Green Mastermix (Life Technologies) was used in place of TaqMan Universal Mastermix II, fluorogenic probes were omitted, and $C_t$ values were generated using the $\Delta R_n$ threshold value of 0.3. A melt curve (temperature elevation from 60 °C to 95 °C in 0.3 °C increments each of 15 s duration) was included at the end of each run to ensure only detectable target sequences were amplified. Template solutions yielding $C_t$ values below the standard curve intercept and melting temperatures ($T_m$) within 1 °C of plasmid $T_m$ values were included in the analysis. The *ITS2* copy number within each cell ($C_{TOTAL}$; as determined from SYBR qPCR analysis) was compared to the sum of those given by the $C100^+$ and $C100^-$ TaqMan assays using linear regression (parameters constrained; intercept = 0, slope = 1). Finally, a mixture test was carried out to assess the ability of the TaqMan qPCR assay to accurately predict the proportion of total *Symbiodinium* clade C *ITS2* copies that were of type C100 ($C_{C100}$:$C_{TOTAL}$ ratio). Eight mixtures were constructed from plasmid C100 and C109 DNA template solutions (diluted to approximately 200 *ITS2* copies $\mu l^{-1}$; $C_{C100}$:$C_{TOTAL}$ ratios = 0, 0.02, 0.10, 0.4, 0.6, 0.9, 0.98 and 1; see *Appendix B* for $C_t$ values) and qPCR reactions were carried out

in duplicate as above. The ability of the combined TaqMan assay to predict $C_{TOTAL}$ and $C_{C100}$:$C_{TOTAL}$ was assessed using linear regression (parameters constrained; intercept = 0, slope = 1).

### *2.2.5. Statistical analysis*

To assess the relationship between the total *ITS2* copy number and the proportion of copies that were of type C100, a non-linear regression curve (second order polynomial) was fitted to the bivariate $C_{C100}$:$C_{TOTAL}$ *versus* $C_{TOTAL}$ data in Sigmaplot v11.0 (Systat). Values of $C_{C100}$:$C_{TOTAL}$ were arcsin transformed and compared between colonies (*Colony*) and between branches within colonies (*Branch*(*Colony*)) using nested ANOVA (lm function in R; R Development Core Team 2011). Three competing hypotheses were evaluated to explain the *ITS2* sequence variation within and between the symbionts of *P. damicornis*: ($H_0$) colonies host a single population of genetically heterogeneous symbionts, *versus* ($H_1$) colonies host two populations of genetically distinct, homogeneous symbionts, *versus* ($H_2$) colonies host distinct populations of genetically homogeneous and heterogeneous symbionts, consistent with the occurrence of hybridization (Figure 2.1) The frequency distribution of $C_{C100}$:$C_{TOTAL}$ within a coral colony (X) is expressed in model form as:

$H_0$: $X \sim \text{Beta}(\alpha, \beta)$, $\alpha > 1$, $\beta > 1$ **Equation 2.1**

$H_1$: $X \sim \text{Beta}(\alpha, \beta)$, $\alpha < 1$, $\beta < 1$ **Equation 2.2**

$H_2$: $X \sim \pi\ \text{Beta}(\alpha_1, \beta_1) + (1 - \pi)\ \text{Beta}(\alpha_2, \beta_2)$, $0 < \pi < 1$ **Equation 2.3**

where $\alpha$ and $\beta$ are the shape parameters of the beta function, and $\pi$ denotes the proportion of symbionts belonging to each component of the mixture model. Mixed beta functions were fitted to the $C_{C100}$:$C_{TOTAL}$ frequency distributions of each coral colony, and maximum likelihood parameter values were solved using the optim function in R (L-BFGS-B method; R Development Core Team 2011). A range of starting parameter values were used at each optimization stage to ensure that a universal log-likelihood maximum was reached. Hypothesis evaluation was based on weighted AICc values ($w_i$), with those above 0.90 considered to provide unambiguous support for a candidate model (Burnham & Anderson 2002).

## 2.3. Results

### *2.3.1. DGGE and DNA sequencing*

The excision and sequencing of DGGE bands revealed that all six *P. damicornis* colonies hosted *Symbiodinium ITS2* types C100 (Genbank accession number HM222433; Wicks *et al.* 2010) and C109 (Genbank accession number KJ530690; novel sequence). Although two divergent *ITS2* sequences were retrieved, three distinct DGGE band profiles were observed among the 180 individual cells analysed. These corresponded to *Symbiodinium* cells featuring a homogeneous C100 array, those featuring a homogeneous C109 array, and those with a heterogeneous mixture of both *ITS2* types (Figure 2.2). Four of the six colonies analysed hosted a consortium of *Symbiodinium* cells that included all three profiles (two colonies from each site), while the remaining two colonies hosted only homogeneous C100 symbionts and those producing the heterogeneous band-pattern (Figure 2.2a). No amplification signal was detected from template-free controls or the extractions with symbiont cells omitted, indicating an absence of extracellular DNA contamination.

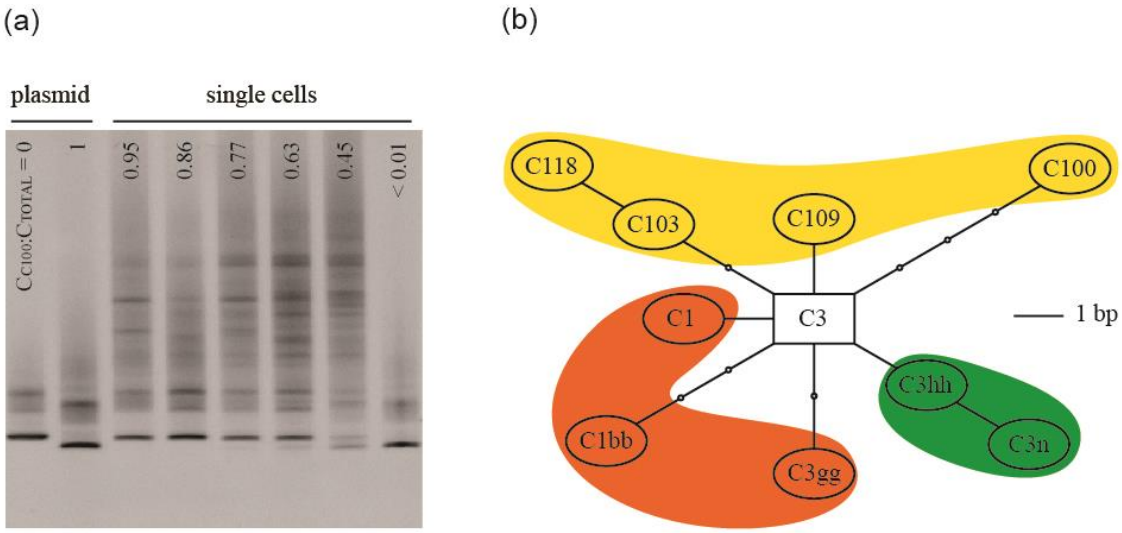


**Figure 2.2 Sequence variation among Pocilloporid-associated *Symbiodinium* at LHI**
*ITS2* sequence variation between and within the *Symbiodinium* genome is shown by: (a) DGGE profiles of individual symbionts from *P. damicornis* colonies at Lord Howe Island, featuring a range of $C_{C100}$:$C_{TOTAL}$ ratios (alongside plasmid-purified C100 and C109 DNA); and (b) an un-rooted statistical parsimony network showing the phylogenetic relationships between derived Pocilloporid-associated *Symbiodinium* types found at Lord Howe Island (ellipses) and the ancestral C3 root (rectangle; modified from Wicks *et al.* 2010). Small circles in (b) represent hypothetical intermediate sequences, each distinguished from its neighbor by a single nucleotide substitution or gap. *P. damicornis*-associated types are shown in yellow, while those found in association with *Stylophora pistillata* and *Seriatopora hystrix* are shown in orange and green, respectively. See *Appendix A* for Genbank accession numbers.

### *2.3.2. qPCR estimation of intra-genomic* ITS2 *ratios*

The universal primers CInnerFor and CInnerRev were identically matched to conserved regions within the *ITS2* of *Symbiodinium* C100 and C109. These primers also share identical sequences or single-base pair mismatches with nearly all clade C sequences currently available in the Genbank database, including those found within the corals of LHI (Wicks *et al.* 2010). A sequence BLAST analysis of the target probe $C100^{+}$ revealed a high specificity for *Symbiodinium* C100, with at least two nucleotide substitutions differentiating it from the majority of other clade C sequences in Genbank (positioned 16 and 18 base pairs from the 5' end of the probe). The cytosine at the 5' end of the probe $C100^{-}$ is mismatched to C100, C109 and the majority of other clade C *Symbiodinium* types (including the ancestral types C1 and C3). This mismatch had no effect on the reaction efficiency when tested on *ITS2* types C109 and C103 (95% < E < 100%; see *Appendix B*); however it served to prevent cross-

hybridization with the C100 sequence. With this exception, $C100^-$ shared an identical sequence to most clade C *Symbiodinium* types available in Genbank, including the ancestral types C1, C3 and all derived types previously found in association with *P. damicornis* at LHI (Wicks *et al.* 2010). Standard curve analysis of both TaqMan assays revealed acceptable reaction efficiencies when matched to their respective target sequences ($C100^+$ to C100; $C100^-$ to both C109 and C103; 95% < E < 100% and $R^2 > 0.99$ in all cases; see *Appendix B*). qPCR analysis of known plasmid DNA mixtures yielded high accuracy and precision in estimating $C_{C100}$:$C_{TOTAL}$ (constrained linear regression; $R^2 = 0.998$; *Appendix B*) and an absence of cross-hybridization. TaqMan qPCR-generated $C_{TOTAL}$ values within each *Symbiodinium* cell were highly correlated with, and not significantly different from those obtained from the SYBR qPCR assay (constrained linear regression; $R^2 = 0.978$; see *Appendix B*), indicating a negligible incidence of clade C *ITS2* types other than those detected by $C100^+$ and $C100^-$. SYBR qPCR melt curve analysis showed no $T_m$ differences between plasmid C100 and C109, and all single-cell templates yielded single $T_m$ peaks within 1°C of the plasmid-generated values.

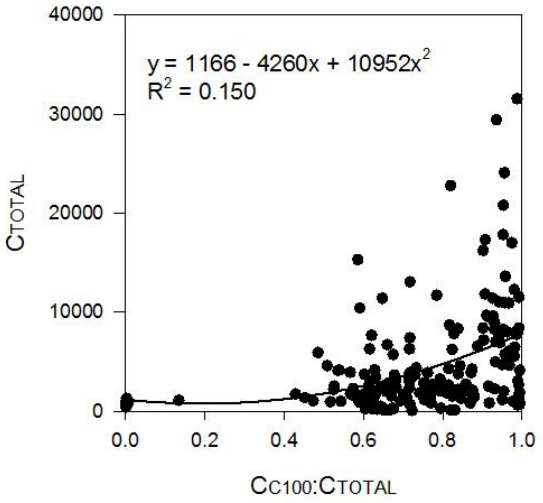


**Figure 2.3 Variation in *ITS2* copy numbers within *Symbiodinium* cells**
A non-linear relationship existed between the proportion of *ITS2* copies of type C100 ($C_{C100}$:$C_{TOTAL}$) and the total number of *ITS2* copies within the cell ($C_{TOTAL}$). Homogeneous C100 cells hosted significantly more *ITS2* copies than the genetically heterogeneous cells, or those featuring a homogeneous C109 array (second order polynomial regression, p = 0.027).

Within-cell *ITS2* copy numbers ($C_{TOTAL}$) were highly variable, ranging from less than 500 to over 30,000. C100 was the dominant *ITS2* type in the majority of cells analysed, with $C_{C100}$:$C_{TOTAL}$ ratios ranging between 0 and 0.987 (Figure 2.3; see *Appendix B* for $C_t$ values). The remaining *ITS2* copies appeared to be primarily of type C109, since this was the only other sequence detected in the DGGE analysis. DGGE band intensities generally reflected

qPCR-generated $C_{TOTAL}$ values, and in cases where both C100- and C109-diagnostic bands were present, their relative intensity gave a qualitative indication of $C_{C100}$:$C_{TOTAL}$. However, the C109 band was generally very faint in cells featuring $C_{C100}$:$C_{TOTAL}$ ratios greater than 0.75, and universally undetectable in those above 0.85 (Figure 2.2a; see *Appendix B*). A significant nonlinear correlation between $C_{C100}$:$C_{TOTAL}$ and $C_{TOTAL}$ revealed that *ITS2* copy numbers were higher on average in genetically homogeneous C100 cells than in either the heterogeneous C100/C109 cells or the homogeneous C109 cells (non-linear regression, $p < 0.027$; $R^2 = 0.15$; Figure 2.3). Within-cell $C_{C100}$:$C_{TOTAL}$ ratios did not differ between branches within colonies, but varied between colonies (nested ANOVA, $p = 0.82$ and $< 0.01$ for *Branch*(*Colony*) and *Colony* effects, respectively; Table 2.1).

**Table 2.1 Nested ANOVA for intra-genomic variation in *ITS2* ratios**

| Source | df | SS | MS | *F* | *P* |
|---|---|---|---|---|---|
| **Between colonies** | 5 | 4.07 | 0.81 | 24.23 | 0.001 |
| **Between branches within colonies** | 12 | 0.40 | 0.03 | 0.61 | 0.82 |
| **Error** | 162 | 8.87 | 0.05 | | |

The model design used in the nested ANOVA analysis was $C_{C100}$:$C_{TOTAL}$ ~ *Colony* x *Branch*(*Colony*). $C_{C100}$:$C_{TOTAL}$ ratios were arcsin transformed prior to analysis. Branches within colonies were pooled for subsequent mixture model fitting.

The application and evaluation of competing beta models based on $C_{C100}$:$C_{TOTAL}$ ratios revealed the presence of multiple symbiont clusters in all six colonies. In all cases, the two-component beta mixture model representative of $H_2$ provided the best fit of the candidate models ($w_i > 0.90$ for all colonies; Table 2.2). Three modes were present in colonies a, b, d and e, representing clusters of genetically homogeneous C100 cells, homogeneous C109 cells, and heterogeneous C100/C109 cells. Two modes were detected in colonies c and f, representing coexisting populations of homogeneous C100 cells and heterogeneous C100/C109 cells (Figure 2.4). The proportion of genetically heterogeneous symbiont cells in the consortium ranged from 7% in colony c to 88.5% in colony a.

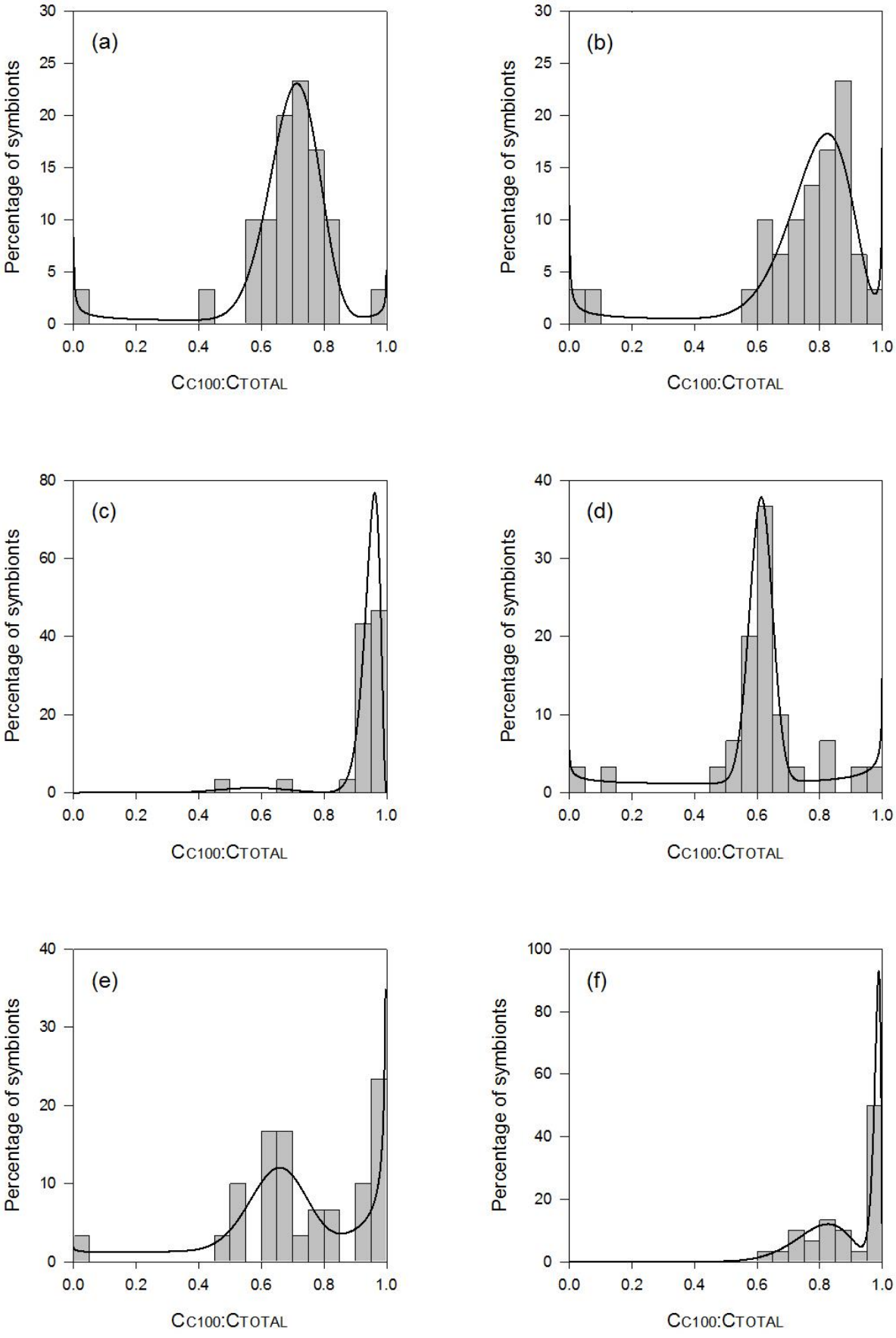
(a)
(b)
(c)
(d)
(e)
(f)
Percentage of symbionts
CC100:CTOTAL

**Figure 2.4 (previous page) Frequency distributions of intra-genomic *ITS2* ratios**
Colonies a-c were sampled from North Bay (1-3m), and colonies d-f from Ned's Beach (14-18m). Vertical bars represent the percentage of symbiont cells within each $C_{C100}$:$C_{TOTAL}$ category ($n$ = 30 cells for each colony). Overlying probability density functions are optimized two-component beta mixtures (see Table 2.2 for parameter estimates).

**Table 2.2 Summary of optimized beta mixture models**

| Colony ID | Site | Best-fit hypothesis | Model Equation | Proportion heterogeneous | $w_i$ |
|---|---|---|---|---|---|
| **a** | North Bay | $H_2$ | X ~ 0.13 x Beta (0.57, 0.53) + 0.87 x Beta (26.08, 10.89) | 0.885 | > 0.99 |
| **b** | North Bay | $H_2$ | X ~ 0.07 x Beta (3.48, 66.21) + 0.93 x Beta (10.99, 2.89) | 0.816 | > 0.99 |
| **c** | North Bay | $H_2$ | X ~ 0.07 x Beta (13.97, 10.32) + 0.93 x Beta (57.10, 3.12) | 0.007 | > 0.99 |
| **d** | Ned's Beach | $H_2$ | X ~ 0.33 x Beta (0.71, 0.57) + 0.67 x Beta (108.55, 68.91) | 0.670 | > 0.99 |
| **e** | Ned's Beach | $H_2$ | X ~ 0.51 x Beta (16.58, 4.28) + 0.49 x Beta (114.8, 2.32) | 0.512 | 0.96 |
| **f** | Ned's Beach | $H_2$ | X ~ 0.55 x Beta (0.90, 0.34) + 0.45 x Beta (19.40, 10.63) | 0.444 | 0.93 |

Model support is indicated by Akaike weights ($w_i$), representing the conditional probability that a particular model provides the best fit of all candidate models (i.e. $H_0$, $H_1$ and $H_2$). These give unambiguous support for a candidate if > 0.9 (Johnson & Omland 2004).

## 2.4. Discussion

The primary focus of this chapter was to establish a molecular and statistical framework by which to assess the incidence of hybridization between divergent *Symbiodinium* lineages. This is made difficult by their apparent haplontic life cycle, a lack of amenability to culture in many types (particularly in clade C *Symbiodinium*), and the paucity of well-characterized genetic markers. This study attempts to circumvent these obstacles by developing protocols to isolate and extract DNA from individual *Symbiodinium* cells, establish and quantify the dominant ribotype(s) within each genome, and test competing hypotheses explaining the observed pattern of intra-genomic variation. Using these techniques, a population of putative hybrids is identified inhabiting the reef building coral *Pocillopora damicornis* at the isolated, high-latitude reef of Lord Howe Island, Australia.

### *2.4.1. Method development*

The single-cell isolation and extraction method described here facilitated the rapid preparation of individual *Symbiodinium* cells prior to PCR (around 20 per hour), with the potential to be further improved with the application of flow-cytometry and fluorescence activated cell sorting (FACS). The protocol also showed good efficiency, with around 85% of isolated cells undergoing successful PCR amplification. The downstream application of DGGE and DNA sequencing successfully revealed the dominant ribotype(s) within individual cells, providing a reliable assessment of inter-genomic *ITS2* diversity within the *P. damicornis* symbiont consortium. Used in conjunction with plasmid cloning, this method could be used to evaluate levels of intra-genomic variation in other genetic markers, providing an important assessment of their phylogenetic utility.

The qPCR assay developed in this study offers sufficient sensitivity to quantify *ITS2* ratios at the subclade level. This represents a significant improvement in resolution from earlier clade-level assays (Ulstrup & van Oppen 2003; Loram *et al.* 2007a; Mieog *et al.* 2007; Correa *et al.* 2009; Yamashita *et al.* 2010; Cunning *et al.* 2013), since the subclade presents a more ecologically-relevant taxonomic unit (LaJeunesse 2005). This assay is also the first to quantify polymorphic rDNA sequences within individual *Symbiodinium* cells, and the second to do so in dinoflagellates (see also Brosnahan *et al.* 2010). This provides an important insight into the level of *ITS2* variation within the *Symbiodinium* genome, underscoring concerns about its utility in establishing diversity estimates (Thornhill *et al.* 2007), and its suitability for quantifying the dynamics of mixed infections (Mieog *et al.* 2007). In particular, substantial differences in rDNA copy numbers observed between *Symbiodinium* types C100 and C109 highlight the pitfalls of using *ITS2*-qPCR to estimate abundance ratios of coexisting symbionts without single-cell validation.

Finally, the statistical methodology developed here identifies admixture in symbiont populations based on intra-genomic *ITS2* ratios. Conflicting hypotheses of one, two and three coexisting populations were formulated, corresponding to the existence of a single symbiont clone harbouring a non-diagnostic polymorphism (NDP), the coexistence of two ‘pure’ (homogeneous) ribotypes, and mixed populations of genetically homogeneous and heterogeneous *Symbiodinium* cells, respectively. The model consistent with the latter hypotheses received unambiguous statistical support in all six *P. damicornis* colonies analysed. However, the model selection approach relies on forming a set of candidate models

that are representative of the biological processes under investigation (Johnson & Omland 2004). While the mixture model representing $H_2$ is consistent with a population of hybrids coexisting with parental genotypes (progenitors), it cannot explicitly infer this scenario. This is because a similar pattern could arise from the incomplete concerted evolution of ancestral polymorphisms (ICEAP).

### *2.4.2. Hybridization or incomplete concerted evolution of ancestral polymorphisms?*

The existence of both C100 and C109 ribotypes in the homogeneous condition affirms their status as diagnostic of separate *Symbiodinium* subclades (i.e. neither sequence represents a degenerating pseudo-gene). Furthermore, these two ribotypes differ at 5 variable nucleotide sites in the *ITS2* region (2% divergence), while NDPs typically feature a single nucleotide substitution or insertion/deletion (indel) that distinguish them from the dominant sequence variant (LaJeunesse 2005; Tonk *et al.* 2013). However, if both ribotypes were present within the genome of the most recent common ancestor of *Symbiodinium* C100 and C109, processes of concerted evolution may not have had sufficient time to homogenize the rDNA arrays of both taxa. Hence copies of the ribotype that is now diagnostic of the sister taxon may remain in the genome of one or both lineages. The *Symbiodinium* genome routinely hosts a diverse assemblage of *ITS2* sequences (Thornhill *et al.* 2007), and several putative cases of ICEAP appear in the literature. For example, the *ITS2* sequence diagnostic of *Symbiodinium glynni* (type D1) also occurs within the genome of *S. trenchii* (type D1a), with the incomplete displacement of a vestigial polymorphism invoked to explain their intra-genomic coexistence (Thornhill *et al.* 2007). However, several features of the data presented here suggest that an alternative explanation of hybridization should not be ruled out. First, the C100 and C109 sequences coalesce at the ancestral type C3, as opposed to either representing an intermediate evolutionary step toward the other (e.g. C103 and C118 in *P. damicornis* and C3hh and C3n in *Seriatopora hystrix*; see Figure 2.2b). If concerted evolution has not had sufficient time to homogenize all C109 rDNA repeats in the C100 genome, then vestigial copies of the intermediate C3 sequence would also likely persist as a non-dominant intra-genomic variant. Rather, the C3 sequence was not detected in any of the cells analysed, despite its characteristic DGGE band pattern (see Wicks *et al.* 2010, supplementary material). Second, concerted evolutionary processes rapidly homogenize intra-genomic co-dominance, either completely displacing a non-dominant polymorphism or leaving only background traces

(Baldwin *et al.* 1995; Wendel *et al.* 1995; Ganley & Scott 2002). This is inconsistent with the similar proportional abundance of *ITS2* polymorphisms within many of the genetically heterogeneous cells observed here, with more than a third of all symbionts featuring $C_{C100}$:$C_{TOTAL}$ ratios between 0.25 and 0.75. Finally, frequency troughs along the $C_{C100}$:$C_{TOTAL}$ spectrum depict a degree of genetic isolation between genetically heterogeneous *Symbiodinium* cells and either of the 'pure' genotypes (i.e. homogeneous C100 and C109 cells), consistent with the substantial fitness loss often experienced by $F_2$ and later-generation backcross genotypes (resulting from 'hybrid breakdown'; see Demuth & Wade 2005).

While hybridization represents a plausible explanation for the intra-genomic co-dominance of the C100 and C109 ribotypes, the distinction between hybridization and ICEAP remains ambiguous. Addressing this question will likely require a significant investment of resources, including the use of WGA and/or the generation of isoclonal cultures (in order to facilitate multi-locus genotyping analysis on individual cells by targeting nuclear microsatellites and/or single nucleotide polymorphisms), and continued attempts to induce the sexual life cycle, both within and between cultured *Symbiodinium* lineages. Next generation sequencing (NGS) platforms also offer tremendous potential for identifying processes underlying intra-genomic variation in *Symbiodinium*, enabling the identification of rare sequence variants and the generation of high-volume sequence data from large numbers of individuals (Arif *et al.* 2014; Thomas *et al.* 2014; Green *et al.* 2014). Another area requiring investigation is the morphological, physiological and ecological characterization of putative *Symbiodinium* hybrids. Concerted evolution operates *via* a series of stochastic processes that occur independently of natural selection (Dover 1982). By contrast, hybridization is often accompanied by drastic changes in morphology, performance and fitness (Barton & Bengtsson 1986; Barton 2001; Arnold 2007; Arnold & Martin 2010), even involving diversification into new habitats (Rieseberg *et al.* 2003). Investigating the form, function, distribution and ecology of genetically heterogeneous *Symbiodinium* cells may therefore provide further insight into the incidence and potential evolutionary effects of hybridization in this genus. The remaining chapters of this thesis are concerned with addressing these objectives.

### *2.4.3. Background symbiont populations*

The results of this study indicate that at least three *ITS2* genotypes can coexist within the symbiont consortium of *P. damicornis* (C100, C100/C109 and C109). While homogeneous *Symbiodinium* C109 cells were only ever detected at background levels (constituting less than 7% of the symbiont population, and possibly suggesting a non-homologous relationship with this host species), the biological relevance of this population may extend well beyond providing a presumably minor contribution to the overall productivity of the symbiosis. Genetically heterogeneous *Symbiodinium* cells outnumbered 'pure' genotypes in more than half of the colonies sampled, suggesting that rare sexual reproduction events between C100 and C109 may facilitate asexual hybrid proliferation, with potentially important functional implications for the coral colony. The evolutionary contribution of *Symbiodinium* C109 may be more important still, if hybrids create a 'bridge' for the migration of genetic material to the dominant C100 lineage (i.e. introgression; see Figure 2.1b). A small number of genetically heterogeneous symbionts featured $C_{C100}$:$C_{TOTAL}$ ratios near 0.75, and thus potentially represent $F_1$ × C100 backcross genotypes. However, this pattern could equally have arisen from ICEAP, differential rDNA inheritance in $F_1$ hybrids (arising from dissimilar copy-numbers between parent taxa; e.g. Brosnahan *et al.* 2010), or even concerted evolution acting to homogenize rDNA variability in the hybrid genome (e.g. Wendel *et al.* 1995). Establishing the incidence of introgression would initially require the identification of individual hybrid- and backcross classes (i.e. $F_1$ hybrid, $F_2$ backcross, etc.). This in turn requires the genotyping of a large number of individuals, and the analysis of at least 13-50 ancestry-informative loci per individual (Epifanio & Phillipp 1997; Fitzpatrick 2012). This project is not sufficiently resourced to carry out such a comprehensive task; however it does serve to highlight the perils of dismissing symbionts that persist in low abundance as biologically-irrelevant or simply representing surface contamination.

### *2.4.4. Conclusion*

While the results presented in this chapter do not provide unequivocal evidence of hybridization between divergent *Symbiodinium* lineages, they provide an initial 'proof of principle' for its occurrence. In doing so, this study draws attention to the important evolutionary implications that may accompany the generation of new genetic diversity in *Symbiodinium*, including the potential for rapid symbiont adaptation through introgression.

Progress in this area has been hindered by a lack of available methodology, an obstacle that is addressed here through the development of new molecular and statistical methods focussed on the individual *Symbiodinium* cell. Through the application of these techniques, colonies of *P. damicornis* inhabiting the reef of Lord Howe Island are identified as representing a putative *Symbiodinium* 'hybrid zone', requiring further molecular, morphological, physiological and ecological assessment. Additional development of this research may help to characterize and predict the evolutionary response of the coral-algal symbiosis to the many anthropogenic impacts currently threatening the world's coral reefs.

# Chapter 3: The spatiotemporal distribution of putative *Symbiodinium* hybrids

## 3.1. Introduction

Providing unequivocal evidence of hybridization has proven difficult in many species. In particular, the persistence of ancestral polymorphisms can leave a similar genomic signature to that of hybridization, and hence distinguishing between these fundamentally different evolutionary processes requires corroborative population-genetic, morphological, physiological and ecological evidence (Vriesendorp & Bakker 2005; Willis *et al.* 2006). Ecological data can be particularly useful for assessing the candidacy of genetically additive individuals as putative hybrids. While concerted evolutionary processes act independently of natural selection (Dover 1982), the ability of hybrids to survive and reproduce is strongly influenced by their biotic and abiotic environment (Lewontin & Birch 1966). As such, hybrids are generally more common at the ecological and/or geographical margin of the parental species range, where selection arising from competition with parents is weak (Arnold 1997; Rieseberg 1997), and opportunities exist for 'transgressive' hybrids to diversify into extreme habitats (see below).

The lack of competition and extreme abiotic conditions found in marginal habitats can create opportunities for hybrids to diversify into vacant niches, through a process called 'transgressive segregation'. When individuals from two divergent lineages cross, the majority of the many possible hybrid recombinants are generally inviable or unfit, since 'hybrid breakdown' arises from the segregation of co-adapted gene complexes or the creation of maladapted gene combinations (Barton 2001; Demuth & Wade 2005). However, the genetic variation created by hybridization can occasionally produce a fit genotype, that may escape this 'rat race' of unfit congeners (Seehausen 2004; Arnold & Martin 2010). Transgressive segregation, the emergence of 'extreme' hybrid phenotypes *via* recombination (Rieseberg *et al.* 1999, 2000; Seehausen 2004; Bell & Travis 2005), can enable hybrids to exploit new environments and even develop into stable, reproductively-isolated lineages (Rieseberg *et al.* 2003; Gompert *et al.* 2006). The ability of a fit hybrid recombinant to reproduce asexually can further increase its chances of establishing a foot-hold in a vacant niche, from where it may rapidly proliferate, stabilize, and adapt to the new conditions (Rieseberg *et al.* 2003).

The best-studied example of hybrid diversification *via* transgressive segregation occurs in the wild sunflower genus *Helianthus*. The hybrid species *H. paradoxus* acquired a particular combination of alleles from *H. annuus* and *H. petiolaris* that conferred additive phenotypic effects, resulting in substantial increases in succulence, calcium uptake, and sodium exclusion relative to both progenitor species (Lexer *et al.* 2003). Positive directional selection acting on these adaptations enabled the hybrid lineage to diversify into extremely saline marshes (Lexer *et al.* 2003; Rieseberg *et al.* 2003), where neither parental species can persist (Welch & Rieseberg 2002). Another hybrid species, *Helianthus deserticola*, diversified into arid areas by acquiring several transgressive 'desert adaptations', including reduced boron uptake, reduced leaf size, and rapid flowering (Rieseberg *et al.* 2003). Hybridization has thus been implicated in major ecological transitions, with hybrids commonly found beyond the range margins of parental taxa (Wang *et al.* 1990; Rieseberg 1991; Morrell & Rieseberg 1998; Rieseberg *et al.* 2003; Barrett *et al.* 2007; Hamilton *et al.* 2009).

Marginal coral reefs may provide a suitable environment in which hybrid diversification could occur. These habitats are characterized by extreme conditions such as atypically high or low temperatures, irradiance levels outside those required for optimum photosynthesis, and/or a reduction in quality of other parameters such as salinity, nutrient loads or pH (Kleypas *et al.* 1999). The world's southernmost coral reef at Lord Howe Island (Australia; 31°33'S) is situated at the transition zone between coral- and macroalgal-dominated benthic assemblages (Allen & Paxton 1974), and is regularly exposed to wide fluctuations in temperature, light and nutrient levels (Harriott & Banks 2002). The extreme abiotic conditions at LHI reef may therefore provide vacant adaptive peaks that select for extreme hybrid phenotypes. Indeed, the lack of evidence for hybridization among other *Symbiodinium* taxa despite several multi-locus genotyping studies (e.g. Santos *et al.* 2003b; Pettay *et al.* 2011; Thornhill *et al.* 2013a; LaJeunesse *et al.* 2014), suggests that if hybridization does occur in symbiotic dinoflagellates, it may well be confined to isolated, marginal habitats such as LHI.

This chapter aimed to assess the candidacy of genetically heterogeneous *Symbiodinium* cells as putative hybrids by examining their ecological characteristics and distribution patterns on the LHI reef. A bulk-cell qPCR method was developed to quantify the number of genetically heterogeneous *Symbiodinium* cells (putative hybrids) as a proportion of the total number of symbionts in the *P. damicornis* consortium (*Symbiodinium* $_{\text{HETEROGENEOUS}}$: *Symbiodinium* $_{\text{TOTAL}}$, hereafter abbreviated to $S_H$:$S_T$). Surveys of $S_H$:$S_T$ were carried out over three nested spatial scales and two summer-winter cycles. Three separate hypotheses were tested to

explain the spatial and temporal distribution of putative *Symbiodinium* hybrids. First, $S_H$:$S_T$ varies within and between *P. damicornis* colonies, and is additionally variable between geographically isolated reef sites. Second, $S_H$:$S_T$ varies within colonies through time, in response to cyclical changes in the abiotic environment. Third, site-averaged $S_H$:$S_T$ values correlate with one or more of a suite of environmental variables obtained from long-term environmental monitoring at the study sites.

## 3.2. Methods

### *3.2.1. Study location and species*

This study was carried out at the high-latitude, marginal coral reef at Lord Howe Island, Australia (-31.5, 159.1). The host species investigated was *Pocillopora damicornis*, a widely distributed reef-building coral that forms a dominant component of the LHI reef (Veron 2000; Miller & Ayre 2004). *P. damicornis* was previously shown to host *Symbiodinium* C100, C103 or C118, with the majority of colonies hosting C100 (Wicks *et al.* 2010). However, single-cell analysis revealed that these colonies also host a cryptic population of *Symbiodinium* C109 (Genbank accession number KJ530690; see chapter 2), and a third population of genetically heterogeneous symbionts, featuring both C100 and C109 ribotypes (see chapter 2). These symbionts may represent C100 × C109 hybrids, or alternatively, *Symbiodinium* cells that host a persistent ancestral polymorphism.

### *3.2.2. Coral sampling and preservation*

To analyse the spatial distribution of genetically heterogeneous *Symbiodinium* cells, and determine whether associations exist between local temperature conditions and their proportional abundance within the symbiont consortium ($S_H$:$S_T$), five *P. damicornis* colonies were sampled from each of eight LHI reef sites (Figure 3.1). Three terminal fragments were removed (using diagonal pliers) from each colony, preserved in DMSO preservation buffer (20% DMSO, 250 mM EDTA, NaCl saturated, pH 8.0; Seutin *et al.* 1991) and stored at -20 °C prior to DNA extraction. Colonies were sampled as near as possible to the *in situ* temperature data loggers operated by the Australian Institute of Marine Science (AIMS); however, a spacing of at least 2 m was maintained between colonies to reduce the risk of

sampling ramets. To explore the relationship between $S_H$:$S_T$ and depth (a proxy for irradiance), a more exhaustive sampling effort was carried out at a single reef margin site featuring a steep sloping profile (The Arch, where *P. damicornis* colonies occur from approximately 4-12 m). Twenty one additional colonies were sampled as above at roughly even intervals along the depth gradient, with their apical depth recorded using a dive computer (Suunto Gekko). Samples were collected within the space of ~ 10 min; therefore negligible differences in tidal height were assumed.

For temporal analysis of $S_H$:$S_T$, numbered cattle ear-tags were attached to five colonies from each of the three inner-lagoon sites (Sylph's Hole, North Bay and Comet's Hole) during March 2011. A single branch tip was sampled from each tagged colony during March 2011, September 2011, March 2012 and September 2012 (six-monthly sampling over 1.5 years). These sampling times were chosen to closely follow the thermal maxima and minima over two seasonal cycles, and hence establish the relationship between the relative abundance of putative hybrids and natural cyclical changes in seawater temperature.

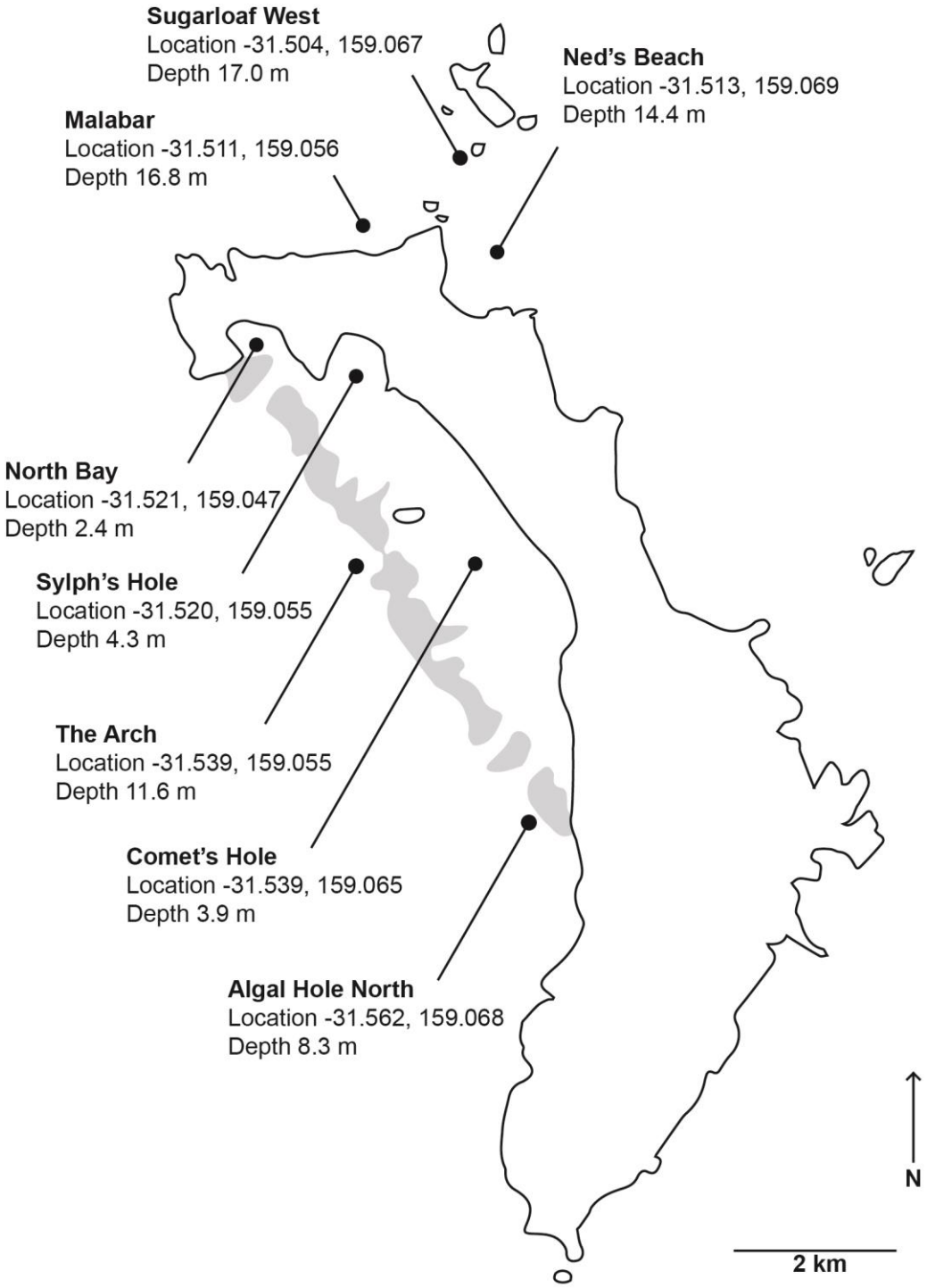


**Figure 3.1 Locations of study sites at Lord Howe Island**

Spatial surveys were carried out at the eight sites indicated. Temporal surveying was carried out at Comet's Hole, North Bay and Sylph's Hole, at six-monthly intervals from March 2011 to September 2012. Australian Institute of Marine Science (AIMS) data loggers are permanently deployed at all sites except The Arch, where a HOBO pendant logger was deployed from September 2011 to September 2012. Logger depths and coordinates are shown for each site.

### *3.2.3. Extraction of bulk-cell* Symbiodinium *DNA*

Preserved coral tissue was separated from the underlying skeleton by centrifugation through a fine plastic-coated wire mesh (grid size 1 mm; 16,100 x g for 10 s). The skeleton was discarded and 200 µl of DMSO buffer were added to the tissue homogenate. The sample was then vortexed and centrifuged for 10 min at 16,100 x g to separate the host and symbiont fractions. The supernatant (host fraction) was discarded and a further 200 µl DMSO buffer were added to the *Symbiodinium* pellet, which was re-suspended by milling without beads for 3 min at 50 Hz (Qiagen TissueLyser LT; Qiagen). A 10 µl sub-sample was added to a 1.7 ml micro-centrifuge tube containing 50 mg acid-washed glass beads (710-1180 µm; Sigma-Aldrich), and milled for 3 min at 50 Hz to disrupt the *Symbiodinium* cells and release nucleic acids. Following a 10 min incubation period at 4 °C, 90 µl of de-ionised water were added. The sample was then vortexed and centrifuged for 10 min at 16,100 x g to pellet cellular debris. The DNA-enriched supernatant (50 µl) was transferred to a new micro-centrifuge tube with an equal volume of 2-propanol for precipitation of nucleic acids, and centrifuged for 10 min at 16,100 x g to collect the DNA pellet. The supernatant was discarded and 200 µl of wash buffer (70% v/v ethanol) were added. The sample was vortexed and returned to the centrifuge for a further 10 min at 16,100 x g. The supernatant was carefully removed with a pipette and the DNA pellet dried under a laminar flow hood for 30 min. Elution buffer (10 mM Tris-HCl; 0.1 mM EDTA; pH = 8.0) was then added to a final volume of 50 µl. Following a 10 min re-hydration period, the DNA was eluted by milling without beads for 1 min at 30 Hz.

### *3.2.4. PCR and electrophoresis*

Denaturing gradient gel electrophoresis (DGGE) was carried out on all samples to establish the presence or absence of *Symbiodinium* types other than C100 and C109. PCR amplification for denaturing gradient gel electrophoresis (DGGE) was carried out with the primers ITSintfor2 and ITS2CLAMP (LaJeunesse 2002). Thermal cycling involved an initial denaturation step of 3 min at 95 °C followed by 40 cycles of 15 s at 95 °C, 15 s at 56 °C and 10 s at 72 °C (Applied Biosystems Veriti thermo-cycler; Life Technologies). Each PCR reaction contained 4 µl of DNA template solution, 1x MyTaq PCR reaction mix (Bioline), 10 pmol each primer, 10 µg bovine serum albumin (BSA; Sigma) and deionised sterile water to a total volume of 20 µl. A template-free control was included with each run. To ensure the

final product was within the intended size range (300-350 bp) and that amplification did not occur in the template-free control reaction, 5 µl of the final PCR product were electrophoresed on a 1.5% agarose gel containing 1x SYBR safe nucleic acid stain (Life Technologies) alongside a DNA standard (Hyperladder™ II; Bioline). Agarose gels were viewed and imaged on a blue light trans-illuminator (Safe Imager; Invitrogen). The remaining PCR product was loaded on a 200 x 200 x 1 mm, 8% denaturing polyacrylamide gel (25-50% denaturant gradient), and run in 1 x TAE at 150 V for 7 h at 60 °C (DCode system; BioRad) alongside known *ITS2* sequences of *Symbiodinium* C100 and C109 (extracted from plasmid DNA; see chapter 2 for cloning methods). Following electrophoresis, denaturing gels were stained with ethidium bromide and viewed on a UV trans-illuminator (FirstLight; UVP) and the presence or absence of each *ITS2* sequence type was recorded.

### *3.2.5. Quantification of genetically heterogeneous* Symbiodinium *cells*

To determine the proportional abundance of *ITS2* type C100 ($C_{C100}$:$C_{TOTAL}$) in bulk-cell *Symbiodinium* samples, quantitative PCR (qPCR) was carried out with the universal primers CInnerFor and CInnerRev, and the TaqMan fluorogenic probes $C100^{+}$ and $C100^{-}$ (see chapter 2 for nucleotide sequences). Each qPCR reaction contained 4 µl DNA template, 1x TaqMan Universal Mastermix II (Life Technologies), 18 pmol each primer, 1x TaqMan fluorogenic probe (Life Technologies), 10 µg BSA (Sigma-Aldrich) and deionised sterile water to a total volume of 20 µl. Thermal cycling involved an initial 10 min, 95 °C denaturation step followed by 40 cycles of 15 s at 95 °C and 1 min at 60 °C (Applied Biosystems StepOne quantitative PCR instrument; Life Technologies). $C_t$ values were determined as the cycle at which the change in fluorescence was significantly different to the background level ($\Delta R_n$ = 0.05; obtained using the instrument's built-in algorithm). Reactions featuring $C_t$ values below the standard curve intercept (36.873 and 37.119 for $C100^{+}$ and $C100^{-}$ assays, respectively; see *Appendix B*) and sufficiently low standard deviations (< 0.5) were included in the analysis. Plasmid DNA template solutions containing pure *Symbiodinium* C100 and C109 sequences were used to construct standard curves (see chapter 2 for cloning methods). To establish standard curve parameter estimates, 6 logarithm serial dilutions of C100 and C109 plasmid DNA were run in duplicate (10 pg $\mu l^{-1}$ to 0.1 fg $\mu l^{-1}$; corresponding to approximately 2,120,000 and 21 *ITS2* copies $\mu l^{-1}$, respectively). DNA template solutions generated from bulk-cell *Symbiodinium* samples were run in duplicate with a template-free control included

for each probe type. The total number of *ITS2* copies ($C_{TOTAL}$) within each sample was estimated as the sum of the C100 copy number ($C_{C100}$) and the number of *Symbiodinium* clade C *ITS2* sequences other than type C100 (as determined by mean $C_t$ values derived from $C100^+$ and $C100^-$ assays, respectively). The proportion of total *Symbiodinium* clade C sequences that were of type C100 was expressed as the bulk-cell $C_{C100}$:$C_{TOTAL}$ ratio.

The proportional abundance of genetically heterogeneous *Symbiodinium* cells ($S_H$:$S_T$) was derived from the bulk-cell $C_{C100}$:$C_{TOTAL}$ ratio using parametric information generated from single-cell qPCR analysis carried out in chapter 2. For each of the six colonies sampled in the chapter 2 analysis, the proportion of individuals assigned to the heterogeneous mixture-model component (see Table 2.2) was plotted against the bulk-cell $C_{C100}$:$C_{TOTAL}$ ratio. A downward parabola was fitted to the bivariate data (form $y = ax^2 + bx$; $a < 0$; where $y = S_H:S_T$ ; $x = C_{C100}:C_{TOTAL}$) using the curve fitter function in Sigmaplot v11.0 (Systat). The bulk-cell $C_{C100}$:$C_{TOTAL}$ ratio approximated $S_H$:$S_T$ *via* the second-order polynomial relationship $y = -3.4484x^2 + 3.3604x$ (Figure 3.2). The parameters generated in this analysis were then used to predict $S_H$:$S_T$ from bulk-cell *ITS2* ratios obtained from each coral sample in the spatiotemporal distribution analysis.

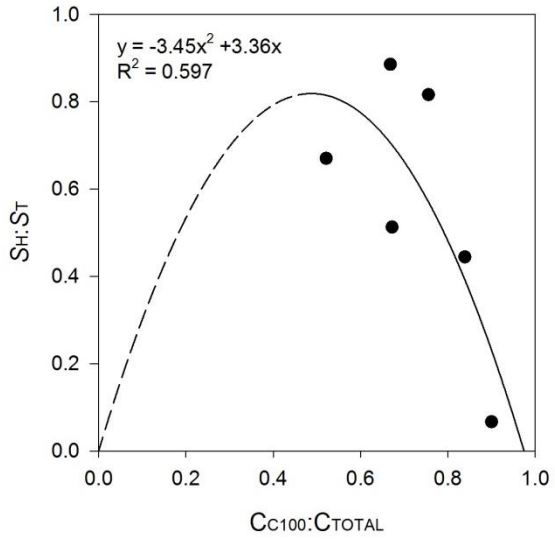


**Figure 3.2 Estimating the proportional abundance of putative *Symbiodinium* hybrids** The application of bulk-cell qPCR enabled the rapid approximation of $S_H$:$S_T$ without the need for single-cell analysis. The qPCR-generated $C_{C100}$:$C_{TOTAL}$ ratio (bulk-cell) predicted the $S_H$:$S_T$ values generated in chapter 2 *via* the polynomial relationship $y = -3.45x^2 + 3.36x$. The curve section from x = 0 to x = 0.5 is shown by a dashed line, since none of the six colonies analysed in chapter 2 or the 61 *P. damicornis* colonies analysed in the present chapter produced $C_{C100}$:$C_{TOTAL}$ ratios less than 0.5.

### *3.2.6. Water temperature monitoring*

To determine whether the distribution of putative *Symbiodinium* hybrids is associated with the local temperature regime, environmental data were obtained from the *in situ* data loggers operated by the Australian Institute of Marine Science (AIMS). Monthly average temperatures from March 2009 to August 2012 were downloaded from the AIMS public website (accessed from http://www.data.aims.gov.au/ on 20/03/2014). These loggers continuously record seawater temperatures at Algal Hole North, Comet's Hole, Malabar, Ned's Beach, North Bay, Sugarloaf West and Sylph's Hole (Figure 3.1). An eighth logger also permanently monitors water temperatures at Wheatsheaf Islet (adjacent to Ball's Pyramid, 20 km to the southeast of Lord Howe Island); however *P. damicornis* colonies were not found at this site despite a thorough sampling effort. AIMS loggers are occasionally retrieved for battery replacement or repairs (I. Kerr, LHIMPA, pers. comm.). To correct for bias associated with these logging gaps, sites featuring missing data were paired with their most proximal site for which logging was continuous from March 2009 to August 2012. A correlation analysis was carried out using the available simultaneous measurements, and missing data were estimated using the slope and intercept of the fitted line (see *Appendix B*). In lieu of an AIMS logger at The Arch, a HOBO pendant logger (Onset Computer Corporation) was deployed at a depth of 11.6 m from 18/09/2011 to 31/08/2012 (measuring and logging temperature at 15 min intervals). Data obtained from this instrument were visually checked for spurious values, month-averaged and temporally aligned with temperature values measured by the AIMS logger deployed at Algal Holes (for which continuous month-averaged temperatures were available from March 2009 to August 2012, inclusive). Month-averaged temperatures at The Arch prior to September 2011 were estimated using correlation analysis as described above, with Algal Hole North used as the predictor site (see *Appendix B*). For each of the study sites, a four-parameter sine function of the form

$$y = a\sin\left(\frac{2\pi x}{b} - c\right) + d \qquad \textbf{Equation 3.1}$$

was fitted to monthly mean temperature data using the curve fitter function in Sigmaplot v11.0 (Systat). The fitted temperature mean ($d$), maximum ($d + a$), minimum ($d – a$), and range ($2a$) were extracted as candidate predictor variables for regression against site-averaged $S_H$:$S_T$ ratios.

### *3.2.7. Statistical analysis*

Spatiotemporal variation in $S_H$:$S_T$ was assessed using a combination of repeated measures analysis of variance (rmANOVA), nested univariate ANOVA and linear regression. Spatial variability in $S_H$:$S_T$ within and between *P. damicornis* colonies was modelled using two-factor nested ANOVA, with *Site* (eight levels, random) and *Colony(Site)* (colony nested within site; five levels, random) as hierarchical factors and *Branch* as the residual. Temporal variation in $S_H$:$S_T$ within and between colonies was assessed using rmANCOVA with *Time* as a within-subject factor (four levels, fixed), *Site* as a between-subject factor (3 levels, random) and *Colony* as the residual. Relative variance components for random effects were estimated using the MINQUE procedure (Rasch & Mašata 2006). In order to assess the effect of depth (a proxy for irradiance) on $S_H$:$S_T$ within colonies, a linear regression analysis was carried out with colony-$S_H$:$S_T$ as the dependent variable and depth (in metres) as the explanatory variable. To establish the best predictor(s) for site-averaged $S_H$:$S_T$, a multiple linear regression analysis was carried out using stepwise addition of candidate explanatory temperature variables (mean, minimum, maximum and range). For each linear model analysis, assumptions of variance homoscedasticity and residual normality were validated using Levene's and Shapiro-Wilk tests, respectively. Statistical analyses were carried out using R v2.13.2 (R Development Core Team 2011) and SPSS Statistics v20 (IBM).

## 3.3. Results

### *3.3.1. Spatiotemporal distribution patterns*

Investigating the spatiotemporal distribution of putative hybrid symbionts involved the analysis of 186 individual branches taken from a total of 61 *P. damicornis* colonies, sampled from eight reef sites around Lord Howe Island. *Symbiodinium* C100 represented the dominant *ITS2* type in all colonies and branches analysed. Approximately two thirds of the colonies also produced a non-dominant DGGE band representative of *Symbiodinium* C109 (41 colonies; see *Appendix B*). No other *Symbiodinium* sequences were detected in this study, including the rare types C103 and C118 previously identified from *P. damicornis* at LHI (Wicks *et al.* 2010). This may arise from differences in host-identification specificity between studies. For example, two ambiguous Sylph's Hole colonies omitted from the present study

(that appeared to be the *P. damicornis* × *Stylophora pistillata* hybrids described by Miller & Ayre 2004) were later found to exclusively host *Symbiodinium* C118 (unpublished data).

The proportional abundance of genetically heterogeneous *Symbiodinium* cells within colonies ($S_H$:$S_T$) ranged from 0.10 to 0.82 (corresponding to bulk-cell $C_{C100}$:$C_{TOTAL}$ ratios of 0.9438 and 0.516, respectively; see *Appendix B*). The $C_{C100}$:$C_{TOTAL}$ ratio was generally reflected in the relative intensity of C100- and C109-diagnostic bands observable on the DGGE gel. Both bands were universally visible in samples where genetically heterogeneous cells constituted more than 60% of the symbiont consortium ($S_H$:$S_T$ > 0.6; $C_{C100}$:$C_{TOTAL}$ < 0.74), while the C109-diagnostic band was either not visible or difficult to detect in samples where less than half of the resident symbionts were classified as heterogeneous ($S_H$:$S_T$ < 0.5; $C_{C100}$:$C_{TOTAL}$ > 0.78; see *Appendix B*). Samples featuring an intermediate proportional abundance of genetically heterogeneous cells (0.6 < $S_H$:$S_T$ < 0.5) either produced a DGGE profile diagnostic of C100 in isolation or that of both C100 and C109, underscoring the limitations of applying this method for DNA quantitation.

The distribution of putative *Symbiodinium* hybrids was variable between colonies over spatial scales of metres to tens of metres, and even more so between sites separated by hundreds to thousands of metres. The majority of spatial variation in $S_H$:$S_T$ partitioned at the level of *Colony(Site)* (colony nested within site; $F_{32,80}$ = 58.76; p < 0.001; 72% of total variance explained; Table 3.1), with colony-averaged $S_H$:$S_T$ values ranging from 0.142 to 0.813. A significant proportion of spatial variation also partitioned at the *Site* level (24% of total variance explained; $F_{7,32}$ = 2.72; p = 0.025; Table 3.1), with site-averaged $S_H$:$S_T$ ratios ranging from 0.323 (Sylph's Hole) to 0.613 (Ned's Beach). However, the proportional abundance of genetically heterogeneous *Symbiodinium* cells was highly conserved between branches within colonies (4% residual variance component; Table 3.1). Furthermore, $S_H$:$S_T$ did not vary within colonies through time. A longitudinal survey of 15 tagged *P. damicornis* colonies at North Bay, Sylph's Hole and Comet's Hole over two summer winter cycles showed a distinct lack of temporal variation in the proportional abundance of genetically heterogeneous *Symbiodinium* cells (Pillai's Trace p = 0.509 and 0.217 for *Time* x *Site* interaction and *Time* main effect, respectively; Table 3.2). When reduced to a two-factor nested ANOVA model ($S_H$:$S_T$ ~ *Site* + *Colony(Site)*; *Branch* as the residual with temporal replication), the error variance accounted for a similar proportion of the total variance in $S_H$:$S_T$ as was explained in the original spatially-nested analysis (3.8%; Figure 3.4a; Table 3.3).

**Table 3.1 Nested ANOVA for spatial distribution of putative *Symbiodinium* hybrids**

| Source of variation | SS | Hypothesis df | Error df | *F* | *P* | Variance component | Variance explained |
|---|---|---|---|---|---|---|---|
| **Between sites** | 1.048 | 7 | 32 | 2.718 | < 0.001 | 0.006 | 24% |
| **Between colonies within sites** | 1.763 | 32 | 80 | 58.761 | 0.025 | 0.018 | 72% |
| **Between branches within colonies (residual)** | 0.075 | 80 | | | | 0.001 | 4% |

**Table 3.2 Repeated measures ANOVA for temporal changes in putative hybrid abundance**

| Source of variation | | SS | Hypothesis df | Error df | *F* | *P* |
|---|---|---|---|---|---|---|
| **Within colonies** | *Time* | 0.002 | 3 | 36 | 1.112 | 0.357 |
| | *Time* × *Site* | 0.005 | 6 | 36 | 1.180 | 0.339 |
| **Between colonies** | *Site* | 0.029 | 2 | 12 | 0.576 | 0.577 |

**Table 3.3 Reduced nested ANOVA for temporal changes in putative hybrid abundance**

| Source of variation | SS | Hypothesis df | Error df | *F* | *P* | Variance component | Variance explained |
|---|---|---|---|---|---|---|---|
| **Between inner-lagoon sites** | 0.114 | 2 | 12 | 0.576 | 0.577 | 0* | 0% |
| **Between colonies within inner-lagoon sites** | 1.191 | 12 | 45 | 150.242 | < 0.001 | 0.025 | 96.2% |
| **Between time-points within colonies (residual)** | 0.030 | | | | | 0.001 | 3.8% |

*Rounded to zero, since estimated variance component was negative

### *3.3.2. Environmental niche partitioning*

Thermal characteristics were variable within and between sites, with the inner-lagoon Sylph's Hole reef experiencing the highest level of seasonal temperature variability (Figure 3.3). This poorly-flushed site experienced the warmest summer maximum and coolest winter minimum during the logging period (March 2009 to August 2012; fitted values = 17.56 °C and 25.18 °C, respectively). Monthly averages and raw data values were occasionally more extreme than the fitted maxima and minima of the climate model, particularly during the anomalously warm summer of 2009/2010 (Figure 3.3). Monthly temperature averages at Sylph's Hole ranged from 17.06 °C in August 2012 to 26.25 °C in January 2010, while actual 10-min logging values at this site ranged from 14.91 °C during July 2011 to 28.05 °C during January 2010. The absolute maximum temperature of 28.16 °C was recorded at Comet's Hole during January 2010. Of the four candidate predictor variables assessed in the stepwise multiple regression analysis (model-fitted temperature mean, minimum, maximum, and range), the fitted thermal maximum emerged as the sole significant predictor of $S_H$:$S_T$ ($F_{1,6} = 23.137$; $p = 0.003$; Figure 3.4b-e). The linear relationship between maximum temperature and $S_H$:$S_T$ featured a strong negative correlation ($R^2 = 0.794$), with a 0.5 °C increase in the thermal maximum (from 24.7 °C to 25.2 °C) corresponding to a 35% reduction in $S_H$:$S_T$. Finally, no clear correlation between $S_H$:$S_T$ and depth was evident among 26 *P. damicornis* colonies sampled along their natural bathymetric distribution at a sloping reef-margin site (The Arch; linear regression, $F_{1,24} = 2.222$; $p = 0.149$; $R^2 = 0.085$; Figure 3.4b).

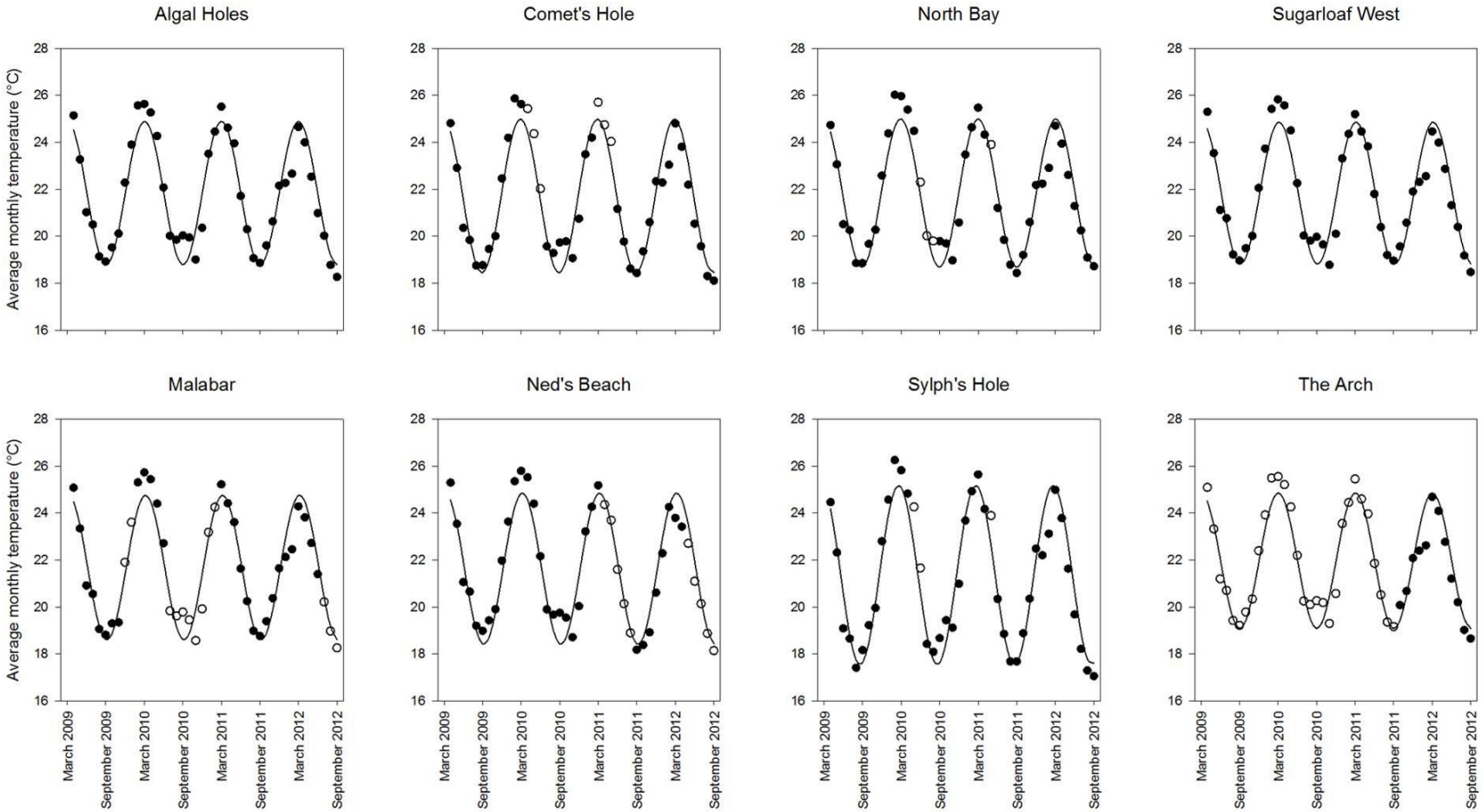


**Figure 3.3 Thermal characteristics of eight Lord Howe Island reef sites**

Average monthly temperatures obtained from data-logger measurements are shown in closed circles. Open circles show average monthly temperatures during logging gaps, estimated using correlation analysis against sites from which continuous measurements were available. Measurements from Algal Hole North, Comet's Hole, Malabar, Ned's Beach, North Bay, Sugarloaf West and Sylph's Hole were acquired from the Australian Institute of Marine Science (AIMS). Measurements from The Arch were obtained from a HOBO data logger, deployed from September 2011 to September 2012. Overlying fitted curves are optimized four-parameter sine functions. Note that extensive coral bleaching occurred during early 2010 (Harrison *et al.* 2011).

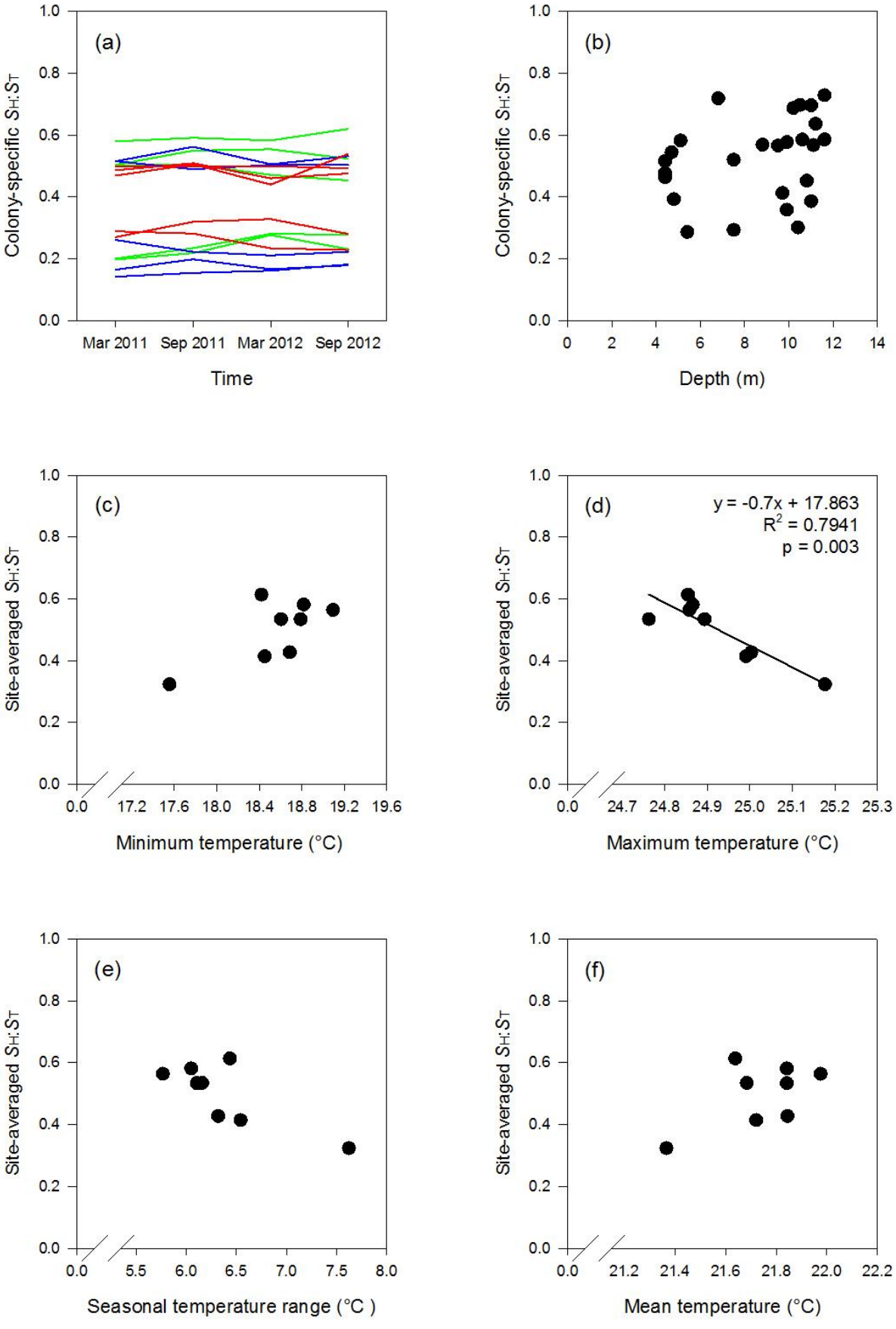
(a)
Colony-specific $S_H:S_T$
1.0
0.8
0.6
0.4
0.2
0.0
Mar 2011
Sep 2011
Mar 2012
Sep 2012
Time
(b)
Colony-specific $S_H:S_T$
0
2
4
6
8
10
12
14
Depth (m)
(c)
Site-averaged $S_H:S_T$
0.0
17.2
17.6
18.0
18.4
18.8
19.2
19.6
Minimum temperature (°C)
(d)
y = -0.7x + 17.863
$R^2$ = 0.7941
p = 0.003
Site-averaged $S_H:S_T$
24.7
24.8
24.9
25.0
25.1
25.2
25.3
Maximum temperature (°C)
(e)
Site-averaged $S_H:S_T$
5.5
6.0
6.5
7.0
7.5
8.0
Seasonal temperature range (°C )
(f)
Site-averaged $S_H:S_T$
21.2
21.4
21.6
21.8
22.0
22.2
Mean temperature (°C)

**Figure 3.4 (previous page) Niche partitioning of putative *Symbiodinium* hybrids**
The proportional abundance of genetically heterogeneous *Symbiodinium* cells ($S_H$:$S_T$) was characterized by: (a) temporal stability within coral colonies over two summer-winter cycles (colonies from Comet's Hole are shown in red, North Bay in green and Sylph's Hole in blue); (b) no association between depth and colony-averaged $S_H$:$S_T$ at a steeply sloping reef-margin site (The Arch); and (c-f) relationships between site-averaged $S_H$:$S_T$ and four candidate thermal predictor variables extracted from the climate model. Of the model-fitted thermal minimum (c), thermal maximum (d), seasonal temperature range (e), and temperature mean (f), only the thermal maximum showed a significant (negative) correlation with $S_H$:$S_T$.

## 3.4. Discussion

This study explored the relationship between the physical environment and the abundance of putative *Symbiodinium* hybrids. The methods described in chapter 2 were expanded in order to measure the proportional abundance of putative hybrids in mixed *Symbiodinium* communities, facilitating a thorough investigation of their spatiotemporal distribution. Each coral colony hosted a specific proportion of putative *Symbiodinium* hybrids that remained stable over two summer-winter cycles. The data show an absence of competition or within-colony niche partitioning between genetically homogeneous and heterogeneous symbionts; however thermal niche-partitioning was evident between colonies hosting different proportional abundances of putative hybrid symbionts. Corals dominated by these symbionts were comparatively rare within the lagoon, but abundant at the reef margin near the transition zone between coral- and macroalgal-dominated benthic communities. While this may have resulted from fine-scale population structure (by geographic distance or physical resistance to connectivity), the significant correlation with maximum temperature strongly suggests a thermal basis for the observed distribution pattern.

### *3.4.1. Method development*

A primary outcome of this study was the quantification of genetically heterogeneous *Symbiodinium* cells using bulk-cell qPCR, a development that circumvented the need to carry out single-cell analysis on each coral colony. rDNA markers (such as the *ITS2*) have been targeted in several quantitative assessments of mixed-clade infections (Ulstrup & van Oppen 2003; Loram *et al.* 2007a; Mieog *et al.* 2007; Venn *et al.* 2008; Correa *et al.* 2009; LaJeunesse *et al.* 2009; Yamashita *et al.* 2010; Green *et al.* 2014). When properly calibrated,

these assays can provide reliable estimates of symbiont relative abundance, despite the high variability in rDNA total copy-numbers often detected between *Symbiodinium* cells (Loram *et al.* 2007a; Mieog *et al.* 2007). In this study, the use of the *ITS2* in determining symbiont community dynamics was validated by single-cell analysis in conjunction with a robust statistical method (model selection; Burnham & Anderson 2002). Yet the conversion of bulk-cell *ITS2* ratios ($C_{C100}$:$C_{TOTAL}$) to the proportional abundance of genetically heterogeneous *Symbiodinium* cells ($S_H$:$S_T$) was supported by a small sample size and only a moderate correlation (six coral colonies; $R^2 = 0.6$), representing an obvious weakness in this analysis. Furthermore, the identification of *Symbiodinium ITS2* types was based on DGGE, an electrophoretic method that lacks sensitivity in detecting background symbiont taxa (Thornhill *et al.* 2006b; LaJeunesse *et al.* 2008). DGGE yielded a minimum $C_{C100}$:$C_{TOTAL}$ detection limit of approximately 15% for nested PCR (see chapter 2) and ~ 20% for direct PCR amplification; therefore other cryptic symbiont types may have gone undetected. Another limitation of DGGE involves sequence co-migration. Though unlikely, other symbiont types may have been present and remained undetected. For example, the C103 sequence migrates to a similar position on the denaturing gradient as C109 (see Wicks *et al.* 2010, supplementary material). These limitations may eventually be overcome through the application of quantitative next-generation sequencing (NGS) to individual cells. Nonetheless, the bulk-cell qPCR method developed here showed an adequate ability to quantify ratios of genetically heterogeneous and homogeneous cells in the *P. damicornis* symbiont consortium.

### *3.4.2. The spatiotemporal distribution of putative* Symbiodinium *hybrids*

Genetically heterogeneous and homogeneous *Symbiodinium* cells were co-dominant within many *P. damicornis* colonies, with $S_H$:$S_T$ values ranging from 15% to 82%. This finding contrasts with several quantitative analyses of mixed-clade infections, in which the most common condition involves a single dominant type coexisting with one or a few cryptic/background populations (Ulstrup & van Oppen 2003; Mieog *et al.* 2007; Correa *et al.* 2009; LaJeunesse *et al.* 2009; Yamashita *et al.* 2010; Byler *et al.* 2013; Cunning *et al.* 2013). For example, in five host species that hosted mixed-clade *Symbiodinium* assemblages, the abundance ratio of non-dominant to dominant symbionts ranged from $10^{-3}$ to $10^{-6}$ (Correa *et al.* 2009). Where symbiont co-dominance does exist, it generally involves either competitive

displacement or within-colony niche-partitioning (Rowan & Knowlton 1995; Rowan *et al.* 1997; van Oppen *et al.* 2001; Ulstrup & van Oppen 2003; Chen *et al.* 2005; Ulstrup *et al.* 2006, 2007; Thornhill *et al.* 2006b; LaJeunesse *et al.* 2010b; Pettay *et al.* 2011). For example, Caribbean *Montastraea* (= *Orbicella*) *annularis* colonies can simultaneously host members of *Symbiodinium* clades A, B and C, with clade C dominating shaded sides, clade B dominating the light-exposed tips and clade A occupying intermediate irradiance-microhabitats (Rowan *et al.* 1997). In a conspicuous example of competition among mixed symbionts, a temporary outbreak of the opportunistic type $B1_{Aiptasia}$ (= *Symbiodinium minutum*) was visible as yellow patches on branches of *Pocillopora* spp. following a cold-water bleaching event in the Gulf of California (LaJeunesse *et al.* 2010b).While samples were not taken from all physical aspects of colonies in the present study, the relative abundance of genetically homogeneous and heterogeneous *Symbiodinium* cells was noticeably uniform across the topography of all colonies. Indeed, the ~ 4% of total $S_H$:$S_T$ variation that was detected within colonies is likely to be an inflated estimate, since this residual variance component also encompasses pipette- and instrument-error. The co-dominant, uniform distribution pattern of coexisting *Symbiodinium* cells within colonies suggests that neither genotype shows opportunistic tendencies, and that symbiont niche-partitioning does not occur within *P. damicornis* colonies.

A lack of competition between genetically homogeneous and heterogeneous *Symbiodinium* cells is further indicated by the absence of dynamic symbiont shuffling. By contrast, competition between symbionts for host resources generally manifests in transient infections or temporal fluctuations in relative abundance (e.g. Thornhill *et al.* 2006; Jones *et al.* 2008; LaJeunesse *et al.* 2009, 2010). The temporal stability in $S_H$:$S_T$ observed here also suggests that the consortium dynamic is not affected by natural fluctuations in the physical environment, as evident in other corals and symbiotic anemones that host mixed *Symbiodinium* infections (Chen *et al.* 2005; Venn *et al.* 2008). Rather, it indicates that either symbiont shuffling is prompted by severe environmental disturbance, through selective symbiont expulsion/regeneration during bleaching (*sensu* Yamashita *et al.* 2010), or non-competitive clonal genotypes establish during early ontogeny/gametogenesis (*sensu* Padilla-Gamiño *et al.* 2012) and are not subject to further modification. Several cases of bleaching-induced symbiont shuffling are reported from tagging and transplantation studies (Baker 2001; Toller *et al.* 2001b; Berkelmans & van Oppen 2006; Thornhill *et al.* 2006b; Jones *et al.* 2008; LaJeunesse *et al.* 2009). Yet in studies employing long-term, follow-up monitoring, the

eventual return to dominance of a homologous type is usually evident (Thornhill *et al.* 2006b; Jones *et al.* 2008; Sampayo *et al.* 2008; LaJeunesse *et al.* 2009). While no observable bleaching occurred during this study, a severe bleaching episode affected the LHI lagoon approximately one year prior to the first round of sampling (Harrison *et al.* 2011). Therefore, if bleaching did cause symbiont shuffling in adult colonies, at least some readjustment in $S_H$:$S_T$ would likely have been observed during this study. The pronounced temporal conservation in $S_H$:$S_T$ within colonies despite previous bleaching suggests that, although thermal stress is important in determining symbiont ratios (see next section), this most likely occurs through early ontogenetic flexibility or natural selection acting on juvenile and/or larval stages.

### *3.4.3. Niche partitioning of putative* Symbiodinium *hybrids and progenitors*

The summer thermal maximum emerged as a significant predictor of $S_H$:$S_T$, while the thermal minimum, average temperature, seasonal temperature variability, and depth (a proxy for irradiance) did not have any detectable influence. Colonies dominated by genetically heterogeneous *Symbiodinium* cells were more common at the reef-margin sites than in the lagoon, where reduced circulation stimulates more pronounced thermal maxima (I. Kerr, LHIMPA, pers. comm.). A degree of niche partitioning between genetically homogeneous and heterogeneous symbionts therefore appears to be supported by differences in thermal tolerance. Symbiont niche partitioning is evident both within and between colonies of many coral species, with temperature and irradiance identified as key drivers (Rowan & Knowlton 1995; Rowan *et al.* 1997; van Oppen *et al.* 2001; Ulstrup & van Oppen 2003; Iglesias-Prieto *et al.* 2004; Ulstrup *et al.* 2006; Berkelmans & van Oppen 2006; Sampayo *et al.* 2007). This pattern is attributable to the evolution of physiological adaptations that enable survival in a particular light or thermal habitat, and the out-competition of extrinsic or generalist types (Ulstrup & van Oppen 2003). The observed thermal niche partitioning between genetically homogeneous and heterogeneous *Symbiodinium* cells therefore supports their delineation as separate genetic and ecological entities, lending further credibility to the hypothesis of symbiont hybridization.

Hybrids are often rapidly out-competed by their progenitors when in the parental habitat (e.g. Brasier 2001). Reduced hybrid fitness is particularly conspicuous in haploids, since detrimental effects arising from the segregation of co-adapted gene complexes during

recombination (hybrid breakdown) cannot be compensated for by heterosis (i.e. 'hybrid vigour' arising from increased heterozygosity in early generation hybrids; Charlesworth & Charlesworth 1987). The reduced abundance of genetically heterogeneous *Symbiodinium* cells within the LHI lagoon is consistent with reduced hybrid fitness in this habitat; yet their ecological prosperity at the transitional reef margin sites remains an intriguing puzzle. The diversification of transgressive hybrids into this 'extreme' habitat presents a plausible explanation that warrants further investigation. In this context, a large-scale assessment of hybrid abundance along a latitudinal gradient spanning both tropical and sub-tropical reefs would provide a valuable contribution to this research.

### *3.4.4. Conclusion*

The application of bulk-cell qPCR enabled the rapid estimation of the proportional abundance of genetically heterogeneous *Symbiodinium* cells in *P. damicornis* colonies. This facilitated a comprehensive assessment of the spatiotemporal distribution of these putative *Symbiodinium* hybrids. Negligible variability in symbiont abundance ratios within colonies suggested an early ontogenetic establishment of a few non-competitive clonal genotypes. While homogeneous and heterogeneous *Symbiodinium* cells were relatively co-dominant within many colonies, a degree of thermal niche-partitioning was evident between *P. damicornis* colonies hosting different symbiont abundance ratios. Specifically, those dominated by heterogeneous symbionts were common at the reef margin, and comparatively rare at the inner lagoon sites that experience more pronounced thermal peaks. Ecological differentiation between genetically homogeneous and heterogeneous *Symbiodinium* cells lends further credibility to the occurrence of hybridization, and may indicate the diversification of hybrids into the 'extreme' habitat at the margin of coral- and macroalgal-dominated benthic assemblages.

# Chapter 4: The form and function of putative *Symbiodinium* hybrids

## 4.1. Introduction

Natural hybridization has played defining roles in the evolution of many species. New genetic variation is created through the migration of genetic material between lineages, *via* the repeated backcrossing of hybrids to parental lineages (introgression; Arnold 2007). Additionally, the substantial genetic variation or 'macro-mutation' that is created during outcrossing has led to several cases of hybrid speciation, and even adaptive radiations in plant and animal taxa (Rieseberg 1997; Bell & Travis 2005; Grant *et al.* 2005; Mallet 2007). However, the potential for hybridization to contribute to adaptation depends on the fitness of $F_1$ hybrids and later-generation hybrid and backcross classes (i.e. $F_2$, $F_3$, etc.; Barton 2001). In particular, gene flow will not overcome barriers of reproductive isolation if the mean fitness of any of the intermediate backcross classes is insurmountably low (Barton & Bengtsson 1986; Ingvarsson & Whitlock 2000; see chapter 2, Figure 2.1). If considerable time has passed since divergence, the vast majority of the innumerable possible hybrid and backcross recombinants will be inviable or unfit, representing biological 'dead ends' with little or no evolutionary significance (Barton 2001). This poor relative fitness arises from epistatic 'hybrid breakdown', the segregation of co-adapted gene complexes or the creation of maladapted gene combinations (Demuth & Wade 2005). Early-generation hybrid breakdown is particularly evident in haploids, whose unpaired chromosomes cannot compensate for the detrimental effects of recombination *via* heterosis (i.e. 'hybrid vigour' arising from increased heterozygosity in diploid or polyploid hybrids; Charlesworth & Charlesworth 1987). In extreme cases, post-zygotic lethality can result from the failure to proceed from meiotic to mitotic cell division (e.g. Brosnahan *et al.* 2010). However, hybrid performance and fitness may occasionally equal or even exceed those of either parent taxon, where conditions are experienced between or outside their environmental optima (Anderson & Stebbins 1954; Arnold & Hodges 1995; Rieseberg *et al.* 2003; Arnold & Martin 2010). Under such conditions, the rate of gene-flow increases and hybridization can stimulate rapid adaptation (Ingvarsson & Whitlock 2000).

Genetically heterogeneous *Symbiodinium* cells can form an abundant component of the symbiont consortium of *P. damicornis* (> 80%; see chapters 2 and 3). The fitness of at least one heterogeneous clone therefore appears sufficient to overcome the selective pressures imposed by the abiotic environment and the coral host. Indeed, the considerable variation in *ITS2* ratios and total copy numbers (see chapter 2) suggest that genetically heterogeneous symbiont populations may be comprised of several fit clonal genotypes. If frequent hybridization underlies this genetic variation, the fitness of each of the many different hybrid recombinants is likely to be correspondingly variable (Barton 2001). Addressing the question of hybrid fitness may be simplified by determining the average fitness of each discrete hybrid class. However, even if the occurrence of hybridization between *Symbiodinium* C100 and C109 can be confirmed, the frequency distribution of *ITS2* ratios in a population (e.g. chapter 2, Figure 2.4) may not provide sufficient resolution to distinguish between classes. This is because variation in *ITS2* ratios may arise from multiple processes, including concerted evolution acting on ancestral polymorphisms, differential rDNA inheritance (arising from dissimilar copy-numbers in parent taxa; e.g. Brosnahan *et al.* 2010), the occurrence of backcrossing, and even the rapid homogenization of intra-genomic variation following hybridization (Wendel *et al.* 1995). The analysis of multiple diagnostic loci is therefore required to establish the incidence of hybridization and backcrossing, and evaluate the fitness of each hybrid class (Nason & Ellstrand 1993; Epifanio & Phillipp 1997; Fitzpatrick 2012). Though technically possible, this is currently a challenging task for individual cells (Handyside *et al.* 2004).

The resource limitations of this project preclude the unambiguous confirmation of genetically heterogeneous *Symbiodinium* cells as hybrid and backcross genotypes. However, it is currently possible to broadly classify individuals into putative-hybrid or non-hybrid classes using mixture-model clustering (see chapter 2), enabling an initial comparative assessment of their performance and fitness relative to the putative progenitor *Symbiodinium* C100. This chapter aims to establish whether genetically homogeneous and heterogeneous *Symbiodinium* cells show overall differences in morphology, physiology and performance, and if so, whether the relative abundance of each type in the symbiont consortium influences the functioning of the coral symbiosis. Assessments of coral- and symbiont physiology were made at both ambient and artificially-elevated seawater temperatures (25 and 29 °C, respectively) to explore the influence of thermal stress on the performance of each symbiont cell-type. The hypotheses tested were that: (1) genetically homogeneous and heterogeneous

*Symbiodinium* cells show differences in morphology and photo-physiology; (2) corals hosting different proportions of genetically homogeneous and heterogeneous symbionts show corresponding physiological differences; and (3) elevated temperatures exacerbate the functional disparities between genetically homogeneous and heterogeneous symbionts, with corresponding effects on the host's physiological performance.

## 4.2. Methods

### *4.2.1. Study location and species*

The corals investigated in this study were *Pocillopora damicornis* colonies inhabiting the reef at North Bay, LHI (-31.521, 159.047). At this location, *P. damicornis* can simultaneously host three genetically distinct *Symbiodinium ITS2* types, C100, C109, and symbiont cells featuring a heterogeneous mixture of C100 and C109 sequences (putative hybrids; see chapters 2 and 3). Genetically heterogeneous *Symbiodinium* cells are generally less common in the LHI lagoon (including North Bay), than at the reef margin. This thermal niche-partitioning pattern appears to be driven by temperature stress, since the site-averaged proportional abundance of genetically heterogeneous *Symbiodinium* cells is negatively correlated with the summer thermal maximum (see chapter 3). The poorly-flushed inner-lagoon sites experience particularly pronounced thermal maxima, with model-fitted values of 25.003 °C, 25.177 °C and 24.991 °C for North Bay, Sylph's Hole and Comet's Hole, respectively. However, the actual temperature can occasionally exceed these values, with the water temperature at Comet's Hole reaching 28.16 °C during January 2010 (see chapter 3).

### *4.2.2. Coral collection and acclimation*

Coral collection, acclimation and oxygen flux analysis was carried out during March 2012. One branch was collected from each of 15 *P. damicornis* colonies by divers using diagonal pliers. Each branch was then divided into two small fragments (surface area approximately 6 $cm^2$), which were then attached to stainless steel bases with marine epoxy putty to maintain an upright orientation (Knead It Aqua; Selleys). One fragment from each colony was assigned to a treatment group and the other to a control group. Fragments were placed in 2 l clear plastic tanks (5 fragments per tank; 3 tanks per treatment; Figure 4.1) and supplied with

flowing seawater at rate of 300 ml $min^{-1}$, drawn from a 200 l reservoir. This reservoir was maintained at 25 °C using submersible heaters and an aquarium chiller unit (Hailea HC500A), and was fed from a larger reservoir, into which fresh seawater was continuously pumped from the LHI lagoon. All fragments were initially acclimated for 5 d at 25 °C, after which the temperature in the three tanks housing the treatment-group fragments was raised to 29 °C over the course of 4 h (constant ramp rate of 1°C $h^{-1}$). This was achieved by switching the water supply of the treatment tanks to a second temperature-controlled 200 l tank (the control tanks remained at 25 °C). All fragments were then left at their respective temperatures for a further 4 d prior to oxygen flux analysis, sample preservation (immediate freezing) and laboratory processing.

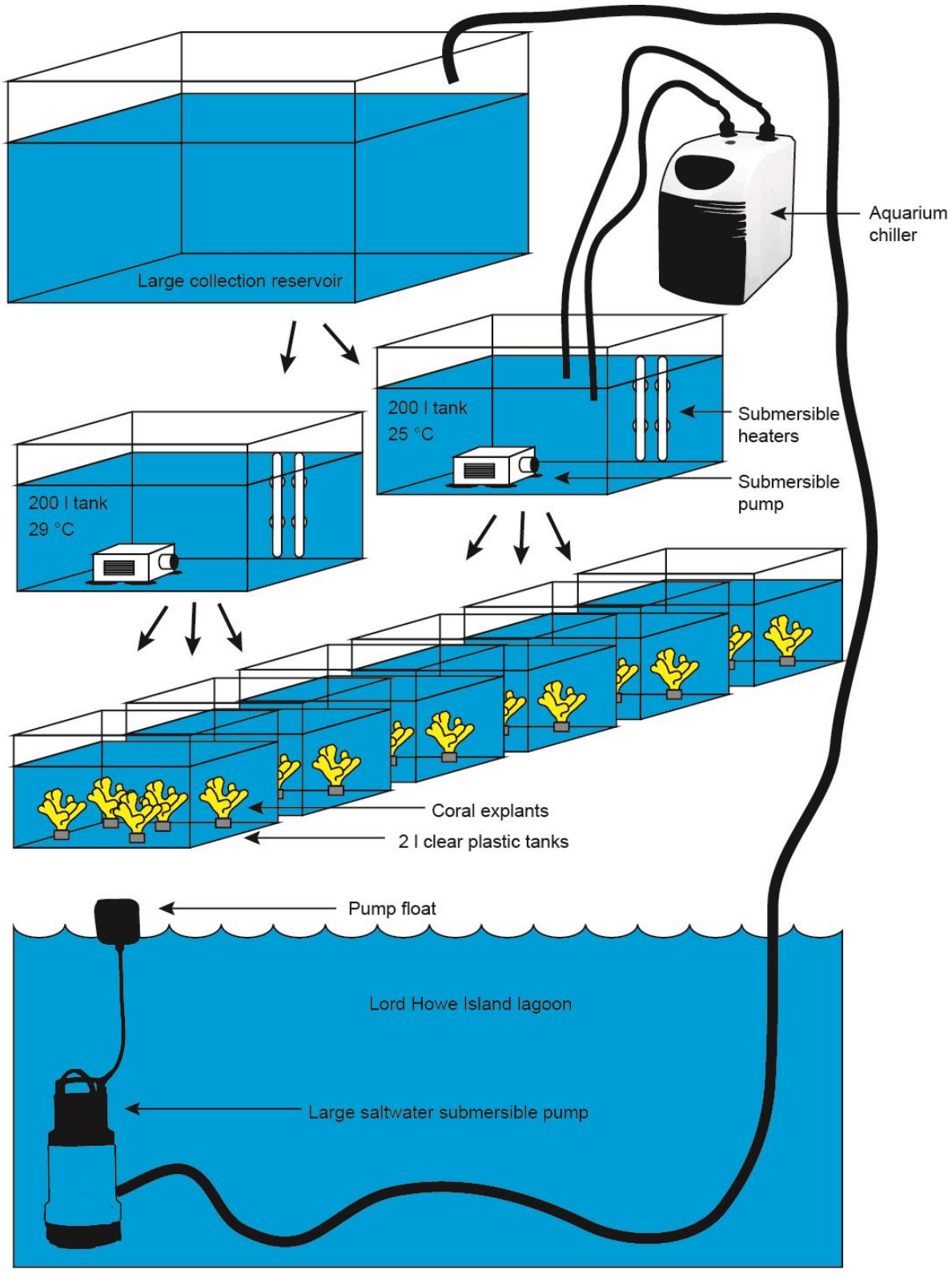


**Figure 4.1 Thermal acclimation of coral fragments prior to oxygen flux analysis**
Seawater was supplied from the LHI lagoon into a large collection reservoir using a submersible pump (Leader Ecosub). The large reservoir fed into two 200 l tanks, in which temperatures were maintained using submersible aquarium heaters, circulation pumps and in the case of the 25 °C tank, an aquarium chiller. Water was then fed from the temperature-controlled tanks into 2 l clear plastic tanks housing coral fragments (five per tank), at a constant rate of 300 ml $min^{-1}$.

### *4.2.3. Analysis of oxygen fluxes*

For the analysis of photosynthetic and respiratory oxygen fluxes, each coral fragment was transferred to an airtight 15 ml glass chamber filled with 1 µm filtered seawater (FSW; Figure 4.2). The volume of the FSW displaced was measured using an analytical balance, and the concentration of dissolved oxygen in the chamber was calculated using coefficients derived from tables of oxygen solubility at 35 ‰ salinity (211.3 and 194.6 µmol $O_2$ $l^{-1}$ for 25 °C and 29 °C, respectively). A pre-calibrated fiber-optic oxygen electrode (FIBOX 3; PreSens GmbH) and temperature sensor were inserted through the sealed openings of the chamber, and a visual check was carried out to ensure that no air bubbles were present. The chamber was then submerged in a temperature-controlled water bath containing a submersible aquarium heater, a temperature probe and an aquarium pump (to ensure even temperature distribution). FSW in the chambers was mixed by a micro-spin bar controlled by a magnetic stirrer, and temperatures were maintained within 0.2 °C of target values (25 °C and 29 °C for control and treatment fragments, respectively) by manually controlling the submersible heater unit. Following a 10 min dark acclimation period, fragments were exposed to eight consecutive irradiance levels (0, 10, 20, 40, 80, 160, 320 and 700 µmol photons $m^{-2}$ $s^{-1}$; measured using a LI-COR LI-190 underwater quantum sensor). Light was provided by a 12V halogen lamp, directed through a series of 50% transmittance neutral density filters. Fragments were acclimated to each light level for 5 min, before the dissolved oxygen in the chamber was measured at 5 s intervals for at least 5 min, until a linear rate of oxygen evolution was observable. Net oxygen evolution rates at each light level were calculated by fitting a linear regression line. Oxygen electrodes were subjected to two-point dissolved oxygen calibration prior to each run. FSW was treated with sodium sulphite (1 $gl^{-1}$ $Na_2SO_3$) for the 0% dissolved oxygen calibration, and oxygenated for 30 min using an aquarium air pump and air-stone for the 100% dissolved oxygen calibration. The oxygen saturation in the chamber was maintained between 50 and 100% (Davies 1984). Following oxygen flux analysis, fragments were frozen at -20 °C for subsequent laboratory analysis.

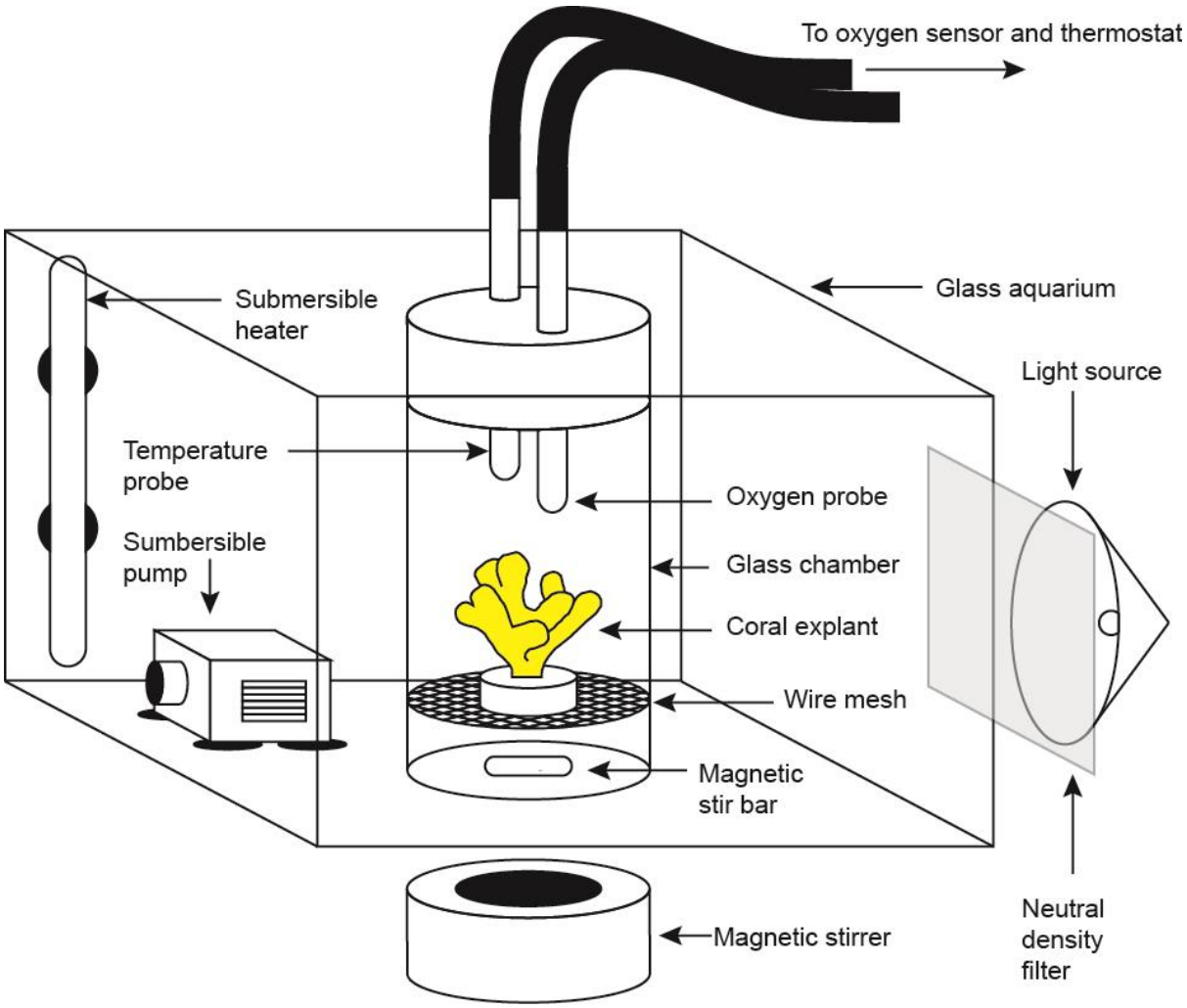


**Figure 4.2 Experimental setup for measuring coral oxygen fluxes**
Coral fragments were individually placed in a sealed 15 ml glass chamber, and maintained at a constant temperature of 25 or 29 °C by manually controlling a submersible heater. Water inside the chamber was mixed by a stir bar, controlled by a magnetic stirrer situated beneath the aquarium. Oxygen fluxes were measured at each of eight light levels ranging from 0 to 700 µmol photons $m^{-2}$ $s^{-1}$, generated by placing a series of neutral density filters between the light source and the aquarium.

### *4.2.4. Assessment of morphology and physiology*

Frozen coral fragments were defrosted and coral tissue was removed from the underlying skeleton with a stream of 50 mM phosphate buffer (1 mM EDTA; pH = 7.8), delivered at high velocity through a compressed-air-generated spray nozzle. The coral skeleton was dried at 70 °C for 24 h and the surface area calculated using the wax method (Stimson & Kinzie 1991). The total homogenate volume was measured using a pipette, and five 1.5 ml aliquots

were taken for cell density and symbiont size measurements (one aliquot), DNA extraction (one aliquot), and measurements of host protein biomass and symbiont chlorophyll composition (three aliquots). Symbiont densities were estimated using a haemocytometer (Neubauer Brightline; eight replicate grids for each sample). The average symbiont size was assessed by measuring the diameter of 50 cells from each coral fragment, using a compound microscope fitted with an eyepiece graticule and a 100x objective oil immersion lens. The three protein/chlorophyll aliquots were centrifuged at 16,100 x g for 5 min to separate host and algal fractions. For host protein biomass estimation, 10 µl of supernatant were added to each of three micro-plate wells, each containing 200 µl of Bradford reagent (Sigma-Aldrich). Sample absorbance was measured at 595 nm, and the content of host-derived soluble protein was estimated by comparing absorbance values to a standard curve obtained using BSA protein standards. The soluble host protein biomass from each coral fragment was normalized to the skeletal surface area, and expressed in mg $cm^{-2}$. To extract and measure chlorophyll from within the *Symbiodinium* cells, algal pellets were re-suspended in 222 µl 90% acetone and incubated in a light-proof container for 24 h at 4 °C. Chlorophyll extracts were then centrifuged at 16,100 x g to pellet cellular debris and chlorophyllases. The supernatant (200 µl) was transferred to a UV-proof micro-plate (Griener) and absorbance values were measured at 630, 665 and 750 nm. The concentration of chlorophylls *a* and $c_2$ were calculated using the equations of Jeffrey & Humphrey (1975) with the coefficients for dinophytes given by Ritchie (2006). Chlorophyll content was expressed as pg $cell^{-1}$.

### *4.2.5. DNA extraction*

For bulk-cell PCR and qPCR analysis of *Symbiodinium ITS2* sequences, a 1.5 ml homogenate sample was centrifuged at 16,100 x g for 5 min, the supernatant was discarded, and 200 µl DMSO preservation buffer (20% DMSO, 250 mM EDTA, NaCl saturated, pH 8.0; Seutin *et al.* 1991) were added. The pellet was re-suspended by milling without beads for 3 min at 50 Hz. Following a 7 d incubation period at -20 °C, the settled *Symbiodinium* cells were re-suspended using a vortex and 10 µl were taken for DNA extraction. Acid-washed glass beads were added (50 mg; 710-1180 µm; Sigma-Aldrich) and the sample was milled at 50 Hz for 3 min (Qiagen TissueLyser LT; Qiagen) to disrupt the cell-walls and enable the release of nucleic acids. Following a 10 min incubation period at 4 °C, 90 µl of de-ionised water were added. The sample was then vortexed and centrifuged for 10 min at 16,100 x g to pellet the

cellular debris. The DNA-enriched supernatant (50 µl) was transferred to a new micro-centrifuge tube with an equal volume of 2-propanol to precipitate the nucleic acids, and centrifuged for 10 min at 16,100 x g to collect the DNA pellet. The supernatant was discarded and 200 µl wash buffer (70% v/v ethanol) were added. The sample was vortexed and returned to the centrifuge for a further 10 min at 16,100 x g. The supernatant was carefully removed with a pipette and the DNA pellet was dried under a laminar flow hood for 30 min. Elution buffer (10 mM Tris-HCl; 0.1 mM EDTA; pH = 8.0) was added to a final volume of 50 µl. Following a 10 min re-hydration period, the DNA was re-suspended by milling without beads for 1 min at 30 Hz.

### *4.2.6. PCR and denaturing gradient gel electrophoresis*

Denaturing gradient gel electrophoresis (DGGE) was carried out on all samples to establish whether *Symbiodinium* types other than C100 and C109 were present in the selected colonies. PCR amplification for DGGE was carried out with the primers ITSintfor2 and ITS2CLAMP (LaJeunesse 2002). Thermal cycling involved an initial denaturation step of 3 min at 95 °C followed by 40 cycles of 15 seconds at 95 °C, 15 seconds at 56 °C and 10 seconds at 72 °C (carried out on an Applied Biosystems Veriti thermo-cycler; Life Technologies). Each reaction contained 4 µl of DNA template solution, 1x MyTaq PCR reaction mix (Bioline), 10 pmol each primer, 10 µg bovine serum albumin (BSA; Sigma) and deionised sterile water to a total volume of 20 µl. A template-free control was included with each run. To ensure the final product was within the intended size range of 300-350 bp, and that amplification did not occur in the template-free control reaction, 5 µl of the final PCR product were electrophoresed on a 1.5 % agarose gel containing 1x SYBR safe nucleic acid stain (Life Technologies) alongside a DNA standard (Hyperladder II; Bioline). Agarose gels were viewed and imaged on a blue light trans-illuminator (Safe Imager; Invitrogen).The remaining PCR product was loaded on a 200 x 200 x 1 mm, 8% denaturing polyacrylamide gel (25-50% urea/formamide denaturant gradient), and run in 1 x TAE at 150 V for 7 h at 60 °C (DCode system; BioRad) alongside known *ITS2* sequences of *Symbiodinium* C100 and C109 (PCR-amplified from plasmid DNA). Following electrophoresis, denaturing gels were stained with ethidium bromide and viewed on a UV trans-illuminator (FirstLight UVP), and the presence or absence of each *ITS2* sequence type was scored.

### *4.2.7. Quantitative PCR*

The bulk-cell qPCR assay developed in chapter 3 was used to establish the relative proportion of putative *Symbiodinium* hybrids within the symbiont consortium of each coral fragment ($S_H$:$S_T$). Each qPCR reaction contained 4 µl DNA template, 1x TaqMan Universal Mastermix II (Life Technologies), 18 pmol each primer (CInnerFor and CInnerRev; see chapter 2 for nucleotide sequences), 1x TaqMan fluorogenic probe ($C100^+$ or $C100^-$; Life Technologies, see chapter 2 for nucleotide sequences), 10 µg BSA (Sigma-Aldrich) and deionised sterile water to a total volume of 20 µl. Thermal cycling involved an initial 10 min, 95 °C denaturation step followed by 40 cycles of 15 seconds at 95 °C and 1 min at 60 °C (Applied Biosystems StepOne qPCR instrument; Life Technologies). DNA template solutions generated from bulk-cell *Symbiodinium* samples were run in duplicate with a template-free control reaction included for each probe type. $C_t$ values were determined as the cycle at which the change in fluorescence was significantly different to the background level ($\Delta R_n$ = 0.05; obtained using the instrument's built-in algorithm). Reactions featuring $C_t$ values below the intercepts of the previously-generated standard curves (36.873 and 37.119 for $C100^+$ and $C100^-$ assays, respectively; see *Appendix B*) and sufficiently low standard deviations (< 0.5) were included in the analysis. The total number of *ITS2* copies in each sample ($C_{TOTAL}$) was estimated as the sum of the C100 copy number and the number of *Symbiodinium* clade C *ITS2* sequences other than type C100 ($C_{C100}$ and $C_{C100}^-$, respectively). The proportion of total *Symbiodinium* clade C sequences that were of type C100 was expressed as the bulk-cell $C_{C100}$:$C_{TOTAL}$ ratio. This ratio were subsequently converted to the proportional abundance of genetically heterogeneous cells ($S_H$:$S_T$) using the polynomial equation developed in chapter 3 ($y = -3.4484x^2 + 3.3604x$; where $y = S_H$:$S_T$ and $x = C_{C100}$:$C_{TOTAL}$).

### *4.2.8. Statistical analysis*

For assessments of photosynthetic performance, a three-parameter hyperbolic tangent function of the form

$$y = a\left(\frac{1\text{-}e^{\frac{-x}{b}}}{1\text{-}e^{\frac{-x}{b}}}\right) + c \qquad \textbf{Equation 4.1}$$

was fitted to the bivariate photosynthesis-irradiance data from each coral fragment (Chalker *et al.* 1983), using the least-squares curve fitter function in Sigmaplot v11.0 (Systat). The parameters *a*, *b* and *c* correspond to $P_{GROSS}$, $I_K$ and *R*, representing the maximum gross rate of photosynthesis (μmol $O_2$ $h^{-1}$), the 50% saturation irradiance (μmol photons $m^{-2}$ $s^{-1}$), and the dark respiration rate (μmol $O_2$ $h^{-1}$), respectively (Figure 4.3). Following parameter estimation, $P_{GROSS}$ and *R* were normalized to host protein biomass, and expressed in nmol $O_2$ $mg^{-1}$ protein $h^{-1}$. The maximum gross photosynthesis to respiration ratio (*P:R*), the light-harvesting efficiency ($\alpha$) and the compensation irradiance ($I_C$) were calculated using the formulae of Chalker *et al.* (1983):

$$P:R = \frac{P_{GROSS}}{R} \qquad \textbf{Equation 4.2}$$

$$\alpha = \frac{P_{GROSS}}{I_K} \qquad \textbf{Equation 4.3}$$

$$I_C = I_K \tanh^{-1} \frac{-R}{P_{GROSS}} \qquad \textbf{Equation 4.4}$$

Parametric multivariate analysis of covariance (MANCOVA) was used to compare the effects of temperature and the proportional abundance of genetically heterogeneous symbionts on the suite of measured photo-physiological response variables ($P_{GROSS}$, *R*, *P:R*, $\alpha$, $I_C$ , and $I_K$) and morphological and physiological attributes (host protein biomass, symbiont density and size, and chlorophyll *a* and $c_2$ content). Significant parameter estimates were then combined to generate an integrated photosynthesis-irradiance model with $S_H$:$S_T$ and temperature as explanatory variables. The average diameter and chlorophyll content of each symbiont cell type (i.e. genetically heterogeneous cells and homogeneous C100 cells) were estimated by extrapolating from the fitted regression lines (assuming hypothetical colonies with $S_H$:$S_T$ ratios of 0 and 1). In all cases, normality and variance homoscedasticity were assessed using Q-Q plots and Box's and Levene's tests of variance equality. All statistical analyses were carried out using SPSS Statistics v20 (IBM).

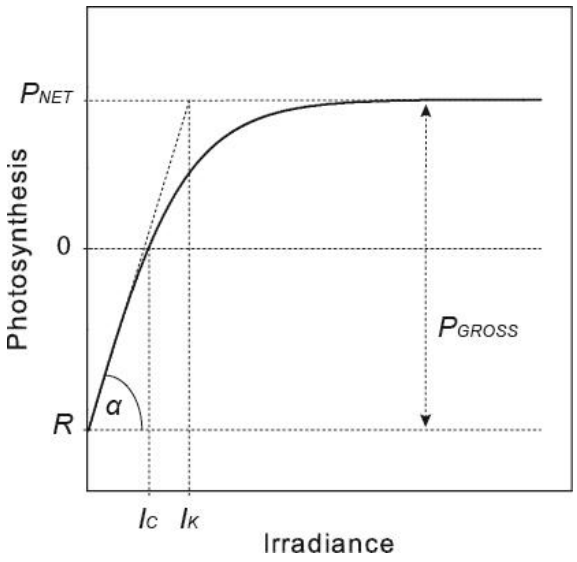


**Figure 4.3 Properties of the photosynthesis-irradiance (PI) curve**
The maximum net photosynthetic rate ($P_{NET}$) is the observed oxygen evolution at maximum irradiance. Respiration ($R$) represents the total oxygen evolution in the dark, expressed as a negative value. The maximum gross photosynthetic rate ($P_{GROSS}$) is the total photosynthetic oxygen evolution at maximum irradiance. The compensation irradiance ($I_C$) is the irradiance at which no net oxygen evolution occurs ($P:R$ = 1; $P_{NET}$ = 0). The sub saturating irradiance ($I_K$) is an indicator of photo-acclimation, calculated as the theoretical point where the initial linear section of the curve intersects $P_{NET}$. The light harvesting efficiency ($\alpha$; also known as the light utilization coefficient) represents the effectiveness of photosynthesis at low light, and is calculated as the angle between the line y = 0 and the initial linear section of the PI curve. Diagram adapted from Chalker *et al.* (1983).

## 4.3. Results

All 30 coral fragments analysed in this study produced bulk-cell DGGE band patterns consistent with the presence of *Symbiodinium* C100, either in apparent isolation or in coexistence with *Symbiodinium* C109. No other *Symbiodinium* sequences were detected, including the rare types C103 and C118 previously identified from *P. damicornis* at LHI (Wicks *et al.* 2010). The relative C100 and C109 band intensities generally corresponded with the relative proportions of each *ITS2* type, as determined by bulk-cell qPCR (see *Appendix B*). Conversion of bulk-cell *ITS2* ratios ($C_{C100}$:$C_{TOTAL}$) to the proportional abundance of genetically heterogeneous symbionts ($S_H$:$S_T$) revealed that genetically heterogeneous *Symbiodinium* cells constituted between 0.15% and 0.72% of the symbiont consortium (Figure 4.4). The variation in $S_H$:$S_T$ between fragments sampled from the same colony was negligible, despite experiencing a 4 °C difference in temperature for 4 d (7.7% residual variance component; Figure 4.4).

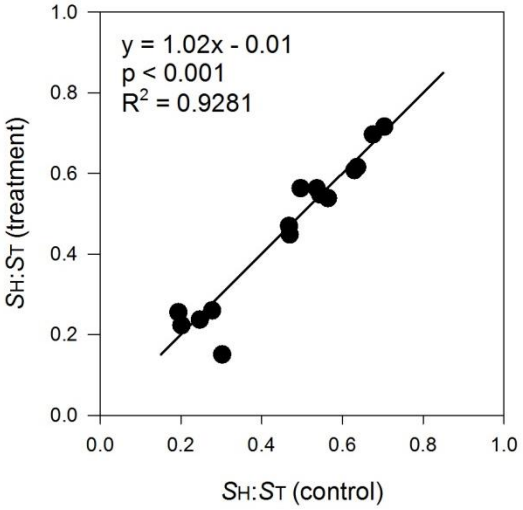


**Figure 4.4 Within-colony variation in symbiont abundance ratios**
Similar $S_H$:$S_T$ ratios between control (25 °C) and treatment (29 °C) fragments reflect a lack of intra-colony variation in the proportional abundance of genetically heterogeneous symbionts following a 4 d exposure to different temperatures. A 7.7% residual variance component (calculated as 1 – $R^2$) corresponds with the low between-branch variability observed in chapters 2 and 3, and suggests that the coral host does not selectively expel symbionts over short time-frames.

### *4.3.1. Morphology and physiology*

Temperature treatment and $S_H$:$S_T$ jointly explained a significant proportion of the variation in the multi-parameter physiological response of *P. damicornis* (MANCOVA, Pillai's Trace p-value = 0.029 and 0.004 for covariate and treatment effects, respectively; Table 4.1). Subsequent univariate testing revealed a significant main effect of $S_H$:$S_T$ on the majority of the variables measured, either in isolation or in conjunction with temperature (Table 4.2). The total soluble protein biomass per unit surface area (used here as a proxy for host tissue thickness) was unaffected by temperature (p = 0.746) and was not significantly correlated with $S_H$:$S_T$. However, a trend towards a higher tissue biomass in corals hosting more putative hybrids was observable (p = 0.075; Figure 4.5a; Table 4.2). Symbiont density was negatively correlated with $S_H$:$S_T$ when normalised to both host protein biomass and coral surface area. A 1% increase in $S_H$:$S_T$ was associated with approximately 13,500 fewer symbiont cells per mg host protein, regardless of temperature (p = 0.002; Figure 4.5b). Similarly, a 1% increase in $S_H$:$S_T$ corresponded to ~ 3,000 fewer symbiont cells per $cm^2$ (p = 0.023; Figure 4.5c). However, in contrast to the host protein-normalized symbiont density, the density of *Symbiodinium* cells per unit surface area was also dependent on temperature, with corals acclimated at 25 °C maintaining around 120,000 more symbiont cells per $cm^2$ than those kept at 29 °C (p = 0.012; Figure 4.5c). A reduced symbiont density in corals hosting proportionally more putative *Symbiodinium* hybrids was consistent with an observed difference in symbiont cell size (p = 0.022; Figure 4.5d); extrapolation from the MANCOVA fitted regression line indicated that the average diameter of genetically heterogeneous

symbionts was 11.53 µm, compared to 10.15 µm for the homogeneous cells (corresponding cell volume = 803 µm3 and 548 µm$^3$ respectively).

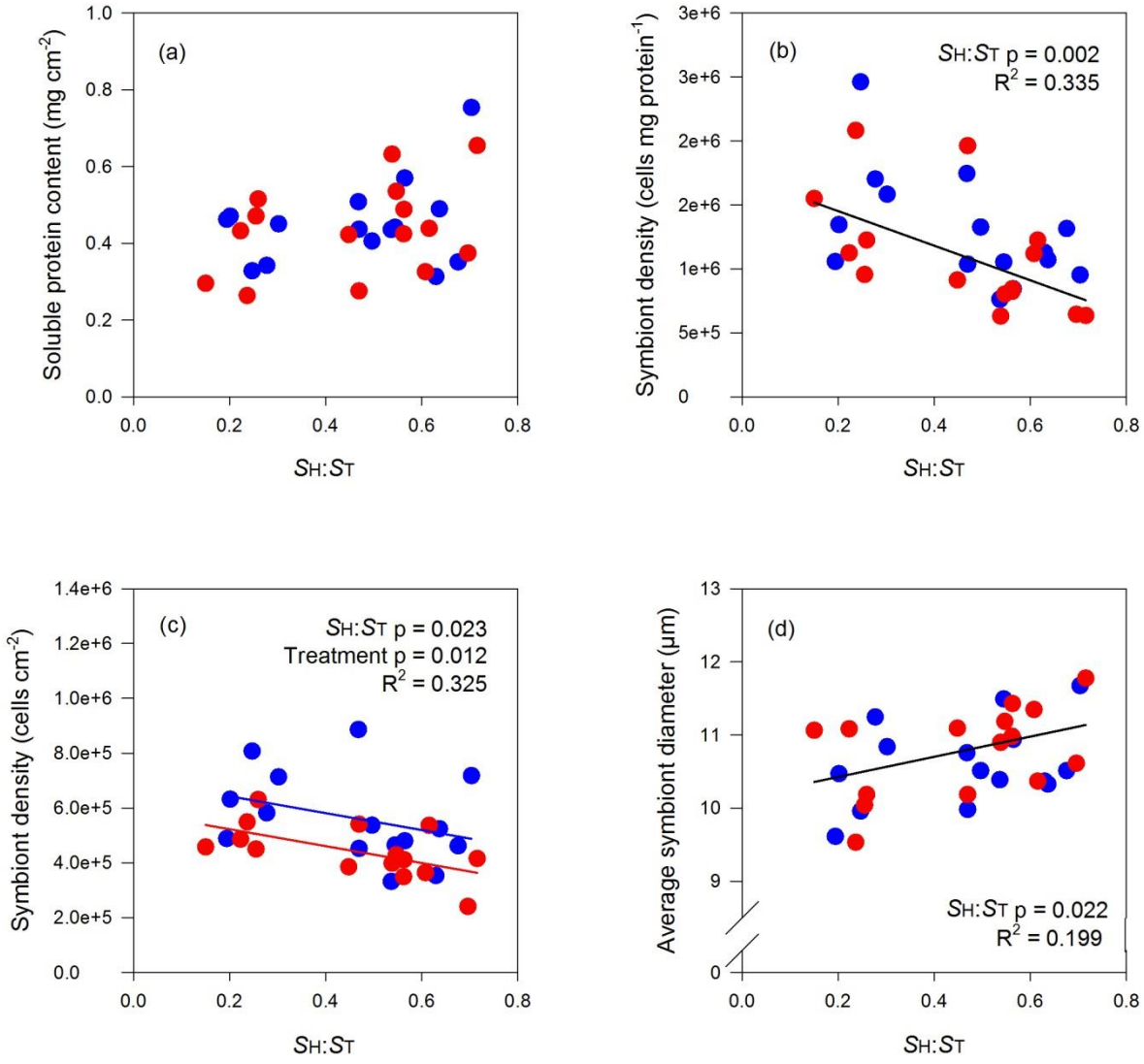


**Figure 4.5 Host protein biomass, symbiont density and cell-size**
Differences in morphology and physiology were evident between genetically homogeneous and heterogeneous symbionts, and between high- and low-$S_H$:$S_T$ colonies, with (a) similar host protein biomass among colonies and temperature treatments (although a positive trend was indicated by a near-significant p-value of 0.075); (b) reduced protein-normalised symbiont densities in high-$S_H$:$S_T$ colonies; (c) reduced surface area-normalised symbiont densities in high-$S_H$:$S_T$ colonies, that were further reduced in all colonies at elevated temperature; and (d) larger average symbiont cell diameters in high-$S_H$:$S_T$ colonies (extrapolated estimates = 11.53 µm and 10.15 µm for genetically heterogeneous and homogeneous symbiont cells, respectively). Blue and red circles represent coral fragments following exposure to 25 °C and 29 °C, respectively. Coloured lines show the ANCOVA model when both $S_H$:$S_T$ and the temperature produced significant effects. A single sloping black line is fitted in cases where temperature effect was non-significant (i.e. reduced to a linear regression), and a single horizontal black line indicates an absence of both $S_H$:$S_T$ and temperature effects.

The total chlorophyll *a* content per *Symbiodinium* cell was similar across all coral fragments, regardless of $S_H$:$S_T$ and temperature (p = 0.221 and 0.497 for $S_H$:$S_T$ and treatment effects, respectively; mean = 3.36 pg cell$^{-1}$; Figure 4.6a). By contrast, the symbionts of colonies hosting comparatively more genetically heterogeneous *Symbiodinium* cells contained more chlorophyll $c_2$ per cell than those of low-$S_H$:$S_T$ colonies, with a 1% increase in $S_H$:$S_T$ conferring an increase of 0.614 pg cell$^{-1}$ (p = 0.006; Figure 4.6b). As such, genetically heterogeneous symbionts featured a correspondingly higher chlorophyll $c_2$:*a* ratio than homogeneous cells (extrapolated estimates = 0.50 for putative hybrids and 0.25 for non-hybrids; p = 0.002; Figure 4.6c). The chlorophyll $c_2$ composition also showed an increase at elevated temperature, with treated symbiont cells containing an additional 0.18 pg chlorophyll $c_2$ at the end of the 4-d acclimation period (p = 0.019; Figure 4.6b). However, this temperature effect was not of sufficient magnitude to significantly increase the $c_2$:*a* ratio (p = 0.248; Figure 4.6c).

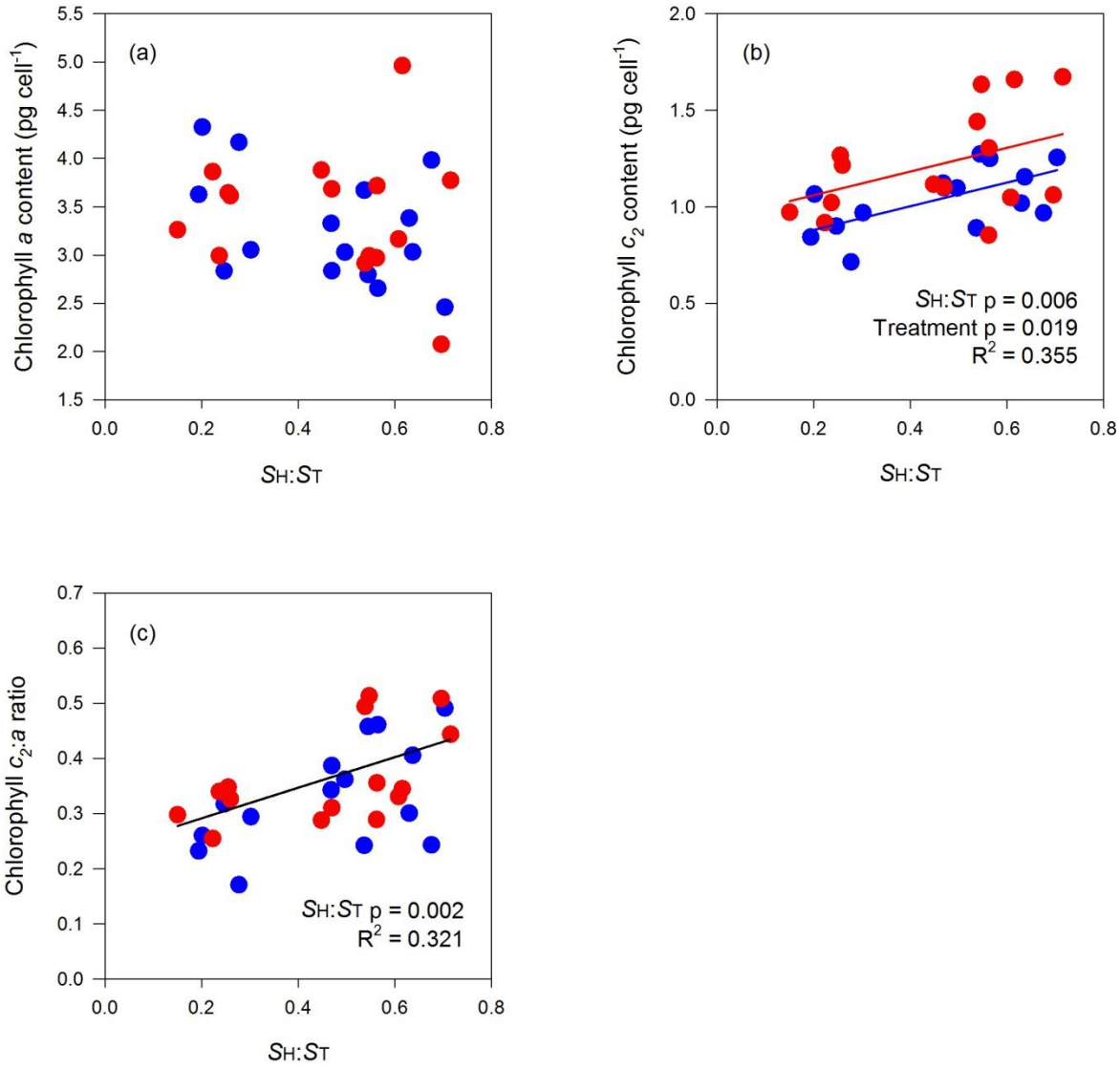


**Figure 4.6 Chlorophyll *a* and $c_2$ content**

The chlorophyll content per-symbiont cell varied among colonies and treatments, with (a) no effect of either $S_H$:$S_T$ or temperature on the content of chlorophyll *a* per cell; (b) a positive correlation between $S_H$:$S_T$ and the chlorophyll $c_2$ content per cell (with a further positive effect of elevated temperature); and (c) increased chlorophyll $c_2$:*a* ratios in colonies dominated by genetically heterogeneous symbionts. Blue and red circles represent coral fragments following exposure to 25 °C and 29 °C, respectively. Coloured lines show the ANCOVA model when both $S_H$:$S_T$ and the temperature produced significant effects. A single sloping black line is fitted in cases where temperature effect was non-significant (i.e. reduced to a linear regression), and a single horizontal black line indicates an absence of both $S_H$:$S_T$ and temperature effects.

### *4.3.2. Photosynthetic efficiency*

All photosynthesis-irradiance parameters were influenced by the proportional abundance of genetically heterogeneous symbionts, either alone or in conjunction with temperature (Figure 4.7; Figure 4.8). The maximum gross photosynthetic rate ($P_{GROSS}$) was not affected by the temperature treatment ($p = 0.972$), but declined by 16 nmol $O_2$ $mg^{-1}$ protein $h^{-1}$ with each 1% increase in $S_H$:$S_T$ ($p = 0.003$; Figure 4.7a). The net oxygen uptake in the dark (respiration; $R$) similarly declined by 6 nmol $O_2$ $mg^{-1}$ protein $h^{-1}$ for each 1% increase in $S_H$:$S_T$ ($p = 0.041$). However, in contrast to $P_{GROSS}$, $R$ was also influenced by temperature, with fragments exposed to 29 °C consuming an additional 0.245 µmol $O_2$ $mg^{-1}$ protein $h^{-1}$ relative to the controls ($p = 0.024$; Figure 4.7b). As such, the maximum photosynthesis to respiration ratio ($P:R$) was dependent on both temperature and the proportional abundance of genetically heterogeneous symbionts. A 1% increase in $S_H$:$S_T$ corresponded to a 5.14 x $10^{-3}$ unit linear reduction in $P:R$, and the temperature-treated fragments exhibited a 0.368 unit reduction in $P:R$ relative to the controls ($p = 0.003$ and $p < 0.001$ for $S_H$:$S_T$ and temperature treatment, respectively; Figure 4.7c).

**Table 4.1 MANCOVA for multi-parameter physiological response**

| Source | Pillai's Trace | Hypothesis df | Error df | F | P |
|---|---|---|---|---|---|
| **$S_H$:$S_T$** | 0.677 | 12 | 16 | 2.791 | 0.029 |
| **Treatment** | 0.793 | 12 | 16 | 5.109 | 0.002 |

$S_H$:$S_T$ was entered as a continuous covariate, and the temperature treatment entered as a fixed factor (at two levels, control and elevated).

An increase in the proportional abundance of genetically heterogeneous symbionts corresponded with a decline in light harvesting efficiency ($\alpha$; $p = 0.001$). However, this parameter remained unaffected by the temperature treatment ($p = 0.831$; Figure 4.7d). The irradiance required to produce net oxygen evolution (compensation irradiance; $I_C$) was significantly higher in corals hosting a relatively higher abundance of genetically heterogeneous *Symbiodinium* cells ($p = 0.012$), with an increase of 0.76 µmol photons $m^{-2}$ $s^{-1}$ for each 1% increase in $S_H$:$S_T$. The average $I_C$ increased by a further 32 µmol photons $m^{-2}$ $s^{-1}$ in fragments exposed to 29 °C relative to those kept at 25 °C ($p = 0.003$; Figure 4.7e). Finally, the 50%-saturation light intensity ($I_K$) declined by 0.402 µmol photons $m^{-2}$ $s^{-1}$ for

every 1% increase in $S_H$:$S_T$ ($p = 0.038$), but was not affected by temperature ($p = 0.786$; Figure 4.7f).

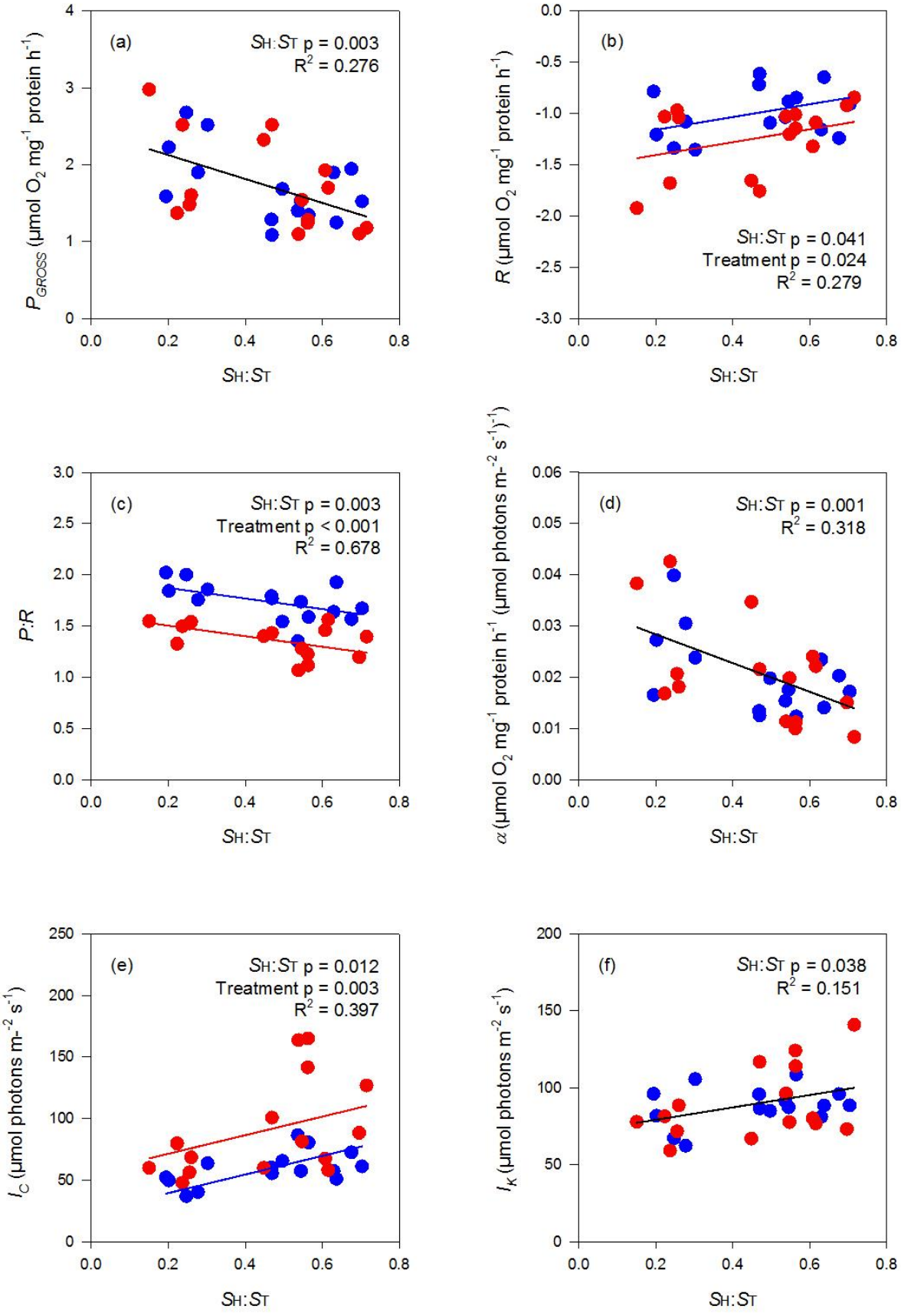
(a)
SH:ST p = 0.003
R2 = 0.276
PGROSS (µmol O2 mg-1 protein h-1)
SH:ST
(b)
SH:ST p = 0.041
Treatment p = 0.024
R2 = 0.279
R (µmol O2 mg-1 protein h-1)
SH:ST
(c)
SH:ST p = 0.003
Treatment p < 0.001
R2 = 0.678
P:R
SH:ST
(d)
SH:ST p = 0.001
R2 = 0.318
α (µmol O2 mg-1 protein h-1 (µmol photons m-2 s-1)-1)
SH:ST
(e)
SH:ST p = 0.012
Treatment p = 0.003
R2 = 0.397
IC (µmol photons m-2 s-1)
SH:ST
(f)
SH:ST p = 0.038
R2 = 0.151
IK (µmol photons m-2 s-1)
SH:ST

**Figure 4.7 (previous page) Respiratory and photosynthetic oxygen fluxes**
The proportional abundance of genetically heterogeneous symbionts had an influence on all measured photosynthesis-irradiance parameters, with (a) a negative linear correlation between $S_H$:$S_T$ and maximum gross photosynthesis; (b) an increase in respiratory oxygen consumption in low-$S_H$:$S_T$ colonies (further intensified in all colonies at elevated temperature); (c) disproportionately high photosynthetic rates relative to respiration in low-$S_H$:$S_T$ colonies, conferring an increase in *P:R*; (d) reduced light harvesting efficiency in genetically heterogeneous *Symbiodinium* cells, compared with homogeneous C100 symbionts; (e) an associated increase in compensation irradiance in high-$S_H$:$S_T$ colonies, particularly at the elevated temperature (corresponding with an increase in respiration); and (f) an increased 50%-saturation irradiance in high-$S_H$:$S_T$ colonies. Blue and red circles represent coral fragments following exposure to 25 °C and 29 °C, respectively. Coloured lines show the ANCOVA model when both $S_H$:$S_T$ and the temperature produced significant effects. A single sloping black line is fitted in cases where temperature effect was non-significant (i.e. reduced to a linear regression), and a single horizontal black line indicates an absence of both $S_H$:$S_T$ and temperature effects.

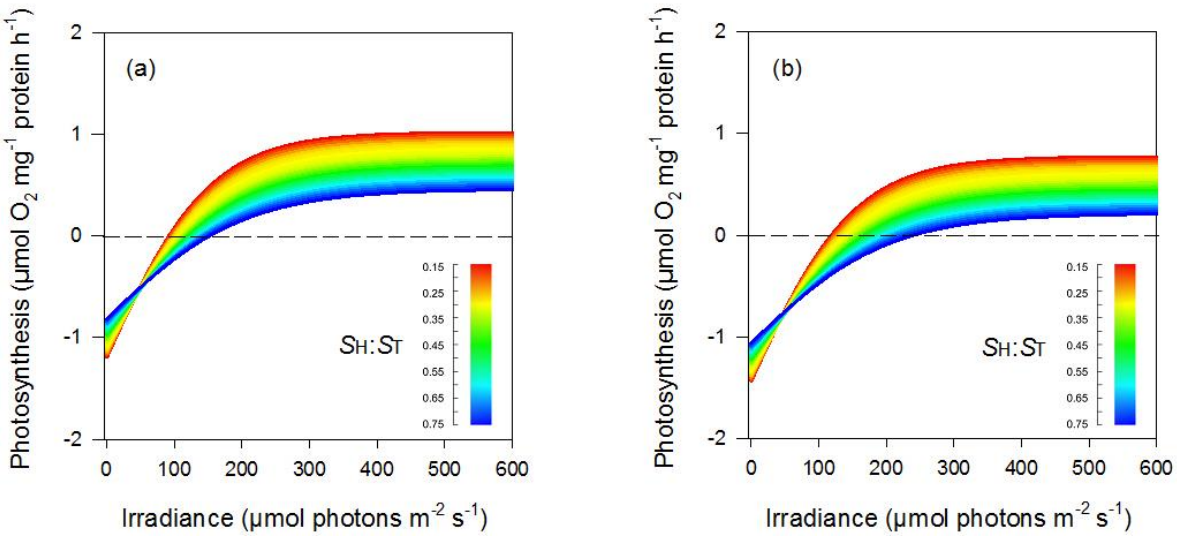


**Figure 4.8 Photosynthesis-irradiance model for *P. damicornis***
The photosynthetic performance of *P. damicornis* is shown at ambient temperature (a) and under thermal stress (b), with the proportional abundance of genetically heterogeneous symbionts depicted as a colour gradient. Ambient and stressful thermal conditions are represented by the average mid-summer temperature at North Bay (25 °C), and that slightly exceeding the thermal maximum experienced in the LHI lagoon (29 °C). An increase in $S_H$:$S_T$ was associated with a reduction in (i) maximum net photosynthetic oxygen evolution ($P_{GROSS}$); (ii) the irradiance required to reach 50% photosynthetic saturation ($I_K$); (iii) the light harvesting efficiency ($\alpha$); and (iv) the ratio of photosynthesis to respiration (*P:R*). A corresponding increase was detected in the irradiance required to meet respiratory oxygen requirements ($I_C$). The total oxygen uptake during respiration (*R*) was lower in colonies hosting comparatively more genetically heterogeneous symbionts, corresponding with a reduced symbiont cell density. Colonies dominated by heterogeneous symbionts were only marginally capable of net photosynthesis at elevated temperature, even under saturating irradiance.

**Table 4.2 Univariate ANCOVA for individual physiological response variables**

| Source | Dependent variable | df | SS | MS | F | P |
|---|---|---|---|---|---|---|
| $S_H$:$S_T$ | Protein (surface area) | 1 | 0.041 | 0.041 | 3.418 | 0.075 |
| | Density (protein) | 1 | 1.67901E+12 | 1.67901E+12 | 11.706 | 0.002 |
| | Density (surface area) | 1 | 87313961439 | 87313961439 | 5.852 | 0.023 |
| | Symbiont diameter | 1 | 1.745 | 1.745 | 5.873 | 0.022 |
| | Chlorophyll *a* (cell) | 1 | 0.572 | 0.572 | 1.572 | 0.221 |
| | Chlorophyll $c_2$ (cell) | 1 | 0.346 | 0.346 | 8.827 | 0.006 |
| | Chlorophyll $c_2$:*a* | 1 | 0.07 | 0.07 | 12.096 | 0.002 |
| | $P_{GROSS}$ (protein) | 1 | 2.22 | 2.22 | 10.301 | 0.003 |
| | *R* (protein) | 1 | 0.361 | 0.361 | 4.608 | 0.041 |
| | *P*:*R* | 1 | 0.243 | 0.243 | 11.063 | 0.003 |
| | $\alpha$ (protein) | 1 | 0.001 | 0.001 | 12.53 | 0.001 |
| | $I_K$ | 1 | 1491.185 | 1491.185 | 4.742 | 0.038 |
| | $I_C$ | 1 | 5242.373 | 5242.373 | 7.305 | 0.012 |
| **Treatment** | Protein (surface area) | 1 | 0.001 | 0.001 | 0.107 | 0.746 |
| | Density (protein) | 1 | 2.86542E+11 | 2.86542E+11 | 1.998 | 0.169 |
| | Density (surface area) | 1 | 1.08932E+11 | 1.08932E+11 | 7.301 | 0.012 |
| | Symbiont diameter | 1 | 0.259 | 0.259 | 0.873 | 0.358 |
| | Chlorophyll *a* (cell) | 1 | 0.173 | 0.173 | 0.474 | 0.497 |
| | Chlorophyll $c_2$ (cell) | 1 | 0.243 | 0.243 | 6.206 | 0.019 |
| | Chlorophyll $c_2$:*a* | 1 | 0.008 | 0.008 | 1.396 | 0.248 |
| | $P_{GROSS}$ (protein) | 1 | 0 | 0 | 0.001 | 0.972 |
| | *R* (protein) | 1 | 0.45 | 0.45 | 5.743 | 0.024 |
| | *P*:*R* | 1 | 1.015 | 1.015 | 46.315 | < 0.001 |
| | $\alpha$ (protein) | 1 | 2.73E-06 | 2.73E-06 | 0.046 | 0.831 |
| | $I_K$ | 1 | 23.742 | 23.742 | 0.076 | 0.786 |
| | $I_C$ | 1 | 7657.407 | 7657.407 | 10.67 | 0.003 |
| **Error** | Protein (surface area) | 27 | 0.326 | 0.012 | | |
| | Density (protein) | 27 | 3.87274E+12 | 1.43435E+11 | | |
| | Density (surface area) | 27 | 4.02825E+11 | 14919426866 | | |
| | Symbiont diameter | 27 | 8.022 | 0.297 | | |
| | Chlorophyll *a* (cell) | 27 | 9.833 | 0.364 | | |
| | Chlorophyll $c_2$ (cell) | 27 | 1.058 | 0.039 | | |
| | Chlorophyll $c_2$:*a* | 27 | 0.157 | 0.006 | | |
| | $P_{GROSS}$ (protein) | 27 | 5.82 | 0.216 | | |
| | *R* (protein) | 27 | 2.117 | 0.078 | | |
| | *P*:*R* | 27 | 0.592 | 0.022 | | |
| | $\alpha$ (protein) | 27 | 0.002 | 5.86E-05 | | |
| | $I_K$ | 27 | 8490.012 | 314.445 | | |
| | $I_C$ | 27 | 19376.082 | 717.633 | | |

$S_H$:$S_T$ was entered as a continuous covariate, and the temperature treatment entered as a fixed factor (at two levels, control and elevated). Denominators for normalised variables are shown in parentheses.

## 4.4. Discussion

The aim of this chapter was to investigate the form and function of genetically heterogeneous *Symbiodinium* cells (putative hybrids) in comparison to genetically homogeneous symbionts (putative progenitors), under ambient and stressful conditions. A suite of diagnostic variables were measured, with morphological and physiological differences observed at both the symbiont- and holobiont level. Consistent with the findings of the previous chapter, genetically heterogeneous symbionts performed poorly at ambient and elevated summer temperatures, with their host colonies suffering substantial reductions in photosynthetic efficiency. However, this did not prevent net photosynthetic production, even when the maximum temperature experienced in their natural habitat was exceeded.

### *4.4.1. Physical attributes of putative* Symbiodinium *hybrids*

Genetically heterogeneous *Symbiodinium* cells were 50% larger by volume (applying the sphere radius to volume conversion $V = 4/3\pi r^3$) than the homogeneous C100 symbionts. This disparity is likely to have an underlying genetic basis, since conspecific *Symbiodinium* cells generally show only minor variation in size (LaJeunesse 2001; LaJeunesse *et al.* 2012, 2014). Corals dominated by these large heterogeneous symbiont cells showed corresponding reductions in symbiont density. However, while two-dimensional space availability is known to be important factor in limiting algal densities in corals (Jones & Yellowlees 1997), an estimated 10% difference in cell diameter did not entirely explain the two-fold difference in density observed between corals at opposite ends of the $S_H$:$S_T$ spectrum (i.e. 15% *versus* 75% proportional abundance of genetically heterogeneous symbionts). Symbionts are typically not space limited in corals during the summer months (Fitt *et al.* 2000), and *P. damicornis* colonies from other locations are known to accommodate a double layer *Symbiodinium* of cells at densities exceeding $10^6$ cm$^{-2}$ (Gates & Muscatine 1992; Muller-Parker *et al.* 1994). This suggests that the colonies dominated by genetically heterogeneous *Symbiodinium* cells were not 'symbiont saturated'. Rather, they appear to have previously experienced higher rates of symbiont loss, and/or suffered from lower symbiont division rates that may have been unable to maintain pace with terminal coral growth (e.g. Oliver 1984).

Rates of temperature-induced symbiont loss were similar among all colonies in this study, with a 4 °C increase in temperature resulting in the expulsion/degradation of an extra ~

30,000 symbionts per $cm^2$ per day. This meant that thermally-stressed colonies dominated by genetically heterogeneous *Symbiodinium* cells lost a greater percentage of their symbionts than those hosting predominantly homogeneous C100 cells (since the former initially hosted fewer symbionts). Under prolonged thermal stress, high-$S_H$:$S_T$ colonies may therefore exhaust their energy reserves sooner unless they can compensate by switching to a heterotrophic feeding mode (e.g. Grottoli *et al.* 2006). Interestingly, colonies dominated by genetically heterogeneous symbionts showed a high protein biomass, even in comparison to nitrogen-enriched *P. damicornis* colonies (Muller-Parker *et al.* 1994). Similar increases in protein biomass were observed in Hawaiian *Montipora capitata* colonies that switched to heterotrophy after bleaching (Grottoli *et al.* 2006), suggesting a possible role of heterotrophic feeding in the survival of the corals analysed here. The influence of symbiont hybridization on the feeding behaviour and morphology of the coral host presents an interesting area for future research.

The concentration of the primary photosynthetic pigment chlorophyll *a* was similar among genetically heterogeneous and homogeneous (C100) *Symbiodinium* cells. However, the former showed a substantially higher content of the accessory pigment chlorophyll $c_2$ and a corresponding two-fold increase in the $c_2$:*a* ratio, suggesting inherent differences in the composition of light harvesting antennae (membrane-bound chlorophyll *a*-chlorophyll $c_2$-peridinin-protein complexes) between the two cell types. The stoichiometry of light-harvesting antennae varies widely among symbiont taxa, with species-specific differences explained by a combination of adaptation and acclimatization to different habitats (Chang *et al.* 1983; Iglesias-Prieto & Trench 1994, 1997). For example, in the symbiont of the shade-adapted coral *Montipora verrucosa* (*Symbiodinium kawagutii*; type F1), $c_2$:*a* was negatively correlated with light intensity (Chang *et al.* 1983; Iglesias-Prieto & Trench 1994), while $c_2$:*a* showed a positive correlation with light intensity in the clade A symbiont of the light-adapted giant clam *Tridacna maxima* (Chang *et al.* 1983). The differences in $c_2$:*a* observed here may represent a heritable modification; however dynamic changes in light-harvesting antennae can also occur within individual cells, through remodelling, *de novo* synthesis, or differential degradation (Iglesias-Prieto & Trench 1997). It is therefore unclear whether the observed differences in $c_2$:*a* represents an adaptive (i.e. genetically encoded) modification, an acclimatory response to subtle differences in microhabitat, or a combination of both processes. The role(s) of accessory pigments in the ecological diversification of genetically

homogeneous and heterogeneous *Symbiodinium* cells presents another area for future investigation.

### *4.4.2. Relative photosynthetic performance of putative* Symbiodinium *hybrids*

Corals dominated by genetically heterogeneous *Symbiodinium* cells showed lower overall rates of gross photosynthesis, respiration, and *P:R* than those predominantly hosting genetically pure C100 symbionts. This loss of photosynthetic performance can be partially attributed to the reduced symbiont densities in these colonies (see above). However, a corresponding reduction in light-harvesting efficiency can be entirely attributed to the photosynthetic function of the symbiont. Symbiont populations at low density generally show increased light harvesting efficiency, reduced compensation irradiance, and higher rates of net photosynthesis (Crossland & Barnes 1977; Muller-Parker 1984). For example, freshly isolated symbionts from the coral *Acropora acuminata* showed high light-harvesting efficiency when maintained at a low density, while this efficiency declined at higher cell concentrations and in the intact symbiosis (as a result of shading; Crossland & Barnes 1977). By contrast, high-$S_H$:$S_T$ colonies (hosting low symbiont densities), showed poor light-harvesting efficiency, and a correspondingly high irradiance was required to meet the comparatively lower overall oxygen demands of the symbiosis. While the underlying cellular mechanisms of this disparity remain unknown, the impaired photosynthetic performance of these genetically heterogeneous cells is consistent with 'hybrid breakdown', a reduction in performance and fitness due to the segregation of co-adapted gene complexes or the creation of maladapted gene combinations (Demuth & Wade 2005). Haploids such as *Symbiodinium* are especially prone to hybrid breakdown, since the deleterious effects of recombination cannot be compensated for by heterosis (Barton 2001). Furthermore, while 'transgressive' hybrids can outperform parental genotypes in extreme habitats (Rieseberg *et al.* 2003), hybrids are generally expected to function poorly in the parental habitat. This is consistent with an overall reduction in performance shown by the genetically heterogeneous symbionts under conditions simulating those within the LHI lagoon (the average and absolute summer thermal maximum) where homogeneous C100 cells tend to be more dominant. While it remains a possibility that the observed physiological disparities arose from fine-scale genetic structure among sympatric asexual *Symbiodinium* populations, the poor photosynthetic performance of genetically heterogeneous *Symbiodinium* cells reinforces their candidacy as

putative hybrids, and suggests that reduced symbiont fitness (and hence host fitness) may accompany the occurrence of hybridization between divergent *Symbiodinium* taxa.

### *4.4.3. Implications of reduced performance in putative* Symbiodinium *hybrids*

Corals dominated by putative *Symbiodinium* hybrids suffered relatively poor overall photosynthetic function under both ambient and extreme summer temperatures. Extrapolation from the photosynthesis irradiance model suggests that a further marginal temperature increase beyond 29 °C would render this symbiosis incapable of net oxygen production, even under saturating irradiance. This would likely result in substantial loss of fitness for both the host and the symbiont, raising several questions about the potential functional and evolutionary role(s) of hybridization in the *Symbiodinium* genus. First, do hybrids out-perform non-hybrids under extreme and/or intermediate conditions (i.e. those between the parental optima)? The putative hybrids studied here may be more suitably adapted to cooler conditions, given that thermal stress appears to drive their distribution patterns (see chapter 3). A physiological assessment over a broader range of temperature and light conditions may reveal 'redeeming' features that offset their relatively poor performance under the conditions simulated in this study. Second, how does the observed physiological performance distribute among the different genotypes and classes (i.e. $F_1$ hybrid, $F_2$ backcross, etc)? If hybridization has occurred among the symbionts of *P. damicornis*, the cluster of genetically heterogeneous cells may solely represent $F_1$ hybrids, or it may also include second- and later-generation backcross genotypes. Backcross genotypes are expected to suffer poor performance relative to the $F_1$ generation, and hence suffer further reductions in fitness (Barton 2001). Furthermore, the functional performance of the putative C109 progenitor remains unknown, since this type has only been detected forming a cryptic population in *P. damicornis* (< 7% proportional representation; see chapter 2). Establishing clonal cultures of the various genotypes would be necessary to address the fine-scale variation in both performance and fitness, and the underlying physiological mechanisms. Finally, does the observed disparity in physiological performance translate to differences in coral growth, survival and reproduction? Symbiont shuffling is not evident in this symbiosis (see chapter 3), suggesting that an individual coral's symbiont compliment is either inherited or determined early in its ontogeny. Natural selection acting on the coral host may therefore play an important role in

determining the distribution of genetically homogeneous and heterogeneous *Symbiodinium* cells. This consideration will be addressed in chapter 5.

### *4.4.4. Conclusion*

Genetically heterogeneous and homogeneous *Symbiodinium* cells were morphologically and physiologically distinct, both in terms of cell size and their constituent photosynthetic pigments. The former also showed poor light-harvesting efficiency, despite being subject to less shading (resulting from low symbiont densities). These physiological differences translated into functional disparities in the coral holobiont, with colonies dominated by genetically heterogeneous *Symbiodinium* cells showing disproportionately low symbiont densities and poor photo-physiological performance under both ambient and elevated summer temperatures. These results add to the accumulating evidence in favour of hybridization between divergent *Symbiodinium* taxa, and provide a conditional indication of the performance and fitness of the resulting progeny. This is an important step towards understanding the potential for hybridization to contribute to adaptation in a changing climate.

# Chapter 5: Symbiont hybridization and coral fitness

## 5.1. Introduction

In obligate mutualisms, the performance of the symbiont is a key determinant of host fitness. Corals are no exception, since the photosynthetic activity of the algal symbiont ultimately supports the energetic requirements of the host through the translocation of energy-rich compounds (Muscatine & Porter 1977; Muscatine 1990; Davy *et al.* 2012). Yet hosting symbionts inevitably incurs a basal metabolic cost (Grube *et al.* 2010), and as such, poor-performing symbionts are expected to occupy a less-beneficial position along the parasitism-mutualism continuum (Cantin *et al.* 2009). For example, under normal conditions, a twofold increase in photosynthate translocation within juvenile *Acropora millepora* colonies hosting *Symbiodinium* C1 (= *S. goreauii*) resulted in substantially higher growth rates than those harbouring clade D (Little *et al.* 2004; Cantin *et al.* 2009; Jones & Berkelmans 2010). Symbiont performance is also an important determinant of host fitness under stressful conditions. There is a firm link between the thermal optimum of the symbiont and the coral host's resistance or susceptibility to bleaching-related mortality (Rowan 2004; Berkelmans & van Oppen 2006; Sampayo *et al.* 2008). However, emerging evidence suggests that the physiological and behavioural attributes of the host can be at least as important as those of the symbiont in determining thermal stress tolerance (e.g. Fitt *et al.* 2009; Paxton *et al.* 2013; Hawkins *et al.* 2014). For example, in *Pocillopora damicornis* and *Acropora millepora* colonies subjected to elevated temperatures, nitric oxide accumulation and host-cell apoptosis preceded symbiont dysfunction by several days (Hawkins *et al.* 2014). Expelled symbionts can be healthy and photosynthetically active upon expulsion, further suggesting that photosynthetic breakdown does not always precede or cause the bleaching response (Bhagooli & Hidaka 2004; Hill & Ralph 2007). Also, some coral species such as *Montipora capitata* can survive the loss of symbionts by switching to a predominantly heterotrophic feeding mode (Grottoli *et al.* 2006), providing another situation where symbiont performance may be uncoupled from the fitness of host. Indeed, high-performing symbionts can even be detrimental to host fitness. Excessive symbiont reproduction *in situ* can lead to burgeoning densities, and an increased bleaching risk *via* a density-dependent signalling cascade (Cunning & Baker 2013). In extreme cases, a functional mutualistic symbiont may even tend

towards parasitism through preferential photosynthate retention and pathogenic proliferation within the host (Sachs & Wilcox 2006; Stat *et al.* 2008b).

The genetically heterogeneous symbionts of *P. damicornis* (putative hybrids) showed relatively poor photosynthetic performance compared to their putative progenitor (*Symbiodinium* C100) in a controlled environment (see chapter 4). In particular, a comparative reduction in light-harvesting efficiency meant that higher levels of photosynthetically active radiation (PAR) were required to meet the overall oxygen demands (and hence energy demands) of the symbiosis. This suggests that symbiont hybridization may associate with negative fitness consequences for the host, by introducing poor-performing hybrids at the expense of highly mutualistic 'pure' genotypes. Alternatively, symbiont hybridization could be of benefit to the host, even at the cost of functional performance, if hybrids show reduced antagonistic/parasitic tendencies (Schardl & Craven 2003). For example, asexual hybrid fungal symbionts of the cool-season grass family Poaceae are selected for by their hosts, since the sexually reproductive progenitor *Epichloë* sp. can 'hijack' the plant's reproductive structures in order to facilitate spore dispersal (choke disease; Schardl & Clay 1997). Biological fitness is broadly defined as the ability of an individual to survive and contribute genes to the next generation (Maynard Smith 1998). Therefore, while short-term assessments of symbiont performance may give an indication of host fitness, establishing this link requires long-term assessments of host survival, growth and reproduction. This objective can only realistically be achieved in a natural setting (Arnold 1983).

This chapter aimed to establish the relationship between symbiont performance and host fitness on the reef, where many biotic and abiotic factors interact to determine coral survival, growth and fecundity (Correa & Baker 2011). The specific objectives of this study were to establish whether observed disparities in functional performance between genetically homogeneous and heterogeneous *Symbiodinium* cells translate to differences in the growth and survival of their coral hosts. This was assessed through the reciprocal transplantation of coral colonies between two reef sites featuring different thermal characteristics, and corresponding differences in the proportional abundance of putative *Symbiodinium* hybrids. The hypothesis tested in this study was that colonies hosting higher proportions of genetically heterogeneous *Symbiodinium* cells show lower growth rates and an increased risk of mortality, compared to those predominantly hosting homogeneous symbionts.

## 5.2. Methods

### *5.2.1. Study location and species*

This study was carried out at two reef sites at Lord Howe Island (Australia), North Bay (-31.521, 159.047) and the reef margin site known as The Arch (-31.539, 159.055; Figure 5.1) The former is a sheltered inner-lagoon site that is subject to pronounced thermal maxima (see chapter 3). Here, *P. damicornis* colonies can grow to several metres in diameter and form large monoculture stands (Miller & Ayre 2004). By contrast, The Arch is an exposed reef-margin location characterised by heavy wave action, where *P. damicornis* forms a small dense clump-like morphology (Veron 2000; Miller & Ayre 2004). The Arch features a lower maximum temperature than North Bay, and *P. damicornis* colonies host a correspondingly higher proportional abundance of genetically heterogeneous *Symbiodinium* cells (putative hybrids; see chapter 3). The genomes of these symbionts feature both C100 and C109-diagnostic *ITS2* sequences (see chapter 2), and they show reduced light-harvesting efficiency compared to their putative progenitor (*Symbiodinium* C100) at both average- and maximum-summer temperatures (25 °C and 29 °C, respectively; see chapter 4). Genetically heterogeneous *Symbiodinium* cells are also approximately 50% larger by volume, feature two-fold higher chlorophyll $c_2$:*a* ratios, and exist in lower densities in the host tissue compared to homogeneous *Symbiodinium* C100 cells. As such, *P. damicornis* colonies dominated by putative hybrids show lower overall photosynthesis-to-respiration ratios (*P*:*R*; see chapter 4). *Symbiodinium* cells with homogeneous C109 arrays are also found in *P. damicornis* colonies at LHI; however these symbionts only form a cryptic population (< 7% proportional abundance; see chapter 2). Therefore, this study invokes the assumption that *Symbiodinium* C109 forms a minor contribution to the overall photosynthetic activity of the symbiosis.

(a)

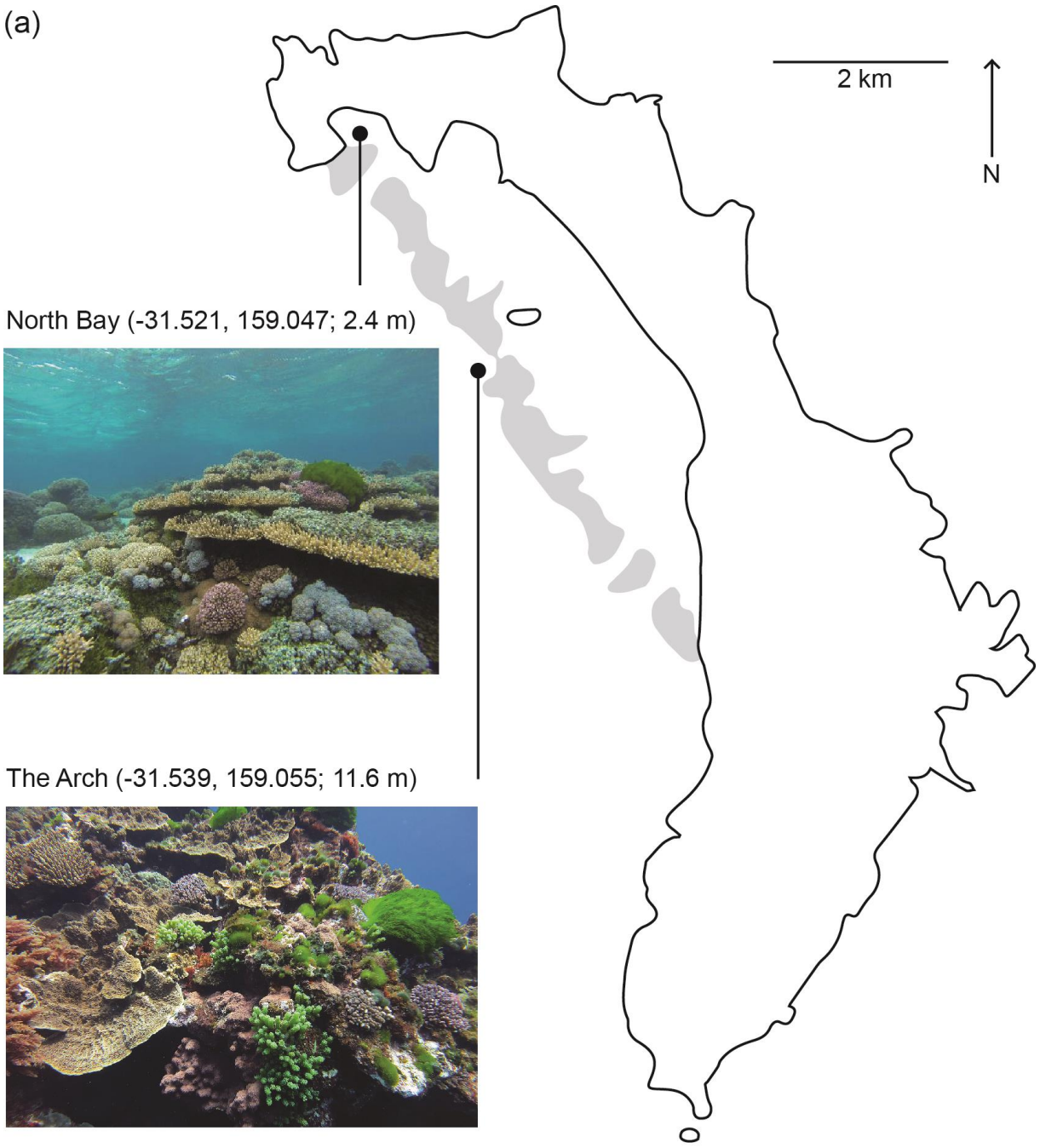
2 km
N
North Bay (-31.521, 159.047; 2.4 m)
The Arch (-31.539, 159.055; 11.6 m)

(b)

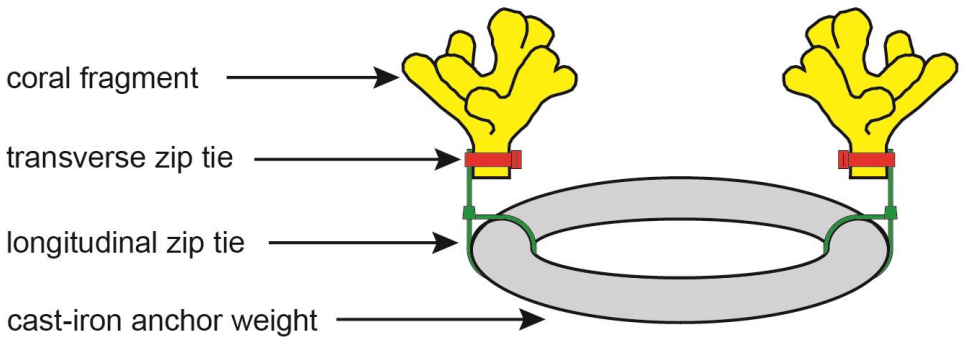
coral fragment
transverse zip tie
longitudinal zip tie
cast-iron anchor weight

**Figure 5.1 (previous page) Location and method of coral transplantation**
Reciprocal transplantation of *P. damicornis* colonies was carried out between North Bay, a sheltered inner-lagoon site, and The Arch, an exposed reef-margin location (a). From each colony, three branch tips were transferred between sites and three were transplanted at the original site from where the parent colony was sampled. The transplantation method is shown in (b); coral fragments were attached to iron anchor weights using two zip ties, a transverse tie around the base of the fragment (red) and a longitudinal tie attached to the weight (green).

### *5.2.2. Coral collection, transplantation and retrieval*

The initial collection of coral samples took place during September 2011, shortly after the winter thermal minimum. A single branch was collected from each of ten *P. damicornis* colonies at each site, and each branch was further divided into seven finger-sized terminal fragments (each approximately 7 g dry weight). One fragment was immediately frozen at -20 °C for DNA analysis, while the remaining six were weighed using the buoyant weight technique (Jokiel *et al.* 1978). These fragments were immediately transplanted onto the reef, three to the original site from where they were collected (transplanted controls) and three to the alternative site (i.e. from North Bay to The Arch or *vice versa*). Corals were attached to large cast-iron anchor weights using two plastic zip-ties, a transverse tie around the base of the fragment, and a larger longitudinal tie attached to the weight (Figure 5.1). The transplant sites were re-visited in March 2012 (shortly after the summer thermal maximum), and the identities of the fragments that had perished recorded. Two live fragments from each colony were retrieved (one from the original site and one from the new site), weighed (using the buoyant weight technique), and frozen at -20 °C prior to DNA analysis. All remaining coral fragments were retrieved, weighed and frozen in September 2012.

### *5.2.3. Skeletal mass estimation*

For each surviving coral fragment, the buoyant mass in water ($M_W$) was converted to dry mass in air ($M_A$) using the formula of (Jokiel *et al.* 1978):

$$M_A = \frac{M_W}{1-\left(\frac{D_W}{D_M}\right)}$$ **Equation 5.1**

where $D_W$ is the density of seawater at a given temperature and salinity (calculated using oceanographic reference tables; UNESCO 1981), and $D_M$ is the species-specific aragonite density (2.703 g $cm^{-3}$ for *P. damicornis*; Spinaze *et al.* 1996). Larger coral fragments are expected to secrete comparatively more calcium (Ferrier-Pagès *et al.* 2000), therefore daily growth rates were converted to compounding growth rates (in % $d^{-1}$; *G*) using the formula:

$$G = \left(\frac{M_A(final)}{M_A(initial)}\right)^{\frac{1}{t}} - 1$$ **Equation 5.2**

where *t* is the time since transplantation (in d) and $M_A(initial)$ and $M_A(final)$ are the initial and final estimated dry masses, respectively.

### *5.2.4. DNA extraction*

DNA analysis of *Symbiodinium ITS2* sequences in bulk-cell samples was similar to that described in chapters 3 and 4. For DNA analysis, a small branch tip was removed from each frozen coral fragment (surface area approximately 5-10 $cm^2$). Coral tissue was removed from the underlying skeleton with a stream of 50 mM phosphate buffer (1 mM EDTA; pH = 7.8), delivered at high velocity through a compressed-air-generated spray nozzle. The homogenate was centrifuged at 16,100 x g for 5 min to pellet the *Symbiodinium* cells, and the supernatant was discarded. DMSO preservation buffer (20% DMSO, 250 mM EDTA, NaCl saturated, pH 8.0; Seutin *et al.* 1991) was added to a volume of 200 µl, and the pellet was re-suspended by milling without beads for 3 min at 50 Hz. Following a 7 d incubation at -20 °C, the settled *Symbiodinium* cells were re-suspended using a vortex, and 10 µl of suspension were taken for DNA extraction. Acid-washed glass beads were added (50 mg; 710-1180 µm; Sigma-Aldrich) and the sample was milled at 50 Hz for 3 min (Qiagen TissueLyser LT; Qiagen) to disrupt the cell-walls and enable the release of nucleic acids. Following a 10 min incubation period at 4 °C, 90 µl of de-ionised water were added. The sample was then vortexed and centrifuged for 10 min at 16,100 x g to pellet the cellular debris. The DNA-enriched supernatant (50 µl) was transferred to a new micro-centrifuge tube with an equal volume of 2-propanol to precipitate the nucleic acids, and centrifuged for 10 min at 16,100 x g to collect

the DNA pellet. The supernatant was discarded and 200 µl wash buffer (70% v/v ethanol) were added. The sample was vortexed and returned to the centrifuge for a further 10 min at 16,100 x g. The supernatant was carefully removed with a pipette and the DNA pellet was dried under a laminar flow hood for 30 min. Elution buffer (10 mM Tris-HCl; 0.1 mM EDTA; pH = 8.0) was added to a final volume of 50 µl. Following a 10 min re-hydration period, the DNA was re-suspended by milling without beads for 1 min at 30 Hz.

### *5.2.5. PCR and denaturing gradient gel electrophoresis*

Denaturing gradient gel electrophoresis (DGGE) was carried out on all samples to establish the presence or absence of *Symbiodinium* types other than C100 and C109. PCR amplification for DGGE was carried out with the primers ITSintfor2 and ITS2CLAMP (LaJeunesse 2002). Thermal cycling involved an initial denaturation step of 3 min at 95 °C followed by 40 cycles of 15 seconds at 95 °C, 15 seconds at 56 °C and 10 seconds at 72 °C (carried out on an Applied Biosystems Veriti thermo-cycler; Life Technologies). Each reaction contained 4 µl of DNA template solution, 1x MyTaq PCR reaction mix (Bioline), 10 pmol each primer, 10 µg bovine serum albumin (BSA; Sigma) and deionised sterile water to a total volume of 20 µl. A template-free control was included with each run. To ensure the final product was within the intended size range (300-350 nucleotides), and that amplification did not occur in the template-free control reaction, 5 µl of the final PCR product were electrophoresed on a 1.5 % agarose gel containing 1x SYBR safe nucleic acid stain (Life Technologies) alongside a DNA standard (Hyperladder II; Bioline). Agarose gels were viewed and imaged on a blue light trans-illuminator (Safe Imager; Invitrogen).The remaining PCR product was loaded on a 200 x 200 x 1 mm, 8% denaturing polyacrylamide gel (25-50% urea/formamide denaturant gradient), and run in 1 x TAE at 150 V for 7 h at 60 °C (DCode system; BioRad) alongside known *ITS2* sequences of *Symbiodinium* C100 and C109 (PCR-amplified from plasmid DNA). Following electrophoresis, denaturing gels were stained with ethidium bromide and viewed on a UV trans-illuminator (FirstLight UVP), and the presence or absence of each *ITS2* sequence type was scored.

### *5.2.6. Quantitative PCR*

The bulk-cell qPCR assay developed in chapter 3 was used to establish the relative proportion of putative hybrids within the symbiont consortium of each coral fragment ($S_H$:$S_T$). Each qPCR reaction contained 4 µl DNA template, 1x TaqMan Universal Mastermix II (Life Technologies), 18 pmol each primer (CInnerFor and CInnerRev; see chapter 2 for nucleotide sequences), 1x TaqMan fluorogenic probe ($C100^+$ or $C100^-$; Life Technologies; see chapter 2 for nucleotide sequences), 10 µg BSA (Sigma-Aldrich) and deionised sterile water to a total volume of 20 µl. Thermal cycling involved an initial 10 min, 95 °C denaturation step followed by 40 cycles of 15 seconds at 95 °C and 1 min at 60 °C (Applied Biosystems StepOne qPCR instrument; Life Technologies). DNA template solutions generated from bulk-cell *Symbiodinium* samples were run in duplicate with a template-free control reaction included for each probe type. $C_t$ values were determined as the cycle at which the change in fluorescence was significantly different to the background level ($\Delta R_n = 0.05$; obtained using the instrument's built-in algorithm). Reactions featuring $C_t$ values below the intercepts of the previously-generated standard curves (36.873 and 37.119 for $C100^+$ and $C100^-$ assays, respectively; see *Appendix B*) and sufficiently low standard deviations (< 0.5) were included in the analysis. The total number of *ITS2* copies in each sample ($C_{TOTAL}$) was estimated as the sum of the C100 copy number and the number of *Symbiodinium* clade C *ITS2* sequences other than type C100 ($C_{C100}$ and $C_{C100}^-$, respectively). The proportion of total *Symbiodinium* clade C sequences that were of type C100 was expressed as the bulk-cell $C_{C100}$:$C_{TOTAL}$ ratio. This ratio were subsequently converted to the proportional abundance of genetically heterogeneous cells ($S_H$:$S_T$) using the polynomial equation developed in chapter 3 ($y = -3.4484x^2 + 3.3604x$; where $y = S_H$:$S_T$ and $x = C_{C100}$:$C_{TOTAL}$).

### *5.2.7. Statistical analysis*

Mortality rates were compared between sites (North Bay and The Arch) and transplant times (195 d and 374 d) using a three-way Pearson's chi-squared cross-tabulation test. For corals transplanted at The Arch, mortality rates were further assessed after 195 d using a binomial logistic regression model, with the proportional abundance of genetically heterogeneous *Symbiodinium* cells ($S_H$:$S_T$) as a putative explanatory variable and mortality as the binary response. Initial dry weight (in g) was added as a nuisance covariate and given first opportunity to explain variance within the model, in order to control the type II error rate (see

Quinn & Keough 2002). Variation in compounding growth rates ($G$; in % $d^{-1}$) and $S_H$:$S_T$ were assessed using blocked MANCOVA, with *Transplant site* and *Time* as factors (fixed-effects; each with two levels), original $S_H$:$S_T$ as a covariate, and *Original site* as a block variable. In all cases, normality and homoscedasticity were assessed using Q-Q plots, and Box's and Levene's tests of variance equality. All statistical analyses were carried out using SPSS Statistics v20 (IBM).

## 5.3. Results

### *5.3.1. Coral mortality*

Coral mortality varied according to transplant-site and time since transplantation, but not as a function of the proportional abundance of genetically heterogeneous *Symbiodinium* cells ($S_H$:$S_T$ ). Mortality was consistently higher at The Arch than at North Bay ($\chi^2_1$ = 6.656 and 30.313; p = 0.010 and < 0.001, after 195 d and 374 d, respectively). A further partial association existed between mortality and time since transplantation, with corals at The Arch experiencing higher mortality rates during the final 179 d of deployment ($\chi^2_1$ = 9.87; p = 0.002). Of the 60 coral fragments deployed at The Arch, 11 perished during the first 195 d, and of the 29 that remained after the first retrieval only seven survived to the end of the 374-d experiment. Conversely, mortality was consistently low at North Bay, with only one of the 60 coral fragments perishing during the first six months, and four more during the subsequent six-month period ($\chi^2_1$ = 0.539; p = 0.463 for 195 d *versus* 374 d comparison). This prevented assessment of the association between $S_H$:$S_T$ and mortality at North Bay, due to a lack of balance in the binomial logistic regression model. Indeed, this assessment could only be reliably carried out at The Arch after the first retrieval round (195 d since transplantation) due to the low number of surviving fragments at this site after 374 d. High mortality in transplanted corals at The Arch was consistent with the established colonies at this site, many of which perished during the particularly cold winter of 2012 (see chapter 3, Figure 3.3), and were overgrown with macroalgae by the end of the experiment. By contrast, very few of the transplanted corals at North Bay perished, and no noticeable mortality occurred among the established *P. damicornis* colonies at this site over the course of the experiment.

The initial dry weight of transplanted coral fragments emerged as a significant factor in determining the likelihood of mortality, with smaller fragments showing a reduced likelihood of survival. A 1.37-fold increase in survival likelihood was associated with a 1 g increase in dry weight (Wald test statistic with one degree of freedom = 4.076; p = 0.043). After accounting for site- and size-related factors, no association was detected between $S_H$:$S_T$ and mortality (binomial logistic regression, $\chi^2_1$ = 0.241; p = 0.632; Figure 5.2).

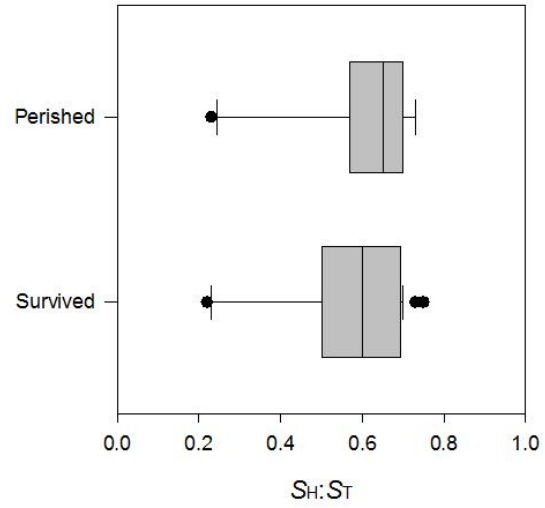


**Figure 5.2 Effect of putative *Symbiodinium* hybrids on coral mortality**
Boxes show the median and interquartile range in the proportional abundance of genetically heterogeneous *Symbiodinium* cells in corals that perished ($n$ = 11) or survived ($n$ = 49) after 195 d of deployment at The Arch. Closed circles represent $10^{th}$/$90^{th}$ percentile outliers. Mortality rates were not significantly affected by $S_H$:$S_T$ (p = 0.632).

### *5.3.2. Physical response to transplantation*

Surviving coral fragments from both sites exhibited high variability in growth, and minor changes in the proportional abundance of genetically heterogeneous *Symbiodinium* cells. A significant interaction between *Transplant site* and *Time* was evident in determining the combined physical response ($G$ and $S_H$:$S_T$; MANCOVA $F_{2,75}$ = 4.337; omnibus p-value = 0.017; Table 5.1). Subsequent univariate testing revealed the *Transplant site* x *Time* interaction applied only to coral growth ($F_{1,76}$ = 8.129 and 0.510; p = 0.006 and 0.477 for $G$ and $S_H$:$S_T$ , respectively; Table 5.2). Simple-effects tests for coral growth at each retrieval time-point revealed that differences between the two sites occurred only during the final 179 d (during which the winter thermal minimum occurred; $F_{1,77}$ = 0.183, p = 0.670 for 195-d and $F_{1,77}$ = 10.761, p = 0.002 for 374-d transplant time; Table 5.3 and Table 5.4, respectively). Average (± S.E.) daily growth rates over the first 195 d were 1.755 x $10^{-3}$ ± 0.119 x $10^{-3}$ % $d^{-1}$ for both sites, and those over the entire 374-d duration were 0.859 x$10^{-3}$ ± 0.374 x$10^{-3}$ % $d^{-1}$ at the Arch and 1.902 x$10^{-3}$ ± 0.160 x $10^{-3}$ % $d^{-1}$ at North Bay. The interpolated growth rates during the final 179 d were therefore -0.133 x$10^{-3}$ ± 0.780 x $10^{-3}$ % $d^{-1}$ at The Arch and 2.044 x$10^{-3}$ ± 0.253 x $10^{-3}$ % $d^{-1}$ at North Bay (Figure 5.3a). The highest growth rate by a single coral fragment was recorded at North Bay, with an increase in dry weight from 8.65 g to 38.83 g in 374 d, representing a compounding growth rate of 4.02 x $10^{-3}$ % $d^{-1}$. Of 84 surviving colonies in total, three recorded net skeletal erosion over the 374-d period, all of which were deployed at The Arch.

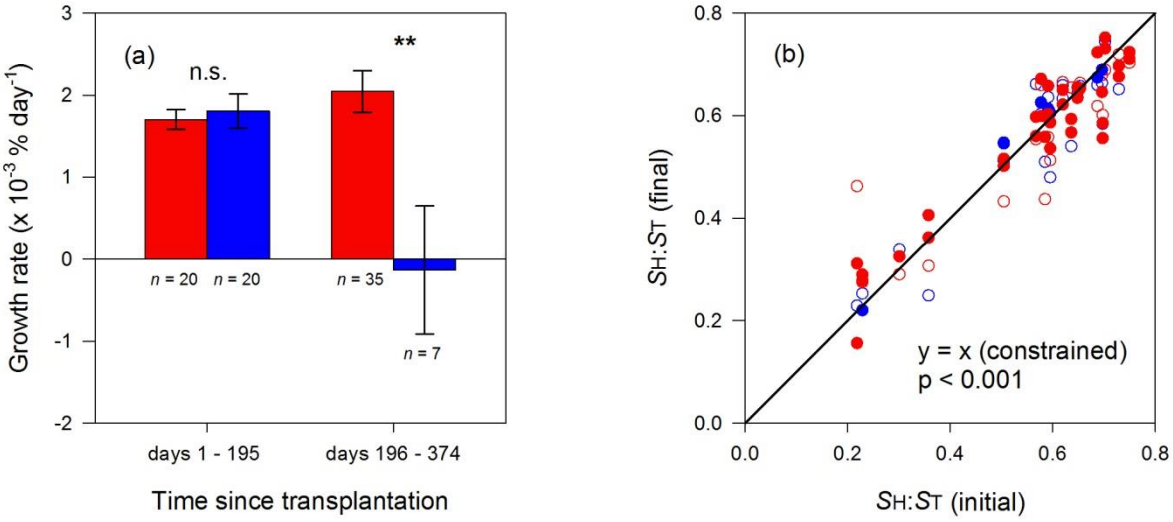


**Figure 5.3 Physical responses of *P. damicornis* colonies following transplantation**
Coral fragments showed a variety of responses to transplantation, with (a) high variation in growth rates between the transplant sites of North Bay and The Arch (shown in red and blue, respectively; double asterisk denotes a p-value of less than 0.01); and (b) minor temporal changes in the proportional abundance of genetically heterogeneous *Symbiodinium* cells. Changes in $S_H$:$S_T$ occurred independently of transplant site and transplant time (shown in red and blue for North Bay and The Arch, and open and closed circles for 195-d and 374-d, respectively). A relatively high level of temporal variation in $S_H$:$S_T$ was detected between ramets of the same parent colony (16.7% residual variance component), compared with an earlier longitudinal analysis of established coral colonies (4% residual variance component; see chapter 3).

An intrinsically higher proportional abundance of genetically heterogeneous *Symbiodinium* cells in *P. damicornis* colonies at The Arch (see chapter 3) was evident in a significant effect of *Original site* (i.e. 'block' effect; mean $S_H$:$S_T$ = 0.583 and 0.551 and The Arch and North Bay, respectively; $F_{1,78}$ = 4.053; p = 0.048; Table 5.2). However, neither *Transplant site* nor *Time* had a significant influence on the $S_H$:$S_T$ ratio measured upon retrieval ($F_{1,76}$ = 0.046 and 1.561, p = 0.830 and 0.215, respectively; Table 5.2). The proportional abundance of homogeneous and heterogeneous *Symbiodinium* cells did not change deterministically throughout the course of the experiment, with the initial $S_H$:$S_T$ (measured from the parent colony prior to transplantation) emerging as a strong predictor of final $S_H$:$S_T$ ($F_{1,76}$ = 486.576; p < 0.001; Table 5.2). As such, when the initial and final $S_H$:$S_T$ ratios were analysed using a before and after paired-differences t-test, no significant change in $S_H$:$S_T$ was detected ($t_{81}$ = 1.112; p = 0.269; Figure 5.3b).

**Table 5.1 MANCOVA for coral growth and temporal changes in the proportional abundance of putative *Symbiodinium* hybrids**

| Source | Pillai's Trace | Hypothesis df | Error df | *F* | *P* |
|---|---|---|---|---|---|
| **Initial $S_H$:$S_T$ (covariate)** | 0.865 | 2 | 75 | 240.094 | < 0.001 |
| **Original site (block)** | 0.052 | 2 | 75 | 2.076 | 0.133 |
| **Transplant site** | 0.068 | 2 | 75 | 2.729 | 0.072 |
| **Time** | 0.063 | 2 | 75 | 2.511 | 0.088 |
| **Transplant site x Time** | 0.104 | 2 | 75 | 4.337 | 0.017 |

**Table 5.2 Univariate ANCOVA for coral growth and temporal changes in the proportional abundance of putative *Symbiodinium* hybrids**

| Source | Variable | df | SS | MS | *F* | *P* |
|---|---|---|---|---|---|---|
| **Initial $S_H$:$S_T$ (covariate)** | Growth | 1 | 0.451 | 0.451 | 0.766 | 0.384 |
| | $S_H$:$S_T$ | 1 | 1.532 | 1.532 | 486.576 | < 0.001 |
| **Original site (block)** | Growth | 1 | 0.062 | 0.062 | 0.105 | 0.746 |
| | $S_H$:$S_T$ | 1 | 0.013 | 0.013 | 4.053 | 0.048 |
| **Transplant site** | Growth | 1 | 3.205 | 3.205 | 5.443 | 0.022 |
| | $S_H$:$S_T$ | 1 | <0.001 | <0.001 | 0.046 | 0.830 |
| **Time** | Growth | 1 | 1.981 | 1.981 | 3.364 | 0.071 |
| | $S_H$:$S_T$ | 1 | 0.005 | 0.005 | 1.561 | 0.215 |
| **Transplant site x Time** | Growth | 1 | 4.786 | 4.786 | 8.129 | 0.006 |
| | $S_H$:$S_T$ | 1 | 0.002 | 0.002 | 0.510 | 0.477 |
| **Error** | Growth | 76 | 44.748 | 0.589 | | |
| | $S_H$:$S_T$ | 76 | 0.239 | 0.003 | | |

**Table 5.3 Simple-effects analysis of coral growth over 195 days**

| Source | df | SS | MS | *F* | *P* |
|---|---|---|---|---|---|
| **Transplant site** | 1 | 0.107 | 0.107 | 0.180 | 0.673 |
| **Error** | 76 | 45.199 | 0.595 | | |

**Table 5.4 Simple-effects analysis of coral growth over 374 days**

| Source | Df | SS | MS | *F* | *P* |
|---|---|---|---|---|---|
| **Transplant site** | 1 | 6.317 | 6.317 | 10.62 | 0.002 |
| **Error** | 76 | 45.199 | 0.595 | | |

## 5.4. Discussion

The photosynthetic performance of the symbiont is often a strong determinant of coral fitness; however the host's physiology and behaviour can uncouple this association (reviewed in Baird *et al.* 2008). Similarly, the performance of the symbiont may not necessarily reflect its mutualistic scope (Stat *et al.* 2008b). This study aimed to determine whether physiological differences observed between genetically homogeneous and heterogeneous *Symbiodinium* cells (see chapter 4) affect the growth and survival of their coral hosts in the natural reef setting. Colonies were reciprocally transplanted between two distinct reef habitats, an inner lagoon site exposed to pronounced thermal peaks, and a well-flushed site situated at the transition zone between coral- and macroalgal-dominated communities. The proportional abundance of putative hybrid symbionts did not influence coral mortality or calcification, nor did it change in response to habitat modification. Instead, coral fitness appeared to be predominantly driven by local environmental factors, with the inner-lagoon site providing a more suitable habitat for coral growth and survival.

### *5.4.1. The influence of putative* Symbiodinium *hybrids on coral fitness*

Coral calcification and mortality were not affected by the proportional abundance of genetically heterogeneous *Symbiodinium* cells. This was inconsistent with the comparatively poor photosynthetic performance shown by these symbionts in a controlled setting (see chapter 4). This discrepancy may have arisen *via* several processes. First, conditions simulated in an experimental setting are not representative of those experienced on the reef. While the earlier assessment of photosynthetic performance was carried out using stable temperatures approximating the summer average and absolute thermal maximum experienced within the Lord Howe Island lagoon (25 and 29 °C, respectively; see chapter 4), pronounced fluctuations in temperature and light characterise the LHI reef environment (Veron & Done 1979; Harrison *et al.* 2011). Coral fragments were also exposed to temperatures that were consistently lower than 25 °C throughout the course of this study. While it is presently unknown how heterogeneous *Symbiodinium* cells perform under cold-stress, their spatial distribution pattern indicates a possible adaptation to cooler environments (see chapter 3). The extreme thermal minimum experienced at LHI plays an important role in determining range boundaries of corals and other reef fauna at this site (Veron & Done 1979), and cold stress is a known causal factor underlying coral bleaching and symbiont community change

in *Pocillopora* colonies in the Gulf of California (LaJeunesse *et al*. 2010b). Cold-adaptation or other factors may have equalized the disparity in photosynthetic performance between homogeneous and heterogeneous *Symbiodinium* cells in their natural setting. Second, the biochemical and/or behavioural activity of the coral host may have compensated for the poor photosynthetic performance of its symbionts. Corals may employ various strategies to ensure that their metabolic requirements are met, with some species even switching to a heterotrophic feeding mode in the absence of symbiont-derived compounds (Grottoli *et al.* 2006). Indeed, *P. damicornis* colonies hosting predominantly heterogeneous *Symbiodinium* cells showed marginal increases in protein biomass, a response consistent with this mode of nutrient assimilation (see chapter 4). Finally, a reduction in photosynthetic performance may be offset if a symbiont occupies a particularly beneficial position along the parasitism-mutualism continuum. In the majority of cases, coral fitness varies according to the degree of host-symbiont co-operation rather than host- or symbiont factors in isolation (Bhagooli & Hidaka 2003; Abrego *et al.* 2008). In particular, the quality and quantity of translocated photosynthate may differ widely among symbiont taxa, with important implications for host fitness (Little *et al.* 2004; Loram *et al.* 2007b; Stat *et al.* 2008b; Cantin *et al.* 2009; Jones & Berkelmans 2010; Starzak *et al.* 2014). For example, the clade A symbionts of the coral *Acropora cytherea* released significantly less carbon compared with those of clade C, with colonies hosting the former showing a corresponding increase in disease risk (Stat *et al.* 2008b). The uncoupling of symbiont performance and host fitness observed in this study suggests that some beneficial feature of putative hybrid *Symbiodinium* cells may warrant their persistence in the *P. damicornis* symbiont consortium. This may explain their widespread abundance on the LHI reef, and the lack of temporal variation within colonies (see chapter 3 and next section). Identification of this 'redeeming' characteristic presents an interesting area for future investigation.

### *5.4.2. Changes in symbiont ratios following transplantation*

Minor temporal changes in ratios of genetically homogeneous and heterogeneous symbionts were apparently random, and not attributable to environmental factors. Corals that transmit their symbionts vertically (such as *P. damicornis*) generally show reduced symbiotic flexibility (Thornhill *et al.* 2006a); however this contrasted with several previous transplant studies that show deterministic symbiont shuffling in both horizontal- and vertical-

transmitting species (Baker 2001; Toller *et al.* 2001b; Berkelmans & van Oppen 2006). For example, colonies of the vertically-transmitting coral *Porites astreoides* underwent a change in dominant symbiont from clade C to clade A when transplanted to a shallower habitat on a Caribbean reef (Baker 2001), a response that ostensibly led to an improvement in thermal tolerance. While no deterministic symbiont shuffling was observed in the present study, symbiont ratios were temporally variable in transplanted corals compared with those established colonies (see chapter 3). This increased random variation in $S_H$:$S_T$ may have arisen from the fragmentation process, causing stochastic drift in the proportional abundance as a result of a 'population bottleneck'. Indeed, the effect may have been compounded by partial bleaching experienced by fragments following transplantation. The sudden exposure of previously-shaded branch areas to excess irradiance resulted in visible paling in all transplanted colonies (including the transplanted controls) on the North Bay reef approximately one week after transplantation, while no such bleaching was apparent in the parent colonies (pers. obs; a follow-up visual assessment of fragments and parent colonies could not be carried out at The Arch, due to difficulties accessing this site). These findings support the assertion made in chapter 3: that the symbiont consortium of *P. damicornis* is determined during early ontogeny and/or bleaching, with genetically homogeneous and heterogeneous *Symbiodinium* cells apparently not subject to intra-specific competition or selective expulsion by the host.

### *5.4.3. Methodological considerations*

While symbiont performance was apparently uncoupled from host fitness in this study, several factors may have prevented the detection of underlying patterns. Stochastic events such as abiotic disturbance, interspecific competition, predation and disease can substantially increase the variability in coral growth and survival on the reef (Correa & Baker 2011). Gaining reliable estimates of fitness in the field is hampered by these processes, particularly when sample sizes are small (Garrison & Ward 2012). Measuring the influence of putative *Symbiodinium* hybrids on host survival was further hindered by the inability to retrieve coral fragments at a time when approximately equal numbers had perished and survived (thus maximizing statistical power; Quinn & Keough 2002). Future assessments of coral- and symbiont-fitness may benefit from employing larger sample sizes and attempting to control for the many sources of extraneous variation encountered in the natural setting. Moreover,

fitness is a measure of an individual's genetic contribution to subsequent generations (Maynard Smith 1998). Estimates of performance, growth and survivorship can give an indication of fitness, but may not provide an absolute measure (Arnold 1983). For example, in a comparison of the effects of different symbiont types on the fitness of the anemone *Aiptasia* sp., homologous algae stimulated increased biomass while heterologous algae prompted an increase in reproductive output (Kinzie & Chee 1979). Further attempts to establish a link between symbiont hybridization and coral fitness should therefore also incorporate measures of reproductive success.

### *5.4.4. Conclusion*

The relative abundance of genetically heterogeneous *Symbiodinium* cells did not appreciably affect the growth or survival of transplanted corals in the field, despite the impaired photosynthetic function of these symbionts at elevated temperature. These findings highlight the fact that a coral's fitness may be uncoupled from the photosynthetic performance of its symbiont, through processes mediated by either or both symbiotic partners. An apparent lack of negative long-term effects associated with hosting putative *Symbiodinium* hybrids may help to explain their temporal stability within colonies and their widespread abundance on the Lord Howe Island reef. Further research into the mutualistic scope of hybrid *Symbiodinium* cells may reveal concealed benefits, such as adaptation to extreme conditions or reduced virulence. Establishing the implications of symbiont hybridization for coral fitness will ultimately help to evaluate the evolutionary significance of this process in a rapidly changing environment.

# Chapter 6: General discussion

The preceding data chapters provide several lines of indirect evidence for hybridization in symbiotic dinoflagellates. These include: (1) the intra-genomic co-dominance of divergent *ITS2* sequences; (2) significant genetic clustering of heterogeneous and homogeneous symbionts; (3); the coexistence of genetically heterogeneous symbionts with both putative progenitors; (4) thermal niche partitioning, consistent with the diversification of hybrids into 'extreme' habitats (i.e. the coral-macroalgal transition zone); (5) differences in morphology and physiology, with putative hybrids 50% larger by volume and showing a two-fold increase in chlorophyll $c_2$:*a*; and (6) disparities in photosynthetic function, consistent with the deleterious segregation of unlinked genes in haploid hybrids ('hybrid breakdown'). A review of the literature also indicates that hybridization may have occurred among other *Symbiodinium* taxa. In particular, this hypothesis is advanced by emerging evidence of sexual reproduction in symbiotic dinoflagellates (Baillie *et al.* 1998, 2000; LaJeunesse 2001; Santos *et al.* 2003b; Pettay *et al.* 2011; Thornhill *et al.* 2013a; Chi *et al.* 2014; Baums *et al.* 2014), a maximum divergence threshold of around 5-10% *ITS* dissimilarity for viable hybridization in other dinoflagellates, diatoms and haplontic green algae (Coleman *et al.* 1994; Edvardsen *et al.* 2003; Vanormelingen *et al.* 2008), and the recent finding of diploidy and allelic additivity in the heat-tolerant species *Symbiodinium trenchii* (LaJeunesse *et al.* 2014). While evidence remains indirect, these results collectively provide a compelling argument that hybridization is a naturally occurring phenomenon in the *Symbiodinium* genus.

### *6.1.1. Confirming hybridization in* Symbiodinium

The findings of this study highlight the need for direct evidence of hybridization in *Symbiodinium*. This is likely best accomplished through continued attempts to induce the sexual life-cycle within and between *Symbiodinium* lineages in culture. While putative gametes have been observed by several authors (Freudenthal 1962; Taylor 1973, 1974; Fitt & Trench 1983), life-cycle stages are often misinterpreted in dinoflagellates (Elbrächter 2003). This is particularly true of gametogenesis, which often involves simple vegetative division (hologamy; Pfiester & Anderson 1987). Conclusive evidence of this process has continued to evade researchers, presenting a major challenge to determining the evolutionary significance

of recombination in the *Symbiodinium* genus. Yet cryptic sexual life cycles have been increasingly exposed in free-living 'asexual' dinoflagellates (e.g. Parrow & Burkholder 2003a; b, 2004), with the simulation of nutrient stress often proving the necessary stimulant (Turpin *et al.* 1978; Anderson *et al.* 1984; Chesnick & Cox 1987; Figueroa *et al.* 2007, 2011). Experimental crossing of closely related types may also help to induce the sexual life-cycle, since mating incompatibilities often prevent isoclonal dinoflagellates from conjugating (Destombe & Cembella 1990; Parrow & Burkholder 2003a). The experimental stimulation of sexual reproduction in *Symbiodinium* would constitute an important scientific breakthrough, with potentially major implications for coral adaptation in a changing climate. As such, research in this area should be a high priority.

In the absence of direct evidence of sexual reproduction and hybridization in culture, convincing evidence of these processes may be obtained from genomic analysis. A preliminary objective is to determine the multi-locus genotype (MLG) of each clone within a symbiont assemblage. Yet MLG techniques require DNA from individual organisms or isoclonal cell-lines (Santos *et al.* 2003b). While some corals appear to harbour a single symbiont genotype (Goulet & Coffroth 2003a; b; Pettay & LaJeunesse 2007; Thornhill *et al.* 2009; Andras *et al.* 2011; Pettay *et al.* 2011; Baums *et al.* 2014), and thus effectively provide a 'culture vessel' of vegetative growth (LaJeunesse *et al.* 2012), this is clearly not the case for many species (e.g. Rowan & Knowlton 1995; Stat *et al.* 2011; Green *et al.* 2014). Indeed, the results presented in this thesis suggest that the *P. damicornis* symbiont consortium can consist of at least three (and possibly many more) clonal genotypes. These symbionts do not readily survive in culture (S. Pontasch, VUW, pers. comm.), a trait characteristic of many vertically-transmitted *Symbiodinium* lineages (Krueger & Gates 2012). However, a solution may be found in whole genome amplification (WGA). Recent developments in WGA using the bacteriophage *Φ*29 DNA polymerase (Dean *et al.* 2002) show promising results for obtaining MLG data from single cells. For example, WGA facilitated the successful amplification of 20 different loci from a single human lymphocyte (Handyside *et al.* 2004). Application of this technology to the unicellular organisms of the coral holobiont could greatly improve the resolution of population genetic studies, and thus help to identify the genealogical origins of non-culturable *Symbiodinium* cells.

The inability to culture *Symbiodinium* C100, C109 or their putative hybrids necessitated genotyping by single-cell PCR (scPCR). While this method enabled the unambiguous distinction of intra- and inter-genomic sequence variation, it is currently restricted to

targeting a single, high-copy-number marker from each *Symbiodinium* cell. The *ITS2* locus was chosen for its wide utility, phylogenetic sensitivity and amenability to scPCR (since it occurs in multiple copies per genome). However, its multi-copy nature also renders it subject to intra-genomic variation arising from the incomplete concerted evolution of ancestral polymorphisms, presenting an unavoidable limitation to this study. Despite its drawbacks, the *ITS2* can reveal important evolutionary processes, including hybridization, hybrid speciation, reticulate evolution and adaptive radiation (Álvarez & Wendel 2003), particularly when used in conjunction with morphological, physiological and ecological data (Peterson *et al.* 2004; Vriesendorp & Bakker 2005). DNA meta-barcoding now offers semi-quantitative estimates of *ITS2* copy numbers and other genetic markers at the subclade level through the generation of high-throughput sequence data (Green *et al.* 2014). Applying this powerful molecular tool to the individual symbiont cell could facilitate large-scale assessments of intra-genomic variation and inter-genomic diversity, helping to establish the incidence of hybridization and solve the complex puzzle of *Symbiodinium* evolution.

### *6.1.2. Implications of* Symbiodinium *hybridization*

Over the past two decades or so, a prolific research effort has sought to predict the future of coral reefs in a changing climate. While symbiont shuffling has been identified as an important acclimatory mechanism offering short-term relief from environmental stress, the so-called ‘adaptive bleaching’ response does not appear to be a heritable modification, and hence its potential benefits are ostensibly limited. Understanding the means by which corals and their symbionts adapt *sensu stricto* is therefore of paramount importance. This will require a major shift in focus towards the evolutionary effects of somatic mutation accumulation and meiotic recombination within and between lineages. In particular, symbiont hybridization has the potential to offer rapid heritable modification to the coral holobiont, and hence play a critical role in its evolution in a shifting adaptive landscape. The putative emergence of this phenomenon prompts several questions about its ecological and evolutionary significance: When, where and how does symbiont hybridization occur? What are the immediate mutualistic effects and long-term adaptive consequences for the coral host? Could symbiont hybridization be applied in future attempts to improve reef resilience? These considerations are discussed in detail below and accompanied by suggested areas for future research.

#### 6.1.2.1. When, where and how does hybridization occur?

For hybridization to contribute to adaptation, reproductive barriers must initially be overcome. Establishing the timing, location and divergence thresholds for sexual reproduction in *Symbiodinium* are therefore important objectives for understanding the evolutionary significance of hybridization in this genus. While the *ITS2* admixture depicted in chapter 2 suggests that frequent recombination events may have produced several hybrid genotypes (see Figure 2.4), the absence of MLG data prevents the identification of individual hybrid classes. On one hand, a single ancient hybridization event may have given rise to a divergent, reproductively isolated hybrid lineage whose genome is in various stages of concerted evolution. On the other hand, hybridization and backcrossing may occur on a regular basis, with the occasional fit recombinant undergoing asexual proliferation. The findings of several fine-scale population-level studies indicate that sexual reproduction occurs frequently within *Symbiodinium* lineages (e.g. Santos *et al.* 2003b; Pettay *et al.* 2011; Thornhill *et al.* 2013a; LaJeunesse *et al.* 2014; Baums *et al.* 2014). However, none of these studies detected the recombination of alleles between lineages, indicating that if successful hybridization does occur in this group it is likely an isolated and/or infrequent occurrence. Competition with parental taxa and 'transgressive segregation' (the emergence of extreme hybrid phenotypes) often confine hybrids to the range margins of parental taxa (Arnold 1997; Rieseberg 1997; Rieseberg *et al.* 2003), and hybrid symbionts of terrestrial plants show a similar distribution pattern (e.g. Barrett *et al.* 2007; Hamilton *et al.* 2009). Therefore, *Symbiodinium* hybridization may occur exclusively in marginal coral reef habitats. Yet hybridization is stimulated both by disturbance (Anderson & Stebbins 1954) and species range shifts (Hoffmann & Sgrò 2011); hence an increase in frequency may occur as conditions continue to deteriorate.

**Ancient hybridization:** Hybridization may not necessarily occur frequently to have important evolutionary effects. The chance occurrence of a single fit hybrid recombinant can give rise to a novel lineage, provided that the adaptive allele combination can stabilize and that reproductive isolation is upheld (Grant 1981; Figure 6.1). This mode of speciation has been implicated in major adaptive radiations, particularly when hybrids occupy vacant niches arising from environmental upheaval (Anderson & Stebbins 1954; Seehausen 2004; Bell & Travis 2005; Grant *et al.* 2005; Mallet 2007). Hybrid speciation is commonly associated with

allopolyploidy (when an $F_1$ hybrid inherits a set of chromosomes from each parent), since chromosome doubling can offer instant genetic isolation from both progenitors (reviewed in Mallet 2007; Abbott *et al.* 2013). Yet an increasing number of cases of homoploid hybrid speciation have been identified, particularly when hybrids diversify into extreme habitats *via* transgressive segregation (Rieseberg 1997; Buerkle *et al.* 2000; Rieseberg *et al.* 2003; Gompert *et al.* 2006). For example, in the wild sunflower genus *Helianthus*, hybrid species have diversified into deserts and salt marshes (Rieseberg *et al.* 2003), and in the butterfly genus *Lycaeides*, a homoploid hybrid species of *L. melissa* and *L. idas* occurs exclusively in extreme alpine habitats (Gompert *et al.* 2006). Hybrid diversification and speciation are also prevalent in symbiont lineages. A hybrid strain of the poplar rust pathogen *Melampsora* sp. occurs at the southern range margin of its progenitor *Melampsora lini* in Australia (Barrett *et al.* 2007), and in the endophytic fungal symbionts of the grass family Poaceae, hybrid species of the genus *Neotyphodium* are common in habitats characterised by low moisture and reduced nutrients, in comparison to their *Epichloë* progenitors (Hamilton *et al.* 2009).

Hybridization may have played an important role in recent adaptive radiations of symbiotic dinoflagellates. Host-taxon niche diversification can present a powerful diverging force (Thornhill *et al.* 2013a), and may provide the ecological isolation necessary to reinforce hybrid speciation (Buerkle *et al.* 2000). The polytomic clade D lineage presents a particularly feasible case of adaptive radiation *via* hybridization. This group includes at least four species that show adaptation to 'extreme' environmental conditions (*Symbiodinium trenchii, S. boreum, S. eurythalpos* and *S. glynni nomen nudum*; LaJeunesse *et al.* 2014). In particular, several characteristics of *S. trenchii* suggest a possible origin of hybrid speciation. *S. trenchii* has one of the largest genomes of all symbiotic dinoflagellates (LaJeunesse *et al.* 2005), it routinely possesses two alleles at microsatellite loci (Pettay & LaJeunesse 2009; Wham *et al.* 2011; LaJeunesse *et al.* 2014), and its *ITS2* profile shows a co-dominant pattern diagnostic of both *Symbiodinium* D1a and *S. glynni* (LaJeunesse 2002).While polyploidy can spontaneously arise in asexual lineages through abnormal mitotic cell division (resulting in whole-genome duplication), this species also shows ecological traits resembling a hybrid species. For example, *S. trenchii* characteristically inhabits thermally-extreme environments (Berkelmans & van Oppen 2006; Keshavmurthy *et al.* 2012) and rapidly colonises bleached corals, aggressively out-competing other symbiont taxa under thermally-stressful conditions (LaJeunesse *et al.* 2009).

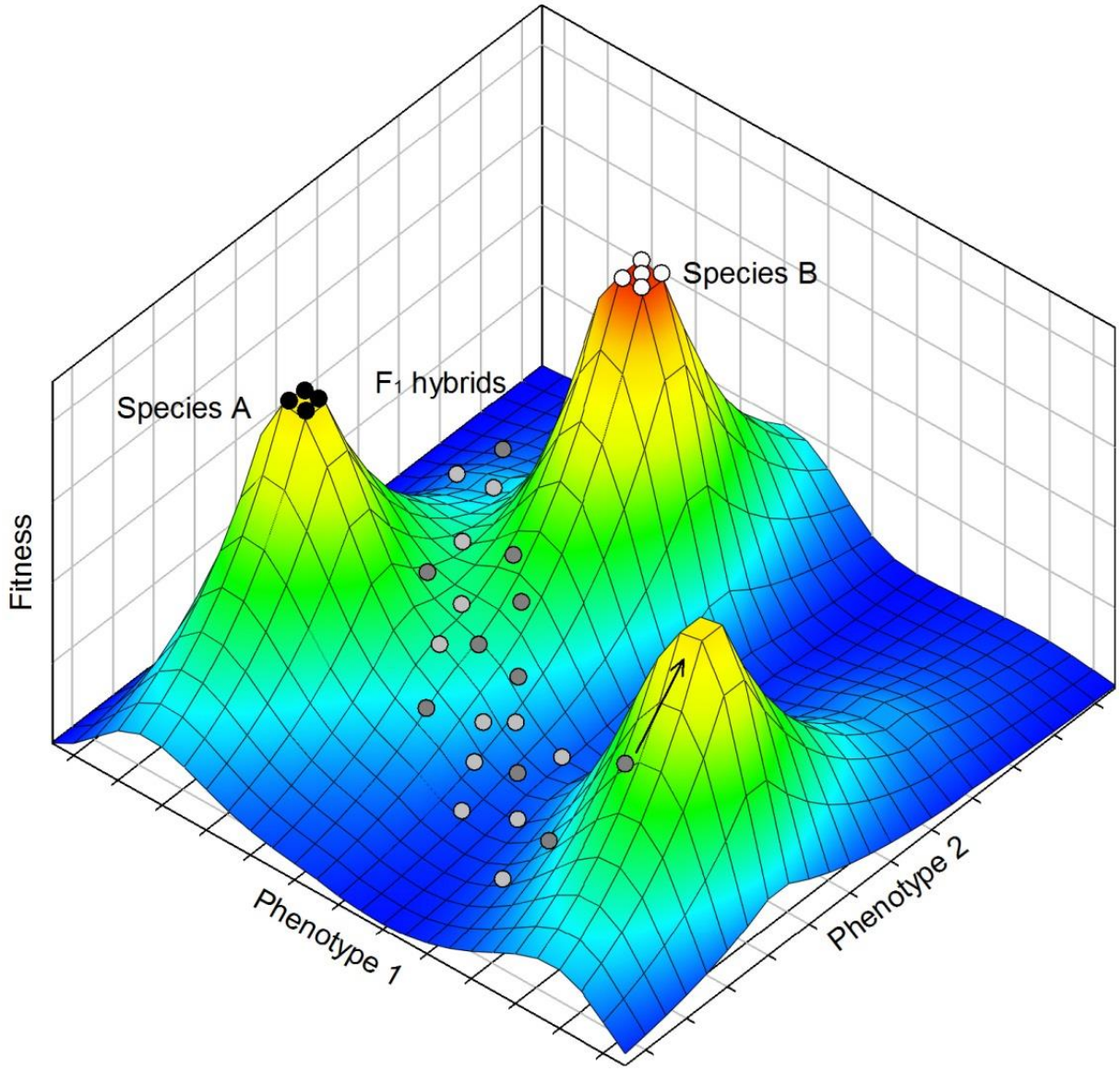


**Figure 6.1 Adaptive divergence *via* hybridization**
Two species, A (black) and B (white) are superimposed on an adaptive landscape alongside A × B hybrids (grey, with many possible haploid genotypes). The plane represents two quantitative phenotypic characters that are subject to 'fitness optima' (shown in a colour gradient). In reality, environmental change causes the landscape to shift continuously, and natural selection simultaneously acts on many phenotypic traits, meaning that the landscape is multi-dimensional (Wright 1932). Hybridization can lead to macro-evolutionary 'jumps'. If a fortunate hybrid recombinant hits an unoccupied adaptive peak, it may exploit the vacant niche, stabilize and undergo hybrid speciation (shown by arrow; adapted from Wright 1932; Simpson 1953; Mallet 2007).

While *S. trenchii* presents an obvious candidate hybrid species, several other symbiotic dinoflagellates also warrant further investigation. For example, the C3m *ITS2* sequence is co-dominant with that of C3 in symbionts of the zoanthid *Protopalythoa* sp. in Hawaii (LaJeunesse *et al.* 2004); yet C3m aligns with the C1 radiation. This suggests that, either the same *ITS2* nucleotide substitution that arose during the divergence of C1 from the C3 lineage arose independently during the more recent divergence of C3m from the C3 lineage (i.e. homoplasy), or hybridization has occurred between members of the C1 and C3 radiations (LaJeunesse *et al.* 2005). Could the genetically heterogeneous *Symbiodinium* C100 × C109 cells represent a divergent, reproductively isolated hybrid species? The diversification of heterogeneous symbionts into a more 'marginal' habitat from that of the putative progenitor (C100) is consistent with hybrid speciation, since niche partitioning is often a necessary precursor for this mode of divergence (Buerkle *et al.* 2000). However, while morphological, physiological and ecological evidence may allude to hybrid speciation, this process can be notoriously difficult to demonstrate. In order to provide convincing evidence that a species is of hybrid origin, natural selection should favour similar gene combinations in experimental crosses (i.e. synthetic hybrids) under similar environmental conditions (e.g. Rieseberg *et al.* 2003). Yet even this may be insufficient to unambiguously confirm a species' genealogical origin (Morrell & Rieseberg 1998).

**Frequent hybridization:** Another scenario that could explain the genotypic clustering patterns observed in chapter 2 is that *Symbiodinium* C100 and C109 remain reproductively compatible. Under this scenario, the cluster of genetically heterogeneous *Symbiodinium* cells may arise from frequent hybridization events, and hybrids may occasionally backcross to the parental types. If this is the case, where and when does hybridization occur? The majority of adult coral colonies appear to host just one or a few *Symbiodinium* clones, and symbiont reproduction appears to be exclusively asexual when *in hospite* (LaJeunesse *et al.* 2012). Here, symbionts are enclosed in membrane-bound vacuoles within the host's gastrodermal cells (see Davy *et al.* 2012), presumably preventing them from accessing potential mates. Furthermore, theory predicts that hosts should actively limit the reproductive opportunities of the symbionts, in order to prevent symbiotic disruption arising from competition between closely-related individuals (Frank 1996a). It therefore seems unlikely that *Symbiodinium* sexual reproduction occurs in the multicellular coral host. By contrast, free-living *Symbiodinium* cells can be highly mobile, showing directed movement towards chemical and physical cues (Fitt 1984; Hollingsworth *et al.* 2005; Pasternak *et al.* 2006), and existing in

high densities in the reef sediment and water column (Coffroth *et al.* 2006; Littman *et al.* 2008; Pochon *et al.* 2010; Takabayashi *et al.* 2011). The unlimited access to potential mates suggests that the symbionts of horizontally-transmitting corals probably undergo sexual reproduction outside of the host (Trench 1997; but see Baums *et al.* 2014). However, extensive recombination of alleles has also occurred in *S. glynni* populations isolated from closely related, vertically-transmitting *Pocillopora* spp. in the Gulf of California (Pettay *et al.* 2011). This is clearly at odds with the theory that symbiont sexual reproduction occurs exclusively *ex hospite*.

Frank (1996a) suggested that symbiotic hosts may derive adaptive benefit from the delineation of symbionts into transmissible germ lineages and non-transmissible somatic lineages. If a portion of a coral's symbionts are sexual, and these symbionts are transmitted to the progeny, then symbiont fusion, plasmogamy and recombination may occur early during the host's ontogenetic development. The ovum of vertically-transmitting corals presents a unique situation where several non-clonal symbionts coexist within a single host cell. Information on the assortment of symbionts into the ovum is scarce (Davy & Turner 2003; Davy *et al.* 2012); however Padilla-Gamiño *et al.* (2012) showed that Hawaiian *Montipora capitata* colonies release eggs containing between 2300 and 4200 *Symbiodinium* cells, and many eggs contain distinct symbiont consortia from that of the parent colony. These authors suggested that adaptive diversification may result from the selective assortment of symbionts into gametes. The hypothesis outlined here takes the suggestion of Padilla-Gamiño *et al.* (2012) a step further, by proposing that under certain conditions, an adaptive advantage may be realized by both partners if symbiont sexual reproduction occurs in synchrony with that of the host. Under this scenario, the onset of symbiont sexual reproduction occurs in the host gamete, zygote and/or developing embryo. Natural selection then acts on a cohort of coral juveniles with a wide range of genotypes and hosting a wide range of recombinant symbionts, thus conferring maximum likelihood of hitting a vacant 'adaptive peak' (see Figure 6.1).

It is not unusual for symbiont sexual reproduction to occur in synchrony with that of the host. For example, the dinoflagellate *Peridinium balticum* and its membrane-bound endosymbiotic heterokont (Bacillariophyta) undergo concomitant sexual reproduction (Chesnick & Cox 1987). Indeed, major hybridization events in symbiont lineages appear to track those of their hosts. For example, a hybrid poplar was widely grown in California on account of its resistance to the two rust pathogens that infected its parent species (*Melampsora medusa*, the parasite of *Populus deltoids*, and *M. occidentalis*, the parasite of *P. trichocarpa*). However, in

1997 these pathogens crossed to produce the hybrid species *Melampsora* × *columbiana*, which was able to infect the hybrid poplar (Newcombe *et al.* 2000). In another example, the tall fescue grass *Lolium arundinaceum* (=*Festuca arundinacea*) and its fungal endosymbiont *Neotyphodium* × *coenophialum* have each undergone two separate hybridizations, culminating in the combination of three plant genomes and three fungal genomes (Tsai *et al.* 1994; Humphreys *et al.* 1995; Schardl & Craven 2003; Moon *et al.* 2004).

The possibility that *P. damicornis* and its symbionts have undergone synchronous hybridization presents an interesting topic for investigation. *P. damicornis* undergoes extensive hybridization in nature (Combosch *et al.* 2008), and shows a predominantly sexual reproductive mode at Lord Howe Island, where it is even known to undergo intergeneric hybridization with *Stylophora pistillata* (Miller & Ayre 2004). While sexual reproduction in *P. damicornis* appears to be more prevalent at marginal reefs, the majority of offspring produced are brooded asexual larvae, and the cryptic simultaneous broadcast-spawning of gametes can be difficult to detect (Combosch & Vollmer 2013). As such, testing the hypothesis that the reproductive mode of the symbiont is intertwined with that of the host will likely require a population genetics approach, tracking the genealogical origins of both symbiotic partners over several generations. In the interim, the feasibility of this hypothesis may be assessed by evaluating the potential costs and benefits in terms of host fitness.

#### 6.1.2.2. How does symbiont hybridization affect coral fitness?

The occurrence of natural hybridization between symbiotic dinoflagellates may have a major influence on the fitness of the coral host. Symbiont-derived compounds constitute the primary source of energy for reef-building corals (Muscatine 1990; but see Grottoli *et al.* 2006), and hence even minor disparities in photosynthetic performance can have a profound impact on the host's ability to survive and reproduce (e.g. Cantin *et al.* 2009). Symbiont hybridization may therefore be detrimental to the host if hybrid breakdown inhibits performance, but similar microbe-associated molecular patterns are inherited (MAMPs; see Davy *et al.* 2012) and hence the host is unable to recognize deleterious hybrids. Alternatively, symbiont hybridization may benefit host fitness through the instantaneous production of a novel asexual lineage with increased competitive ability (Stebbins 1950) and a 'clean slate' from deleterious mutations.

The effects of symbiont hybridization on host fitness are highlighted by the example of symbiotic fungi in the genera *Epichloë* and *Neotyphodium*. These endophytic ascomycetes infect cool-season grasses of the family Poaceae (subfamily Poöideae), an association that spans the parasitism-mutualism continuum. Most asexual *Neotyphodium* spp. symbionts are of hybrid origin (Schardl *et al.* 1994; Tsai *et al.* 1994; Moon *et al.* 2004; Hamilton *et al.* 2009), a process that has been implicated in their recent radiation (Tsai *et al.* 1994). Hybridization has also been central to the evolution of mutualism in *Neotyphodium* spp., which are transmitted from parent to offspring and offer a wide range of adaptive benefits to their hosts. For example, repeated hybridization events have led to the accumulation of alkaloid-production genes in the hybrid species *Neotyphodium* × *coenophialum*, which can produce three of the four known classes of endophyte- associated anti-herbivore alkaloids (Clay & Schardl 2002). Indeed, grasses hosting asexual *Neotyphodium* hybrids often show increased fitness compared to those that host 'pure' types, including resistance to herbivory and disease, and the ability to survive in extreme environments (Malinowski & Belesky 2000; Clay & Schardl 2002; Hamilton *et al.* 2009; Saari & Faeth 2012). By contrast, the horizontally-transmitted, sexual progenitor *Epichloë* sp. can reduce host fitness by 'hijacking' the plant's reproductive structures in order to facilitate spore dispersal (choke disease; Schardl & Clay 1997). Hybridization may also benefit both symbiotic partners by preventing the accumulation of deleterious mutations in a vertically-transmitted symbiont lineage (i.e. the counteraction of Muller's ratchet; Muller 1964; Felsenstein 1974). The occasional recombination that occurs between *Neotyphodium* and *Epichloë* lineages is thought to play a key role in preventing 'ratchet clicks' in mutualistic fungal endophytes (Schardl *et al.* 1991; Clay & Schardl 2002; Schardl & Craven 2003). While fungal hybridization outside the symbiosphere is uncommon, the diverse array of fungal hybrids in vertically-transmitting grasses implies a host role in the outcrossing process (Clay & Schardl 2002). It is not known whether the host actively selects beneficial asexual hybrid genotypes or the particular ecological niche simply favours hybrids when they occur (Schardl & Craven 2003; Moon *et al.* 2004). However, the hybrid fungal endophyte example serves to illustrate the substantial fitness benefits that a host may derive from symbiont hybridization.

The corals that were dominated by putative hybrid symbionts in this study showed significant reductions in overall photosynthetic performance (*P:R*; see chapter 4). Yet these colonies did not suffer from decreased growth rates or higher mortality in the field (chapter 5). The apparent uncoupling of symbiont photosynthetic performance and host fitness suggests that

corals may realize compensatory adaptive benefits from hosting hybrid *Symbiodinium*. The literature on fungal-plant mutualisms suggests that these benefits could include an increased ability to survive in extreme environments, a reduced risk of symbiont virulence, the production of secondary compounds, and the release from mutation accumulation in vertically-transmitted symbiont lineages. This suite of potential adaptive benefits indicates that the coral host may indeed play an active role in the creation of new symbiont lineages.

#### 6.1.2.3. What are the evolutionary implications of symbiont hybridization?

Hybridization can expedite the evolutionary process by providing the raw genetic material necessary for adaptation (Anderson 1949). In spatial areas where related species hybridize frequently ('hybrid zones'), fertile $F_1$ hybrids may 'backcross' with individuals from one or both progenitor populations. The mating of progenitors with progressively later-generation backcross genotypes can lead to the migration of genetic material between lineages (introgression; see Figure 2.1b). Introgressive hybridization can incur profound evolutionary consequences for the recipient population(s). These range from the introduction of 'genetic pollution' to a native lineage (even leading to extinction; reviewed in Rhymer & Simberloff 1996) to the acquisition of novel genetic diversity, providing a 'fast track' to adaptive evolution (Anderson & Stebbins 1954; Lewontin & Birch 1966; Arnold & Martin 2010). Adaptive trait introgression may be particularly important in a changing environment, since this mechanism can confer rapid evolutionary modification. In their pioneering experiments on the fruit fly *Dacus tryoni*, Lewontin & Birch (1966) showed that the introduction of genes from another species (*Dacus neohumeralis*) was responsible for substantial changes in thermal optima, despite the absence of heterosis (i.e. $F_1$ hybrids and backcross generations were less fit than either progenitor). The introgressive transfer of thermally-adaptive gene combinations was thus identified as the mechanism underlying the rapid shift southward of this invasive Australian pest during the twentieth century (Lewontin & Birch 1966).

Introgressive hybridization can lead to rapid evolution in symbiont lineages, with important effects on their mutualistic scope. Recent studies, particularly those focussed on plant-pathogen interactions, have revealed extensive evolutionary developments arising from introgression. These can range from the acquisition of new host specificities and pathogenic aggressiveness to the adaptive divergence of new symbiont taxa (Brasier 1995, 2000; Et-Touil *et al.* 1999; Brasier *et al.* 1999; Schardl & Craven 2003). A particularly well studied

case is the fungal agent of Dutch elm disease, *Ophiostoma novo-ulmi*, the cause of devastating losses of elms across Europe, Asia and America. While *O. novo-ulmi* × *O. ulmi* $F_1$ hybrids are severely unfit and are quickly outcompeted by parental taxa, they serve to provide a bridge for unidirectional flow of genes, and possibly even viruses (Brasier 2001). *O. novo-ulmi* recently acquired the pathogenicity gene *Pat1* from *O. ulmi via* introgressive hybridization, a factor implicated in its increased virulence and concomitant intercontinental spread (Et-Touil *et al.* 1999).

Introgression can represent an especially potent macro-evolutionary force in haplontic organisms, particularly those with rapid generation times (Schardl & Craven 2003). The potential for accelerated *Symbiodinium* evolution through introgressive hybridization may therefore have profound implications for corals in a shifting adaptive landscape. In particular, the transfer of genes between divergent *Symbiodinium* lineages has the potential to produce novel, host-compatible algal phenotypes, facilitating rapid adaptation of the symbiosis to warming ocean temperatures. In plants, introgressive hybridization can even lead to the transfer of chloroplasts between lineages ('chloroplast capture'; Rieseberg & Soltis 1991). Chloroplast capture could have major implications for corals, since the symbiont chloroplast has been identified as a key target for oxidative damage, a precursor to thermal bleaching (reviewed in Lesser 2006). Yet the occurrence of introgression depends on many factors, including the frequency of hybridization events, the regions of the genome that are permeable to gene-flow, the relative fitness of each hybrid and backcross genotype, and the associated genotype × environment interactions (Barton 2001; Arnold 2007; Taylor *et al.* 2009). The abundance of putative *Symbiodinium* hybrids observed within many *P. damicornis* colonies suggests that a fitness advantage may be realized by some hybrid genotypes/classes under certain conditions; however further analyses of multiple diagnostic loci are needed to confirm this. The potential for introgression to expedite coral adaptation highlights the need to make timely progress in this area.

#### 6.1.2.4. Could hybridization be applied to improve reef resilience?

The profound influence of hybridization on species evolution makes it a potentially powerful tool for restoring ecological systems. Attempts to improve habitats impacted by human activity can be enhanced by the directed translocation and/or outcrossing of individuals, with the intention of facilitating adaptation to changing conditions (assisted gene flow or AGF;

Aitken & Whitlock 2013). AGF is an emerging field that holds promise for mitigating maladaptation in a rapidly shifting adaptive landscape (Thomas *et al.* 2013; Aitken & Whitlock 2013). However, there are several risks associated with restorative outcrossing, including the dilution of locally-adapted alleles (Montalvo & Ellstrand 2000; Fenster & Galloway 2000), the segregation of co-adapted gene complexes (Edmands 2007; Schiffers *et al.* 2013), the introduction of 'genetic pollution'(Rhymer & Simberloff 1996; Hufford & Mazer 2003), and in the case of symbiotic organisms, the stimulation of virulence (Brasier 2001). These factors could impart unforeseeable, possibly unmanageable consequences, and hence extensive feasibility assessments are necessary before any genetic interventions should be considered (Thomas *et al.* 2013).

For corals, the genetic enhancement of host-symbiont combinations through directed hybridization could enable the introduction of pre-adapted host-symbiont combinations to denuded reefs. These actions may expedite the restoration process and promote increased resilience to future environmental perturbation. Human-assisted evolution of symbiotic dinoflagellates could yield particularly effective results, due to their short generation times and known potential for rapid adaptation (van Oppen *et al.* 2011; Howells *et al.* 2011). Initially, establishing the efficacy of AGF in *Symbiodinium* would benefit from research aimed at inducing the sexual life cycle, determining the frequency and location of hybridization events, establishing barriers of genetic exchange, and identifying areas of the genome permeable to introgressive gene flow. While such 'evolutionary rescue' is fundamentally reactive in scope, this emerging area of research is a priority due to the continued reef degradation caused by human activity.

### *6.1.3. Concluding remarks*

While usually deleterious in nature, hybridization can occasionally produce a fit individual whose genetic contribution can have a disproportionately large influence on adaptation. The resulting burst of genetic variation can provide evolutionary innovation two or three orders of magnitude greater than that offered by the gradual accumulation of mutations (Grant & Grant 1994). The immense biodiversity and ecosystem services provided by the world's coral reefs emphasize the need to better understand the 'macro-evolutionary' potential of the many species constituting the coral holobiont. In particular, the integral roles of the symbiotic alga *Symbiodinium* in coral productivity, reef accretion and thermal bleaching highlight the critical

importance of this research. This thesis takes a tentative step forward by providing indirect evidence of natural hybridization between two *Symbiodinium* lineages. Gaining a wider understanding of sexual reproduction and hybridization in both the host and the symbiont is needed to assess the potential for coral adaptation, both natural and human-assisted, as our destructive activity continues to jeopardize their future.

# References


Abbott R, Albach D, Ansell S *et al.* (2013) Hybridization and speciation. *Journal of Evolutionary Biology*, **26**, 229–246.

Abrego D, Ulstrup KE, Willis BL, van Oppen MJH (2008) Species-specific interactions between algal endosymbionts and coral hosts define their bleaching response to heat and light stress. *Proceedings of the Royal Society B*, **275**, 2273–2282.

Aitken SN, Whitlock MC (2013) Assisted gene flow to facilitate local adaptation to climate change. *Annual Review of Ecology, Evolution, and Systematics*, **44**, 367–388.

Allemand D, Tambutté É, Zoccola D, Tambutté S (2011) Coral calcification, cells to reefs. In: *Coral Reefs: An Ecosystem in Transition* (eds Dubinsky Z, Stambler N), pp. 119–150. Springer, New York.

Allen GR, Paxton JR (1974) A tropical outpost in the Pacific. *Australian Natural History*, **18**, 50–55.

Altschul SF, Gish W, Miller W, Myers EW, Lipman DJ (1990) Basic local alignment search tool. *Journal of Molecular Biology*, **215**, 403–410.

Álvarez I, Wendel JF (2003) Ribosomal ITS sequences and plant phylogenetic inference. *Molecular Phylogenetics and Evolution*, **29**, 417–434.

Anderson E (1949) *Introgressive Hybridization*. John Wiley and Sons, New York.

Anderson DM, Kulis DM, Binder BJ (1984) Sexuality and cyst formation in the dinoflagellate *Gonyaulax tamarensis*: cyst yield in batch cultures. *Journal of Phycology*, **20**, 418–425.

Anderson E, Stebbins GL Jr (1954) Hybridization as an evolutionary stimulus. *Evolution*, **8**, 378–388.

Andersson L (1990) The driving force: species concepts and ecology. *Taxon*, **39**, 375–382.

Andras JP, Kirk NL, Harvell CD (2011) Range-wide population genetic structure of *Symbiodinium* associated with the Caribbean Sea fan coral, *Gorgonia ventalina*. *Molecular Ecology*, **20**, 2525–2542.

Anthony KRN, Kline DI, Diaz-Pulido G, Dove S, Hoegh-Guldberg O (2008) Ocean acidification causes bleaching and productivity loss in coral reef builders. *Proceedings of the National Academy of Sciences of the United States of America*, **105**, 17442–17446.

Arif C, Daniels C, Bayer T *et al.* (2014) Assessing *Symbiodinium* diversity in scleractinian corals via next-generation sequencing- based genotyping of the ITS2 rDNA region. *Molecular Ecology*, **23**, 4418–4433.

Arnheim N, Krystal M, Schmickel R *et al.* (1980) Molecular evidence for genetic exchanges among ribosomal genes on nonhomologous chromosomes in man and apes. *Proceedings of the National Academy of Sciences of the United States of America*, **77**, 7323–7327.

Arnold SJ (1983) Morphology, performance and fitness. *American Zoologist*, **23**, 347–361.

Arnold ML (1997) *Natural Hybridization and Evolution*. Oxford University Press, Oxford.

Arnold ML (2007) *Evolution through Genetic Exchange*. Oxford University Press, Oxford.

Arnold ML, Hodges SA (1995) Are natural hybrids fit or unfit relative to their parents? *Trends in Ecology and Evolution*, **10**, 67–71.

Arnold ML, Martin NH (2010) Hybrid fitness across time and habitats. *Trends in Ecology and Evolution*, **25**, 530–536.

Van Baalen M, Sabelis MW (1995) The dynamics of multiple infection and the evolution of virulence. *The American Naturalist*, **146**, 881–910.

Bachvaroff TR, Place AR (2008) From stop to start: tandem gene arrangement, copy number and trans-splicing sites in the dinoflagellate *Amphidinium carterae*. *PLoS ONE*, **3**, e2929.

Baillie BK, Monje V, Silvestre V, Sison M, Belda-Baillie CA (1998) Allozyme electrophoresis as a tool for distinguishing different zooxanthellae symbiotic with giant clams. *Proceedings of the Royal Society of London B*, **265**, 1949–1956.

Baillie BK, Belda-Baillie CA, Silvestre V *et al.* (2000) Genetic variation in *Symbiodinium* isolates from giant clams based on random-amplified-polymorphic DNA (RAPD) patterns. *Marine Biology*, **136**, 829–836.

Baird AH, Bhagooli R, Ralph PJ, Takahashi S (2008) Coral bleaching: the role of the host. *Trends in Ecology and Evolution*, **24**, 16–20.

Baird AH, Guest JR, Willis BL (2009) Systematic and biogeographical patterns in the reproductive biology of scleractinian corals. *Annual Review of Ecology, Evolution, and Systematics*, **40**, 551–571.

Baker AC (2001) Reef corals bleach to survive change. *Nature*, **411**, 765–766.

Baker AC (2003) Flexibility and specificity in coral-algal symbiosis: diversity, ecology, and biogeography of *Symbiodinium*. *Annual Review of Ecology, Evolution, and Systematics*, **34**, 661–689.

Baker AC, Rowan R (1997) Diversity of symbiotic dinoflagellates (zooxanthellae) in scleractinian corals of the Caribbean and Eastern Pacific. *Proceedings of the 8th International Coral Reef Symposium*, **2**, 1301–1306.

Baker AC, Starger CJ, McClanahan TR, Glynn PW (2004) Corals' adaptive response to climate change. *Nature*, **430**, 741.

Baker AC, Romanski AM (2007) Multiple symbiotic partnerships are common in scleractinian corals, but not in octocorals: Comment on Goulet (2006). *Marine Ecology Progress Series*, **335**, 237–242.

Baldwin BG, Sanderson MJ, Porter JM *et al.* (1995) The ITS region of nuclear ribosomal DNA: a valuable source of evidence on angiosperm phylogeny. *Annals of the Missouri Botanical Garden*, **82**, 247–277.

Banaszak AT, Iglestas-Prieto R, Trench RK (1993) *Scrippsiella velellae* sp. nov. (Peridiniales) and *Gloeodinium viscum* sp. nov. (Phytodiniales), dinoflagellate symbionts of two hydrozoans (Cnidaria). *Journal of Phycology*, **29**, 517–528.

Banaszak AT, LaJeunesse TC, Trench RK (2000) The synthesis of mycosporine-like amino acids (MAAs) by cultured, symbiotic dinoflagellates. *Journal of Experimental Marine Biology and Ecology*, **249**, 219–233.

Barbrook AC, Voolstra CR, Howe CJ (2014) The chloroplast genome of a *Symbiodinium* sp. clade C3 isolate. *Protist*, **165**, 1–13.

Barnes DJ, Chalker BE (1990) Calcification and photosynthesis in reef-building corals and algae. In: *Ecosystems of the World, 25: Coral Reefs* (ed Dubinsky Z), pp. 109–131. Elsevier, New York.

Barrett LG, Thrall PH, Burdon JJ (2007) Evolutionary diversification through hybridization in a wild host-pathogen interaction. *Evolution*, **61**, 1613–1621.

Barton NH (2001) The role of hybridization in evolution. *Molecular Ecology*, **10**, 551–568.

Barton N, Bengtsson BO (1986) The barrier to genetic exchange between hybridising populations. *Heredity*, **57**, 357–376.

Baums IB, Devlin-Durante MK, LaJeunesse TC (2014) New insights into the dynamics between reef corals and their associated dinoflagellate endosymbionts from population genetic studies. *Molecular Ecology*, DOI: 10.1111/mec.12788.

Bell JJ, Davy SK, Jones T, Taylor MW, Webster NS (2013) Could some coral reefs become sponge reefs as our climate changes? *Global Change Biology*, **19**, 2613–2624.

Bell MA, Travis MP (2005) Hybridization, transgressive segregation, genetic covariation, and adaptive radiation. *Trends in Ecology and Evolution*, **20**, 358–361.

Berkelmans R, van Oppen MJH (2006) The role of zooxanthellae in the thermal tolerance of corals: a "nugget of hope" for coral reefs in an era of climate change. *Proceedings of the Royal Society B*, **273**, 2305–2312.

Bhagooli R, Hidaka M (2003) Comparison of stress susceptibility of *in hospite* and isolated zooxanthellae among five coral species. *Journal of Experimental Marine Biology and Ecology*, **291**, 181–197.

Bhagooli R, Hidaka M (2004) Release of zooxanthellae with intact photosynthetic activity by the coral *Galaxea fascicularis* in response to high temperature stress. *Marine Biology*, **145**, 329–337.

Blackburn SI, Bolch CJS, Haskard KA, Hallegraeff GM (2001) Reproductive compatibility among four global populations of the toxic dinoflagellate *Gymnodinium catenatum* (Dinophyceae). *Phycologia*, **40**, 78–87.

Blank RJ, Huss VAR (1989) DNA divergency and speciation in *Symbiodinium* (Dinophyceae). *Plant Systematics and Evolution*, **163**, 153–163.

Brasier CM (1995) Episodic selection as a force in fungal microevolution, with special reference to clonal speciation and hybrid introgression. *Canadian Journal of Botany*, **73**, S1213–S1221.

Brasier C (2000) The rise of the hybrid fungi. *Nature*, **405**, 134–135.

Brasier CM (2001) Rapid evolution of introduced plant pathogens *via* interspecific hybridization. *BioScience*, **51**, 123–133.

Brasier CM, Cooke DEL, Duncan JM (1999) Origin of a new *Phytophthora* pathogen through interspecific hybridization. *Proceedings of the National Academy of Sciences of the United States of America*, **96**, 5878–5883.

Briggs JC (1999) Coincident biogeographic patterns: Indo-West Pacific Ocean. *Evolution*, **53**, 326–335.

Brodie J, Fabricius K, De'ath G, Okaji K (2005) Are increased nutrient inputs responsible for more outbreaks of crown-of-thorns starfish? An appraisal of the evidence. *Marine Pollution Bulletin*, **51**, 266–278.

Brosnahan ML, Kulis DM, Solow AR *et al.* (2010) Outbreeding lethality between toxic Group I and nontoxic Group III *Alexandrium tamarense* spp. isolates: Predominance of heterotypic encystment and implications for mating interactions and biogeography. *Deep Sea Research Part II: Topical Studies in Oceanography*, **57**, 175–189.

Brown DD, Wensink PC, Jordan E (1972) A comparison of the ribosomal DNA's of *Xenopus laevis* and *Xenopus mulleri*: the evolution of tandem genes. *Journal of Molecular Biology*, **63**, 57–64.

Bruno JF, Selig ER, Casey KS *et al.* (2007) Thermal stress and coral cover as drivers of coral disease outbreaks. *PLoS Biology*, **5**, e124.

Bryant D, Burke L, McManus J, Spalding M (1998) *Reefs at Risk: A Map-based Indicator of Threats to the World's Coral Reefs*. World Resources Institute, Washington D.C.

Buckler ES IV, Ippolito A, Holtsford TP (1997) The evolution of ribosomal DNA: divergent paralogues and phylogenetic implications. *Genetics*, **145**, 821–832.

Buddemeier RW, Fautin DG (1993) Coral bleaching as an adaptive mechanism. *BioScience*, **43**, 320–326.

Buerkle CA, Morris RJ, Asmussen MA, Rieseberg LH (2000) The likelihood of homoploid hybrid speciation. *Heredity*, **84**, 441–451.

Burke L, Reytar K, Spalding M, Perry A (2011) *Reefs at Risk Revisited*. World Resources Institute, Washington D.C.

Burnham KP, Anderson DR (2002) *Model Selection and Multimodel Inference: A Practical Information-Theoretic Approach (2nd edition)*. Springer, New York.

Burriesci MS, Raab TK, Pringle JR (2012) Evidence that glucose is the major transferred metabolite in dinoflagellate-cnidarian symbiosis. *The Journal of Experimental Biology*, **215**, 3467–3477.

Byler KA, Carmi-Veal M, Fine M, Goulet TL (2013) Multiple symbiont acquisition strategies as an adaptive mechanism in the coral *Stylophora pistillata*. *PLoS ONE*, **8**, e59596.

Cadenas E (1989) Biochemistry of oxygen toxicity. *Annual Review of Biochemistry*, **58**, 79–110.

Cantin NE, van Oppen MJH, Willis BL, Mieog JC, Negri AP (2009) Juvenile corals can acquire more carbon from high-performance algal symbionts. *Coral Reefs*, **28**, 405–414.

Carlos AA, Baillie BK, Kawachi M, Maruyama T (1999) Phylogenetic position of *Symbiodinium* (Dinophyceae) isolates from Tridacnids (Bivalvia), Cardiids (Bivalvia), a sponge (Porifera), a soft coral (Anthozoa), and a free-living strain. *Journal of Phycology*, **35**, 1054–1062.

Carpenter KE, Abrar M, Aeby G *et al.* (2008) One-third of reef-building corals face elevated extinction risk from climate change and local impacts. *Science*, **321**, 560–563.

Carté BK (1996) Biomedical potential of marine natural products. *BioScience*, **46**, 271–286.

Casteleyn G, Adams NG, Vanormelingen P *et al.* (2009) Natural hybrids in the marine diatom *Pseudo-nitzschia* pungens (Bacillariophyceae): genetic and morphological evidence. *Protist*, **160**, 343–354.

De Castro O, Di Maio A, Lozada García JA *et al.* (2013) Plastid DNA sequencing and nuclear SNP genotyping help resolve the puzzle of central American *Platanus*. *Annals of Botany*, **112**, 589–602.

Cesar H (1996) *Economic Analysis of Indonesian Coral Reefs*. The World Bank, Washington D.C.

Chalker BE, Dunlap WC, Oliver JK (1983) Bathymetric adaptations of reef-building corals at Davies Reef, Great Barrier Reef, Australia. II. Light saturation curves for photosynthesis and respiration. *Journal of Experimental Marine Biology and Ecology*, **73**, 37–56.

Chang SS, Prézelin BB, Trench RK (1983) Mechanisms of photoadaptation in three strains of the symbiotic dinoflagellate *Symbiodinium microadriaticum*. *Marine Biology*, **76**, 219–229.

Charlesworth D, Charlesworth B (1987) Inbreeding depression and its evolutionary consequences. *Annual Review of Ecology and Systematics*, **18**, 237–268.

Chen CA, Wang J-T, Fang L-S, Yang Y-W (2005) Fluctuating algal symbiont communities in *Acropora palifera* (Scleractinia: Acroporidae) from Taiwan. *Marine Ecology Progress Series*, **295**, 113–121.

Chesnick JM, Cox ER (1987) Synchronized sexuality of an algal symbiont and its dinoflagellate host, *Peridinium balticum* (Levander) Lemmermann. *Biosystems*, **21**, 69–78.

Chi J, Parrow MW, Dunthorn M (2014) Cryptic sex in *Symbiodinium* (Alveolata, Dinoflagellata) is supported by an inventory of meiotic genes. *Journal of Eukaryotic Microbiology*, **61**, 322–327.

Clay K, Schardl C (2002) Evolutionary origins and ecological consequences of endophyte symbiosis with grasses. *The American Naturalist*, **160**, S99–S127.

Clement M, Posada D, Crandall KA (2000) TCS: a computer program to estimate gene genealogies. *Molecular Ecology*, **9**, 1657–1659.

Coates AG, Jackson JBC (1987) Clonal growth, algal symbiosis, and reef formation by corals. *Paleobiology*, **13**, 363–378.

Coffroth MA, Santos SR (2005) Genetic diversity of symbiotic dinoflagellates in the genus *Symbiodinium*. *Protist*, **156**, 19–34.

Coffroth MA, Santos SR, Goulet TL (2001) Early ontogenetic expression of specificity in a cnidarian-algal symbiosis. *Marine Ecology Progress Series*, **222**, 85–96.

Coffroth MA, Lewis CF, Santos SR, Weaver JL (2006) Environmental populations of symbiotic dinoflagellates in the genus *Symbiodinium* can initiate symbioses with reef cnidarians. *Current Biology*, **16**, R985–R987.

Coffroth MA, Poland DM, Petrou EL, Brazeau DA, Holmberg JC (2010) Environmental symbiont acquisition may not be the solution to warming seas for reef-building corals. *PLoS ONE*, **5**, e13258.

Coleman AW, Suarez A, Goff LJ (1994) Molecular delineation of species and syngens in Volvocacean green algae (Chlorophyta). *Journal of Phycology*, **30**, 80–90.

Coles SL, Jokiel PL (1978) Synergistic effects of temperature, salinity and light on the hermatypic coral *Montipora verrucosa*. *Marine Biology*, **195**, 187–195.

Colombo-Pallotta MF, Rodríguez-Román A, Iglesias-Prieto R (2010) Calcification in bleached and unbleached *Montastraea faveolata*: evaluating the role of oxygen and glycerol. *Coral Reefs*, **29**, 899–907.

Combosch DJ, Vollmer S V (2013) Mixed asexual and sexual reproduction in the Indo-Pacific reef coral *Pocillopora damicornis*. *Ecology and Evolution*, **3**, 3379–3387.

Combosch DJ, Guzman HM, Schuhmacher H, Vollmer S V (2008) Interspecific hybridization and restricted trans-Pacific gene flow in the Tropical Eastern Pacific *Pocillopora*. *Molecular Ecology*, **17**, 1304–1312.

Cook CB (1971) Transfer of $35^{S}$-labeled material from food ingested by *Aiptasia* sp. to its endosymbiotic zooxanthellae. In: *Experimental Coelenterate Biology* (eds Lenhoff HM, Muscatine L, Davis LV), pp. 218–224. University of Hawaii Press, Honolulu.

Correa AMS, Baker AC (2009) Understanding diversity in coral-algal symbiosis: a cluster-based approach to interpreting fine-scale genetic variation in the genus *Symbiodinium*. *Coral Reefs*, **28**, 81–93.

Correa AMS, Baker AC (2011) Disaster taxa in microbially mediated metazoans: how endosymbionts and environmental catastrophes influence the adaptive capacity of reef corals. *Global Change Biology*, **17**, 68–75.

Correa AMS, McDonald MD, Baker AC (2009) Development of clade-specific *Symbiodinium* primers for quantitative PCR (qPCR) and their application to detecting clade *D* symbionts in Caribbean corals. *Marine Biology*, **156**, 2403–2411.

Coskun S, Alsmadi O (2007) Whole genome amplification from a single cell: a new era for preimplantation genetic diagnosis. *Prenatal Diagnosis*, **27**, 297–302.

Costanza R, D'Arge R, de Groot R *et al.* (1997) The value of the world's ecosystem services and natural capital. *Nature*, **387**, 253–260.

Cronn RC, Zhao X, Paterson AH, Wendel JF (1996) Polymorphism and concerted evolution in a tandemly repeated gene family: 5S ribosomal DNA in diploid and allopolyploid cottons. *Journal of Molecular Evolution*, **42**, 685–705.

Crossland CJ, Barnes DJ (1977) Gas-exchange studies with the staghorn coral *Acropora acuminata* and its zooxanthellae. *Marine Biology*, **40**, 185–194.

Crow JF (1994) Advantages of sexual reproduction. *Developmental Genetics*, **15**, 205–213.

Cunning R, Baker AC (2013) Excess algal symbionts increase the susceptibility of reef corals to bleaching. *Nature Climate Change*, **3**, 259–262.

Cunning R, Glynn PW, Baker AC (2013) Flexible associations between *Pocillopora* corals and *Symbiodinium* limit utility of symbiosis ecology in defining species. *Coral Reefs*, **32**, 795–801.

Davies PS (1984) The role of zooxanthellae in the nutritional energy requirements of *Pocillopora eydouxi*. *Coral Reefs*, **2**, 181–186.

Davy SK, Turner JR (2003) Early development and acquisition of zooxanthellae in the temperate symbiotic sea anemone *Anthopleura ballii* (Cocks). *The Biological Bulletin*, **205**, 66–72.

Davy SK, Lucas IAN, Turner JR (1997) Uptake and persistence of homologous and heterologous zooxanthellae in the temperate sea anemone *Cereus pedunculatus* (Pennant). *The Biological Bulletin*, **192**, 208–216.

Davy SK, Allemand D, Weis VM (2012) Cell biology of cnidarian-dinoflagellate symbiosis. *Microbiology and Molecular Biology Reviews*, **76**, 229–261.

Dean FB, Hosono S, Fang L *et al.* (2002) Comprehensive human genome amplification using multiple displacement amplification. *Proceedings of the National Academy of Sciences of the United States of America*, **99**, 5261–5266.

Demuth JP, Wade MJ (2005) On the theoretical and empirical framework for studying genetic interactions within and among species. *The American Naturalist*, **165**, 524–536.

Destombe C, Cembella A (1990) Mating-type determination, gametic recognition and reproductive success in *Alexandrium excavatum* (Gonyaulacales, Dinophyta), a toxic red-tide dinoflagellate. *Phycologia*, **29**, 316–325.

Diekmann OE, Bak RPM, Tonk L, Stam WT, Olsen JL (2002) No habitat correlation of zooxanthellae in the coral genus *Madracis* on a Curaçao reef. *Marine Ecology Progress Series*, **227**, 221–232.

Dobzhansky T (1968) On some fundamental concepts of Darwinian biology. In: *Evolutionary Biology* (eds Dobzhansky T, Hecht MK, Steere WC), pp. 1–34. Plenum Press, New York.

Douglas AE (1998) Host benefit and the evolution of specialization in symbiosis. *Heredity*, **81**, 599–603.

Dover G (1982) Molecular drive: a cohesive mode of species evolution. *Nature*, **299**, 111–117.

Drew EA (1972) The biology and physiology of alga-invertebrate symbioses. II. The density of symbiotic algal cells in a number of hermatypic hard corals and alcyonarians from various depths. *Journal of Experimental Marine Biology and Ecology*, **9**, 71–75.

Dunn SR, Weis VM (2009) Apoptosis as a post-phagocytic winnowing mechanism in a coral-dinoflagellate mutualism. *Environmental Microbiology*, **11**, 268–276.

Edmands S (2007) Between a rock and a hard place: evaluating the relative risks of inbreeding and outbreeding for conservation and management. *Molecular Ecology*, **16**, 463–475.

Edvardsen B, Shalchian-Tabrizi K, Jakobsen KS *et al.* (2003) Genetic variability and molecular phylogeny of *Dinophysis* species (Dinophyceae) from Norwegian waters inferred from single cell analyses of rDNA. *Journal of Phycology*, **39**, 395–408.

Elbrächter M (2003) Dinophyte reproduction: progress and conflicts. *Journal of Phycology*, **39**, 629–632.

Epifanio JM, Phillipp DP (1997) Sources for misclassifying genealogical origins in mixed hybrid populations. *Journal of Heredity*, **88**, 62–65.

Et-Touil A, Brasier CM, Bernier L (1999) Localization of a pathogenicity gene in *Ophiostoma novo-ulmi* and evidence that it may be introgressed from *O. ulmi*. *Molecular Plant-Microbe Interactions*, **12**, 6–15.

Fabricius KE, Langdon C, Uthicke S *et al.* (2011) Losers and winners in coral reefs acclimatized to elevated carbon dioxide concentrations. *Nature Climate Change*, **1**, 165–169.

Fadlallah YH (1983) Sexual reproduction, development and larval biology in scleractinian corals. *Coral Reefs*, **2**, 129–150.

Falkowski PG, Dubinsky Z (1981) Light-shade adaptation of *Stylophora pistillata*, a hermatypic coral from the Gulf of Eilat. *Nature*, **289**, 172–174.

Fautin DG, Buddemeier RW (2004) Adaptive bleaching: a general phenomenon. *Hydrobiologia*, **530/531**, 459–467.

Felsenstein J (1974) The evolutionary advantage of recombination. *Genetics*, **78**, 737–756.

Fenster CB, Galloway LF (2000) Inbreeding and outbreeding depression in natural populations of *Chamaecrista fasciculata* (Fabaceae). *Conservation Biology*, **14**, 1406–1412.

Ferrier-Pagès C, Gattuso J-P, Dallot S, Jaubert J (2000) Effect of nutrient enrichment on growth and photosynthesis of the zooxanthellate coral *Stylophora pistillata*. *Coral Reefs*, **19**, 103–113.

Figueroa RI, Garcés E, Bravo I (2007) Comparative study of the life cycles of *Alexandrium tamutum* and *Alexandrium minutum* (Gonyaulacales, Dinophyceae) in culture. *Journal of Phycology*, **43**, 1039–1053.

Figueroa RI, Vázquez JA, Massanet A, Murado MA, Bravo I (2011) Interactive effects of salinity and temperature on planozygote and cyst formation of *Alexandrium minutum* (Dinophyceae) in culture. *Journal of Phycology*, **47**, 13–24.

Figueroa RI, Cuadrado A, Stüken A, Rodríguez F, Fraga S (2014) Ribosomal DNA organization patterns within the dinoflagellate genus *Alexandrium* as revealed by FISH: life cycle and evolutionary implications. *Protist*, **165**, 343–363.

Finney JC, Pettay DT, Sampayo EM *et al.* (2010) The relative significance of host-habitat, depth, and geography on the ecology, endemism, and speciation of coral endosymbionts in the genus *Symbiodinium*. *Microbial Ecology*, **60**, 250–263.

Fisher PL, Malme MK, Dove S (2011) The effect of temperature stress on coral–*Symbiodinium* associations containing distinct symbiont types. *Coral Reefs*, **31**, 473–485.

Fitt WK (1984) The role of chemosensory behavior of *Symbiodinium microadriaticum*, intermediate hosts, and host behavior in the infection of coelenterates and molluscs with zooxanthellae. *Marine Biology*, **81**, 9–17.

Fitt WK, Trench RK (1983) The relation of diel patterns of cell division to diel patterns of motility in the symbiotic dinoflagellate *Symbiodinium microadriaticum* Freudenthal in culture. *New Phytologist*, **94**, 421–432.

Fitt WK, Warner ME (1995) Bleaching patterns of four species of Caribbean reef corals. *The Biological Bulletin*, **189**, 298–307.

Fitt WK, Mcfarland FK, Warner ME, Chilcoa GC (2000) Seasonal patterns of tissue biomass and densities of symbiotic dinoflagellates in reef corals and relation to coral bleaching. *Limnology and Oceanography*, **45**, 677–685.

Fitt WK, Gates RD, Hoegh-Guldberg O *et al.* (2009) Response of two species of Indo-Pacific corals, *Porites cylindrica* and *Stylophora pistillata*, to short-term thermal stress: The host does matter in determining the tolerance of corals to bleaching. *Journal of Experimental Marine Biology and Ecology*, **373**, 102–110.

Fitzpatrick BM (2012) Estimating ancestry and heterozygosity of hybrids using molecular markers. *BMC Evolutionary Biology*, **12**, 131.

Flores-Moya A, Costas E, López-Rodas V (2008) Roles of adaptation, chance and history in the evolution of the dinoflagellate *Prorocentrum triestinum*. *Naturwissenschaften*, **95**, 697–703.

Flot J-F, Hespeels B, Li X *et al.* (2013) Genomic evidence for ameiotic evolution in the bdelloid rotifer *Adineta vaga*. *Nature*, **500**, 453–457.

Frade PR, Englebert N, Faria J, Visser PM, Bak RPM (2008) Distribution and photobiology of *Symbiodinium* types in different light environments for three colour morphs of the coral *Madracis pharensis*: is there more to it than total irradiance? *Coral Reefs*, **27**, 913–925.

Frank SA (1996a) Host control of symbiont transmission: the separation of symbionts into germ and soma. *The American Naturalist*, **148**, 1113–1124.

Frank SA (1996b) Host-symbiont conflict over the mixing of symbiotic lineages. *Proceedings of the Royal Society of London B*, **263**, 339–344.

Franklin EC, Stat M, Pochon X, Putnam HM, Gates RD (2012) GeoSymbio: a hybrid, cloud-based web application of global geospatial bioinformatics and ecoinformatics for *Symbiodinium*-host symbioses. *Molecular Ecology Resources*, **12**, 369–373.

Freudenthal HD (1962) *Symbiodinium* gen. nov. and *Symbiodinium microadriaticum* sp. nov., a zooxanthella: taxonomy, life cycle, and morphology. *Journal of Eukaryotic Microbiology*, **9**, 45–52.

Ganley ARD, Scott B (2002) Concerted evolution in the ribosomal RNA genes of an *Epichloë* endophyte hybrid: comparison between tandemly arranged rDNA and dispersed 5S rrn genes. *Fungal Genetics and Biology*, **35**, 39–51.

Gardner JPA (1997) Hybridization in the sea. *Advances in Marine Biology*, **31**, 1–78.

Garrison VH, Ward G (2012) Transplantation of storm-generated coral fragments to enhance Caribbean coral reefs: a successful method but not a solution. *Revista de Biología Tropical*, **60**, 59–70.

Gates RD, Baghdasarian G, Muscatine L (1992) Temperature stress causes host cell detachment in symbiotic cnidarians: implications for coral bleaching. *The Biological Bulletin*, **182**, 324–332.

Gates RD, Muscatine L (1992) Three methods for isolating viable anthozoan endoderm cells with their intracellular symbiotic dinoflagellates. *Coral Reefs*, **11**, 143–145.

Gates RD, Hoegh-Guldberg O, McFall-Ngai MJ, Bil KY, Muscatine L (1995) Free amino acids exhibit anthozoan "host factor" activity: They induce the release of photosynthate from symbiotic dinoflagellates *in vitro*. *Proceedings of the National Academy of Sciences of the United States of America*, **92**, 7430–7434.

Geneious version 7.0 created by Biomatters. Available from http://www.geneious.com

Gleason DF, Wellington GM (1993) Ultraviolet radiation and coral bleaching. *Nature*, **365**, 836–838.

Glynn PW (1996) Coral reef bleaching: facts, hypotheses and implications. *Global Change Biology*, **2**, 495–509.

Gompert Z, Fordyce JA, Forister ML, Shapiro AM, Nice CC (2006) Homoploid hybrid speciation in an extreme habitat. *Science*, **314**, 1923–1925.

Gordo I, Charlesworth B (2000) The degeneration of asexual haploid populations and the speed of Muller's ratchet. *Genetics*, **154**, 1379–1387.

Goreau TF, Goreau NI (1959) The physiology of skeleton formation in corals. II. Calcium deposition by hermatypic corals under various conditions in the reef. *The Biological Bulletin*, **117**, 239–250.

Goulet TL (2006) Most corals may not change their symbionts. *Marine Ecology Progress Series*, **321**, 1–7.

Goulet TL, Coffroth MA (2003a) Stability of an octocoral-algal symbiosis over time and space. *Marine Ecology Progress Series*, **250**, 117–124.

Goulet TL, Coffroth MA (2003b) Genetic composition of zooxanthellae between and within colonies of the octocoral *Plexaura kuna*, based on small subunit rDNA and multilocus DNA fingerprinting. *Marine Biology*, **142**, 233–239.

Goulet TL, Cook CB, Goulet D (2005) Effect of short-term exposure to elevated temperatures and light levels on photosynthesis of different host–symbiont combinations in the *Aiptasia pallida/Symbiodinium* symbiosis. *Limnology and Oceanography*, **50**, 1490–1498.

Grant V (1981) *Plant Speciation*. Columbia University Press, New York.

Grant PR, Grant BR (1994) Phenotypic and genetic effects of hybridization in Darwin' s finches. *Evolution*, **48**, 297–316.

Grant PR, Grant BR, Petren K (2005) Hybridization in the recent past. *The American Naturalist*, **166**, 56–67.

Green DM (2005) Designatable units for species status assessment and protection. *Conservation Biology*, **19**, 1813–1820.

Green EA, Davies SW, Matz M V., Medina M (2014) Quantifying cryptic *Symbiodinium* diversity within *Orbicella faveolata* and *Orbicella franksi* at the Flower Garden Banks, Gulf of Mexico. *PeerJ*, **2**, e386.

Green AL, Mous PJ (2008) *Delineating the Coral Triangle, its Ecoregions and Functional Seascapes*. Version 5.0. TNC Coral Triangle Program Report 1/08. 44 pp.

Grottoli AG, Rodrigues LJ, Palardy JE (2006) Heterotrophic plasticity and resilience in bleached corals. *Nature*, **440**, 1186–1189.

Grube M, White JF, Seckbach J (2010) Symbioses and stress. In: *Symbioses and Stress: Cellular Origin, Life in Extreme Habitats and Astrobiology, Volume 17* (eds Seckbach J, Grube M), pp. 21–36. Springer, Dordrecht.

Hackett JD, Anderson DM, Erdner DL, Bhattacharya D (2004) Dinoflagellates: a remarkable evolutionary experiment. *American Journal of Botany*, **91**, 1523–1534.

Hamilton CE, Faeth SH, Dowling TE (2009) Distribution of hybrid fungal symbionts and environmental stress. *Microbial Ecology*, **58**, 408–413.

Handyside AH, Robinson MD, Simpson RJ *et al.* (2004) Isothermal whole genome amplification from single and small numbers of cells: a new era for preimplantation genetic diagnosis of inherited disease. *Molecular Human Reproduction*, **10**, 767–772.

Hansen G, Daugbjerg N (2009) *Symbiodinium natans* sp. nov.: a "free-living" dinoflagellate from Tenerife (Northeast-Atlantic Ocean). *Journal of Phycology*, **45**, 251–263.

Harriott VJ, Banks SA (2002) Latitudinal variation in coral communities in eastern Australia: a qualitative biophysical model of factors regulating coral reefs. *Coral Reefs*, **21**, 83–94.

Harriott VJ, Harrison PL, Banks SA (1995) The coral communities of Lord Howe Island. *Marine and Freshwater Research*, **46**, 457–465.

Harrison PL, Dalton SJ, Carroll AG (2011) Extensive coral bleaching on the world's southernmost coral reef at Lord Howe Island, Australia. *Coral Reefs*, **30**, 775.

Harrison PL, Wallace CC (1990) Reproduction, dispersal and recruitment of scleractinian corals. In: *Ecosystems of the World, 25. Coral Reefs* (ed Dubinsky Z), pp. 133–207. Elsevier, Amsterdam.

Hart MC, Green DH, Bresnan E, Bolch CJ (2007) Large subunit ribosomal RNA gene variation and sequence heterogeneity of *Dinophysis* (Dinophyceae) species from Scottish coastal waters. *Harmful Algae*, **6**, 271–287.

Hasegawa M, Kishino H, Yano T (1985) Dating of the human-ape splitting by a molecular clock of mitochondrial DNA. *Journal of Molecular Evolution*, **22**, 160–174.

Hawkins TD, Krueger T, Becker S, Fisher PL, Davy SK (2014) Differential nitric oxide synthesis and host apoptotic events correlate with bleaching susceptibility in reef corals. *Coral Reefs*, **33**, 141–153.

Hill R, Ralph PJ (2007) Post-bleaching viability of expelled zooxanthellae from the scleractinian coral *Pocillopora damicornis*. *Marine Ecology Progress Series*, **352**, 137–144.

Hoegh-Guldberg O (1999) Climate change, coral bleaching and the future of the world's coral reefs. *Marine and Freshwater Research*, **50**, 839–866.

Hoegh-Guldberg O, Jones RJ, Ward S, Loh WK (2002) Is coral bleaching really adaptive? *Nature*, **415**, 601–602.

Hoegh-Guldberg O, Mumby PJ, Hooten AJ *et al.* (2007) Coral reefs under rapid climate change and ocean acidification. *Science*, **318**, 1737–1742.

Hoffmann AA, Sgrò CM (2011) Climate change and evolutionary adaptation. *Nature*, **470**, 479–485.

Hollingsworth LL, Kinzie RA III, Lewis TD, Krupp DA, Leong J-AC (2005) Phototaxis of motile zooxanthellae to green light may facilitate symbiont capture by coral larvae. *Coral Reefs*, **24**, 523.

Hou Y, Lin S (2009) Distinct gene number-genome size relationships for eukaryotes and non-eukaryotes: gene content estimation for dinoflagellate genomes. *PLoS ONE*, **4**, e6978.

Howells EJ, van Oppen MJH, Willis BL (2009) High genetic differentiation and cross-shelf patterns of genetic diversity among Great Barrier Reef populations of *Symbiodinium*. *Coral Reefs*, **28**, 215–225.

Howells EJ, Beltran VH, Larsen NW *et al.* (2011) Coral thermal tolerance shaped by local adaptation of photosymbionts. *Nature Climate Change*, **2**, 116–120.

Howells EJ, Willis BL, Bay LK, van Oppen MJH (2013) Spatial and temporal genetic structure of *Symbiodinium* populations within a common reef-building coral on the Great Barrier Reef. *Molecular Ecology*, **22**, 3693–3708.

Hufford KM, Mazer SJ (2003) Plant ecotypes: genetic differentiation in the age of ecological restoration. *Trends in Ecology and Evolution*, **18**, 147–155.

Hughes TP, Baird AH, Bellwood DR *et al.* (2003) Climate change, human impacts, and the resilience of coral reefs. *Science*, **301**, 929–933.

Humphreys MW, Thomas HM, Morgan WG *et al.* (1995) Discriminating the ancestral progenitors of hexaploid *Festuca arundinacea* using genomic *in situ* hybridization. *Heredity*, **75**, 171–174.

Iglesias-Prieto R, Trench RK (1994) Acclimation and adaptation to irradiance in symbiotic dinoflagellates. I. Responses of the photosynthetic unit to changes in photon flux density. *Marine Ecology Progress Series*, **113**, 163–175.

Iglesias-Prieto R, Trench RK (1997) Acclimation and adaptation to irradiance in symbiotic dinoflagellates. II. Response of chlorophyll-protein complexes to different photon-flux densities. *Marine Biology*, **130**, 23–33.

Iglesias-Prieto R, Matta JL, Robins WA, Trench RK (1992) Photosynthetic response to elevated temperature in the symbiotic dinoflagellate *Symbiodinium microadriaticum* in culture. *Proceedings of the National Academy of Sciences of the United States of America*, **89**, 10302–10305.

Iglesias-Prieto R, Beltrán VH, LaJeunesse TC, Reyes-Bonilla H, Thomé PE (2004) Different algal symbionts explain the vertical distribution of dominant reef corals in the eastern Pacific. *Proceedings of the Royal Society of London B*, **271**, 1757–1763.

Ingvarsson PK, Whitlock MC (2000) Heterosis increases the effective migration rate. *Proceedings of the Royal Society of London B*, **267**, 1321–1326.

Jeffrey SW, Humphrey GF (1975) New spectrophotometric equations for determining chlorophylls *a*, *b*, $c_1$ and $c_2$ in higher plants, algae and natural phytoplankton. *Biochemie und Physiologie der Pflanzen*, **167**, 191–194.

Jeong HJ, Lee SY, Kang NS *et al.* (2014) Genetics and morphology characterize the dinoflagellate *Symbiodinium voratum*, n. sp., (Dinophyceae) as the sole representative of *Symbiodinium* Clade E. *Journal of Eukaryotic Microbiology*, **61**, 75–94.

Johnson JB, Omland KS (2004) Model selection in ecology and evolution. *Trends in Ecology and Evolution*, **19**, 101–108.

Jokiel PL, Coles SL (1977) Effects of temperature on the mortality and growth of Hawaiian reef corals. *Marine Biology*, **43**, 201–208.

Jokiel PL, Maracios JE, Franzisket L (1978) Coral growth: buoyant weight technique. In: *Coral Reefs: Research Methods* (eds Stoddard DR, Juhannes RE), pp. 529–541. UNESCO, Paris.

Jones A, Berkelmans R (2010) Potential costs of acclimatization to a warmer climate: growth of a reef coral with heat tolerant vs. sensitive symbiont types. *PLoS ONE*, **5**, e10437.

Jones AM, Berkelmans R, van Oppen MJH, Mieog JC, Sinclair W (2008) A community change in the algal endosymbionts of a scleractinian coral following a natural bleaching event: field evidence of acclimatization. *Proceedings of the Royal Society B*, **275**, 1359–1365.

Jones RJ, Yellowlees D (1997) Regulation and control of intracellular algae (= zooxanthellae) in hard corals. *Philosophical Transactions of the Royal Society of London B*, **352**, 457–468.

Jones RJ, Hoegh-Guldberg O, Larkum AWD, Schreiber U (1998) Temperature-induced bleaching of corals begins with impairment of the $CO_2$ fixation mechanism in zooxanthellae. *Plant, Cell and Environment*, **21**, 1219–1230.

Judson OP, Normark BB (1996) Ancient asexual scandals. *Trends in Ecology and Evolution*, **11**, 41–46.

Kawaguti S (1944) On the physiology of reef corals. VII. Zooxanthella of the reef corals is *Gymnodinium* sp., Dinoflagellata; its culture *in vitro*. *Palao Tropical Biology Station Studies*, **2**, 675–679.

Keshavmurthy S, Hsu C-M, Kuo C-Y *et al.* (2012) Symbiont communities and host genetic structure of the brain coral *Platygyra verweyi*, at the outlet of a nuclear power plant and adjacent areas. *Molecular Ecology*, **21**, 4393–4407.

Kevin MJ, Hall WT, McLaughlin JJA, Zahl PA (1969) *Symbiodinium microadriaticum* Freudenthal, a revised taxonomic description, ultrastructure. *Journal of Phycology*, **5**, 341–350.

Kim S, Bachvaroff TR, Handy SM, Delwiche CF (2011) Dynamics of actin evolution in dinoflagellates. *Molecular Biology and Evolution*, **28**, 1469–1480.

Kinzie RA III, Chee GS (1979) The effect of different zooxanthellae on the growth of experimentally reinfected hosts. *The Biological Bulletin*, **156**, 315–327.

Kinzie RA III, Takayama M, Santos SR, Coffroth MA (2001) The adaptive bleaching hypothesis: experimental tests of critical assumptions. *The Biological Bulletin*, **200**, 51–58.

Kirk NL, Ward JR, Coffroth MA (2005) Stable *Symbiodinium* composition in the sea fan *Gorgonia ventalina* during temperature and disease stress. *The Biological Bulletin*, **209**, 227–234.

Kirk NL, Andras JP, Harvell CD, Santos SR, Coffroth MA (2009) Population structure of *Symbiodinium* sp. associated with the common sea fan, *Gorgonia ventalina*, in the Florida Keys across distance, depth, and time. *Marine Biology*, **156**, 1609–1623.

Kirtman B, Power SB, Adedoyin JA *et al.* (2013) Near-term climate change: projections and predictability. In: *Climate Change 2013: The Physical Science Basis. Contribution of Working Group I to the Fifth Assessment Report of the Intergovernmental Panel on Climate Change* (eds Stocker TF, Qin D, Plattner G-K, et al.). Cambridge University Press, Cambridge.

Kleypas JA, McManus JW, Meñez LAB (1999) Environmental limits to coral reef development: where do we draw the line? *American Zoologist*, **39**, 146–159.

Knowlton N (2001) Coral reef biodiversity–habitat size matters. *Science*, **292**, 1493–1495.

Koike K, Jimbo M, Sakai R *et al.* (2004) Octocoral chemical signaling selects and controls dinoflagellate symbionts. *The Biological Bulletin*, **207**, 80–86.

Kopp C, Pernice M, Domart-Coulon I *et al.* (2013) Highly dynamic cellular-level response of symbiotic coral to a sudden increase in environmental nitrogen. *mBio*, **4**, e00052–13.

Koumandou VL, Howe CJ (2007) The copy number of chloroplast gene minicircles changes dramatically with growth phase in the dinoflagellate *Amphidinium operculatum*. *Protist*, **158**, 89–103.

Krueger T, Gates RD (2012) Cultivating endosymbionts — Host environmental mimics support the survival of *Symbiodinium* C15 *ex hospite*. *Journal of Experimental Marine Biology and Ecology*, **413**, 169–176.

LaJeunesse TC (2001) Investigating the biodiversity, ecology, and phylogeny of endosymbiotic dinoflagellates in the genus *Symbiodinium* using the ITS region: in search of a "species" level marker. *Journal of Phycology*, **37**, 866–880.

LaJeunesse TC (2002) Diversity and community structure of symbiotic dinoflagellates from Caribbean coral reefs. *Marine Biology*, **141**, 387–400.

LaJeunesse TC (2005) "Species" radiations of symbiotic dinoflagellates in the Atlantic and Indo-Pacific since the Miocene-Pliocene transition. *Molecular Biology and Evolution*, **22**, 570–581.

LaJeunesse TC, Pinzón JH (2007) Screening intragenomic rDNA for dominant variants can provide a consistent retrieval of evolutionarily persistent ITS (rDNA) sequences. *Molecular Phylogenetics and Evolution*, **45**, 417–422.

LaJeunesse TC, Trench RK (2000) Biogeography of two species of *Symbiodinium* (Freudenthal) inhabiting the intertidal sea anemone *Anthopleura elegantissima* (Brandt). *The Biological Bulletin*, **199**, 126–134.

LaJeunesse TC, Thornhill DJ (2011) Improved resolution of reef-coral endosymbiont (*Symbiodinium*) species diversity, ecology, and evolution through *psbA* non-coding region genotyping. *PLoS ONE*, **6**, e29013.

LaJeunesse TC, Loh WKW, van Woesik R *et al.* (2003) Low symbiont diversity in southern Great Barrier Reef corals, relative to those of the Caribbean. *Limnology and Oceanography*, **48**, 2046–2054.

LaJeunesse TC, Thornhill DJ, Cox EF *et al.* (2004) High diversity and host specificity observed among symbiotic dinoflagellates in reef coral communities from Hawaii. *Coral Reefs*, **23**, 596–603.

LaJeunesse TC, Lambert G, Andersen RA, Coffroth MA, Galbraith DW (2005) *Symbiodinium* (Pyrrhophyta) genome sizes (DNA content) are smallest among dinoflagellates. *Journal of Phycology*, **41**, 880–886.

LaJeunesse TC, Bonilla HR, Warner ME *et al.* (2008) Specificity and stability in high latitude eastern Pacific coral-algal symbioses. *Limnology and Oceanography*, **53**, 719–727.

LaJeunesse TC, Smith RT, Finney J, Oxenford H (2009) Outbreak and persistence of opportunistic symbiotic dinoflagellates during the 2005 Caribbean mass coral "bleaching" event. *Proceedings of the Royal Society B*, **276**, 4139–4148.

LaJeunesse TC, Pettay DT, Sampayo EM *et al.* (2010a) Long-standing environmental conditions, geographic isolation and host-symbiont specificity influence the relative ecological dominance and genetic diversification of coral endosymbionts in the genus *Symbiodinium*. *Journal of Biogeography*, **37**, 785–800.

LaJeunesse TC, Smith R, Walther M *et al.* (2010b) Host-symbiont recombination versus natural selection in the response of coral-dinoflagellate symbioses to environmental disturbance. *Proceedings of the Royal Society B*, **277**, 2925–2934.

LaJeunesse TC, Parkinson JE, Reimer JD (2012) A genetics-based description of *Symbiodinium minutum* sp. nov. and *S. psygmophilum* sp. nov. (Dinophyceae), two dinoflagellates symbiotic with cnidaria. *Journal of Phycology*, **48**, 1380–1391.

LaJeunesse TC, Wham DC, Pettay DT *et al.* (2014) Ecologically differentiated stress-tolerant endosymbionts in the dinoflagellate genus *Symbiodinium* (Dinophyceae) Clade D are different species. *Phycologia*, **53**, 305–319.

Law R, Lewis DH (1983) Biotic environments and the maintenance of sex–some evidence from mutualistic symbioses. *Biological Journal of the Linnean Society*, **20**, 249–276.

Lesser MP (1996) Elevated temperatures and ultraviolet radiation cause oxidative stress and inhibit photosynthesis in symbiotic dinoflagellates. *Limnology and Oceanography*, **41**, 271–283.

Lesser MP (1997) Oxidative stress causes coral bleaching during exposure to elevated temperatures. *Coral Reefs*, **16**, 187–192.

Lesser MP (2006) Oxidative stress in marine environments: biochemistry and physiological ecology. *Annual Review of Physiology*, **68**, 253–278.

Lesser MP, Shick JM (1989) Effects of irradiance and ultraviolet radiation on photoadaptation in the zooxanthellae of *Aiptasia pallida*: primary production, photoinhibition, and enzymic defenses against oxygen toxicity. *Marine Biology*, **102**, 243–255.

Lesser MP, Farrell JH (2004) Exposure to solar radiation increases damage to both host tissues and algal symbionts of corals during thermal stress. *Coral Reefs*, **23**, 367–377.

Lesser MP, Stochaj WR, Tapley DW, Shick JM (1990) Bleaching in coral reef anthozoans: effects of irradiance, ultraviolet radiation, and temperature on the activities of protective enzymes against active oxygen. *Coral Reefs*, **8**, 225–232.

Lewis CL, Coffroth MA (2004) The acquisition of exogenous algal symbionts by an octocoral after bleaching. *Science*, **304**, 1490–1492.

Lewontin RC, Birch LC (1966) Hybridization as a source of variation for adaptation to new environments. *Evolution*, **20**, 315–336.

Lexer C, Welch ME, Raymond O, Rieseberg LH (2003) The origin of ecological divergence in *Helianthus paradoxus* (Asteraceae): selection on transgressive characters in a novel hybrid habitat. *Evolution*, **57**, 1989–2000.

Litaker WR, Vandersea MW, Kibler SR *et al.* (2007) Recognizing dinoflagellate species using ITS rDNA sequences. *Journal of Phycology*, **43**, 344–355.

Little AF, van Oppen MJH, Willis BL (2004) Flexibility in algal endosymbioses shapes growth in reef corals. *Science*, **304**, 1492–1494.

Littman RA, van Oppen MJH, Willis BL (2008) Methods for sampling free-living *Symbiodinium* (zooxanthellae) and their distribution and abundance at Lizard Island (Great Barrier Reef). *Journal of Experimental Marine Biology and Ecology*, **364**, 48–53.

Lobban CS, Schefter M, Simpson AGB *et al.* (2002) *Maristentor dinoferus* n. gen., n. sp., a giant heterotrich ciliate (Spirotrichea: Heterotrichida) with zooxanthellae, from coral reefs on Guam, Mariana Islands. *Marine Biology*, **140**, 411–423.

Loh WKW, Loi T, Carter D, Hoegh-Guldberg O (2001) Genetic variability of the symbiotic dinoflagellates from the wide ranging coral species *Seriatopora hystrix* and *Acropora longicyathus* in the Indo-West Pacific. *Marine Ecology Progress Series*, **222**, 97–107.

Loram JE, Boonham N, O'Toole P, Trapido-Rosenthal HG, Douglas AE (2007a) Molecular quantification of symbiotic dinoflagellate algae of the genus *Symbiodinium*. *The Biological Bulletin*, **212**, 259–268.

Loram JE, Trapido-Rosenthal HG, Douglas AE (2007b) Functional significance of genetically different symbiotic algae *Symbiodinium* in a coral reef symbiosis. *Molecular Ecology*, **16**, 4849–4857.

Lupínková L, Komenda J (2004) Oxidative modifications of the photosystem II D1 protein by reactive oxygen species: from isolated protein to cyanobacterial cells. *Photochemistry and Photobiology*, **79**, 152–162.

Macdonald AHH, Sampayo EM, Ridgway T, Schleyer MH (2008) Latitudinal symbiont zonation in *Stylophora pistillata* from southeast Africa. *Marine Biology*, **154**, 209–217.

Magalon H, Baudry E, Husté A, Adjeroud M, Veuille M (2006) High genetic diversity of the symbiotic dinoflagellates in the coral *Pocillopora meandrina* from the South Pacific. *Marine Biology*, **148**, 913–922.

Malinowski DP, Belesky DP (2000) Adaptations of endophyte-infected cool-season grasses to environmental stresses: mechanisms of drought and mineral stress tolerance. *Crop Science*, **40**, 923–940.

Mallet J (2005) Hybridization as an invasion of the genome. *Trends in Ecology and Evolution*, **20**, 229–237.

Mallet J (2007) Hybrid speciation. *Nature*, **446**, 279–283.

Markell DA, Trench RK (1993) Macromolecules exuded by symbiotic dinoflagellates in culture: amino acid and sugar composition. *Journal of Phycology*, **29**, 64–68.

Maynard Smith J (1998) *Evolutionary Genetics (2nd edition)*. Oxford University Press, Oxford.

Mayr E (1942) *Systematics and the Origin of Species*. Columbia University Press, New York.

Mayr E (1963) *Animal Species and Evolution*. Harvard University Press, Cambridge MA.

Mayr E (1999) Understanding evolution. *Trends in Ecology and Evolution*, **14**, 372–373.

McNally KL, Govind NS, Thomé PE, Trench RK (1994) Small subunit ribosomal DNA sequence analysis and reconstruction of the inferred phylogeny among symbiotic dinoflagellates (Pyrrophyta). *Journal of Phycology*, **30**, 316–329.

Mieog JC, van Oppen MJH, Cantin NE, Stam WT, Olsen JL (2007) Real-time PCR reveals a high incidence of *Symbiodinium* clade D at low levels in four scleractinian corals across the Great Barrier Reef: implications for symbiont shuffling. *Coral Reefs*, **26**, 449–457.

Mieog JC, van Oppen MJH, Berkelmans R, Stam WT, Olsen JL (2009) Quantification of algal endosymbionts (*Symbiodinium*) in coral tissue using real-time PCR. *Molecular Ecology Resources*, **9**, 74–82.

Miller KJ, Ayre DJ (2004) The role of sexual and asexual reproduction in structuring high latitude populations of the reef coral *Pocillopora damicornis*. *Heredity*, **92**, 557–568.

Miranda LN, Zhuang Y, Zhang H, Lin S (2012) Phylogenetic analysis guided by intragenomic SSU rDNA polymorphism refines classification of "*Alexandrium tamarense*" species complex. *Harmful Algae*, **16**, 35–48.

Montalvo AM, Ellstrand NC (2000) Transplantation of the subshrub *Lotus scoparius*: testing the home-site advantage hypothesis. *Conservation Biology*, **14**, 1034–1045.

Moon CD, Craven KD, Leuchtmann A, Clement SL, Schardl CL (2004) Prevalence of interspecific hybrids amongst asexual fungal endophytes of grasses. *Molecular Ecology*, **13**, 1455–1467.

Moore RB (2003) Highly organized structure in the non-coding region of the *psbA* minicircle from clade C *Symbiodinium*. *International Journal of Systematic and Evolutionary Microbiology*, **53**, 1725–1734.

Morrell PL, Rieseberg LH (1998) Molecular tests of the proposed diploid hybrid origin of *Gilia achilleifolia* (Polemoniaceae). *American Journal of Botany*, **85**, 1439–1453.

Muller HJ (1964) The relation of recombination to mutational advance. *Mutation Research*, **1**, 2–9.

Muller-Parker G (1984) Photosynthesis-irradiance responses and photosynthetic periodicity in the sea anemone *Aiptasia pulchella* and its zooxanthellae. *Marine Biology*, **82**, 225–232.

Muller-Parker G, D'Elia CF (1997) Interactions between corals and their symbiotic algae. In: *Life and Death of Coral Reefs* (ed Birkeland C), pp. 96–113. Chapman and Hall, New York.

Muller-Parker G, McCloskey LR, Hoegh-Guldberg O, McAuley PJ (1994) Effect of ammonium enrichment on animal and algal biomass of the coral *Pocillopora damicornis*. *Pacific Science*, **48**, 273–283.

Muscatine L (1990) The role of symbiotic algae in carbon and energy flux in reef corals. In: *Ecosystems of the World, 25: Coral Reefs* (ed Dubinsky Z), pp. 75–87. Elsevier, Amsterdam.

Muscatine L, Porter JW (1977) Reef corals: mutualistic symbioses adapted to nutrient-poor environments. *BioScience*, **27**, 454–460.

Nason JD, Ellstrand NC (1993) Estimating the frequencies of genetically distinct classes of individuals in hybridized populations. *Journal of Heredity*, **84**, 1–12.

Nei M, Rooney AP (2005) Concerted and birth-and-death evolution of multigene families. *Annual Review of Genetics*, **39**, 121–152.

Newcombe G, Stirling B, McDonald S, Bradshaw HD (2000) *Melampsora ×columbiana*, a natural hybrid of *M . medusae* and *M . occidentalis*. *Mycological Research*, **3**, 261–274.

Nybakken JW, Bertness MD (2005) *Marine Biology: An Ecological Approach (6th edition)*. Pearson/Benjamin Cummings, San Francisco.

Nyholm S V, McFall-Ngai MJ (2004) The winnowing: establishing the squid-*vibrio* symbiosis. *Nature Reviews Microbiology*, **2**, 632–642.

Nyström M (2006) Redundancy and response diversity of functional groups: implications for the resilience of coral reefs. *Ambio*, **35**, 30–35.

Odum HT, Odum EP (1955) Trophic structure and productivity of a windward coral reef community on Eniwetok atoll. *Ecological Monographs*, **25**, 291–320.

Ogden JC (1988) The influence of adjacent systems on the structure and function of coral reefs. *Proceedings of the 6th International Coral Reef Symposium*, **1**, 123–129.

Oliver JK (1984) Intra-colony variation in the growth of *Acropora formosa*: extension rates and skeletal structure of white (zooxanthellae-free) and brown-tipped branches. *Coral Reefs*, **3**, 139–147.

Oliver TA, Palumbi SR (2011) Many corals host thermally resistant symbionts in high-temperature habitat. *Coral Reefs*, **30**, 241–250.

Omilian AR, Cristescu MEA, Dudycha JL, Lynch M (2006) Ameiotic recombination in asexual lineages of *Daphnia*. *Proceedings of the National Academy of Sciences of the United States of America*, **103**, 18638–18643.

Van Oppen MJH, Gates RD (2006) Conservation genetics and the resilience of reef-building corals. *Molecular Ecology*, **15**, 3863–3883.

Van Oppen MJH, Palstra FP, Piquet AM-T, Miller DJ (2001) Patterns of coral-dinoflagellate associations in *Acropora*: significance of local availability and physiology of *Symbiodinium* strains and host-symbiont selectivity. *Proceedings of the Royal Society of London B*, **268**, 1759–1767.

Van Oppen MJH, Souter P, Howells EJ, Heyward A, Berkelmans R (2011) Novel genetic diversity through somatic mutations: fuel for adaptation of reef corals? *Diversity*, **3**, 405–423.

Padilla-Gamiño JL, Pochon X, Bird C, Concepcion GT, Gates RD (2012) From parent to gamete: vertical transmission of *Symbiodinium* (Dinophyceae) ITS2 sequence assemblages in the reef building coral *Montipora capitata*. *PLoS ONE*, **7**, e38440.

Palumbi SR, Barshis DJ, Traylor-Knowles N, Bay RA (2014) Mechanisms of reef coral resistance to future climate change. *Science*, **344**, 895–898.

Pandolfi JM, Connolly SR, Marshall DJ, Cohen AL (2011) Projecting coral reef futures under global warming and ocean acidification. *Science*, **333**, 418–422.

Parrow MW, Burkholder JM (2003a) Reproduction and sexuality in *Pfiesteria shumwayae* (Dinophyceae). *Journal of Phycology*, **39**, 697–711.

Parrow MW, Burkholder JM (2003b) Estuarine heterotrophic cryptoperidiniopsoids (Dinophyceae): life cycle and culture studies. *Journal of Phycology*, **39**, 678–696.

Parrow MW, Burkholder JM (2004) The sexual life cycles of *Pfiesteria piscicida* and Cryptoperidiniopsoids (Dinophyceae). *Journal of Phycology*, **40**, 664–673.

Pasternak Z, Blasius B, Abelson A, Achituv Y (2006) Host-finding behaviour and navigation capabilities of symbiotic zooxanthellae. *Coral Reefs*, **25**, 201–207.

Paulay G (1997) Diversity and distribution of reef organisms. In: *Life and Death of Coral Reefs* (ed Birkeland C), pp. 298–345. Chapman and Hall, New York.

Pawlowski J, Holzmann M, Fahrni JF, Pochon X, Lee JJ (2001) Molecular identification of algal endosymbionts in large miliolid Foraminifera: 2. Dinoflagellates. *The Journal of Eukaryotic Microbiology*, **48**, 368–373.

Pawlowski J, Audic S, Adl S *et al.* (2012) CBOL protist working group: barcoding eukaryotic richness beyond the animal, plant, and fungal kingdoms. *PLoS Biology*, **10**, e1001419.

Paxton CW, Davy SK, Weis VM (2013) Stress and death of cnidarian host cells play a role in cnidarian bleaching. *The Journal of Experimental Biology*, **216**, 2813–2820.

Pearse VB, Muscatine L (1971) Role of symbiotic algae (zooxanthellae) in coral calcification. *The Biological Bulletin*, **141**, 350–363.

Peterson A, John H, Koch E, Peterson J (2004) A molecular phylogeny of the genus *Gagea* (Liliaceae) in Germany inferred from non-coding chloroplast and nuclear DNA sequences. *Plant Systematics and Evolution*, **245**, 145–162.

Pettay DT, LaJeunesse TC (2007) Microsatellites from clade B *Symbiodinium* spp. specialized for Caribbean corals in the genus *Madracis*. *Molecular Ecology Notes*, **7**, 1271–1274.

Pettay DT, LaJeunesse TC (2009) Microsatellite loci for assessing genetic diversity, dispersal and clonality of coral symbionts in "stress-tolerant" clade D *Symbiodinium*. *Molecular Ecology Resources*, **9**, 1022–1025.

Pettay DT, Wham DC, Pinzón JH, LaJeunesse TC (2011) Genotypic diversity and spatial-temporal distribution of *Symbiodinium* clones in an abundant reef coral. *Molecular Ecology*, **20**, 5197–5212.

Pfiester LA (1989) Dinoflagellate sexuality. In: *International Review of Cytology: A Survey of Cell Biology, Volume 114* (eds Bourne GH, Jeon KW, Friedlander M), pp. 249–270. Academic Press, New York.

Pfiester LA, Anderson DM (1987) Dinoflagellate reproduction. In: *The Biology of Dinoflagellates* (ed Taylor FJR), pp. 611–648. Blackwell Scientific, London.

Pinzón JH, Devlin-Durante MK, Weber MX, Baums IB, LaJeunesse TC (2011) Microsatellite loci for *Symbiodinium* A3 (*S. fitti*) a common algal symbiont among Caribbean *Acropora* (stony corals) and Indo-Pacific giant clams (*Tridacna*). *Conservation Genetics Resources*, **3**, 45–47.

Pochon X, Gates RD (2010) A new *Symbiodinium* clade (Dinophyceae) from soritid foraminifera in Hawai'i. *Molecular Phylogenetics and Evolution*, **56**, 492–497.

Pochon X, Pawlowski J, Zaninetti L, Rowan R (2001) High genetic diversity and relative specificity among *Symbiodinium*-like endosymbiotic dinoflagellates in soritid foraminiferans. *Marine Biology*, **139**, 1069–1078.

Pochon X, Stat M, Takabayashi M *et al.* (2010) Comparison of endosymbiotic and free-living *Symbiodinium* (Dinophyceae) diversity in a Hawaiian reef environment. *Journal of Phycology*, **46**, 53–65.

Pochon X, Putnam HM, Burki F, Gates RD (2012) Identifying and characterizing alternative molecular markers for the symbiotic and free-living dinoflagellate genus *Symbiodinium*. *PLoS ONE*, **7**, e29816.

Pochon X, Putnam HM, Gates RD (2014) Multi-gene analysis of *Symbiodinium* dinoflagellates: a perspective on rarity, symbiosis, and evolution. *PeerJ*, **2**, e394.

Putnam HM, Stat M, Pochon X, Gates RD (2012) Endosymbiotic flexibility associates with environmental sensitivity in scleractinian corals. *Proceedings of the Royal Society B*, **279**, 4352–4361.

Quigley KM, Davies SW, Kenkel CD *et al.* (2014) Deep-sequencing method for quantifying background abundances of *Symbiodinium* types: exploring the rare *Symbiodinium* biosphere in reef-building corals. *PLoS ONE*, **9**, e94297.

Quinn GP, Keough MJ (2002) *Experimental Design and Data Analysis for Biologists*. Cambridge University Press, Cambridge.

R Development Core Team (2011) R: A Language and Environment for Statistical Computing.

Ragni M, Airs RL, Hennige SJ *et al.* (2010) PSII photoinhibition and photorepair in *Symbiodinium* (Pyrrhophyta) differs between thermally tolerant and sensitive phylotypes. *Marine Ecology Progress Series*, **406**, 57–70.

Rasch D, Mašata O (2006) Methods of variance component estimation. *Czech Journal of Animal Science*, **51**, 227–235.

Renger G, Völker M, Eckert HJ *et al.* (1989) On the mechanism of photosystem II deterioration by UV-B irradiation. *Photochemistry and Photobiology*, **49**, 97–105.

Rhymer JM, Simberloff D (1996) Extinction by hybridization and introgression. *Annual Review of Ecology and Systematics*, **27**, 83–109.

Richmond RH, Hunter CL (1990) Reproduction and recruitment of corals: comparisons among the Caribbean, the Tropical Pacific, and the Red Sea. *Marine Ecology Progress Series*, **60**, 185–203.

Rieseberg LH (1991) Homoploid reticulate evolution in *Helianthus* (Asteraceae): evidence from ribosomal genes. *American Journal of Botany*, **78**, 1218–1237.

Rieseberg LH (1997) Hybrid origins of plant species. *Annual Review of Ecology and Systematics*, **28**, 359–389.

Rieseberg L, Soltis DE (1991) Phylogenetic consequences of cytoplasmic gene flow in plants. *Evolutionary Trends in Plants*, **5**, 65–84.

Rieseberg LH, Whitton J, Linder CR (1996) Molecular marker incongruence in plant hybrid zones and phylogenetic trees. *Acta Botanica Neerlandica*, **45**, 243–262.

Rieseberg LH, Archer MA, Wayne RK (1999) Transgressive segregation, adaptation and speciation. *Heredity*, **83**, 363–372.

Rieseberg LH, Baird SJE, Gardner KA (2000) Hybridization, introgression, and linkage evolution. *Plant Molecular Biology*, **42**, 205–224.

Rieseberg LH, Raymond O, Rosenthal DM *et al.* (2003) Major ecological transitions in wild sunflowers facilitated by hybridization. *Science*, **301**, 1211–1216.

Ritchie RJ (2006) Consistent sets of spectrophotometric chlorophyll equations for acetone, methanol and ethanol solvents. *Photosynthesis Research*, **89**, 27–41.

Ritchie RJ, Grant AJ, Eltringham K, Hinde R (1997) Clotrimazole, a model compound for the host release factor of the coral *Plesiastrea versipora*. *Functional Plant Biology*, **24**, 283–290.

Rodriguez-Lanetty M (2003) Evolving lineages of *Symbiodinium*-like dinoflagellates based on ITS1 rDNA. *Molecular Phylogenetics and Evolution*, **28**, 152–168.

Rodriguez-Lanetty M, Loh W, Carter D, Hoegh-Guldberg O (2001) Latitudinal variability in symbiont specificity within the widespread scleractinian coral *Plesiastrea versipora*. *Marine Biology*, **138**, 1175–1181.

Rohwer F, Breitbart M, Jara J, Azam F, Knowlton N (2001) Diversity of bacteria associated with the Caribbean coral *Montastraea franksi*. *Coral Reefs*, **20**, 85–91.

Rohwer F, Seguritan V, Azam F, Knowlton N (2002) Diversity and distribution of coral-associated bacteria. *Marine Ecology Progress Series*, **243**, 1–10.

Rosenberg E, Ben-Haim Y (2002) Microbial diseases of corals and global warming. *Environmental Microbiology*, **4**, 318–326.

Rowan R (1998) Diversity and ecology of zooxanthellae on coral reefs. *Journal of Phycology*, **34**, 407–417.

Rowan R (2004) Thermal adaptation in reef coral symbiosis. *Nature*, **430**, 742.

Rowan R, Powers DA (1991a) Molecular genetic identification of symbiotic dinoflagellates (zooxanthellae). *Marine Ecology Progress Series*, **71**, 65–73.

Rowan R, Powers DA (1991b) A molecular genetic classification of zooxanthellae and the evolution of animal-algal symbioses. *Science*, **251**, 1348–1351.

Rowan R, Powers DA (1992) Ribosomal RNA sequences and the diversity of symbiotic dinoflagellates (zooxanthellae). *Proceedings of the National Academy of Sciences of the United States of America*, **89**, 3639–3643.

Rowan R, Knowlton N (1995) Intraspecific diversity and ecological zonation in coral-algal symbiosis. *Proceedings of the National Academy of Sciences of the United States of America*, **92**, 2850–2853.

Rowan R, Knowlton N, Baker A, Jara J (1997) Landscape ecology of algal symbionts creates variation in episodes of coral bleaching. *Nature*, **388**, 265–269.

Saari S, Faeth SH (2012) Hybridization of *Neotyphodium* endophytes enhances competitive ability of the host grass. *New Phytologist*, **195**, 231–236.

Sachs JL, Wilcox TP (2006) A shift to parasitism in the jellyfish symbiont *Symbiodinium microadriaticum*. *Proceedings of the Royal Society B*, **273**, 425–429.

Sampayo EM, Franceschinis L, Hoegh-Guldberg O, Dove S (2007) Niche partitioning of closely related symbiotic dinoflagellates. *Molecular Ecology*, **16**, 3721–3733.

Sampayo EM, Ridgway T, Bongaerts P, Hoegh-Guldberg O (2008) Bleaching susceptibility and mortality of corals are determined by fine-scale differences in symbiont type. *Proceedings of the National Academy of Sciences of the United States of America*, **105**, 10444–10449.

Sampayo EM, Dove S, LaJeunesse TC (2009) Cohesive molecular genetic data delineate species diversity in the dinoflagellate genus *Symbiodinium*. *Molecular Ecology*, **18**, 500–519.

Sang T, Crawford DJ, Stuessy TF (1995) Documentation of reticulate evolution in peonies (*Paeonia*) using internal transcribed spacer sequences of nuclear ribosomal DNA: implications for biogeography and concerted evolution. *Proceedings of the National Academy of Sciences of the United States of America*, **92**, 6813–6817.

Santos SR, Coffroth MA (2003) Molecular genetic evidence that dinoflagellates belonging to the genus *Symbiodinium* Freudenthal are haploid. *The Biological Bulletin*, **204**, 10–20.

Santos SR, Taylor DJ, Coffroth MA (2001) Genetic comparisons of freshly isolated versus cultured symbiotic dinoflagellates: implications for extrapolating to the intact symbiosis. *Journal of Phycology*, **37**, 900–912.

Santos SR, Gutierrez-Rodriguez C, Coffroth MA (2003a) Phylogenetic identification of symbiotic dinoflagellates via length heteroplasmy in domain V of chloroplast large subunit (cp23S)–ribosomal DNA sequences. *Marine Biotechnology*, **5**, 130–140.

Santos SR, Gutiérrez-Rodríguez C, Lasker HR, Coffroth MA (2003b) *Symbiodinium* sp. associations in the gorgonian *Pseudopterogorgia elisabethae* in the Bahamas: high

levels of genetic variability and population structure in symbiotic dinoflagellates. *Marine Biology*, **143**, 111–120.

Santos SR, Shearer TL, Hannes AR, Coffroth MA (2004) Fine-scale diversity and specificity in the most prevalent lineage of symbiotic dinoflagellates (*Symbiodinium*, Dinophyceae) of the Caribbean. *Molecular Ecology*, **13**, 459– 469.

Santos SR, Taylor DJ, Kinzie RA III *et al.* (2002) Molecular phylogeny of symbiotic dinoflagellates inferred from partial chloroplast large subunit (23S)-rDNA sequences. *Molecular Phylogenetics and Evolution*, **23**, 97–111.

Savage AM, Trapido-Rosenthal H, Douglas AE (2002) On the functional significance of molecular variation in *Symbiodinium*, the symbiotic algae of Cnidaria: photosynthetic response to irradiance. *Marine Ecology Progress Series*, **244**, 27–37.

Schardl CL, Clay K (1997) Evolution of mutualistic endophytes from plant pathogens. In: *The Mycota V: Plant Relationships Part B* (eds Carroll GC, Tudzynski P), pp. 221–238. Springer-Verlag, Berlin.

Schardl CL, Craven KD (2003) Interspecific hybridization in plant-associated fungi and oomycetes: a review. *Molecular Ecology*, **12**, 2861–2873.

Schardl CL, Liu J-S, White JF Jr *et al.* (1991) Molecular phylogenetic relationships of nonpathogenic grass mycosymbionts and clavicipitaceous plant pathogens. *Plant Systematics and Evolution*, **178**, 27–41.

Schardl CL, Leuchtmann A, Tsai H-F *et al.* (1994) Origin of a fungal symbiont of perennial ryegrass by interspecific hybridization of a mutualist with the ryegrass choke pathogen, *Epichloë typhina*. *Genetics*, **136**, 1307–1317.

Schiffers K, Bourne EC, Lavergne S, Thuiller W, Travis JMJ (2013) Limited evolutionary rescue of locally adapted populations facing climate change. *Philosophical Transactions of the Royal Society of London B*, **368**, 20120083.

Schoenberg DA, Trench RK (1976) Specificity of symbioses between marine cnidarians and zooxanthellae. In: *Coelenterate Ecology and Behavior* (ed Mackie GO), pp. 423–432. Plenum Press, New York.

Schoenberg DA, Trench RK (1980a) Genetic variation in *Symbiodinium* (=*Gymnodinium*) *microadriaticum* Freudenthal, and specificity in its symbiosis with marine invertebrates. I. Isoenzyme and soluble protein patterns of axenic cultures of *Symbiodinium microadriaticum*. *Proceedings of the Royal Society of London. Series B, Biological Sciences*, **207**, 405–427.

Schoenberg DA, Trench RK (1980b) Genetic variation in *Symbiodinium* (=*Gymnodinium*) *microadriaticum* Freudenthal, and specificity in its symbiosis with marine invertebrates. II. Morphological variation in *Symbiodinium microadriaticum*. *Proceedings of the Royal Society of London. Series B, Biological Sciences*, **207**, 429–444.

Schoenberg DA, Trench RK (1980c) Genetic variation in *Symbiodinium* (=*Gymnodinium*) *microadriaticum* Freudenthal, and specificity in its symbiosis with marine invertebrates. III. Specificity and infectivity of *Symbiodinium microadriaticum*. *Proceedings of the Royal Society of London. Series B, Biological Sciences*, **207**, 445–460.

Schön I, Martens K (1998) DNA repair in ancient asexuals - a new solution to an old problem? *Journal of Natural History*, **32**, 943–948.

Seehausen O (2004) Hybridization and adaptive radiation. *Trends in Ecology and Evolution*, **19**, 198–207.

Seutin G, White BN, Boag PT (1991) Preservation of avian blood and tissue samples for DNA analyses. *Canadian Journal of Zoology*, **69**, 82–90.

Sheppard CRC, Davy SK, Pilling GM (2009) *The Biology of Coral Reefs*. Oxford University Press, New York.

Shoguchi E, Shinzato C, Kawashima T *et al.* (2013) Draft assembly of the *Symbiodinium minutum* nuclear genome reveals dinoflagellate gene structure. *Current Biology*, **23**, 1399–1408.

Silverstein RN, Correa AMS, LaJeunesse TC, Baker AC (2011) Novel algal symbiont (*Symbiodinium* spp.) diversity in reef corals of Western Australia. *Marine Ecology Progress Series*, **422**, 63–75.

Silverstein RN, Correa AMS, Baker AC (2012) Specificity is rarely absolute in coral-algal symbiosis: implications for coral response to climate change. *Proceedings of the Royal Society B*, **279**, 2609–2618.

Simpson GG (1953) *The Major Features of Evolution*. Columbia University Press, New York.

Small AM, Adey WH, Spoon D (1998) Are current estimates of coral reef biodiversity too low? The view through the window of a microcosm. *Atoll Research Bulletin*, **458**, 1–20.

Small RL, Cronn RC, Wendel JF (2004) Use of nuclear genes for phylogeny reconstruction in plants. *Australian Systematic Biology*, **17**, 145–170.

Smith S (1978) Coral-reef area and the contributions of reefs to processes and resources of the world's oceans. *Nature*, **273**, 225–226.

Soltis PS, Soltis DE, Doyle JJ (1992) *Molecular Systematics of Plants*. Chapman and Hall, New York.

Spinaze KA, Smith SDA, Simpson RD (1996) The effect of depth and wave exposure on the density and porosity of *Pocillopora damicornis* in the Solitary Islands Marine Reserve, New South Wales. *Proceedings of The Great Barrier Reef, Science, Use and Management Conference*, **2**, 72–76.

Stambler N (2011) Zooxanthellae: the yellow symbionts inside animals. In: *Coral Reefs: An Ecosystem in Transition* (eds Dubinsky Z, Stambler N), pp. 87–106. Springer, New York.

Stanley GD Jr, Swart PK (1995) Evolution of the coral-zooxanthellae symbiosis during the Triassic: a geochemical approach. *Paleobiology*, **21**, 179–199.

Starzak DE, Quinnell RG, Nitschke MR, Davy SK (2014) The influence of symbiont type on photosynthetic carbon flux in a model cnidarian–dinoflagellate symbiosis. *Marine Biology*, **161**, 711–724.

Stat M, Carter D, Hoegh-Guldberg O (2006) The evolutionary history of *Symbiodinium* and scleractinian hosts— Symbiosis, diversity, and the effect of climate change. *Perspectives in Plant Ecology, Evolution and Systematics*, **8**, 23–43.

Stat M, Loh WKW, Hoegh-Guldberg O, Carter DA (2008a) Symbiont acquisition strategy drives host–symbiont associations in the southern Great Barrier Reef. *Coral Reefs*, **27**, 763–772.

Stat M, Morris E, Gates RD (2008b) Functional diversity in coral–dinoflagellate symbiosis. *Proceedings of the National Academy of Sciences of the United States of America*, **105**, 9256–9261.

Stat M, Pochon X, Cowie ROM, Gates RD (2009) Specificity in communities of *Symbiodinium* in corals from Johnston Atoll. *Marine Ecology Progress Series*, **386**, 83–96.

Stat M, Bird CE, Pochon X *et al.* (2011) Variation in *Symbiodinium* ITS2 sequence assemblages among coral colonies (D Steinke, Ed,). *PLoS ONE*, **6**, e15854.

Stat M, Baker AC, Bourne DG *et al.* (2012) Molecular delineation of species in the coral holobiont. In: *Advances in Marine Biology, Vol 63* (ed Lesser MP), pp. 1–65. Academic Press, Amsterdam.

Stebbins GL Jr (1950) *Variation and Evolution in Plants*. Columbia University Press, New York.

Steen RG, Muscatine L (1984) Daily budgets of photosynthetically fixed carbon in symbiotic zoanthids. *The Biological Bulletin*, **167**, 477–487.

Steen RG, Muscatine L (1987) Low temperature evokes rapid exocytosis of symbiotic algae by a sea anemone. *The Biological Bulletin*, **172**, 246–263.

Stern RF, Horak A, Andrew RL *et al.* (2010) Environmental barcoding reveals massive dinoflagellate diversity in marine environments. *PLoS ONE*, **5**, e13991.

Stern RF, Andersen RA, Jameson I *et al.* (2012) Evaluating the ribosomal internal transcribed spacer (ITS) as a candidate dinoflagellate barcode marker. *PLoS ONE*, **7**, e42780.

Stimson J, Kinzie RA III (1991) The temporal pattern and rate of release of zooxanthellae from the reef coral *Pocillopora damicornis* (Linnaeus) under nitrogen-enrichment and control conditions. *Journal of Experimental Marine Biology and Ecology*, **153**, 63–74.

Takabayashi M, Santos SR, Cook CB (2004) Mitochondrial DNA phylogeny of the symbiotic dinoflagellates (*Symbiodinium*, Dinophyta). *Journal of Phycology*, **40**, 160–164.

Takabayashi M, Adams LM, Pochon X, Gates RD (2011) Genetic diversity of free-living *Symbiodinium* in surface water and sediment of Hawai'i and Florida. *Coral Reefs*, **31**, 157–167.

Tanaka Y, Miyajima T, Koike I, Hayashibara T, Ogawa H (2006) Translocation and conservation of organic nitrogen within the coral-zooxanthella symbiotic system of *Acropora pulchra*, as demonstrated by dual isotope-labeling techniques. *Journal of Experimental Marine Biology and Ecology*, **336**, 110–119.

Taylor DL (1969) Identity of zooxanthellae isolated from some Pacific Tridacnidae. *Journal of Phycology*, **5**, 336–340.

Taylor DL (1973) The cellular interactions of algal invertebrate symbiosis. *Advances in Marine Biology*, **11**, 1–56.

Taylor DL (1974) Symbiotic marine algae: taxonomy and biological fitness. In: *Symbiosis in the Sea* (ed Vernberg WB), pp. 245–262. University of South Carolina Press, Colombia.

Taylor SJ, Arnold M, Martin NH (2009) The genetic architecture of reproductive isolation in Louisiana irises: hybrid fitness in nature. *Evolution*, **63**, 2581–2594.

Tchernov D, Gorbunov MY, de Vargas C *et al.* (2004) Membrane lipids of symbiotic algae are diagnostic of sensitivity to thermal bleaching in corals. *Proceedings of the National Academy of Sciences of the United States of America*, **101**, 13531–13535.

Templeton AR (1989) The meaning of species and speciation: a genetic perspective. In: *Speciation and its Consequences* (eds Otte D, Endler JA), pp. 3–27. Sinauer, Sunderland MA.

Tengs T, Dahlberg OJ, Shalchian-Tabrizi K *et al.* (2000) Phylogenetic analyses indicate that the 19'hexanoyloxy-fucoxanthin-containing dinoflagellates have tertiary plastids of haptophyte origin. *Molecular Biology and Evolution*, **17**, 718–729.

Thomas L, Kendrick GA, Kennington WJ, Richards ZT, Stat M (2014) Exploring *Symbiodinium* diversity and host specificity in *Acropora* corals from geographical extremes of Western Australia with 454 amplicon pyrosequencing. *Molecular Ecology*, DOI: 10.1111/mec.12801.

Thomas MA, Roemer GW, Donlan CJ *et al.* (2013) Gene tweaking for conservation. *Nature*, **501**, 485–486.

Thornhill DJ, Fitt WK, Schmidt GW (2006a) Highly stable symbioses among western Atlantic brooding corals. *Coral Reefs*, **25**, 515–519.

Thornhill DJ, LaJeunesse TC, Kemp DW, Fitt WK, Schmidt GW (2006b) Multi-year, seasonal genotypic surveys of coral-algal symbioses reveal prevalent stability or post-bleaching reversion. *Marine Biology*, **148**, 711–722.

Thornhill DJ, Doubleday K, Kemp DW, Santos SR (2010) Host hybridization alters specificity of cnidarian–dinoflagellate associations. *Marine Ecology Progress Series*, **420**, 113–123.

Thornhill DJ, LaJeunesse TC, Santos SR (2007) Measuring rDNA diversity in eukaryotic microbial systems: how intragenomic variation, pseudogenes, and PCR artifacts confound biodiversity estimates. *Molecular Ecology*, **16**, 5326–5340.

Thornhill DJ, Xiang Y, Fitt WK, Santos SR (2009) Reef endemism, host specificity and temporal stability in populations of symbiotic dinoflagellates from two ecologically dominant Caribbean corals. *PLoS ONE*, **4**, e6262.

Thornhill DJ, Lewis AM, Wham DC, LaJeunesse TC (2013a) Host-specialist lineages dominate the adaptive radiation of reef coral endosymbionts. *Evolution*, **68**, 352–367.

Thornhill DJ, Xiang Y, Pettay DT, Zhong M, Santos SR (2013b) Population genetic data of a model symbiotic cnidarian system reveal remarkable symbiotic specificity and vectored introductions across ocean basins. *Molecular Ecology*, **22**, 4499–4515.

Tibayrenc M, Kjellberg F, Arnaud J *et al.* (1991) Are eukaryotic microorganisms clonal or sexual? A population genetics vantage. *Proceedings of the National Academy of Sciences of the United States of America*, **88**, 5129–5133.

Titlyanov EA, Titlyanova T V, Leletkin VA *et al.* (1996) Degradation of zooxanthellae and regulation of their density in hermatypic corals. *Marine Ecology Progress Series*, **139**, 167–178.

Toller WW, Rowan R, Knowlton N (2001a) Zooxanthellae of the *Montastraea annularis* species complex: patterns of distribution of four taxa of *Symbiodinium* on different reefs and across depths. *The Biological Bulletin*, **201**, 348–359.

Toller WW, Rowan R, Knowlton N (2001b) Repopulation of zooxanthellae in the Caribbean corals *Montastraea annularis* and *M. faveolata* following experimental and disease-associated bleaching. *The Biological Bulletin*, **201**, 360–373.

Tomascik T, Sander F (1985) Effects of eutrophication on reef-building corals. I. Growth rate of the reef-building coral *Montastrea annularis*. *Marine Biology*, **87**, 143–155.

Tomascik T, Sander F (1987a) Effects of eutrophication on reef-building corals. II. Structure of scleractinian coral communities on fringing reefs, Barbados, West Indies. *Marine Biology*, **94**, 53–75.

Tomascik T, Sander F (1987b) Effects of eutrophication on reef-building corals. III. Reproduction of the reef-building coral *Porites porites*. *Marine Biology*, **94**, 77–94.

Tonk L, Bongaerts P, Sampayo EM, Hoegh-Guldberg O (2013) SymbioGBR: a web-based database of *Symbiodinium* associated with cnidarian hosts on the Great Barrier Reef. *BMC Ecology*, **13**, 7.

Trench RK (1971) The physiology and biochemistry of zooxanthellae symbiotic with marine coelenterates. III. The effect of homogenates of host tissues on the excretion of photosynthetic products *in vitro* by zooxanthellae from two marine coelenterates. *Proceedings of the Royal Society of London. Series B, Biological Sciences*, **177**, 251–264.

Trench RK (1987) Dinoflagellates in non-parasitic symbioses. In: *The Biology of Dinoflagellates* (ed Taylor FJR), pp. 530–570. Blackwell, Oxford.

Trench RK (1993) Microalgal-invertebrate symbioses: a review. *Endocytobiosis and Cell Research*, **9**, 135–175.

Trench RK (1997) Diversity of symbiotic dinoflagellates and the evolution of microalgal-invertebrate symbiosis. *Proceedings of the 8th International Coral Reef Symposium*, **2**, 1275–1286.

Trench R (2000) Validation of some currently used invalid names of dinoflagellates. *Journal of Phycology*, **36**, 972.

Trench RK, Blank RJ (1987) *Symbiodinium microadriaticum* Freudenthal, *S. goreauii* sp. nov., *S. kawagutii* sp. nov., and *S. pilosum* sp. nov.: Gymnodinioid dinoflagellate symbionts of marine invertebrates. *Journal of Phycology*, **23**, 469–481.

Trench RK, Thinh L-V (1995) *Gymnodinium linucheae* sp. nov.: the dinoflagellate symbiont of the jellyfish *Linuche unguiculata*. *European Journal of Phycology*, **30**, 149–154.

Tsai H-F, Liu J-S, Staben C *et al.* (1994) Evolutionary diversification of fungal endophytes of tall fescue grass by hybridization with *Epichloë* species. *Proceedings of the National Academy of Sciences of the United States of America*, **91**, 2542–2546.

Tsitrone A, Kirkpatrick M, Levin DA (2003) A model for chloroplast capture. *Evolution*, **57**, 1776–1782.

Turpin DH, Dobell PER, Taylor FJR (1978) Sexuality and cyst formation in Pacific strains of the toxic dinoflagellate *Gonyaulax tamarensis*. *Journal of Phycology*, **14**, 235–238.

Ulstrup KE, van Oppen MJH (2003) Geographic and habitat partitioning of genetically distinct zooxanthellae (*Symbiodinium*) in *Acropora* corals on the Great Barrier Reef. *Molecular Ecology*, **12**, 3477–3484.

Ulstrup KE, Berkelmans R, Ralph PJ, van Oppen MJH (2006) Variation in bleaching sensitivity of two coral species across a latitudinal gradient on the Great Barrier Reef: the role of zooxanthellae. *Marine Ecology Progress Series*, **314**, 135–148.

Ulstrup KE, van Oppen MJH, Kühl M, Ralph PJ (2007) Inter-polyp genetic and physiological characterisation of *Symbiodinium* in an *Acropora valida* colony. *Marine Biology*, **153**, 225–234.

Ulstrup KE, Hill R, van Oppen MJH, Larkum AWD, Ralph PJ (2008) Seasonal variation in the photo-physiology of homogeneous and heterogeneous *Symbiodinium* consortia in two scleractinian corals. *Marine Ecology Progress Series*, **361**, 139–150.

UNESCO (1981) Tenth report of the joint panel on oceanographic tables and standards. *Unesco Technical Papers in Marine Science*, **36**, 1–25.

Van Valen L (1976) Ecological species, multispecies, and oaks. *Taxon*, **25**, 233–239.

Vandermeulen JH, Davis ND, Muscatine L (1972) The effect of inhibitors of photosynthesis on zooxanthellae in corals and other marine invertebrates. *Marine Biology*, **16**, 185–191.

Vanormelingen P, Chepurnov VA, Mann DG, Sabbe K, Vyverman W (2008) Genetic divergence and reproductive barriers among morphologically heterogeneous sympatric clones of *Eunotia bilunaris* sensu lato (Bacillariophyta). *Protist*, **159**, 73–90.

Venn AA, Loram JE, Trapido-Rosenthal HG, Joyce DA, Douglas AE (2008) Importance of time and place: patterns in abundance of *Symbiodinium* clades A and B in the tropical sea anemone *Condylactis gigantea*. *The Biological Bulletin*, **215**, 243–252.

Veron JEN (1995) *Corals in Space and Time*. University of New South Wales Press, Sydney.

Veron JEN (2000) *Corals of the World*. Australian Institute of Marine Science, Townsville.

Veron JEN, Done TJ (1979) Corals and coral communities of Lord Howe Island. *Australian Journal of Marine and Freshwater Research*, **30**, 203–236.

Vriesendorp B, Bakker FT (2005) Reconstructing patterns of reticulate evolution in angiosperms: what can we do? *Taxon*, **54**, 593–604.

Wakefield TS, Farmer MA, Kempf SC (2000) Revised description of the fine structure of *in situ* "zooxanthellae" genus *Symbiodinium*. *The Biological Bulletin*, **199**, 76–84.

Wakefield TS, Kempf SC (2001) Development of host- and symbiont-specific monoclonal antibodies and confirmation of the origin of the symbiosome membrane in a cnidarian-dinoflagellate symbiosis. *The Biological Bulletin*, **200**, 127–143.

Wang J-T, Douglas AE (1997) Nutrients, signals, and photosynthate release by symbiotic alge. *Plant Physiology*, **114**, 631–636.

Wang J-T, Douglas AE (1998) Nitrogen recycling or nitrogen conservation in an alga-invertebrate symbiosis? *The Journal of Experimental Biology*, **201**, 2445–2453.

Wang XR, Szmidt AE, Lewandowski A, Wang ZR (1990) Evolutionary analysis of *Pinus densata* Masters, a putative Tertiary hybrid. 1. Allozyme variation. *Theoretical and Applied Genetics*, **80**, 635–640.

Warner ME, Fitt WK, Schmidt GW (1999) Damage to photosystem II in symbiotic dinoflagellates: A determinant of coral bleaching. *Proceedings of the National Academy of Sciences of the United States of America*, **96**, 8007–8012.

Welch ME, Rieseberg LH (2002) Habitat divergence between a homoploid hybrid sunflower species, *Helianthus paradoxus* (Asteraceae), and its progenitors. *American Journal of Botany*, **89**, 472–478.

Wendel JF, Schnabel A, Seelanan T (1995) Bidirectional interlocus concerted evolution following allopolyploid speciation in cotton (*Gossypium*). *Proceedings of the National Academy of Sciences of the United States of America*, **92**, 280–284.

Wham DC, Pettay DT, LaJeunesse TC (2011) Microsatellite loci for the host-generalist "zooxanthella" *Symbiodinium trenchi* and other Clade D *Symbiodinium*. *Conservation Genetics Resources*, **3**, 541–544.

Whitehead LF, Douglas AE (2003) Metabolite comparisons and the identity of nutrients translocated from symbiotic algae to an animal host. *The Journal of Experimental Biology*, **206**, 3149–3157.

Wicks LC, Sampayo EM, Gardner JPA, Davy SK (2010) Local endemicity and high diversity characterise high-latitude coral–*Symbiodinium* partnerships. *Coral Reefs*, **29**, 989–1003.

Wicks LC, Gardner JPA, Davy SK (2012) Host tolerance, not symbiont tolerance, determines the distribution of coral species in relation to their environment at a Central Pacific atoll. *Coral Reefs*, **31**, 389–398.

Wilcox TP (1998) Large-subunit ribosomal RNA systematics of symbiotic dinoflagellates: morphology does not recapitulate phylogeny. *Molecular Phylogenetics and Evolution*, **10**, 436–448.

Wilkerson FP, Kobayashi D, Muscatine L (1988) Mitotic index and size of symbiotic algae in Caribbean Reef corals. *Coral Reefs*, **7**, 29–36.

Wilkinson C, Lindén O, Cesar H *et al.* (1999) Ecological and socioeconomic impacts of 1998 coral mortality in the Indian Ocean: an ENSO impact and a warning of future change? *Ambio*, **28**, 188–196.

Willis BL, van Oppen MJH, Miller DJ, Vollmer S V, Ayre DJ (2006) The role of hybridization in the evolution of reef corals. *Annual Review of Ecology, Evolution, and Systematics*, **37**, 489–517.

Wright S (1932) The roles of mutation, inbreeding, crossbreeding and selection in evolution. *Proceedings of the 6th International Congress of Genetics*, **1**, 356–366.

Xiang T, Hambleton EA, DeNofrio JC, Pringle JR, Grossman AR (2013) Isolation of clonal axenic strains of the symbiotic dinoflagellate *Symbiodinium* and their growth and host specificity. *Journal of Phycology*, **49**, 447–458.

Yachi S, Loreau M (1999) Biodiversity and ecosystem productivity in a fluctuating environment: The insurance hypothesis. *Proceedings of the National Academy of Sciences of the United States of America*, **96**, 1463–1468.

Yamashita H, Suzuki G, Hayashibara T, Koike K (2010) Do corals select zooxanthellae by alternative discharge? *Marine Biology*, **158**, 87–100.

Yellowlees D, Rees TA V, Leggat W (2008) Metabolic interactions between algal symbionts and invertebrate hosts. *Plant, Cell and Environment*, **31**, 679–694.

Zardoya R, Costas E, López-Rodas V, Garrido-Pertierra A, Bautista JM (1995) Revised dinoflagellate phylogeny inferred from molecular analysis of large-subunit ribosomal RNA gene sequences. *Journal of Molecular Evolution*, **41**, 637–645.

Zhang H, Bhattacharya D, Lin S (2005) Phylogeny of dinoflagellates based on mitochondrial cytochrome *b* and nuclear small subunit rDNA sequence comparisons. *Journal of Phycology*, **41**, 411–420.

Zhang H, Hou Y, Lin S (2006) Isolation and characterization of proliferating cell nuclear antigen from the dinoflagellate *Pfiesteria piscicida*. *Journal of Eukaryotic Microbiology*, **53**, 142–150.

# Appendix A: Nucleotide sequences and alignments

**Table A.1 Genbank accession numbers for sequences used in rDNA phylogeny (Figure 1.4)**

| Alphanumeric designation | Species name | Genbank accession number(s) |
|---|---|---|
| **A1** | *Symbiodinium microadriaticum* | AF333505, U63483 |
| **A2** | *Symbiodinium pilosum* | AF333506, JN558097, AF060894 |
| **A3** | *'Symbiodinium fitti'* | AF333507, JN558091, KF364601 |
| **A4** | *Symbiodinium linucheae* | AF427465, AY074949, AF333509 |
| **$A_{III}$** | *Symbiodinium natans* | AB704015, AB704056, EU315917 |
| **B1** | *Symbiodinium minutum* | AF333511, JN558059, AF060892 |
| **B2** | *Symbiodinium psygmophilum* | AF333512, JN558061 |
| **C1** | *Symbiodinium goreauii* | AF333515, JN558040, JN558041 |
| **C3** | | AB 294654, EU786077, FJ529524, JF834208, J834209 |
| **C3nt** | | FJ529569, FJ529594-FJ529604, FJ529530 |
| **C8a** | | FJ529563, FJ529612-FJ529619, FJ529526 |
| **C33** | | FJ529566, FJ529567, AY258498, AY765400, FJ529532 |
| **C33a** | | FJ529564, FJ529565, FJ529624- FJ529626, FJ529531 |
| **C35a** | | FJ529559, FJ529584-FJ529593, FJ529529, EF541146, EU808002, AY258501 |
| **C42a** | | FJ529561, FJ529634-FJ529655, FJ529525, HQ650837 |
| **C78a** | | FJ529562, FJ529605-FJ529611, FJ529527, EU808000 |
| **C79** | | FJ529560, FJ529570-FJ525581, FJ529528, AY765414, EU807997 |
| **C91** | | AJ291519, JN558048 |
| **D1a** | *Symbiodinium trenchii* | EU074894, EU074898, EU074903-EU074906, JN558078, KJ019889, KF740689 |
| **D1** | *'Symbiodinium glynni'* | AF334660, JN558075, JN558076, AF396626-AF396628, JN601885, DQ312315 |
| **E1** | *Symbiodinium voratum* | AF334659, JN558084- JN558086, KF364603- KF364605 |
| **F1** | *Symbiodinium kawagutii* | AF360577, AF333517, JN558066, AF427462 |
| **F2** | | AF333516, JN558065, KF740673 |
| **G** | | AJ291537 |
| **H** | | AJ291513 |
| **I** | | FN561559 |
| | *Polarella glacialis* | GQ375263, AB704041, AB704042, FJ939578, AY571373 |
| | *Protodinium simplex* | JF791031, AY686651, JN558103, AF060900 |

*Species names in inverted commas are yet to be formally described

**Table A.2 Deposition of novel internal transcribed spacer 2 (*ITS2*) sequence (chapter 2)**

> **KJ530690** *Symbiodinium* sp. C109 5.8S ribosomal RNA gene, partial sequence; internal transcribed spacer 2, complete sequence; and 28S ribosomal RNA gene, partial sequence

AACCAATGGCCTCCTGAACGTGCGTTGCACTCTTGGGATTTCCTGAGAGTACGTCTGCTTCAGTGC
TTAACTTGCCCCAACTTTGCAAGCAGGATGTGTTTCTGCCTTGCGTTCTTATGAGCTATTGCCCTCT
GAGCCAATGGCTTGTTAATTGCTTGGTTCTTGCAAAATGCTTTGCGCGCTGTTATTCAAGTTTCTAC
CTTCGTGGTTTTACTTGAGTGACGCTGCTCATGCTTGCAACCGCTGGGATGCAGGTGCATGCCTCTA
GCATGAAGTCAGACAAGTGA

**Table A.3 *ITS2* sequences used in statistical parsimony network (Figure 2.2)**

| Alphanumeric designation | Genbank accession number |
|---|---|
| **C1 (*Symbiodinium goreauii*)** | AF333515 |
| **C1bb** | HM222430 |
| **C100** | HM222433 |
| **C103** | HM222435 |
| **C109** | KJ530690 |
| **C118** | HM222440 |
| **C3** | GU111863 |
| **C3gg** | HM222431 |
| **C3hh** | HM222432 |
| **C3n** | EU449106 |

# Appendix B: Supplementary data tables and figures

**Table B.1 Standard curve analysis for nested qPCR (North Bay colonies; chapter 2)**

| Assay | Template sequence | Concentration (ng µl$^{-1}$) | Concentration (copies µl$^{-1}$) | Mean $C_t$ | Slope | Intercept | Efficiency |
|---|---|---|---|---|---|---|---|
| **C100$^{+}$ (TaqMan)** | C100 | 1 x 10$^{-3}$ | 212345 | 7.66 | -3.5255 | 26.472 | 96.08% |
| | | 1 x 10$^{-4}$ | 21234 | 11.12 | | | |
| | | 1 x 10$^{-5}$ | 2123 | 14.91 | | | |
| | | 1 x 10$^{-6}$ | 212 | 18.34 | | | |
| | | 1 x 10$^{-7}$ | 21 | 21.68 | | | |
| | C103 | 1 x 10$^{-3}$ | 212345 | - | | | |
| | C109 | 2.5 x 10$^{-3}$ | 530862 | - | | | |
| | C118 | 1 x 10$^{-3}$ | 212345 | - | | | |
| | C3 | 1 x 10$^{-3}$ | 212345 | - | | | |
| | | | | | | | |
| **C100$^{-}$ (TaqMan)** | C109 | 2.5 x 10$^{-3}$ | 530862 | 6.14 | -3.5296 | 26.392 | 96.00% |
| | | 2.5 x 10$^{-4}$ | 53086 | 9.66 | | | |
| | | 2.5 x 10$^{-5}$ | 5309 | 13.4 | | | |
| | | 2.5 x 10$^{-6}$ | 531 | 16.8 | | | |
| | | 2.5 x 10$^{-7}$ | 53 | 20.22 | | | |
| | C103 | 1 x 10$^{-3}$ | 212345 | 8.33 | -3.5305 | 27.054 | 95.99% |
| | | 1 x 10$^{-4}$ | 21234 | 11.67 | | | |
| | | 1 x 10$^{-5}$ | 2123 | 15.45 | | | |
| | | 1 x 10$^{-6}$ | 212 | 18.54 | | | |
| | | 1 x 10$^{-7}$ | 21 | 22.51 | | | |
| | C100 | 1 x 10$^{-3}$ | 212345 | - | | | |
| | | | | | | | |
| **SYBR** | C100/C109 | 1 x 10$^{-3}$ | 212345 | 5.79 | -3.4024 | 23.775 | 98.37% |
| | | 1 x 10$^{-4}$ | 21234 | 8.9 | | | |
| | | 1 x 10$^{-5}$ | 2123 | 12.48 | | | |
| | | 1 x 10$^{-6}$ | 212 | 15.73 | | | |
| | | 1 x 10$^{-7}$ | 21 | 19.38 | | | |

Mean cycling threshold ($C_t$) values were calculated from triplicate reactions. Template solutions were plasmid-purified DNA of known *ITS2* sequences. A C100/C109 mixture with $C_{C100}$:$C_{TOTAL}$ = 0.5 was used for calibration of the SYBR assay. Dashes represent no-amplification reactions, and show an absence of cross-hybridization. $R^2$ values exceeded 0.99 in all cases

**Table B.2 Standard curve analysis for nested qPCR (Ned's Beach colonies; chapter 2)**

| qPCR assay | Template sequence | Concentration (ng µl$^{-1}$) | Concentration (copies µl$^{-1}$) | Mean $C_t$ | Slope | Intercept | Efficiency |
|---|---|---|---|---|---|---|---|
| **C100$^{+}$** | C100 | 6.67 x 10$^{-4}$ | 142,271 | 7.66 | -3.5325 | 30.057 | 95.95% |
| | | 1 x 10$^{-4}$ | 21,234 | 11.12 | | | |
| | | 1 x 10$^{-5}$ | 2,123 | 14.91 | | | |
| | | 1 x 10$^{-6}$ | 212 | 18.34 | | | |
| | | 1 x 10$^{-7}$ | 21 | 21.68 | | | |
| | | | | | | | |
| | C109 | 1 x 10$^{-3}$ | 212,344 | - | | | |
| | | | | | | | |
| **C100$^{-}$** | C109 | 1 x 10$^{-3}$ | 212,344 | 6.14 | -3.553 | 29.866 | 95.59% |
| | | 2.5 x 10$^{-4}$ | 53,086 | 9.66 | | | |
| | | 2.5 x 10$^{-5}$ | 5,309 | 13.4 | | | |
| | | 2.5 x 10$^{-6}$ | 531 | 16.8 | | | |
| | | 2.5 x 10$^{-7}$ | 53 | 20.22 | | | |
| | | | | | | | |
| | C100 | 6.67 x 10$^{-4}$ | 142,271 | - | | | |

Mean cycling threshold ($C_t$) values are calculated from triplicate reactions. Template solutions were plasmid-purified DNA of known *ITS2* sequences (C100 or C109). Dashes represent no-amplification reactions, and show an absence of cross-hybridization. $R^2$ values exceeded 0.99 in both cases.

**Table B.3 Assay validation for TaqMan nested qPCR (chapter 2)**

| Mixture | $C_{C100}$:$C_{TOTAL}$ (actual) | Mean $C_t$ ($C100^+$) | Mean $C_t$ ($C100^-$) | $C_{TOTAL}$ (predicted) | $C_{C100}$:$C_{TOTAL}$ (predicted) |
|---|---|---|---|---|---|
| **1** | 1 | 18.45 | - | 188 | 1 |
| **2** | 0.98 | 18.44 | 23.7 | 195 | 0.970 |
| **3** | 0.9 | 18.53 | 21.26 | 207 | 0.863 |
| **4** | 0.6 | 19.09 | 19.54 | 211 | 0.586 |
| **5** | 0.4 | 19.67 | 19.08 | 203 | 0.418 |
| **6** | 0.1 | 21.49 | 18.51 | 197 | 0.132 |
| **7** | 0.02 | 24.99 | 18.38 | 189 | 0.014 |
| **8** | 0 | - | 18.4 | 184 | 0 |

Mixtures were generated from plasmid C100 and C109 template solutions diluted to approximately 200 *ITS2* copies $\mu l^{-1}$. The assay predicted $C_{C100}$:$C_{TOTAL}$ with a high degree of accuracy and precision (linear regression with constrained parameters; intercept = 0 and slope = 1; $R^2 = 0.998$). Dashes represent no-amplification reactions, and show an absence of cross-hybridization.

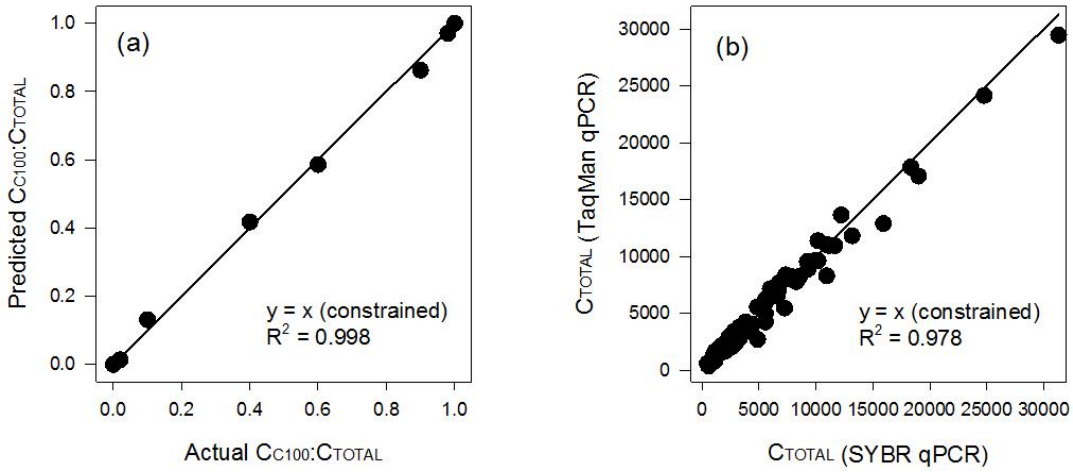


**Figure B.1 Single-cell qPCR assay validation (chapter 2)**

The TaqMan qPCR assay was validated by: (a) testing with known mixtures of clonal DNA; and (b) comparing copy-number estimates for each *Symbiodinium* cell (North Bay colonies) with those obtained from the independent SYBR qPCR assay. TaqMan and SYBR qPCR methods gave highly congruent results, implying that the number of *ITS2* copies present within the genome that were not detected by either TaqMan probe was negligible.

**Table B.4 Mean $C_t$ values for individual *Symbiodinium* cells (colony a; chapter 2)**

| Branch | C100 band | C109 band | Mean $C_t$ ($C100^+$) | Mean $C_t$ ($C100^-$) | Mean $C_t$ (SYBR) | $C_{TOTAL}$ (TaqMan) | $C_{TOTAL}$ (SYBR) | $C_{C100}$:$C_{TOTAL}$ |
|---|---|---|---|---|---|---|---|---|
| **1** | Y | Y | 19.72 | 20.89 | 16.97 | 2364 | 1998 | 0.6945 |
| | Y | N | 20.45 | 24.89 | 17.89 | 1077 | 1072 | 0.9505 |
| | N | Y | - | 21.22 | 19.26 | 584 | 426 | 0 |
| | Y | Y | 19.32 | 20.73 | 16.65 | 2944 | 2479 | 0.7278 |
| | Y | Y | 19.75 | 20.69 | 16.84 | 2435 | 2178 | 0.6616 |
| | Y | Y | 21.43 | 21.69 | 18.12 | 970 | 917 | 0.5566 |
| | Y | Y | 20.52 | 21.13 | 17.35 | 1598 | 1542 | 0.6111 |
| | Y | Y | 21 | 22.25 | 18 | 1010 | 995 | 0.7049 |
| | Y | N | 19.37 | 21.24 | 16.65 | 2644 | 2482 | 0.7822 |
| | Y | Y | 20.69 | 22.4 | 17.88 | 1145 | 1083 | 0.7639 |
| **2** | Y | Y | 20.24 | 21.54 | 17.79 | 1645 | 1150 | 0.7126 |
| | Y | Y | 20.95 | 20.51 | 17.21 | 1662 | 1701 | 0.4424 |
| | Y | Y | 22.34 | 23.25 | 18.97 | 453 | 516 | 0.6561 |
| | Y | Y | 21.19 | 23.05 | 17.86 | 809 | 1097 | 0.7805 |
| | Y | N | 19.31 | 21.58 | 16.82 | 2606 | 2215 | 0.8233 |
| | Y | Y | 19.52 | 20.56 | 16.26 | 2767 | 3226 | 0.6758 |
| | Y | Y | 19.09 | 20.49 | 16.46 | 3426 | 2825 | 0.7254 |
| | Y | Y | 18.82 | 20.6 | 15.93 | 3828 | 4031 | 0.7721 |
| | Y | Y | 21.69 | 23.12 | 18.36 | 625 | 782 | 0.7288 |
| | Y | N | 19.89 | 22.1 | 17.16 | 1804 | 1758 | 0.8179 |
| **3** | Y | Y | 17.05 | 18.48 | 13.91 | 12896 | 15919 | 0.7292 |
| | Y | Y | 19.27 | 20.42 | 16.4 | 3200 | 2947 | 0.692 |
| | Y | Y | 22.08 | 22.78 | 18.5 | 565 | 710 | 0.625 |
| | Y | N | 18.97 | 20.5 | 16.26 | 3626 | 3224 | 0.7418 |
| | Y | Y | 19.3 | 21.02 | 16.5 | 2830 | 2755 | 0.7646 |
| | Y | N | 19.03 | 21.09 | 16.36 | 3210 | 3033 | 0.8025 |
| | Y | Y | 20.66 | 21.15 | 17.57 | 1504 | 1331 | 0.5924 |
| | Y | Y | 20.43 | 21.52 | 17.27 | 1515 | 1627 | 0.6826 |
| | Y | Y | 19.27 | 19.49 | 15.8 | 4004 | 4416 | 0.55 |
| | Y | Y | 19.53 | 20.26 | 16.73 | 2948 | 2360 | 0.6302 |

C100- and C109-diagnostic DGGE bands are scored as present or absent (Y or N). Dashes represent no-amplification reactions

**Table B.5 Mean $C_t$ values for individual *Symbiodinium* cells (colony b; chapter 2)**

| Branch | C100 band | C109 band | Mean $C_t$ ($C100^+$) | Mean $C_t$ ($C100^-$) | Mean $C_t$ (SYBR) | $C_{TOTAL}$ (TaqMan) | $C_{TOTAL}$ (SYBR) | $C_{C100}$:$C_{TOTAL}$ |
|---|---|---|---|---|---|---|---|---|
| **1** | Y | Y | 20.14 | 21.99 | 17.3 | 1607 | 1603 | 0.7798 |
| | Y | Y | 18.72 | 21.25 | 16.17 | 3736 | 3446 | 0.8466 |
| | Y | N | 19.51 | 21.26 | 16.45 | 2459 | 2852 | 0.7682 |
| | Y | N | 20.13 | 22.74 | 17.35 | 1475 | 1550 | 0.8532 |
| | Y | Y | 19.99 | 21 | 16.87 | 2057 | 2138 | 0.672 |
| | Y | Y | 20.01 | 20.87 | 16.54 | 2094 | 2667 | 0.6499 |
| | Y | Y | 20.38 | 21.2 | 17.27 | 1663 | 1638 | 0.6434 |
| | Y | N | 19.43 | 21.45 | 16.57 | 2489 | 2626 | 0.7977 |
| | Y | Y | 18.57 | 20.84 | 16.02 | 4245 | 3812 | 0.8232 |
| | Y | N | 19.78 | 22.72 | 17.31 | 1800 | 1588 | 0.878 |
| **2** | N | Y | - | 21.89 | 18.81 | 377 | 577 | 0 |
| | Y | N | 19.18 | 21.94 | 15.66 | 2708 | 4864 | 0.8653 |
| | Y | Y | 19.7 | 21.11 | 16.43 | 2298 | 2884 | 0.7276 |
| | N | Y | 25.18 | 20.74 | 18.32 | 848 | 801 | 0.0549 |
| | Y | N | 18.13 | 22.15 | 15.46 | 4974 | 5542 | 0.9361 |
| | Y | N | 19.55 | 22.19 | 16.98 | 2149 | 1987 | 0.8552 |
| | Y | N | 20.11 | 23.16 | 17.5 | 1439 | 1401 | 0.8853 |
| | Y | Y | 18.2 | 19.22 | 15.38 | 6597 | 5882 | 0.6727 |
| | Y | N | 20.35 | 22.96 | 17.78 | 1277 | 1160 | 0.8528 |
| | Y | N | 19.53 | 21.74 | 16.96 | 2282 | 2017 | 0.8178 |
| **3** | Y | Y | 20.52 | 21.88 | 17.75 | 1354 | 1178 | 0.7203 |
| | Y | N | 17.5 | 20.02 | 14.46 | 8302 | 10922 | 0.8462 |
| | Y | Y | 20.52 | 20.93 | 16.93 | 1683 | 2052 | 0.5812 |
| | Y | Y | 19.29 | 20.1 | 15.87 | 3393 | 4212 | 0.6438 |
| | Y | N | 20.54 | 26.28 | 17.9 | 985 | 1066 | 0.9781 |
| | Y | N | 19.55 | 22.53 | 17.3 | 2088 | 1602 | 0.8808 |
| | Y | N | 19.33 | 21.03 | 16.51 | 2783 | 2727 | 0.7626 |
| | Y | Y | 18.92 | 20.34 | 16.24 | 3803 | 3289 | 0.7279 |
| | Y | N | 17.97 | 20.34 | 15.47 | 6187 | 5535 | 0.832 |
| | Y | N | 17.61 | 21.04 | 15.35 | 7168 | 5981 | 0.9082 |

C100- and C109-diagnostic DGGE bands are scored as present or absent (Y or N). Dashes represent no-amplification reactions

**Table B.6 Mean $C_t$ values for individual *Symbiodinium* cells (colony c; chapter 2)**

| Branch | C100 band | C109 band | Mean $C_t$ ($C100^+$) | Mean $C_t$ ($C100^-$) | Mean $C_t$ (SYBR) | $C_{TOTAL}$ (TaqMan) | $C_{TOTAL}$ (SYBR) | $C_{C100}$:$C_{TOTAL}$ |
|---|---|---|---|---|---|---|---|---|
| **1** | Y | N | 16.87 | 20.74 | 14.57 | 11391 | 10152 | 0.9299 |
| | Y | N | 17.88 | 23.9 | 15.67 | 5557 | 4834 | 0.9817 |
| | Y | N | 17.36 | 23.9 | 14.87 | 7778 | 8259 | 0.9869 |
| | Y | N | 16.54 | 21.34 | 14.3 | 13651 | 12210 | 0.9603 |
| | Y | N | 17.24 | 21.22 | 14.7 | 8895 | 9301 | 0.9345 |
| | Y | N | 17.6 | 21.65 | 15.19 | 7026 | 6683 | 0.9372 |
| | Y | N | 15.67 | 20.37 | 13.25 | 24149 | 24764 | 0.958 |
| | Y | N | 16.18 | 21.75 | 13.64 | 17066 | 18997 | 0.9757 |
| | Y | N | 17.6 | 21.96 | 15.23 | 6915 | 6473 | 0.9478 |
| | Y | N | 17.77 | 22.99 | 15.44 | 6048 | 5620 | 0.9695 |
| **2** | Y | N | 17.93 | 23.1 | 15.07 | 5460 | 7233 | 0.9686 |
| | Y | N | 16.14 | 20.73 | 13.7 | 17854 | 18335 | 0.955 |
| | Y | N | 17.12 | 21.02 | 14.57 | 9625 | 10166 | 0.931 |
| | Y | N | 15.4 | 19.49 | 12.91 | 29461 | 31310 | 0.9388 |
| | Y | N | 17.16 | 20.78 | 14.71 | 9559 | 9239 | 0.9184 |
| | Y | N | 17.35 | 22.28 | 14.95 | 8019 | 7854 | 0.9635 |
| | Y | N | 18.47 | 21.43 | 15.46 | 4231 | 5547 | 0.8799 |
| | Y | Y | 21.24 | 20.95 | 18.07 | 1305 | 951 | 0.4659 |
| | Y | N | 17.45 | 21.7 | 15.18 | 7667 | 6733 | 0.9445 |
| | Y | N | 17.31 | 23.75 | 15.01 | 8034 | 7554 | 0.986 |
| **3** | Y | N | 16.84 | 20.33 | 14.19 | 11815 | 13153 | 0.9116 |
| | Y | N | 16.89 | 21.16 | 14.46 | 11056 | 10918 | 0.945 |
| | Y | N | 17.35 | 21.32 | 14.98 | 8266 | 7697 | 0.9338 |
| | Y | Y | 19.52 | 20.56 | 16.7 | 2776 | 2396 | 0.6758 |
| | Y | N | 17.15 | 20.7 | 14.59 | 9661 | 10009 | 0.9149 |
| | Y | N | 16.87 | 22.02 | 14.37 | 10947 | 11643 | 0.9684 |
| | Y | N | 17.38 | 20.77 | 15.05 | 8387 | 7339 | 0.9066 |
| | Y | N | 16.88 | 21.62 | 14.43 | 10956 | 11144 | 0.959 |
| | Y | N | 17.65 | 23.72 | 15.21 | 6491 | 6571 | 0.9824 |
| | Y | N | 17.32 | 21.89 | 14.82 | 8276 | 8585 | 0.9545 |

C100- and C109-diagnostic DGGE bands are scored as present or absent (Y or N). Dashes represent no-amplification reactions

**Table B.7 Mean $C_t$ values for individual *Symbiodinium* cells (colony d; chapter 2)**

| Branch | C100 band | C109 band | Mean $C_t$ ($C100^+$) | Mean $C_t$ ($C100^-$) | $C_{C100}$ | $C_{TOTAL}$ | $C_{C100}$:$C_{TOTAL}$ |
|---|---|---|---|---|---|---|---|
| **1** | N | Y | 27.01 | 23.92 | 146 | 1092 | 0.1339 |
| | Y | Y | 23.26 | 23.75 | 1685 | 2741 | 0.6147 |
| | Y | Y | 23.63 | 23.56 | 1324 | 2515 | 0.5264 |
| | Y | Y | 24.01 | 24.49 | 1033 | 1685 | 0.6132 |
| | Y | Y | 24.64 | 25 | 683 | 1153 | 0.5925 |
| | Y | Y | 25.16 | 24.78 | 487 | 1029 | 0.4732 |
| | Y | Y | 22.58 | 23.16 | 2616 | 4164 | 0.6282 |
| | Y | Y | 25.02 | 25.36 | 533 | 905 | 0.589 |
| | Y | Y | 22.28 | 23.6 | 3192 | 4356 | 0.7327 |
| | Y | Y | 23.65 | 23.88 | 1307 | 2278 | 0.5737 |
| **2** | Y | N | 23.25 | 30.62 | 1690 | 1703 | 0.9928 |
| | Y | Y | 26.5 | 27.41 | 203 | 301 | 0.6741 |
| | Y | Y | 22.76 | 22.58 | 2334 | 4589 | 0.5086 |
| | Y | N | 23.13 | 25.44 | 1828 | 2180 | 0.8385 |
| | Y | Y | 21.98 | 22.47 | 3868 | 6282 | 0.6158 |
| | Y | Y | 20.69 | 20.98 | 8968 | 15307 | 0.5859 |
| | Y | Y | 28.19 | 28.94 | 68 | 104 | 0.6495 |
| | Y | Y | 23.4 | 23.88 | 1533 | 2501 | 0.613 |
| | Y | Y | 27.72 | 28.52 | 92 | 140 | 0.6565 |
| | Y | Y | 22.84 | 23.02 | 2208 | 3898 | 0.5665 |
| **3** | Y | Y | 26.96 | 27.41 | 151 | 250 | 0.6052 |
| | Y | N | 21.19 | 23.37 | 6474 | 7821 | 0.8278 |
| | Y | Y | 24.32 | 24.89 | 844 | 1349 | 0.6259 |
| | Y | Y | 21.67 | 22.19 | 4750 | 7653 | 0.6207 |
| | Y | Y | 25.2 | 25.73 | 476 | 769 | 0.6191 |
| | Y | Y | 26.77 | 27.69 | 171 | 253 | 0.6753 |
| | Y | Y | 27.33 | 27.98 | 118 | 186 | 0.6354 |
| | Y | N | 19.94 | 23.11 | 14622 | 16221 | 0.9014 |
| | N | Y | 32.31 | 24.13 | 5 | 828 | 0.0056 |
| | Y | Y | 21.27 | 21.6 | 6145 | 10400 | 0.5908 |

C100- and C109-diagnostic DGGE bands are scored as present or absent (Y or N). Dashes represent no-amplification reactions

**Table B.8 Mean $C_t$ values for individual *Symbiodinium* cells (colony e; chapter 2)**

| Branch | C100 band | C109 band | Mean $C_t$ ($C100^+$) | Mean $C_t$ ($C100^-$) | $C_{C100}$ | $C_{TOTAL}$ | $C_{C100}$:$C_{TOTAL}$ |
|---|---|---|---|---|---|---|---|
| **1** | Y | N | 20.81 | 28.04 | 8320 | 8386 | 0.9922 |
| | Y | N | 23.74 | 30.54 | 1232 | 1245 | 0.9896 |
| | Y | N | 23.73 | 25.9 | 1236 | 1498 | 0.825 |
| | Y | Y | 23.6 | 25 | 1350 | 1820 | 0.7418 |
| | Y | Y | 23.34 | 25.19 | 1599 | 2013 | 0.7943 |
| | Y | N | 21.36 | 24.31 | 5814 | 6548 | 0.8878 |
| | Y | N | 24.62 | 27.33 | 692 | 796 | 0.8696 |
| | Y | N | 18.78 | 25.26 | 31145 | 31541 | 0.9875 |
| | Y | N | 19.48 | 23.86 | 19799 | 20783 | 0.9527 |
| | Y | Y | 21.75 | 22.94 | 4494 | 6274 | 0.7163 |
| **2** | Y | Y | 20.66 | 22.41 | 9175 | 11692 | 0.7847 |
| | Y | Y | 21.5 | 22.69 | 5307 | 7399 | 0.7172 |
| | Y | N | 21.45 | 26 | 5482 | 5727 | 0.9572 |
| | Y | N | 20.24 | 26.01 | 12025 | 12268 | 0.9802 |
| | Y | Y | 23.67 | 24.45 | 1290 | 1959 | 0.6585 |
| | Y | N | 21.99 | 24.35 | 3843 | 4557 | 0.8434 |
| | Y | N | 22.37 | 29.11 | 3010 | 3042 | 0.9893 |
| | Y | N | 22.58 | 29.74 | 2625 | 2646 | 0.9918 |
| | Y | N | 20.32 | 27.56 | 11414 | 11503 | 0.9923 |
| | Y | N | 27.74 | 29.88 | 91 | 111 | 0.8204 |
| **3** | Y | N | 23.64 | 30.62 | 1315 | 1328 | 0.9908 |
| | Y | N | 24.39 | 31.05 | 804 | 813 | 0.9885 |
| | Y | N | 24.83 | 31.47 | 604 | 611 | 0.9884 |
| | Y | N | 19.83 | 23.11 | 15709 | 17308 | 0.9076 |
| | Y | N | 21.34 | 26.63 | 5890 | 6053 | 0.973 |
| | Y | Y | 21.05 | 23.12 | 7092 | 8681 | 0.817 |
| | Y | Y | 26.72 | 27.19 | 176 | 290 | 0.6077 |
| | Y | N | 21.76 | 26.76 | 4479 | 4629 | 0.9676 |
| | Y | N | 23.07 | 27.5 | 1907 | 2000 | 0.9535 |
| | Y | N | 22.19 | 24.91 | 3373 | 3870 | 0.8717 |

C100- and C109-diagnostic DGGE bands are scored as present or absent (Y or N). Dashes represent no-amplification reactions

**Table B.9 Mean $C_t$ values for individual *Symbiodinium* cells (colony f; chapter 2)**

| Branch | C100 band | C109 band | Mean $C_t$ ($C100^+$) | Mean $C_t$ ($C100^-$) | $C_{C100}$ | $C_{TOTAL}$ | $C_{C100}$:$C_{TOTAL}$ |
|---|---|---|---|---|---|---|---|
| **1** | Y | N | 27.91 | 30.16 | 81 | 98 | 0.8306 |
| | Y | Y | 26.25 | 28.12 | 240 | 302 | 0.7947 |
| | Y | N | 24.37 | 32.07 | 815 | 819 | 0.9941 |
| | Y | Y | 22.59 | 23.17 | 2608 | 4146 | 0.629 |
| | Y | Y | 22.83 | 22.84 | 2230 | 4135 | 0.5393 |
| | Y | Y | 22.68 | 23.59 | 2459 | 3627 | 0.678 |
| | Y | Y | 22.44 | 22.12 | 2866 | 5904 | 0.4855 |
| | Y | N | 21.9 | 29.65 | 4075 | 4098 | 0.9944 |
| | Y | N | 24.68 | 32.27 | 666 | 670 | 0.9937 |
| | Y | Y | 28.9 | 30.18 | 43 | 59 | 0.7227 |
| **2** | Y | N | 21.77 | 26.08 | 4450 | 4684 | 0.9502 |
| | N | Y | 32.94 | 23.46 | 3 | 1274 | 0.0024 |
| | Y | N | 23.09 | 30.7 | 1882 | 1894 | 0.9938 |
| | Y | Y | 20.99 | 21.69 | 7375 | 11389 | 0.6476 |
| | Y | Y | 25.18 | 25.07 | 480 | 929 | 0.5169 |
| | Y | Y | 28.12 | 29 | 71 | 106 | 0.6678 |
| | Y | Y | 26.99 | 27.55 | 148 | 238 | 0.622 |
| | Y | N | 24.51 | 28 | 746 | 813 | 0.9173 |
| | Y | N | 23.56 | 30.55 | 1386 | 1399 | 0.9908 |
| | Y | Y | 22.92 | 23.87 | 2096 | 3073 | 0.682 |
| **3** | Y | Y | 21.99 | 22.88 | 3843 | 5693 | 0.675 |
| | Y | N | 22.93 | 26.7 | 2082 | 2239 | 0.9303 |
| | Y | N | 19.57 | 21.65 | 18671 | 22777 | 0.8197 |
| | Y | Y | 22.88 | 24.71 | 2151 | 2717 | 0.792 |
| | Y | Y | 24.29 | 25.36 | 861 | 1233 | 0.6982 |
| | Y | Y | 25.27 | 25.73 | 455 | 746 | 0.609 |
| | Y | N | 23.4 | 30.44 | 1538 | 1552 | 0.9911 |
| | Y | Y | 23.84 | 23.76 | 1154 | 2201 | 0.5246 |
| | Y | N | 22.78 | 26.21 | 2304 | 2518 | 0.9151 |
| | Y | Y | 22.82 | 23.23 | 2237 | 3717 | 0.6019 |

C100- and C109-diagnostic DGGE bands are scored as present or absent (Y or N). Dashes represent no-amplification reactions

**Table B.10 Standard curve parameter estimation for bulk-cell qPCR analysis (chapter 3)**

| qPCR assay | Template sequence | Concentration (ng µl$^{-1}$) | Concentration (copies µl$^{-1}$) | Mean $C_t$ | Slope | Intercept | Efficiency |
|---|---|---|---|---|---|---|---|
| **C100$^{+}$** | C100 | 1 x 10$^{-2}$ | 2,123,448 | 15.41 | -3.379 | 36.873 | 98.84% |
| | | 1 x 10$^{-3}$ | 212,345 | 18.87 | | | |
| | | 1 x 10$^{-4}$ | 21,234 | 22.16 | | | |
| | | 1 x 10$^{-5}$ | 2,123 | 25.91 | | | |
| | | 1 x 10$^{-6}$ | 212 | 29.2 | | | |
| | | 1 x 10$^{-7}$ | 21 | 32.11 | | | |
| | | | | | | | |
| | C109 | 2.5 x 10$^{-2}$ | 5,308,621 | - | | | |
| | | | | | | | |
| **C100$^{-}$** | C109 | 2.5 x 10$^{-2}$ | 5,308,621 | 14.59 | -3.373 | 37.119 | 98.96% |
| | | 2.5 x 10$^{-3}$ | 53,0862 | 17.83 | | | |
| | | 2.5 x 10$^{-4}$ | 53,086 | 20.68 | | | |
| | | 2.5 x 10$^{-5}$ | 5,309 | 24.94 | | | |
| | | 2.5 x 10$^{-6}$ | 531 | 27.82 | | | |
| | | 2.5 x 10$^{-7}$ | 53 | 31.35 | | | |
| | | | | | | | |
| | C100 | 1 x 10$^{-2}$ | 2,123,448 | - | | | |

Mean cycling threshold ($C_t$) values are calculated from triplicate reactions. Template solutions were plasmid-purified DNA of known *ITS2* sequences (C100 or C109). Dashes represent no-amplification reactions, and show an absence of cross-hybridization. $R^2$ values exceeded 0.99 in both cases.

**Table B.11 Nested analysis of spatial variance in $S_H$:$S_T$ (chapter 3)**

| Site | ID | Branch | C100 band | C109 band | Mean $C_t$ ($C100^+$) | Mean $C_t$ ($C100^-$) | $C_{C100}$ | $C_{C100}^-$ | $C_{TOTAL}$ | $C_{100}$:$C_{TOTAL}$ | $S_H$:$S_T$ |
|---|---|---|---|---|---|---|---|---|---|---|---|
| **Sylph's** | 1 | 1 | Y | N | 21.62 | 25.6 | 32698 | 2609 | 35306 | 0.926 | 0.154 |
| **Hole** | | 2 | Y | N | 21.14 | 25 | 45173 | 3915 | 49088 | 0.92 | 0.172 |
| | | 3 | Y | N | 21.35 | 25.76 | 39250 | 2338 | 41588 | 0.944 | 0.1 |
| | 2 | 1 | Y | Y | 25.63 | 27.89 | 2128 | 545 | 2673 | 0.796 | 0.49 |
| | | 2 | Y | Y | 20.25 | 22.52 | 82843 | 21228 | 104071 | 0.796 | 0.49 |
| | | 3 | Y | Y | 24.44 | 26.85 | 4772 | 1111 | 5883 | 0.811 | 0.457 |
| | 3 | 1 | Y | Y | 27.33 | 29.28 | 666 | 210 | 876 | 0.76 | 0.562 |
| | | 2 | Y | Y | 25.36 | 27.41 | 2561 | 755 | 3317 | 0.772 | 0.539 |
| | | 3 | Y | N | 22.7 | 24.7 | 15628 | 4795 | 20423 | 0.765 | 0.552 |
| | 4 | 1 | Y | N | 28.55 | 31.85 | 290 | 37 | 326 | 0.888 | 0.264 |
| | | 2 | Y | N | 29.61 | 33.31 | 141 | 13 | 155 | 0.913 | 0.194 |
| | | 3 | Y | N | 19.33 | 22.88 | 155268 | 16667 | 171936 | 0.903 | 0.222 |
| | 5 | 1 | Y | N | 24.02 | 27.7 | 6379 | 620 | 7000 | 0.911 | 0.198 |
| | | 2 | Y | N | 25.83 | 29.73 | 1856 | 156 | 2012 | 0.923 | 0.165 |
| | | 3 | Y | N | 24.96 | 28.15 | 3348 | 455 | 3804 | 0.88 | 0.286 |
| **North** | 6 | 1 | Y | Y | 24.97 | 26.87 | 3329 | 1096 | 4426 | 0.752 | 0.576 |
| **Bay** | | 2 | Y | Y | 24.02 | 25.85 | 6347 | 2188 | 8535 | 0.744 | 0.592 |
| | | 3 | Y | Y | 23.42 | 25.25 | 9584 | 3295 | 12878 | 0.744 | 0.591 |
| | 7 | 1 | Y | N | 26.8 | 30.26 | 958 | 108 | 1066 | 0.899 | 0.235 |
| | | 2 | Y | N | 24.22 | 27.56 | 5540 | 683 | 6223 | 0.89 | 0.259 |
| | | 3 | Y | N | 23.58 | 27.08 | 8588 | 947 | 9535 | 0.901 | 0.229 |
| | 8 | 1 | Y | N | 20.95 | 24.51 | 51669 | 5464 | 57133 | 0.904 | 0.219 |
| | | 2 | Y | N | 22.43 | 26.03 | 18771 | 1942 | 20714 | 0.906 | 0.213 |
| | | 3 | Y | N | 19.97 | 23.23 | 100557 | 13159 | 113717 | 0.884 | 0.275 |
| | 9 | 1 | Y | Y | 23.87 | 26.07 | 7059 | 1889 | 8948 | 0.789 | 0.505 |
| | | 2 | Y | N | 23.94 | 26.44 | 6725 | 1468 | 8194 | 0.821 | 0.435 |
| | | 3 | Y | N | 23.38 | 25.35 | 9822 | 3091 | 12913 | 0.761 | 0.561 |
| | 10 | 1 | Y | Y | 20.98 | 22.99 | 50532 | 15412 | 65944 | 0.766 | 0.55 |
| | | 2 | Y | Y | 24.43 | 26.25 | 4804 | 1672 | 6476 | 0.742 | 0.595 |
| | | 3 | Y | Y | 20.18 | 22.12 | 86928 | 28009 | 114936 | 0.756 | 0.569 |
| **Comet's** | 11 | 1 | Y | N | 24.86 | 27.08 | 3592 | 947 | 4539 | 0.791 | 0.5 |
| **Hole** | | 2 | Y | Y | 22.33 | 24.58 | 20130 | 5223 | 25353 | 0.794 | 0.494 |
| | | 3 | Y | Y | 22.1 | 24.26 | 23474 | 6483 | 29957 | 0.784 | 0.516 |

| | | | | | | | | | | | |
|---|---|---|---|---|---|---|---|---|---|---|---|
| | 12 | 1 | Y | N | 25.35 | 28.56 | 2579 | 346 | 2925 | 0.882 | 0.282 |
| | | 2 | Y | N | 20.42 | 24.04 | 73843 | 7566 | 81409 | 0.907 | 0.211 |
| | | 3 | Y | N | 20.68 | 24.29 | 62054 | 6376 | 68429 | 0.907 | 0.212 |
| | 13 | 1 | Y | Y | 23.83 | 26.01 | 7245 | 1961 | 9206 | 0.787 | 0.509 |
| | | 2 | Y | N | 24.67 | 26.8 | 4099 | 1149 | 5248 | 0.781 | 0.521 |
| | | 3 | Y | Y | 26.12 | 28.19 | 1525 | 444 | 1968 | 0.774 | 0.534 |
| | 14 | 1 | Y | N | 23.46 | 26.48 | 9335 | 1426 | 10761 | 0.867 | 0.32 |
| | | 2 | Y | N | 19.81 | 23.04 | 112118 | 14917 | 127035 | 0.883 | 0.28 |
| | | 3 | Y | N | 19.28 | 22.43 | 161302 | 22583 | 183885 | 0.877 | 0.294 |
| | 15 | 1 | Y | Y | 27.65 | 29.84 | 536 | 144 | 680 | 0.789 | 0.506 |
| | | 2 | Y | N | 21.8 | 23.93 | 28813 | 8141 | 36954 | 0.78 | 0.524 |
| | | 3 | Y | N | 20.82 | 23.03 | 56351 | 15078 | 71430 | 0.789 | 0.505 |
| **The Arch** | 16 | 1 | Y | N | 23.18 | 26.02 | 11273 | 1949 | 13222 | 0.853 | 0.358 |
| | | 2 | Y | N | 22.68 | 25.84 | 15821 | 2213 | 18034 | 0.877 | 0.294 |
| | | 3 | Y | N | 22.6 | 25.62 | 16790 | 2572 | 19362 | 0.867 | 0.321 |
| | 17 | 1 | Y | Y | 26.89 | 28.82 | 902 | 289 | 1191 | 0.757 | 0.567 |
| | | 2 | Y | Y | 23.93 | 25.86 | 6770 | 2171 | 8941 | 0.757 | 0.567 |
| | | 3 | Y | Y | 23.82 | 25.7 | 7288 | 2423 | 9711 | 0.75 | 0.58 |
| | 18 | 1 | Y | Y | 23.82 | 25.21 | 7303 | 3399 | 10702 | 0.682 | 0.687 |
| | | 2 | Y | Y | 24.25 | 25.67 | 5443 | 2481 | 7924 | 0.687 | 0.681 |
| | | 3 | Y | Y | 22.44 | 23.86 | 18674 | 8506 | 27180 | 0.687 | 0.681 |
| | 19 | 1 | Y | Y | 23.7 | 25.56 | 7906 | 2671 | 10576 | 0.747 | 0.585 |
| | | 2 | Y | N | 29.48 | 31.84 | 154 | 37 | 191 | 0.808 | 0.463 |
| | | 3 | Y | N | 26.05 | 28.05 | 1597 | 487 | 2084 | 0.766 | 0.55 |
| | 20 | 1 | Y | Y | 24.4 | 25.56 | 4917 | 2664 | 7582 | 0.649 | 0.729 |
| | | 2 | Y | Y | 25.46 | 26.77 | 2387 | 1169 | 3556 | 0.671 | 0.702 |
| | | 3 | Y | Y | 25.82 | 27.19 | 1873 | 880 | 2753 | 0.68 | 0.69 |
| **Malabar** | 21 | 1 | Y | Y | 20.21 | 22.15 | 85302 | 27453 | 112755 | 0.757 | 0.569 |
| | | 2 | Y | N | 22.41 | 24.43 | 19120 | 5779 | 24899 | 0.768 | 0.547 |
| | | 3 | Y | Y | 20.22 | 22.02 | 84787 | 30006 | 114793 | 0.739 | 0.601 |
| | 22 | 1 | Y | Y | 20.22 | 22.5 | 84570 | 21636 | 106206 | 0.796 | 0.489 |
| | | 2 | Y | N | 24.41 | 26.97 | 4879 | 1020 | 5899 | 0.827 | 0.42 |
| | | 3 | Y | N | 21.75 | 24.28 | 29954 | 6397 | 36351 | 0.824 | 0.428 |
| | 23 | 1 | Y | Y | 21.88 | 23.82 | 27294 | 8748 | 36042 | 0.757 | 0.567 |
| | | 2 | Y | Y | 19.61 | 21.76 | 128258 | 35751 | 164009 | 0.782 | 0.519 |

| | | | | | | | | | | | |
|---|---|---|---|---|---|---|---|---|---|---|---|
| | | 3 | Y | Y | 20.04 | 22.09 | 95688 | 28596 | 124284 | 0.77 | 0.543 |
| | 24 | 1 | Y | Y | 22.62 | 24.6 | 16492 | 5157 | 21648 | 0.762 | 0.559 |
| | | 2 | Y | Y | 20.59 | 22.63 | 65731 | 19824 | 85555 | 0.768 | 0.546 |
| | | 3 | Y | N | 19.9 | 22.25 | 105462 | 25629 | 131091 | 0.804 | 0.472 |
| | 25 | 1 | Y | Y | 21.92 | 23.76 | 26660 | 9119 | 35779 | 0.745 | 0.589 |
| | | 2 | Y | N | 20.55 | 22.53 | 67606 | 21174 | 88780 | 0.761 | 0.559 |
| | | 3 | Y | Y | 23.33 | 25.12 | 10159 | 3618 | 13777 | 0.737 | 0.603 |
| **Sugarloaf** | 26 | 1 | Y | Y | 24.12 | 26.01 | 5944 | 1963 | 7907 | 0.752 | 0.577 |
| **West** | | 2 | Y | Y | 25.46 | 27.31 | 2386 | 811 | 3197 | 0.746 | 0.587 |
| | | 3 | Y | Y | 23.19 | 25.21 | 11177 | 3394 | 14571 | 0.767 | 0.549 |
| | 27 | 1 | Y | Y | 25.97 | 27.7 | 1690 | 622 | 2311 | 0.731 | 0.614 |
| | | 2 | Y | Y | 24.19 | 25.66 | 5664 | 2499 | 8163 | 0.694 | 0.671 |
| | | 3 | Y | Y | 23.61 | 25.09 | 8396 | 3682 | 12078 | 0.695 | 0.67 |
| | 28 | 1 | Y | Y | 29.23 | 31.14 | 182 | 59 | 241 | 0.755 | 0.572 |
| | | 2 | Y | Y | 26.25 | 27.96 | 1388 | 520 | 1908 | 0.728 | 0.619 |
| | | 3 | Y | Y | 28.13 | 30.21 | 388 | 112 | 499 | 0.777 | 0.53 |
| | 29 | 1 | Y | N | 23.61 | 25.89 | 8419 | 2130 | 10549 | 0.798 | 0.486 |
| | | 2 | Y | N | 24.45 | 26.89 | 4749 | 1078 | 5827 | 0.815 | 0.448 |
| | | 3 | Y | N | 25.57 | 28.06 | 2218 | 486 | 2705 | 0.82 | 0.436 |
| | 30 | 1 | Y | Y | 23.62 | 25.06 | 8384 | 3757 | 12141 | 0.691 | 0.676 |
| | | 2 | Y | Y | 20.98 | 22.48 | 50567 | 21956 | 72523 | 0.697 | 0.667 |
| | | 3 | Y | Y | 23.51 | 25.24 | 9013 | 3334 | 12347 | 0.73 | 0.615 |
| **Ned's** | 31 | 1 | Y | Y | 22.18 | 23.91 | 22299 | 8260 | 30559 | 0.73 | 0.616 |
| **Beach** | | 2 | Y | Y | 22.51 | 23.94 | 17835 | 8098 | 25933 | 0.688 | 0.68 |
| | | 3 | Y | Y | 21.8 | 23.38 | 28896 | 11878 | 40775 | 0.709 | 0.65 |
| | 32 | 1 | Y | Y | 24.84 | 25.2 | 3651 | 3424 | 7075 | 0.516 | 0.816 |
| | | 2 | Y | Y | 26.96 | 27.41 | 861 | 759 | 1620 | 0.532 | 0.812 |
| | | 3 | Y | Y | 23.4 | 23.86 | 9744 | 8561 | 18305 | 0.532 | 0.812 |
| | 33 | 1 | Y | N | 21.65 | 24.39 | 31960 | 5936 | 37897 | 0.843 | 0.381 |
| | | 2 | Y | N | 25.06 | 27.64 | 3141 | 645 | 3786 | 0.83 | 0.414 |
| | | 3 | Y | N | 24.06 | 26.8 | 6204 | 1144 | 7349 | 0.844 | 0.379 |
| | 34 | 1 | Y | Y | 22.34 | 23.89 | 19933 | 8366 | 28299 | 0.704 | 0.656 |
| | | 2 | Y | Y | 26.6 | 27.9 | 1098 | 542 | 1640 | 0.669 | 0.704 |
| | | 3 | Y | Y | 25.15 | 26.34 | 2946 | 1574 | 4520 | 0.652 | 0.725 |
| | 35 | 1 | Y | Y | 21.72 | 23.97 | 30438 | 7936 | 38374 | 0.793 | 0.496 |

| | | | | | | | | | | |
|---|---|---|---|---|---|---|---|---|---|---|
| | | 2 | Y | N | 24.03 | 26.23 | 6313 | 1694 | 8007 | 0.788 | 0.506 |
| | | 3 | Y | Y | 23.29 | 25.28 | 10464 | 3231 | 13695 | 0.764 | 0.554 |
| **Algal** | 36 | 1 | Y | Y | 22.31 | 24.12 | 20411 | 7165 | 27576 | 0.74 | 0.598 |
| **Hole** | | 2 | Y | Y | 22.48 | 24.38 | 18165 | 5986 | 24150 | 0.752 | 0.577 |
| **North** | | 3 | Y | Y | 25.4 | 27.36 | 2480 | 780 | 3260 | 0.761 | 0.561 |
| | 37 | 1 | Y | Y | 24.48 | 26.14 | 4661 | 1797 | 6458 | 0.722 | 0.629 |
| | | 2 | Y | Y | 23.09 | 24.76 | 11959 | 4614 | 16573 | 0.722 | 0.629 |
| | | 3 | Y | Y | 22.99 | 24.52 | 12878 | 5436 | 18314 | 0.703 | 0.658 |
| | 38 | 1 | Y | Y | 21.16 | 23.3 | 44704 | 12503 | 57207 | 0.781 | 0.52 |
| | | 2 | Y | Y | 22.53 | 24.65 | 17613 | 4983 | 22596 | 0.779 | 0.524 |
| | | 3 | Y | Y | 19.95 | 21.99 | 101930 | 30586 | 132516 | 0.769 | 0.545 |
| | 39 | 1 | Y | N | 20.62 | 22.96 | 64765 | 15802 | 80568 | 0.804 | 0.473 |
| | | 2 | Y | N | 21.47 | 23.79 | 36084 | 8931 | 45015 | 0.802 | 0.478 |
| | | 3 | Y | N | 21.93 | 24.45 | 26359 | 5692 | 32051 | 0.822 | 0.431 |
| | 40 | 1 | Y | N | 21.38 | 23.72 | 38501 | 9381 | 47881 | 0.804 | 0.472 |
| | | 2 | Y | N | 22.39 | 24.92 | 19308 | 4138 | 23447 | 0.824 | 0.429 |
| | | 3 | Y | N | 18.3 | 20.74 | 313079 | 71992 | 385071 | 0.813 | 0.453 |

**Table B.12 Variation in $S_H$:$S_T$ along a depth gradient at The Arch (chapter 3)**

| ID | Depth (m) | C100 band | C109 band | Mean $C_t$ ($C100^+$) | Mean $C_t$ ($C100^-$) | $C_{C100}$ | $C_{C100}^-$ | $C_{TOTAL}$ | $C_{C100}$:$C_{TOTAL}$ | $S_H$:$S_T$ |
|---|---|---|---|---|---|---|---|---|---|---|
| **1** | 9.5 | Y | Y | 21.24 | 23.18 | 42460 | 13556 | 56016 | 0.758 | 0.566 |
| **2** | 7.5 | Y | N | 22.16 | 25.32 | 22613 | 3152 | 25765 | 0.878 | 0.293 |
| **3** | 5.1 | Y | Y | 20.6 | 22.47 | 65548 | 21976 | 87524 | 0.749 | 0.583 |
| **4** | 4.4 | Y | N | 26.12 | 28.44 | 1521 | 375 | 1896 | 0.802 | 0.477 |
| **5** | 4.4 | Y | Y | 22.34 | 24.72 | 20025 | 4753 | 24778 | 0.808 | 0.463 |
| **6** | 9.7 | Y | N | 21.04 | 23.64 | 48649 | 9939 | 58588 | 0.83 | 0.413 |
| **7** | 7.5 | Y | Y | 23.16 | 25.3 | 11401 | 3190 | 14591 | 0.781 | 0.52 |
| **8** | 5.4 | Y | N | 19.34 | 22.53 | 154749 | 21089 | 175838 | 0.88 | 0.287 |
| **9** | 8.8 | Y | Y | 20.3 | 22.23 | 80366 | 25883 | 106249 | 0.756 | 0.569 |
| **10** | 11 | Y | N | 23.77 | 26.49 | 7542 | 1421 | 8963 | 0.841 | 0.386 |
| **11** | 11.6 | Y | Y | 25.2 | 27.05 | 2854 | 966 | 3820 | 0.747 | 0.586 |
| **12** | 4.4 | Y | N | 27.34 | 29.49 | 662 | 183 | 844 | 0.784 | 0.516 |
| **13** | 4.7 | Y | Y | 20.12 | 22.16 | 90742 | 27213 | 117955 | 0.769 | 0.544 |
| **14** | 4.8 | Y | N | 20.96 | 23.65 | 51184 | 9847 | 61030 | 0.839 | 0.393 |
| **15** | 10.8 | Y | Y | 22.26 | 24.69 | 21140 | 4856 | 25997 | 0.813 | 0.452 |
| **16** | 6.8 | Y | Y | 21.82 | 23.05 | 28543 | 14876 | 43419 | 0.657 | 0.719 |
| **17*** | 9.9 | Y | N | 23.18 | 26.02 | 11273 | 1949 | 13222 | 0.853 | 0.358 |
| **18*** | 11.1 | Y | Y | 26.89 | 28.82 | 902 | 289 | 1191 | 0.757 | 0.567 |
| **19*** | 10.2 | Y | Y | 23.82 | 25.21 | 7303 | 3399 | 10702 | 0.682 | 0.687 |
| **20*** | 10.6 | Y | Y | 23.7 | 25.56 | 7906 | 2671 | 10576 | 0.747 | 0.585 |
| **21*** | 11.6 | Y | Y | 24.4 | 25.56 | 4917 | 2664 | 7582 | 0.649 | 0.729 |
| **22** | 9.9 | Y | Y | 21.86 | 23.76 | 27675 | 9134 | 36809 | 0.752 | 0.577 |
| **23** | 11.2 | Y | Y | 23.44 | 25.07 | 9442 | 3724 | 13167 | 0.717 | 0.636 |
| **24** | 10.5 | Y | Y | 22.36 | 23.7 | 19756 | 9532 | 29288 | 0.675 | 0.698 |
| **25** | 11 | Y | Y | 22.65 | 23.99 | 16239 | 7797 | 24036 | 0.676 | 0.696 |
| **26** | 10.4 | Y | N | 23.06 | 26.18 | 12250 | 1756 | 14006 | 0.875 | 0.301 |

Asterisks indicate colonies used in nested analysis

**Table B.13 Longitudinal analysis of temporal variation in $S_H$:$S_T$ (chapter 3)**

| Site | ID | Time | $C_t$ ($C100^+$) | $C_t$ ($C100^-$) | $C_{C100}$ | $C_{C100}^-$ | $C_{TOTAL}$ | $C_{100}$:$C_{TOTAL}$ | $S_H$:$S_T$ |
|---|---|---|---|---|---|---|---|---|---|
| **Comet's** | 1 | Mar 2011 | 22.41 | 24.63 | 19090 | 5030 | 24119 | 0.791 | 0.5 |
| **Hole** | | Sep 2011 | 24.86 | 27.08 | 3592 | 947 | 4539 | 0.791 | 0.5 |
| | | Mar 2012 | 19.74 | 21.97 | 117800 | 31077 | 148877 | 0.791 | 0.5 |
| | | Sep 2012 | 18.68 | 20.94 | 242570 | 62740 | 305310 | 0.795 | 0.493 |
| | 2 | Mar 2011 | 20.88 | 24.06 | 54042 | 7424 | 61466 | 0.879 | 0.289 |
| | | Sep 2011 | 25.35 | 28.56 | 2579 | 346 | 2925 | 0.882 | 0.282 |
| | | Mar 2012 | 20.93 | 24.41 | 52327 | 5880 | 58207 | 0.899 | 0.234 |
| | | Sep 2012 | 19.38 | 22.89 | 150383 | 16518 | 166902 | 0.901 | 0.228 |
| | 3 | Mar 2011 | 27.8 | 30.07 | 485 | 123 | 608 | 0.797 | 0.487 |
| | | Sep 2011 | 23.83 | 26.01 | 7245 | 1961 | 9206 | 0.787 | 0.509 |
| | | Mar 2012 | 23.57 | 25.96 | 8675 | 2040 | 10715 | 0.81 | 0.46 |
| | | Sep 2012 | 20.83 | 23.16 | 55972 | 13777 | 69749 | 0.802 | 0.476 |
| | 4 | Mar 2011 | 19.14 | 22.42 | 177333 | 22833 | 200166 | 0.886 | 0.271 |
| | | Sep 2011 | 23.46 | 26.48 | 9335 | 1426 | 10761 | 0.867 | 0.32 |
| | | Mar 2012 | 21.26 | 24.24 | 41778 | 6560 | 48338 | 0.864 | 0.328 |
| | | Sep 2012 | 20.56 | 23.78 | 67451 | 8993 | 76444 | 0.882 | 0.28 |
| | 5 | Mar 2011 | 21.44 | 23.79 | 36954 | 8920 | 45875 | 0.806 | 0.469 |
| | | Sep 2011 | 27.65 | 29.84 | 536 | 144 | 680 | 0.789 | 0.506 |
| | | Mar 2012 | 21.82 | 24.3 | 28414 | 6301 | 34715 | 0.818 | 0.44 |
| | | Sep 2012 | 20.59 | 22.65 | 65985 | 19505 | 85491 | 0.772 | 0.539 |
| **North** | 6 | Mar 2011 | 22.37 | 24.26 | 19579 | 6514 | 26093 | 0.75 | 0.58 |
| **Bay** | | Sep 2011 | 23.42 | 25.25 | 9584 | 3295 | 12878 | 0.744 | 0.591 |
| | | Mar 2012 | 24.9 | 26.77 | 3500 | 1174 | 4673 | 0.749 | 0.583 |
| | | Sep 2012 | 21.82 | 23.53 | 28446 | 10662 | 39109 | 0.727 | 0.62 |
| | 7 | Mar 2011 | 23.5 | 27.17 | 9047 | 889 | 9935 | 0.911 | 0.201 |
| | | Sep 2011 | 26.8 | 30.26 | 958 | 108 | 1066 | 0.899 | 0.235 |
| | | Mar 2012 | 24.29 | 27.51 | 5288 | 706 | 5995 | 0.882 | 0.281 |
| | | Sep 2012 | 24.36 | 27.59 | 5057 | 668 | 5725 | 0.883 | 0.278 |
| | 8 | Mar 2011 | 19.95 | 23.65 | 101785 | 9855 | 111640 | 0.912 | 0.197 |
| | | Sep 2011 | 20.95 | 24.51 | 51669 | 5464 | 57133 | 0.904 | 0.219 |
| | | Mar 2012 | 21.09 | 24.34 | 46818 | 6158 | 52976 | 0.884 | 0.276 |
| | | Sep 2012 | 22.51 | 26 | 17804 | 1980 | 19784 | 0.9 | 0.231 |
| | 9 | Mar 2011 | 24.86 | 27.07 | 3582 | 951 | 4533 | 0.79 | 0.502 |

| | | | | | | | | | |
|---|---|---|---|---|---|---|---|---|---|
| | | Sep 2011 | 23.87 | 26.07 | 7059 | 1889 | 8948 | 0.789 | 0.505 |
| | | Mar 2012 | 21.31 | 23.65 | 40406 | 9819 | 50225 | 0.804 | 0.472 |
| | | Sep 2012 | 21.07 | 23.49 | 47457 | 10949 | 58406 | 0.813 | 0.454 |
| | 10 | Mar 2011 | 23.06 | 25.26 | 12258 | 3272 | 15531 | 0.789 | 0.504 |
| | | Sep 2011 | 20.98 | 22.99 | 50532 | 15412 | 65944 | 0.766 | 0.55 |
| | | Mar 2012 | 24.37 | 26.36 | 5019 | 1551 | 6569 | 0.764 | 0.555 |
| | | Sep 2012 | 23.75 | 25.87 | 7654 | 2164 | 9818 | 0.78 | 0.524 |
| **Sylph's** | 11 | Mar 2011 | 22.3 | 26.37 | 20525 | 1539 | 22064 | 0.93 | 0.142 |
| **Hole** | | Sep 2011 | 21.62 | 25.6 | 32698 | 2609 | 35306 | 0.926 | 0.154 |
| | | Mar 2012 | 20.56 | 24.49 | 67320 | 5550 | 72870 | 0.924 | 0.161 |
| | | Sep 2012 | 18.14 | 21.94 | 350788 | 31739 | 382527 | 0.917 | 0.182 |
| | 12 | Mar 2011 | 25.97 | 28.12 | 1689 | 467 | 2156 | 0.784 | 0.516 |
| | | Sep 2011 | 25.63 | 27.89 | 2128 | 545 | 2673 | 0.796 | 0.49 |
| | | Mar 2012 | 19.35 | 21.56 | 153834 | 41070 | 194903 | 0.789 | 0.504 |
| | | Sep 2012 | 20.98 | 23.19 | 50579 | 13482 | 64061 | 0.79 | 0.504 |
| | 13 | Mar 2011 | 27.15 | 29.3 | 754 | 208 | 961 | 0.784 | 0.515 |
| | | Sep 2011 | 27.33 | 29.28 | 666 | 210 | 876 | 0.76 | 0.562 |
| | | Mar 2012 | 24.27 | 26.47 | 5358 | 1437 | 6795 | 0.788 | 0.506 |
| | | Sep 2012 | 19.57 | 21.66 | 132194 | 38247 | 170441 | 0.776 | 0.532 |
| | 14 | Mar 2011 | 25.08 | 28.4 | 3093 | 385 | 3477 | 0.889 | 0.261 |
| | | Sep 2011 | 19.33 | 22.88 | 155268 | 16667 | 171936 | 0.903 | 0.222 |
| | | Mar 2012 | 23.22 | 26.83 | 10997 | 1127 | 12124 | 0.907 | 0.211 |
| | | Sep 2012 | 19.49 | 23.03 | 139659 | 15004 | 154663 | 0.903 | 0.223 |
| | 15 | Mar 2011 | 21.17 | 25.08 | 44297 | 3716 | 48013 | 0.923 | 0.165 |
| | | Sep 2011 | 24.02 | 27.7 | 6379 | 620 | 7000 | 0.911 | 0.198 |
| | | Mar 2012 | 22.54 | 26.43 | 17497 | 1478 | 18975 | 0.922 | 0.166 |

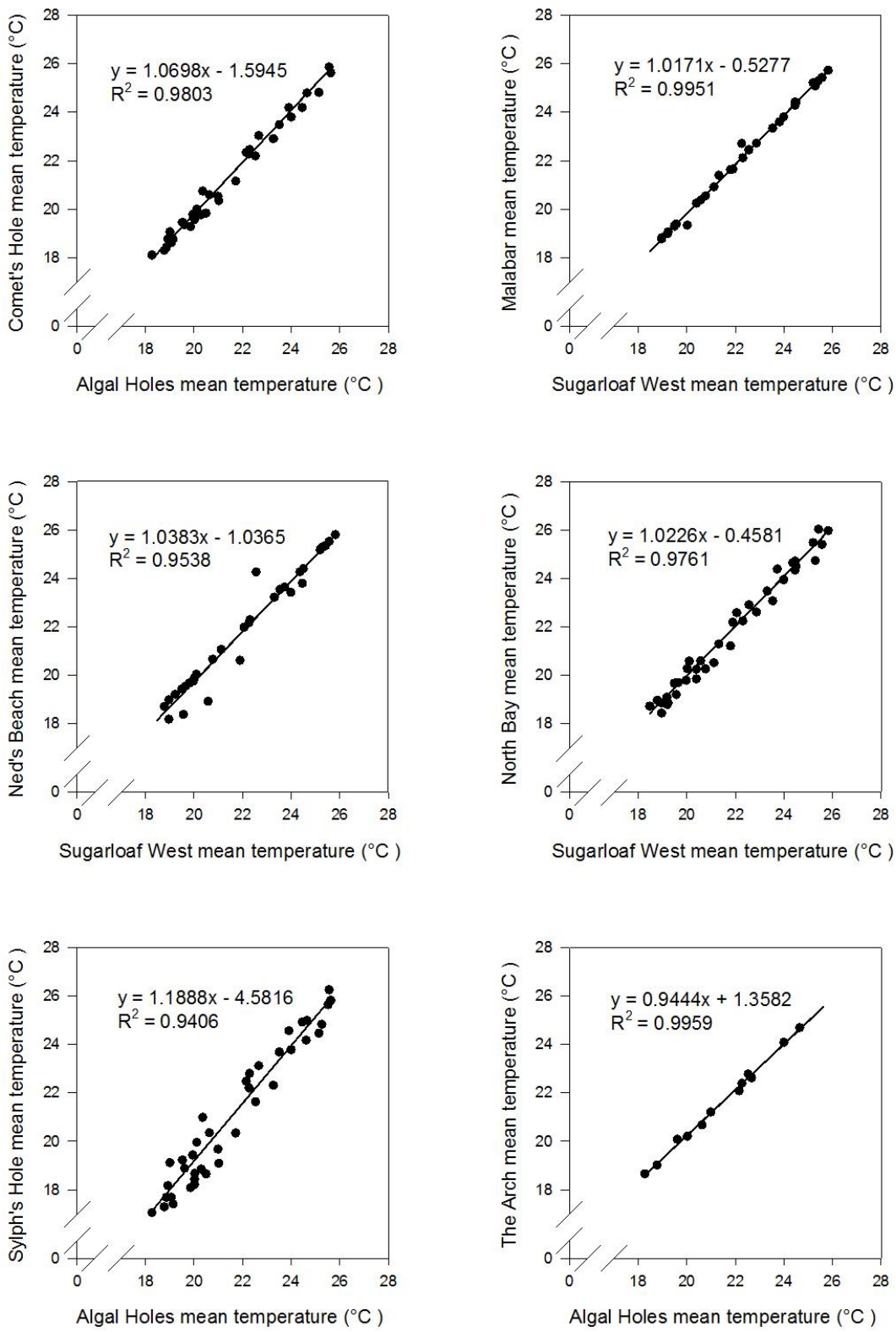


**Figure B.2 Site-correlation to estimate missing temperature data (chapter 3)**
Donor sites were either Algal Holes or Sugarloaf West, both of which had continuous temperature measurements available over the entire period. Circles represent monthly average temperatures during periods of simultaneous logging. Following correlation analysis, the parameters of the fitted line were used to predict missing monthly-temperature values.

**Table B.14 Climate model parameters for eight LHI study sites (chapter 3)**

| Site | a | b | c | d | d + a | d - a | 2a | $R^2$ |
|---|---|---|---|---|---|---|---|---|
| **Algal Holes** | 3.052 | 11.977 | 1.537 | 21.841 | 24.893 | 18.789 | 6.104 | 0.91 |
| **Comet's Hole** | 3.271 | 11.985 | -4.659 | 21.72 | 24.991 | 18.45 | 6.541 | 0.912 |
| **Malabar** | 3.079 | 11.997 | 1.472 | 21.683 | 24.762 | 18.604 | 6.158 | 0.909 |
| **Ned's Beach** | 3.217 | 12.007 | 1.48 | 21.637 | 24.854 | 18.42 | 6.434 | 0.919 |
| **North Bay** | 3.159 | 12.07 | -4.627 | 21.844 | 25.003 | 18.686 | 6.317 | 0.909 |
| **Sugarloaf West** | 3.024 | 11.996 | 1.489 | 21.842 | 24.866 | 18.817 | 6.048 | 0.91 |
| **Sylph's Hole** | 3.811 | 12.021 | 1.788 | 21.366 | 25.177 | 17.555 | 7.621 | 0.918 |
| **The Arch** | 2.883 | 11.992 | 1.544 | 21.975 | 24.857 | 19.092 | 5.765 | 0.909 |

The four sine-function parameters a, b, c and d represent the amplitude, period, phase shift and vertical shift, respectively. Parameter information can be interpreted as: d, mean temperature; d + a, temperature maximum; d – a, temperature minimum; 2a, seasonal temperature variability.

**Table B.15 Calculation of $S_H$:$S_T$ ratios for physiology analysis (chapter 4)**

| Fragment no. | Colony no. | Temperature | C100 band | C109 band | $C_t$ ($C100^+$) | $C_t$ ($C100^-$) | $C_{C100}$ | $C_{TOTAL}$ | $C_{C100}$:$C_{TOTAL}$ | $S_H$:$S_T$ |
|---|---|---|---|---|---|---|---|---|---|---|
| **1** | 1 | 25 °C | Y | Y | 22.55 | 24 | 17284 | 25024 | 0.691 | 0.676 |
| **2** | 2 | 25 °C | Y | Y | 22.43 | 23.73 | 18871 | 28172 | 0.67 | 0.704 |
| **3** | 3 | 25 °C | Y | N | 22.16 | 24.52 | 22567 | 28021 | 0.805 | 0.47 |
| **4** | 4 | 25 °C | Y | N | 22.93 | 24.88 | 13362 | 17614 | 0.759 | 0.565 |
| **5** | 5 | 25 °C | Y | Y | 24.49 | 26.52 | 4622 | 6011 | 0.769 | 0.545 |
| **6** | 6 | 25 °C | Y | Y | 23.62 | 25.25 | 8337 | 11632 | 0.717 | 0.637 |
| **7** | 7 | 25 °C | Y | N | 21.94 | 25.05 | 26269 | 30049 | 0.874 | 0.302 |
| **8** | 8 | 25 °C | Y | Y | 22.45 | 24.11 | 18562 | 25734 | 0.721 | 0.63 |
| **9** | 9 | 25 °C | Y | Y | 24.52 | 26.75 | 4526 | 5709 | 0.793 | 0.497 |
| **10** | 10 | 25 °C | Y | N | 22.82 | 25.18 | 14422 | 17892 | 0.806 | 0.468 |
| **11** | 11 | 25 °C | Y | N | 23.89 | 25.96 | 6942 | 8979 | 0.773 | 0.537 |
| **12** | 12 | 25 °C | Y | N | 21.99 | 25.39 | 25410 | 28411 | 0.894 | 0.247 |
| **13** | 13 | 25 °C | Y | N | 22.52 | 26.23 | 17687 | 19376 | 0.913 | 0.194 |
| **14** | 14 | 25 °C | Y | N | 21.52 | 24.76 | 34956 | 39569 | 0.883 | 0.277 |
| **15** | 15 | 25 °C | Y | N | 20.94 | 24.61 | 51927 | 57050 | 0.91 | 0.202 |
| **16** | 1 | 29 °C | Y | Y | 24.1 | 25.45 | 6018 | 8908 | 0.676 | 0.696 |
| **17** | 2 | 29 °C | Y | Y | 23.69 | 24.93 | 7992 | 12106 | 0.66 | 0.716 |
| **18** | 3 | 29 °C | Y | N | 22.58 | 25.02 | 17004 | 20863 | 0.815 | 0.448 |
| **19** | 4 | 29 °C | Y | N | 23.36 | 25.42 | 9987 | 12930 | 0.772 | 0.538 |
| **20** | 5 | 29 °C | Y | Y | 24.63 | 26.65 | 4196 | 5464 | 0.768 | 0.547 |
| **21** | 6 | 29 °C | Y | Y | 23.39 | 25.12 | 9784 | 13403 | 0.73 | 0.616 |
| **22** | 7 | 29 °C | Y | N | 21.02 | 25.03 | 49136 | 52979 | 0.927 | 0.15 |
| **23** | 8 | 29 °C | Y | Y | 22.21 | 23.97 | 21872 | 29775 | 0.735 | 0.608 |
| **24** | 9 | 29 °C | Y | N | 24 | 25.95 | 6454 | 8498 | 0.759 | 0.563 |
| **25** | 10 | 29 °C | Y | N | 23.95 | 26.3 | 6688 | 8303 | 0.805 | 0.47 |
| **26** | 11 | 29 °C | Y | N | 24.22 | 26.18 | 5552 | 7306 | 0.76 | 0.562 |
| **27** | 12 | 29 °C | Y | N | 24.2 | 27.66 | 5617 | 6255 | 0.898 | 0.237 |
| **28** | 13 | 29 °C | Y | N | 23.48 | 26.83 | 9200 | 10320 | 0.891 | 0.255 |
| **29** | 14 | 29 °C | Y | N | 22.2 | 25.53 | 22071 | 24803 | 0.89 | 0.26 |
| **30** | 15 | 29 °C | Y | N | 21.84 | 25.38 | 28141 | 31168 | 0.903 | 0.223 |

**Table B.16 Physiological diagnostics (chapter 4)**

| Fragment no. | Colony no. | Treatment Temperature | $S_H$:$S_T$ | Surface area ($cm^2$) | Host protein ($mg\ cm^{-2}$) | Symbiont density ($x\ 10^3$ cells $mg^{-1}$) | Symbiont density ($x\ 10^3$ cells $cm^{-2}$) | Chlorophyll *a* ($pg\ cell^{-1}$) | Chlorophyll $c_2$ ($pg\ cell^{-1}$) | Chlorophyll $c_2$:*a* ratio |
|---|---|---|---|---|---|---|---|---|---|---|
| **1** | 1 | 25 °C | 0.676 | 5.71 | 0.351 | 1314 | 461 | 3.98 | 0.97 | 0.243 |
| **2** | 2 | 25 °C | 0.704 | 5.29 | 0.754 | 952 | 717 | 2.46 | 1.26 | 0.491 |
| **3** | 3 | 25 °C | 0.47 | 6.58 | 0.436 | 1036 | 452 | 2.84 | 1.1 | 0.387 |
| **4** | 4 | 25 °C | 0.565 | 5.96 | 0.57 | 843 | 480 | 2.66 | 1.25 | 0.461 |
| **5** | 5 | 25 °C | 0.545 | 6.11 | 0.442 | 1052 | 465 | 2.8 | 1.27 | 0.458 |
| **6** | 6 | 25 °C | 0.637 | 4.38 | 0.489 | 1070 | 524 | 3.03 | 1.15 | 0.406 |
| **7** | 7 | 25 °C | 0.302 | 3.86 | 0.45 | 1582 | 713 | 3.05 | 0.97 | 0.294 |
| **8** | 8 | 25 °C | 0.63 | 6.38 | 0.313 | 1127 | 353 | 3.38 | 1.02 | 0.301 |
| **9** | 9 | 25 °C | 0.497 | 4.32 | 0.405 | 1325 | 537 | 3.03 | 1.1 | 0.362 |
| **10** | 10 | 25 °C | 0.468 | 5.16 | 0.508 | 1744 | 886 | 3.33 | 1.12 | 0.343 |
| **11** | 11 | 25 °C | 0.537 | 8.76 | 0.435 | 762 | 332 | 3.67 | 0.89 | 0.242 |
| **12** | 12 | 25 °C | 0.247 | 5.41 | 0.328 | 2461 | 807 | 2.84 | 0.9 | 0.317 |
| **13** | 13 | 25 °C | 0.194 | 7.26 | 0.462 | 1056 | 488 | 3.63 | 0.84 | 0.232 |
| **14** | 14 | 25 °C | 0.277 | 5.44 | 0.342 | 1702 | 582 | 4.17 | 0.71 | 0.171 |
| **15** | 15 | 25 °C | 0.202 | 4.26 | 0.47 | 1344 | 632 | 4.33 | 1.07 | 0.26 |
| **16** | 1 | 29 °C | 0.696 | 7.77 | 0.374 | 643 | 240 | 2.08 | 1.06 | 0.509 |
| **17** | 2 | 29 °C | 0.716 | 3.74 | 0.654 | 635 | 415 | 3.77 | 1.67 | 0.443 |
| **18** | 3 | 29 °C | 0.448 | 4.57 | 0.422 | 912 | 385 | 3.88 | 1.12 | 0.288 |
| **19** | 4 | 29 °C | 0.538 | 3.64 | 0.632 | 630 | 398 | 2.91 | 1.44 | 0.494 |
| **20** | 5 | 29 °C | 0.547 | 4.41 | 0.535 | 802 | 429 | 2.99 | 1.63 | 0.513 |
| **21** | 6 | 29 °C | 0.616 | 4.75 | 0.438 | 1224 | 536 | 4.96 | 1.66 | 0.345 |
| **22** | 7 | 29 °C | 0.15 | 5.06 | 0.295 | 1549 | 457 | 3.26 | 0.97 | 0.298 |
| **23** | 8 | 29 °C | 0.608 | 8.28 | 0.325 | 1118 | 363 | 3.17 | 1.05 | 0.331 |
| **24** | 9 | 29 °C | 0.563 | 4.55 | 0.488 | 842 | 411 | 3.72 | 1.3 | 0.356 |
| **25** | 10 | 29 °C | 0.47 | 4.97 | 0.276 | 1961 | 540 | 3.69 | 1.1 | 0.311 |
| **26** | 11 | 29 °C | 0.562 | 6.11 | 0.424 | 822 | 349 | 2.97 | 0.85 | 0.289 |
| **27** | 12 | 29 °C | 0.237 | 4.57 | 0.264 | 2081 | 548 | 2.99 | 1.02 | 0.34 |
| **28** | 13 | 29 °C | 0.255 | 5.43 | 0.471 | 955 | 450 | 3.64 | 1.27 | 0.348 |
| **29** | 14 | 29 °C | 0.26 | 4.98 | 0.515 | 1224 | 630 | 3.61 | 1.22 | 0.326 |
| **30** | 15 | 29 °C | 0.223 | 4.71 | 0.432 | 1124 | 486 | 3.86 | 0.92 | 0.255 |

**Table B.17 Photosynthesis-irradiance measurements (chapter 4)**

| Fragment no. | Colony no. | Treatment temperature | $S_H$:$S_T$ | $P_{GROSS}$ (µmol $O_2$ $mg^{-1}$ protein $h^{-1}$) | $R$ (µmol $O_2$ $mg^{-1}$ protein $h^{-1}$) | $P$:$R$ | $\alpha$ (µmol $O_2$ $mg^{-1}$ protein $h^{-1}$ (µmol photons $m^{-2}$ $s^{-1}$)$^{-1}$) | $I_K$ (µmol photons $m^{-2}$ $s^{-1}$) | $I_C$ (µmol photons $m^{-2}$ $s^{-1}$) |
|---|---|---|---|---|---|---|---|---|---|
| **1** | 1 | 25 °C | 0.676 | 1.95 | -1.24 | 1.57 | 0.0203 | 95.8 | 72.4 |
| **2** | 2 | 25 °C | 0.704 | 1.52 | -0.91 | 1.67 | 0.0172 | 88.5 | 61 |
| **3** | 3 | 25 °C | 0.47 | 1.09 | -0.61 | 1.77 | 0.0126 | 86.5 | 55.3 |
| **4** | 4 | 25 °C | 0.565 | 1.35 | -0.85 | 1.59 | 0.0124 | 108.5 | 80.4 |
| **5** | 5 | 25 °C | 0.545 | 1.53 | -0.88 | 1.74 | 0.0176 | 87.2 | 57.2 |
| **6** | 6 | 25 °C | 0.637 | 1.25 | -0.65 | 1.93 | 0.0141 | 88.4 | 50.8 |
| **7** | 7 | 25 °C | 0.302 | 2.52 | -1.36 | 1.86 | 0.0239 | 105.6 | 63.5 |
| **8** | 8 | 25 °C | 0.63 | 1.9 | -1.16 | 1.64 | 0.0234 | 80.9 | 57.4 |
| **9** | 9 | 25 °C | 0.497 | 1.68 | -1.09 | 1.54 | 0.0198 | 84.9 | 65.5 |
| **10** | 10 | 25 °C | 0.468 | 1.29 | -0.72 | 1.79 | 0.0135 | 95.6 | 60.2 |
| **11** | 11 | 25 °C | 0.537 | 1.4 | -1.04 | 1.35 | 0.0154 | 91.1 | 86.4 |
| **12** | 12 | 25 °C | 0.247 | 2.68 | -1.34 | 2 | 0.0399 | 67.1 | 36.8 |
| **13** | 13 | 25 °C | 0.194 | 1.59 | -0.79 | 2.02 | 0.0165 | 95.9 | 52 |
| **14** | 14 | 25 °C | 0.277 | 1.9 | -1.08 | 1.76 | 0.0305 | 62.2 | 40.2 |
| **15** | 15 | 25 °C | 0.202 | 2.23 | -1.21 | 1.84 | 0.0273 | 81.6 | 49.6 |
| **16** | 1 | 29 °C | 0.696 | 1.1 | -0.92 | 1.2 | 0.0151 | 73 | 88.2 |
| **17** | 2 | 29 °C | 0.716 | 1.18 | -0.85 | 1.4 | 0.0084 | 140.9 | 126.7 |
| **18** | 3 | 29 °C | 0.448 | 2.32 | -1.66 | 1.4 | 0.0347 | 66.9 | 59.8 |
| **19** | 4 | 29 °C | 0.538 | 1.1 | -1.03 | 1.07 | 0.0114 | 96.1 | 163.6 |
| **20** | 5 | 29 °C | 0.547 | 1.54 | -1.2 | 1.28 | 0.0199 | 77.6 | 81.2 |
| **21** | 6 | 29 °C | 0.616 | 1.7 | -1.09 | 1.56 | 0.0222 | 76.6 | 58.1 |
| **22** | 7 | 29 °C | 0.15 | 2.98 | -1.92 | 1.55 | 0.0383 | 77.7 | 59.7 |
| **23** | 8 | 29 °C | 0.608 | 1.93 | -1.32 | 1.46 | 0.0241 | 80 | 67.2 |
| **24** | 9 | 29 °C | 0.563 | 1.28 | -1.15 | 1.12 | 0.0112 | 114 | 164.9 |
| **25** | 10 | 29 °C | 0.47 | 2.52 | -1.76 | 1.43 | 0.0216 | 116.7 | 100.6 |
| **26** | 11 | 29 °C | 0.562 | 1.24 | -1.01 | 1.23 | 0.01 | 124.1 | 141.5 |
| **27** | 12 | 29 °C | 0.237 | 2.52 | -1.68 | 1.5 | 0.0426 | 59.1 | 47.6 |
| **28** | 13 | 29 °C | 0.255 | 1.48 | -0.97 | 1.53 | 0.0207 | 71.6 | 56.2 |
| **29** | 14 | 29 °C | 0.26 | 1.6 | -1.04 | 1.54 | 0.0181 | 88.4 | 68.4 |
| **30** | 15 | 29 °C | 0.223 | 1.37 | -1.03 | 1.33 | 0.0168 | 81.3 | 79.7 |

**Table B.18 Mortality, growth, and temporal changes in $S_H$:$S_T$ (chapter 5)**

| Colony | Original site | Transplant site | Survived 195 d | Survived 374 d | Initial dry weight (g) | Final dry weight (g) | Time (d) | Growth (mg $d^{-1}$) | Growth ($\times 10^3$ % $d^{-1}$) | Original $S_H$:$S_T$ | Mean $C_t$ ($C100^+$) | Mean $C_t$ ($C100^-$) | $C_{C100}$ | $C_{TOTAL}$ | $C_{100}$: $C_{TOTAL}$ | Final $S_H$:$S_T$ |
|---|---|---|---|---|---|---|---|---|---|---|---|---|---|---|---|---|
| **1** | North Bay | North Bay | Y | *N/A | 6.20 | 8.91 | 195 | 13.88 | 1.86 | 0.70 | 23.41 | 24.79 | 9655 | 14175 | 0.68 | 0.69 |
| | | North Bay | Y | Y | 9.05 | 26.26 | 374 | 46.02 | 2.85 | | 24.61 | 25.64 | 4251 | 6783 | 0.63 | 0.75 |
| | | North Bay | Y | Y | 6.30 | 14.28 | 374 | 21.33 | 2.19 | | 24.70 | 25.86 | 4001 | 6184 | 0.65 | 0.73 |
| | | The Arch | Y | *N/A | 5.80 | 8.97 | 195 | 16.26 | 2.24 | | 25.14 | 26.22 | 2962 | 4669 | 0.63 | 0.74 |
| | | The Arch | Y | N | 8.26 | | | | | | | | | | | |
| | | The Arch | Y | N | 7.52 | | | | | | | | | | | |
| **2** | North Bay | North Bay | Y | *N/A | 10.37 | 13.66 | 195 | 16.87 | 1.41 | 0.65 | 21.90 | 23.55 | 26925 | 37475 | 0.72 | 0.63 |
| | | North Bay | Y | Y | 10.50 | 24.76 | 374 | 38.12 | 2.30 | | 23.65 | 25.20 | 8188 | 11613 | 0.71 | 0.65 |
| | | North Bay | Y | Y | 7.99 | 20.22 | 374 | 32.69 | 2.49 | | 24.27 | 25.90 | 5372 | 7488 | 0.72 | 0.64 |
| | | The Arch | Y | *N/A | 10.58 | 15.78 | 195 | 26.69 | 2.05 | | 28.78 | 30.38 | 248 | 348 | 0.71 | 0.64 |
| | | The Arch | N | N | 9.50 | | | | | | | | | | | |
| | | The Arch | Y | N | 7.25 | | | | | | | | | | | |
| **3** | North Bay | North Bay | Y | *N/A | 9.73 | 13.03 | 195 | 16.91 | 1.50 | 0.60 | 23.97 | 26.13 | 6600 | 8409 | 0.78 | 0.51 |
| | | North Bay | Y | Y | 12.36 | 21.34 | 374 | 24.02 | 1.46 | | 28.37 | 30.22 | 328 | 439 | 0.75 | 0.59 |
| | | North Bay | Y | Y | 4.80 | 10.71 | 374 | 15.80 | 2.15 | | 24.64 | 26.70 | 4183 | 5408 | 0.77 | 0.54 |
| | | The Arch | Y | *N/A | 4.66 | 6.11 | 195 | 7.44 | 1.39 | | 30.71 | 33.01 | 67 | 84 | 0.80 | 0.48 |
| | | The Arch | Y | N | 17.14 | | | | | | | | | | | |
| | | The Arch | Y | Y | 8.25 | 7.55 | 374 | -1.86 | -0.24 | | 23.16 | 24.94 | 11413 | 15504 | 0.74 | 0.61 |
| **4** | North Bay | North Bay | Y | *N/A | 11.66 | 15.36 | 195 | 18.96 | 1.41 | 0.62 | 25.62 | 27.12 | 2139 | 3063 | 0.70 | 0.67 |
| | | North Bay | Y | Y | 10.95 | 31.49 | 374 | 54.92 | 2.83 | | 23.41 | 24.98 | 9657 | 13627 | 0.71 | 0.65 |
| | | North Bay | Y | Y | 10.70 | 14.72 | 374 | 10.74 | 0.85 | | 24.82 | 26.52 | 3694 | 5086 | 0.73 | 0.62 |
| | | The Arch | Y | *N/A | 11.39 | 14.02 | 195 | 13.47 | 1.06 | | 25.43 | 27.07 | 2437 | 3387 | 0.72 | 0.63 |
| | | The Arch | Y | N | 12.16 | | | | | | | | | | | |
| | | The Arch | Y | N | 10.18 | | | | | | | | | | | |
| **5** | North Bay | North Bay | Y | *N/A | 10.95 | 15.29 | 195 | 22.27 | 1.71 | 0.50 | 25.04 | 27.55 | 3177 | 3865 | 0.82 | 0.43 |
| | | North Bay | Y | Y | 13.48 | 19.31 | 374 | 15.59 | 0.96 | | 23.05 | 25.21 | 12286 | 15676 | 0.78 | 0.52 |
| | | North Bay | Y | Y | 14.13 | 26.34 | 374 | 32.65 | 1.67 | | 25.33 | 27.54 | 2607 | 3299 | 0.79 | 0.50 |
| | | The Arch | Y | *N/A | 12.92 | 16.37 | 195 | 17.71 | 1.22 | | 26.59 | 28.76 | 1103 | 1404 | 0.79 | 0.51 |
| | | The Arch | Y | N | 13.47 | | | | | | | | | | | |
| | | The Arch | Y | Y | 9.78 | 8.54 | 374 | -3.32 | -0.36 | | 28.88 | 30.90 | 232 | 302 | 0.77 | 0.55 |
| **6** | North Bay | North Bay | Y | *N/A | 5.80 | 10.81 | 195 | 25.69 | 3.20 | 0.59 | 27.35 | 29.32 | 657 | 862 | 0.76 | 0.56 |
| | | North Bay | Y | Y | 7.99 | 13.66 | 374 | 15.17 | 1.44 | | 25.30 | 26.83 | 2655 | 3775 | 0.70 | 0.66 |

| | | | | | | | | | | | | | | | | |
|---|---|---|---|---|---|---|---|---|---|---|---|---|---|---|---|---|
| | | North Bay | Y | Y | 9.75 | 20.51 | 374 | 28.76 | 1.99 | | 22.96 | 24.75 | 13078 | 17730 | 0.74 | 0.60 |
| | | The Arch | Y | *N/A | 6.41 | 11.93 | 195 | 28.31 | 3.19 | | 24.78 | 26.42 | 3782 | 5269 | 0.72 | 0.64 |
| | | The Arch | N | N | 3.91 | | | | | | | | | | | |
| | | The Arch | Y | Y | 6.41 | 11.27 | 374 | 12.99 | 1.51 | | 23.59 | 25.33 | 8526 | 11658 | 0.73 | 0.61 |
| **7** | North Bay | North Bay | Y | *N/A | 11.81 | 14.63 | 195 | 14.48 | 1.10 | 0.22 | 22.23 | 24.61 | 21575 | 26676 | 0.81 | 0.46 |
| | | North Bay | Y | Y | 6.75 | 12.97 | 374 | 16.63 | 1.75 | | 21.66 | 25.63 | 31702 | 34251 | 0.93 | 0.16 |
| | | North Bay | Y | Y | 7.70 | 16.92 | 374 | 24.66 | 2.11 | | 22.37 | 25.43 | 19655 | 22573 | 0.87 | 0.31 |
| | | The Arch | Y | *N/A | 9.12 | 9.80 | 195 | 3.48 | 0.37 | | 22.30 | 25.80 | 20530 | 22794 | 0.90 | 0.23 |
| | | The Arch | Y | N | 5.72 | | | | | | | | | | | |
| | | The Arch | Y | N | 6.57 | | | | | | | | | | | |
| **8** | North Bay | North Bay | Y | *N/A | 7.12 | 10.87 | 195 | 19.24 | 2.17 | 0.23 | 23.03 | 26.28 | 12506 | 14144 | 0.88 | 0.28 |
| | | North Bay | Y | Y | 12.23 | 26.87 | 374 | 39.15 | 2.11 | | 24.36 | 27.59 | 5057 | 5725 | 0.88 | 0.28 |
| | | North Bay | Y | Y | 5.46 | 10.92 | 374 | 14.60 | 1.86 | | 25.88 | 29.05 | 1787 | 2033 | 0.88 | 0.29 |
| | | The Arch | Y | *N/A | 14.06 | 22.09 | 195 | 41.20 | 2.32 | | 24.68 | 28.04 | 4071 | 4562 | 0.89 | 0.25 |
| | | The Arch | N | N | 4.54 | | | | | | | | | | | |
| | | The Arch | Y | Y | 7.73 | 9.25 | 374 | 4.06 | 0.48 | | 22.58 | 26.14 | 16923 | 18725 | 0.90 | 0.22 |
| **9** | North Bay | North Bay | Y | *N/A | 3.62 | 6.45 | 195 | 14.52 | 2.97 | 0.65 | 25.70 | 27.20 | 2030 | 2902 | 0.70 | 0.66 |
| | | North Bay | Y | N | 5.56 | | | | | | | | | | | |
| | | North Bay | Y | Y | 8.25 | 15.42 | 374 | 19.17 | 1.67 | | 23.68 | 25.24 | 8019 | 11349 | 0.71 | 0.65 |
| | | The Arch | Y | *N/A | 3.13 | 4.55 | 195 | 7.27 | 1.92 | | 23.49 | 25.03 | 9126 | 12970 | 0.70 | 0.66 |
| | | The Arch | N | N | 3.56 | | | | | | | | | | | |
| | | The Arch | Y | N | 7.75 | | | | | | | | | | | |
| **10** | North Bay | North Bay | Y | *N/A | 7.30 | 9.37 | 195 | 10.63 | 1.28 | 0.75 | 24.02 | 25.33 | 6356 | 9480 | 0.67 | 0.70 |
| | | North Bay | Y | Y | 5.01 | 8.10 | 374 | 8.27 | 1.29 | | 26.66 | 27.92 | 1056 | 1589 | 0.66 | 0.71 |
| | | North Bay | Y | Y | 7.14 | 15.86 | 374 | 23.32 | 2.14 | | 25.61 | 26.80 | 2157 | 3302 | 0.65 | 0.72 |
| | | The Arch | Y | *N/A | 8.13 | 10.29 | 195 | 11.08 | 1.21 | | 23.98 | 25.18 | 6549 | 10014 | 0.65 | 0.72 |
| | | The Arch | Y | N | 6.07 | | | | | | | | | | | |
| | | The Arch | Y | N | 10.63 | | | | | | | | | | | |
| **11** | The Arch | North Bay | Y | *N/A | 2.87 | 4.22 | 195 | 6.94 | 1.98 | 0.36 | 24.86 | 27.95 | 3581 | 4105 | 0.87 | 0.31 |
| | | North Bay | Y | Y | 4.38 | 7.91 | 374 | 9.44 | 1.58 | | 26.15 | 28.77 | 1489 | 1787 | 0.83 | 0.41 |
| | | North Bay | Y | Y | 3.91 | 7.07 | 374 | 8.45 | 1.59 | | 24.39 | 27.21 | 4958 | 5824 | 0.85 | 0.36 |
| | | The Arch | Y | *N/A | 3.29 | 4.84 | 195 | 7.94 | 1.98 | | 27.37 | 30.75 | 651 | 729 | 0.89 | 0.25 |
| | | The Arch | Y | N | 4.80 | | | | | | | | | | | |
| | | The Arch | Y | N | 4.22 | | | | | | | | | | | |
| **12** | The Arch | North Bay | Y | *N/A | 2.53 | 3.51 | 195 | 5.02 | 1.68 | 0.57 | 22.06 | 24.06 | 24190 | 31640 | 0.76 | 0.55 |

| | | | | | | | | | | | | | | | | |
|---|---|---|---|---|---|---|---|---|---|---|---|---|---|---|---|---|
| | | North Bay | Y | Y | 8.09 | 15.57 | 374 | 20.00 | 1.75 | | 24.46 | 26.43 | 4719 | 6198 | 0.76 | 0.56 |
| | | North Bay | Y | Y | 3.21 | 5.05 | 374 | 4.92 | 1.21 | | 25.37 | 27.18 | 2531 | 3417 | 0.74 | 0.60 |
| | | The Arch | Y | *N/A | 5.49 | 8.58 | 195 | 15.87 | 2.29 | | 26.49 | 28.00 | 1182 | 1687 | 0.70 | 0.66 |
| | | The Arch | N | N | 1.64 | | | | | | | | | | | |
| | | The Arch | Y | N | 6.28 | | | | | | | | | | | |
| **13** | The Arch | North Bay | Y | *N/A | 4.43 | 5.70 | 195 | 6.53 | 1.30 | 0.69 | 26.03 | 27.74 | 1619 | 2223 | 0.73 | 0.62 |
| | | North Bay | Y | N | 3.03 | | | | | | | | | | | |
| | | North Bay | Y | Y | 2.08 | 3.97 | 374 | 5.05 | 1.73 | | 25.14 | 26.34 | 2968 | 4538 | 0.65 | 0.72 |
| | | The Arch | Y | *N/A | 2.77 | 4.82 | 195 | 10.52 | 2.85 | | 25.33 | 26.85 | 2610 | 3717 | 0.70 | 0.66 |
| | | The Arch | N | N | 4.25 | | | | | | | | | | | |
| | | The Arch | Y | Y | 3.80 | 8.90 | 374 | 13.64 | 2.28 | | 24.88 | 26.33 | 3539 | 5115 | 0.69 | 0.67 |
| **14** | The Arch | North Bay | Y | *N/A | 11.36 | 15.01 | 195 | 18.73 | 1.43 | 0.59 | 25.29 | 27.78 | 2676 | 3263 | 0.82 | 0.44 |
| | | North Bay | N | N | 7.97 | | | | | | | | | | | |
| | | North Bay | Y | Y | 13.14 | 27.10 | 374 | 37.33 | 1.94 | | 23.50 | 25.47 | 9086 | 11922 | 0.76 | 0.56 |
| | | The Arch | Y | *N/A | 6.62 | 6.45 | 195 | -0.86 | -0.13 | | 25.21 | 27.39 | 2833 | 3601 | 0.79 | 0.51 |
| | | The Arch | Y | N | 10.04 | | | | | | | | | | | |
| | | The Arch | Y | N | 4.72 | | | | | | | | | | | |
| **15** | The Arch | North Bay | Y | *N/A | 5.62 | 7.07 | 195 | 7.41 | 1.17 | 0.73 | 25.65 | 26.86 | 2103 | 3200 | 0.66 | 0.72 |
| | | North Bay | Y | Y | 3.43 | 4.04 | 374 | 1.64 | 0.44 | | 26.52 | 27.86 | 1158 | 1715 | 0.68 | 0.70 |
| | | North Bay | Y | Y | 3.37 | 4.65 | 374 | 3.42 | 0.86 | | 24.93 | 26.37 | 3422 | 4954 | 0.69 | 0.68 |
| | | The Arch | Y | *N/A | 9.57 | 10.70 | 195 | 5.78 | 0.57 | | 25.25 | 26.81 | 2749 | 3885 | 0.71 | 0.65 |
| | | The Arch | N | N | 3.59 | | | | | | | | | | | |
| | | The Arch | N | N | 3.01 | | | | | | | | | | | |
| **16** | The Arch | North Bay | Y | *N/A | 5.73 | 7.90 | 195 | 11.13 | 1.65 | 0.58 | 25.23 | 26.76 | 2782 | 3961 | 0.70 | 0.66 |
| | | North Bay | Y | Y | 10.60 | 20.74 | 374 | 27.11 | 1.80 | | 22.29 | 24.10 | 20638 | 27895 | 0.74 | 0.60 |
| | | North Bay | Y | Y | 6.38 | 13.52 | 374 | 19.08 | 2.01 | | 25.21 | 26.68 | 2830 | 4078 | 0.69 | 0.67 |
| | | The Arch | Y | *N/A | 3.99 | 6.02 | 195 | 10.43 | 2.11 | | 24.26 | 26.04 | 5407 | 7334 | 0.74 | 0.60 |
| | | The Arch | Y | N | 11.74 | | | | | | | | | | | |
| | | The Arch | Y | Y | 6.14 | 11.24 | 374 | 13.62 | 1.62 | | 24.91 | 26.59 | 3464 | 4785 | 0.72 | 0.63 |
| **17** | The Arch | North Bay | Y | *N/A | 3.61 | 5.00 | 195 | 7.14 | 1.67 | 0.64 | 26.18 | 27.72 | 1462 | 2072 | 0.71 | 0.65 |
| | | North Bay | Y | Y | 8.65 | 38.83 | 374 | 80.69 | 4.02 | | 23.27 | 25.09 | 10641 | 14321 | 0.74 | 0.59 |
| | | North Bay | Y | Y | 5.17 | 20.48 | 374 | 40.92 | 3.69 | | 23.79 | 25.73 | 7439 | 9820 | 0.76 | 0.57 |
| | | The Arch | Y | *N/A | 3.33 | 6.15 | 195 | 14.45 | 3.15 | | 24.31 | 26.36 | 5224 | 6771 | 0.77 | 0.54 |
| | | The Arch | N | N | 5.38 | | | | | | | | | | | |
| | | The Arch | Y | N | 9.70 | | | | | | | | | | | |

| | | | | | | | | | | | | | | | | |
|---|---|---|---|---|---|---|---|---|---|---|---|---|---|---|---|---|
| **18** | The Arch | North Bay | Y | *N/A | 3.96 | 5.37 | 195 | 7.22 | 1.56 | 0.70 | 26.77 | 28.56 | 976 | 1322 | 0.74 | 0.60 |
| | | North Bay | Y | Y | 9.57 | 22.45 | 374 | 34.44 | 2.28 | | 25.52 | 27.38 | 2290 | 3063 | 0.75 | 0.59 |
| | | North Bay | Y | Y | 2.27 | 5.01 | 374 | 7.34 | 2.12 | | 25.57 | 27.55 | 2214 | 2900 | 0.76 | 0.56 |
| | | The Arch | Y | *N/A | 4.64 | 6.92 | 195 | 11.70 | 2.05 | | 24.66 | 26.53 | 4112 | 5495 | 0.75 | 0.58 |
| | | The Arch | N | N | 2.92 | | | | | | | | | | | |
| | | The Arch | Y | N | 7.30 | | | | | | | | | | | |
| **19** | The Arch | North Bay | Y | *N/A | 7.81 | 10.49 | 195 | 13.73 | 1.51 | 0.70 | 24.86 | 26.29 | 3600 | 5227 | 0.69 | 0.68 |
| | | North Bay | Y | N | 2.35 | | | | | | | | | | | |
| | | North Bay | Y | Y | 4.72 | 8.35 | 374 | 9.72 | 1.53 | | 22.95 | 24.54 | 13217 | 18585 | 0.71 | 0.65 |
| | | The Arch | Y | *N/A | 7.23 | 13.13 | 195 | 30.28 | 3.07 | | 23.32 | 24.83 | 10268 | 14683 | 0.70 | 0.66 |
| | | The Arch | Y | N | 10.31 | | | | | | | | | | | |
| | | The Arch | Y | Y | 3.99 | 5.24 | 374 | 3.34 | 0.73 | | 25.67 | 27.05 | 2068 | 3036 | 0.68 | 0.69 |
| **20** | The Arch | North Bay | Y | *N/A | 5.48 | 7.31 | 195 | 9.37 | 1.48 | 0.30 | 24.29 | 27.46 | 5287 | 6017 | 0.88 | 0.29 |
| | | North Bay | Y | N | 8.89 | | | | | | | | | | | |
| | | North Bay | Y | Y | 3.46 | 7.15 | 374 | 9.88 | 1.94 | | 23.16 | 26.16 | 11403 | 13176 | 0.87 | 0.33 |
| | | The Arch | Y | *N/A | 2.08 | 2.63 | 195 | 2.84 | 1.21 | | 24.05 | 26.98 | 6245 | 7258 | 0.86 | 0.34 |
| | | The Arch | N | N | 13.32 | | | | | | | | | | | |
| | | The Arch | Y | N | 3.87 | | | | | | | | | | | |

Asterisks indicate coral fragments collected after 195 d